Hydrogen Metabolizers: Drivers of Anaerobic Degradation Processes in Peatlands and Earthworm Guts

Dissertation

To obtain the Academic Degree
Doctor rerum naturalium
(Dr. rer. nat.)
Submitted to the Faculty of Biology, Chemistry, and Geosciences
of the University of Bayreuth

by
Oliver Schmidt

Bayreuth, April 2016

This doctoral thesis was supervised by Prof. Harold L. Drake and prepared at the Department of Ecological Microbiology, University of Bayreuth, from Januar 2010 until April 2016.

This is a full reprint of the dissertation submitted to obtain the academic degree of Doctor of Natural Sciences (Dr. rer. nat.) and approved by the Faculty of Biology, Chemistery and Geosciences of the University of Bayreuth.

Date of submission: 07.04.2016

Date of defence: 14.06.2016

Acting dean: Prof. Dr. Stefan Schuster

Doctoral committee:

Prof. Harold Drake, PHD   (1st reviewer)
Prof. Dr. Ortwin Rabenbauer   (2nd reviewer)
Prof. Dr. Dirk Schüler   (chairman)
Prof. Dr. Egbert Matzner

"Thermodynamics sets the frame, evolution draws the picture."

Barbara Schoepp-Cothenet (2013)

CONTENTS

FIGURES

TABLES

APPENDIX TABLES

EQUATIONS

ABBREVIATIONS

ATP	adenosine triphosphate
BLAST	basic local alignment search tool
cDNA	complementary DNA
CH_4	methane
CO	carbon monoxide
CO_2	carbon dioxide
CsTFA	cesium trifluoroacetate
ddH_2O	deionized double destilled water
ΔG	Gibbs free energy
DNRA	dissimilatory reduction of nitrate to ammonium
EDTA	ethylenediaminetetraacetate
e.g.	for example
ETP	electron transport phosphorylation
Fd	oxidized ferredoxin
Fd^{2-}	reduced ferredoxin
Fdh-H	formate dehydrogenase H of *Escherichia coli*
Fe^{2+}	ferrous iron
Fe^{3+}	ferric iron
FHL	formate hydrogenlyase
FHL-1	formate hydrogenlyase 1 from *E. coli*
FHL-2	formate hydrogenlyase 2 from *E. coli*
g_{DW}	grams of dry weight
g_{FW}	grams of fresh weight
H^+	protons
H_2	molecular hydrogen
HycE	large subunit of the hydrogenase 3 of *E. coli*
HYD3	hydrogenase 3 of *E. coli*
HYD4	hydrogenase 4 of *E. coli*
HyfG	large subunit of the hydrogenase 4 of *E. coli*
i.e.	that is
IPTG	isopropyl-β-D-galactopyranoside
lacZ	gene encoding for β-galactosidase
LB	lysogeny broth
MCS	multiple cloning site
Mn^{4+}	manganese(IV)

N$_2$	dinitrogen
NAD$^+$	oxidized nicotinamide adenine dinucleotide
NADH	reduced nicotinamide adenine dinucleotide
NADP$^+$	oxidized nicotinamide adenine dinucleotide phosphate
NADPH	reduced nicotinamide adenine dinucleotide phosphate
NH$_4^+$	ammonium
O$_2$	molecular oxygen
OTU	operational taxonomic unit
PCR	polymerase chain reation
PCR-H$_2$O	autoclaved and sterile filtered ddH$_2$O
pmf	proton motive force
Rnf	ferredoxin:NAD$^+$-oxidoreductase
S^{2-}	sulfide anion
SIP	stable isotope probing
SLP	substrate level phosphorylation
smf	sodium motive force
X-Gal	5-bromo-4-chloro-3-indolyl-β-D-galactopyranoside

1. INTRODUCTION

Molecular hydrogen (H_2) is a central intermediate during the anaerobic degradation of organic matter in natural (wetlands, limnic or marine sediments, and the digestive tract of ruminants or termites) and anthropogenic (wastewater treatment plants, biogas plants, and landfills) ecosystems that are permanently or temporarily anoxic [60, 307, 398, 475]. In such ecosystems, H_2 metabolizing microbes produce (e.g., primary or secondary fermenters) or consume (e.g., methanogens, acetogens, and sulfate reducers) H_2 as part of their dissimilatory metabolism [398]. In this dissertation, H_2 producing and H_2 consuming processes and associated microbes were investigated in two contrasting natural ecosystems: (i) peatlands that are generally characterized by a relatively limited amount of easily degradable carbon sources, stable anoxic conditions, and low in situ H_2 concentrations [313, 445], and (ii) the gut of earthworms that is a transient anoxic microhabitat in aerated soils, characterized by high concentrations of mucus-derived sugars and high in situ concentrations of H_2 [488].

1.1. Peatlands: sources and sinks for greenhouse gases

Peatlands constitute the single most important type of anoxic terrestrial ecosystem, they cover 400×106 km^2 worldwide (3% of the terrestrial surface on earth), and 90% of the total peatland area is located in subarctic, boreal, and temperate zones of the northern hemisphere (especially in Russia, Scandinavia, and Canada) [56, 139, 313]. Peatland ecosystems are substantial sinks for the greenhouse gas carbon dioxide (CO_2) and store 200-455 Pg carbon (20-30% of the global soil carbon pool) [128, 139, 408]. On the other hand, peatlands emit methane (CH_4; the second most important greenhouse gas after CO_2 [354]) and contribute to up to 7% of the global CH_4 emissions [314, 352, 357]. Thus, peatlands are of extreme importance for the global carbon cycle and effect the global climate. In turn, the sink/source relationship for greenhouse gases in peatlands is effected by global warming, and CO_2 and CH_4 production from the decomposition of accumulated peat are expected to increase alongside with increasing temperatures [79]. However, the effect of the expected temperature increase on the composition of the microbial community, which is the driver of organic matter decomposition in peat soils, is not well understood. Temperature-induced changes of the plant vegetation and the microbial community might alter the biogeochemical pathways that eventually lead to the production of CO_2 and CH_4 [405, 424, 445, 471]. As part of this dissertation, the effect of temperature on H_2 metabolizers, which are of central importance for the anaerobic decomposition of organic matter to CO_2 and CH_4, was studied in the model peatland Fen Schlöppnerbrunnen. Understanding the temperature-dependent process and

community dynamics is crucial for a prediction of the role of peatlands as sources and sinks for greenhouse gases in a future with globally increasing temperatures.

1.1.1.   Formation and classification of peatlands

Wetlands are soil ecosystems that are permanently or at least periodically saturated or covered with water [304, 475]. Peatlands (also called mires [313]), swamps, marshes, and lagoons are examples for natural wetlands whereas rice paddy soils are important man-made wetlands [8, 501]. Limnic and marine sediments are not considered as wetlands as they are no soil ecosystems. Peatlands can be differentiated from other wetlands by the formation and accumulation of peat [139, 313, 475]. Peat forms when the annual primary production exceeds the annual degradation of plant material [54, 136]. The imbalance between production and degradation of organic material is caused by the limited availability of molecular oxygen (O_2) in the water saturated soil (peat typically contains 80-90% water) [313]. The solubility of O_2 in water is relatively low (Table 8) and the diffusion of O_2 from the atmosphere into the pore water of peatlands is slower than the O_2 consumption by microbes [38, 475]. As a result, peatland soils are considered mainly anoxic habitats, and the degradation of organic matter is generally impaired under anoxic compared to oxic conditions [272]. Degradation of organic material in peat is further hindered by a relatively high degree of recalcitrant compounds in peat-forming plants, poor nutrient conditions, low pH, and low temperatures [459, 475].

Peatlands can be differentiated according to shape, source of water, availability of nutrients, pH, and peat soil covering vegetation [138, 313, 475]. However, these factors are often linked and in general peatlands are classified either as fens or bogs. Fens receive water in form of groundwater or catchment surface water in addition to precipitation. The nutrient supply to a fen depends on the mineral nutrient content of the catchment soils. Fens are therefore termed minerotrophic ("fed with mineral-derived nutrients" [427]). The amount of nutrients that are supplied is generally lower when the groundwater is stagnant (i.e., topogenous fens) and higher when the fen is fed by moving groundwater (i.e., soligenous fens). Fens can be classified as eutrophic (nutrient rich), mesotrophic (in-between nutrient rich and nutrient poor), or oligotrophic (nutrient poor) according to the amount of nutrients that are supplied by the groundwater [118]. Bogs are characterized by a thick peat layer that is raised above the local groundwater level [304]. Precipitation is the exclusive source of water and nutrients for the bog peat. Bogs are therefore considered ombrotrophic ("fed by rain" [427]). The amount of nutrients in precipitations vary and may be higher if they originate from urban or marine areas [138, 313]. However, most bogs are oligotrophic (nutrient poor) [313].

1.1.2. Vegetation and its effect on the microbial community in peatlands

Bogs are typically covered with thick lawns of *Sphagnum* mosses [459]. *Sphagnum* mosses have a very high cation exchange capacity allowing them to compete for nutrients in extremely nutrient-poor environments like oligotrophic peatlands [54, 413]. The high cation exchange capacity of *Sphagnum* plant tissue results from high amounts of polyuronic and phenolic acids in the cell wall [319, 459]. These organic acids bind (i) metal ions that are essential for the synthesis of enzymes and (ii) ammonium (NH_4^+) that is an important source of nitrogen [459]. In exchange for cations polyuronic and phenolic acids release protons (H^+) into the pore water and thereby acidify the environment [313]. The organic acids of the cell wall are released and the pH is further lowered during the decomposition of *Sphagnum* biomass. The pH of bogs is typically ≤ 4 as a result of the acidifying activity of living and dead *Sphagnum* biomass [313].

Fens are typically characterized by higher nutrient concentrations and a higher pH (5-7) compared to bogs (1.1.1). The higher nutrient concentrations are a prerequisite for the growth of vascular plants that are not as competitive for nutrients as *Sphagnum* mosses. Different genera (e.g., *Carex*, *Molinia*, *Juncus*, and *Eriophorum*) of the order *Poales* (hereafter termed 'sedges' for simplification [424]) can be commonly found in fens in addition to *Sphagnum* mosses [118, 205, 326]. The biomass of these sedges contains a high degree of polymers (e.g., cellulose and hemicellulose) that are more easily degradable under oxic and anoxic conditions compared to the aromatic compounds present in *Sphagnum* biomass and ligneous plant biomass [71, 201, 305]. Faster degradation of sedge biomass compared to *Sphagnum* biomass is reflected by a smaller fraction of carbohydrate polymers in peat from sites covered with *Carex* than sites covered solely with *Sphagnum* [313, 441]. How the contrasting conditions in fens and bogs effect the microbial community is summarized in Figure 1.

The vegetation effects the microbial community not only by representing the dominant source of dead organic matter in peatlands but also by the excretion of root exudates and by facilitating gas exchange between peat soil and the atmosphere [38, 424]. Root exudates include organic acids (e.g., formate and acetate), sugars, amino acids, phenols, enzymes, and mucilage [206, 448, 464]. Roots deposit easily degradable organics in peat soil either actively [12, 188] or passively by leakage [226]. As a result of the rhizodeposition of organic compounds, the rhizosphere represents a hot spot for microbial activity in peat soils [313]. As a consequence of low O_2 diffusion rates in water, many wetland plants have evolved a porous tissue (called aerenchyma) that connects the root with the stem and leaves [183]. The aerenchyma provides the root cells with O_2 that is necessary for root respiration [38]. Some of the O_2 transported to the roots will leak into the surrounding peat soil providing oxic microzones at close proximity to the roots [422, 424]. This is important for the reoxidation of

reduced terminal electron acceptors (e.g., ferric iron [Fe^{3+}], manganese(IV) [Mn^{4+}], sulfate, and nitrate) and the oxidation of CH_4 by aerobic peat microbes [84, 424, 475]. On the other hand, the aerenchyma in plants facilitates the diffusion of methane formed under anoxic conditions in the peat soil to the atmosphere [38, 424]. Thus, the rhizosphere and associated microbes are important for biogeochemical cycling and the emission of the greenhouse gas CH_4.
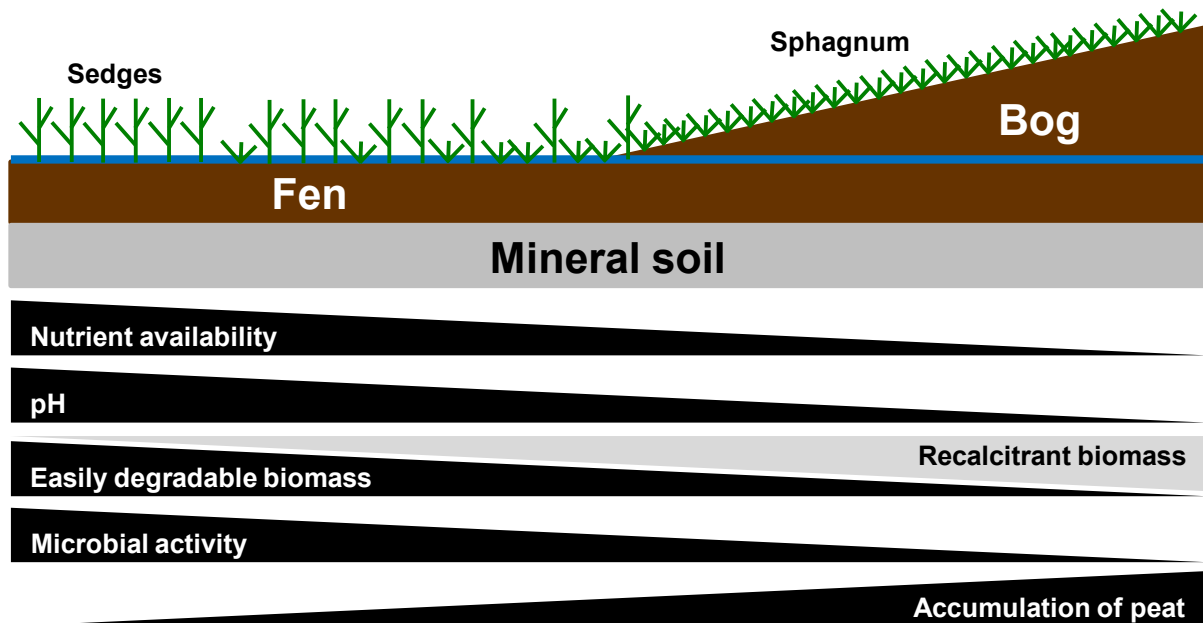
Figure 1   Model of contrasting conditions that effect the microbes in fens and bogs.
Colors: brown, peat; blue, groundwater level.

1.1.3.   Flow of carbon and reductant in peatlands

Photosynthesis by sedges and *Sphagnum* mosses is the single most abundant source of primary production in peatlands [475]. Dead plant material and root exudates are mineralized by aerobic and anaerobic microbes. The plant biomass is heterogenous [441] and cellulose and hemicellulose are more abundant than phenolic polymers when sedges dominate over *Sphagnum* mosses (this is the case in the sampling site of this study; 2.1.1). Exoenzymes excreted by microorganisms catalyze the depolymerization of the insoluble biopolymers of plant-derived organic matter, and soluble oligomers and monomers that can be incorporated by microbial cells are released [90, 299]. Cellulose is more easily degradable than hemicellulose, and phenolic biopolymers like lignin or *Sphagnum* biomass are more recalcitrant [71, 201, 305]. Fungi dominate depolymerization and completely mineralize their substrate under oxic conditions whereas hydrolytic fermenting bacteria dominate depolymerization in the absence of O_2 [17, 241, 267, 475, 479, 480]. Under anoxic conditions, soluble sugars, which are released during depolymerization, and fermentation products, which

are formed by primary and secondary fermenters, are either completely mineralized by anaerobic respiratory processes or are converted to CH_4 and CO_2 by an interwoven food web of syntrophs, acetogens, and methanogens (Figure 2) [100, 282, 494].

Methanogenic processes and the associated methanogenic archaea have been extensively studied in diverse peatlands [168, 176, 178, 212, 289, 290, 445]. However, little is known about the hydrolytic fermenters, which initiate organic matter decomposition, and syntrophs, which convert primary fermentation products to substrates for methanogens (e.g., H_2) [100]. As part of this dissertation, hydrolytic and syntrophic fermentation processes and the associated H_2-metabolizing taxa were studied in the Fen Schlöppnerbrunnen to resolve the drivers of the anaerobic intermediary ecosystem metabolism in this well-studied model peatland. Furthermore, the effect of supplemental formate, which is commonly excreted by roots and is rapidly converted by the fen microbes [178 ,206], on H_2 metabolizers in the rhizosphere of sedges from the Fen Schlöppnerbrunnen was studied.
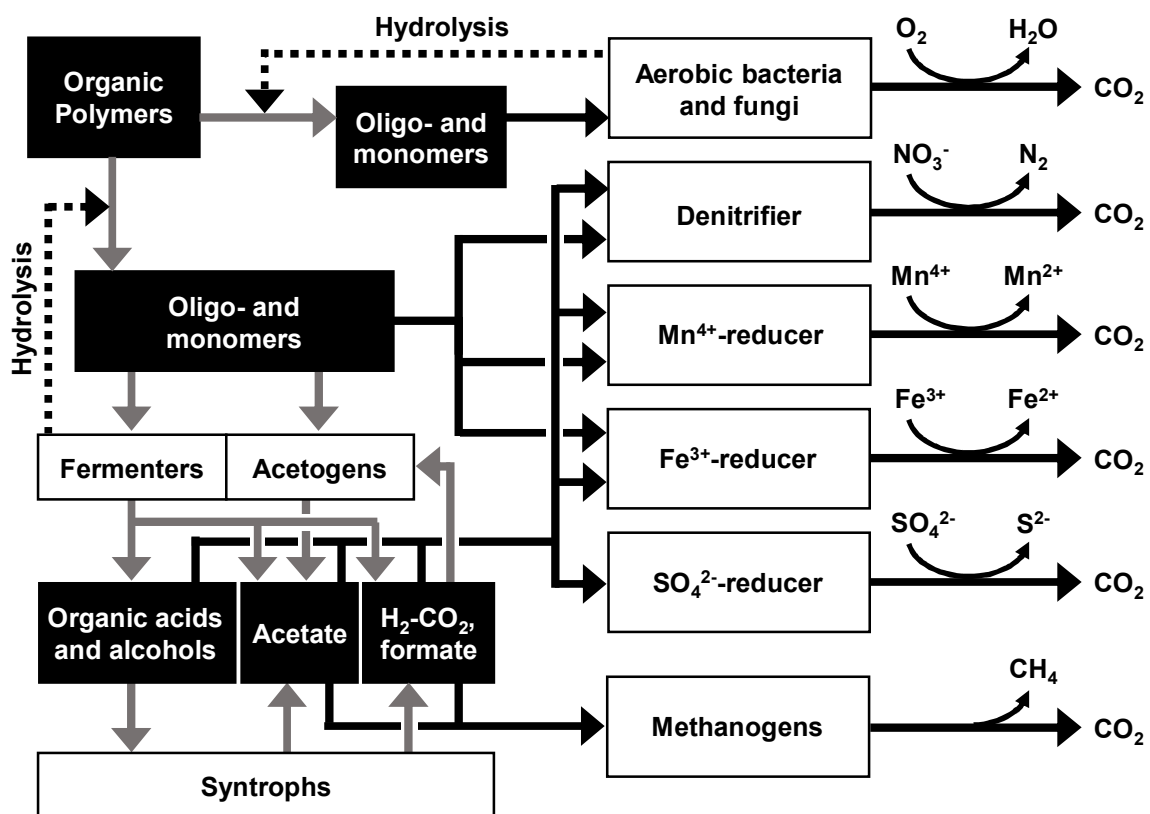
Figure 2   Flow of carbon and reductant during the degradation of organic matter in peatlands. Arrows: dotted, depolymerization of organic polymers (e.g., cellulose) by hydrolytic exoenzymes; grey, intermediary metabolic processes; black, terminal processes that lead to a complete mineralization of organic compounds. Modified from ref [475].

1.2.   Earthworms: engineers that promote soil fertility

In the late 19th century, Charles Darwin already recognized the importance of earthworms as soil engineers that promote soil fertility by their feeding and burrowing activities [78]. Earthworms are a major part of the soil macrofauna and account for up to 90% of the invertebrate biomass in soils [109, 239]. They feed either on mineral soil or the overlying organic litter and contribute significantly to the decomposition of organic matter in soils [35, 36, 74, 109, 239]. Ingested material is mixed with intestinal mucus that is produced in the alimentary canal of earthworms [35, 36]. The excreted materials (i.e., earthworm casts) are characterized by relatively high concentrations of easily degradable organic carbon and macro nutrients compared to the surrounding soil [24, 35, 36, 373, 440]. Earthworms deposit part of their casts in nutrient-poor soil layers and thereby fertilize the soil [35, 36, 109, 274]. As a result of the fertilizing activity of earthworms, plant growth is increased in the presence of earthworms [114, 233]. Most earthworm species form burrows and therefore alter soil structure [109, 239]. Those burrows represent macro-pores that enhance aeration and water absorption capacity in soils and facilitate the growth of plant roots [35, 78, 255, 465]. Earthworms influence the distribution and germination of plant seeds by ingesting and excreting plant seeds [4, 37, 115, 334]. Because of the numerous beneficial effects of earthworms on soil fertility and soil structure, earthworms were termed 'ecosystem engineers' [187, 190, 237].

1.2.1.   Earthworm ecotypes

Earthworms are classified according to their feeding and living habitats into three different ecotypes (also known as feeding guilds): epigeic, endogeic, and anecic earthworms [15, 30]. Epigeic earthworms live in the litter and surface soil, feed predominantly on the organic rich leaf litter, and do not form permanent burrows. *Eudrillus eugeniae* is a typically epigeic earthworm, displays a high casting activity and is used economically for vermicomposting (i.e., the conversion of organic litter into nutrient-rich casts that are used as fertilizers) [131]. Endogeic earthworms (e.g., *Aporrectodea caliginosa*) form primarily horizontal burrows in the upper part of the mineral soil or in the rhizosphere [15, 109]. Their diet is relatively poor in nutrients compared to the organic rich litter that is ingested by epigeic and anecic earthworms. Anecic earthworms (e.g., *Lumbricus terrestris*) form vertical burrows that can reach several meters in depth [109, 239]. They ingest organic litter from the soil surface in addition to mineral soil, and deposit the resulting casts in deeper, nutrient poor layers of the soil, thereby fertilizing it [35, 36, 109, 274]. Living individuals of *L. terrestris* emitted H_2 and high H_2 concentrations were measured in their guts [488]. Therefore, *L. terrestris* was selected here as a model to study processes involved in H_2 production in the gut of earthworms and to identify H_2-metabolizing taxa in this H_2-saturated habitat.

1.2.2.   Digestive system of *Lumbricus terrestris*

The alimentary canal of *L. terrestris* is subdivided in the mouth, pharynx, esophagus, crop, gizzard, intestine (consisting of the foregut, midgut, and hindgut region), and the anus (Figure 3) [32, 423, 438, 476]. The ingested materials (e.g., fungal and prokaryotic cells, plant litter, and soil particles) are homogenized and physically disrupted by grinding in the gizzard, which is made of thick, chitin-containing walls [35, 333, 348, 391, 484]. Intestinal mucus that consists of monomeric, oligomeric, and polymeric sugars as well as glycoproteins is produced by the earthworm especially in the pharynx and the foregut [32, 275, 442]. The mucus is a necessary highly energetic investment for the earthworm that facilitates the transport of the ingested material through the alimentary canal, protects the gut tissue from damage by sharp-edged soil or organic particles, and activates ingested soil microbes [95, 109]. Hydrolysis of organic polymers is supposed to be conducted by exoenzymes (e.g., cellulases, chitinases, lipases, and proteases) that may be excreted by ingested microbes and/or the earthworm [35, 234, 316, 339]. Soluble organics and inorganic nutrients are absorbed by the earthworm primarily at the midgut and hindgut region, and undigested materials are excreted as casts [32, 109]. The average gut passage time of *L. terrestris* is 11 h [490].
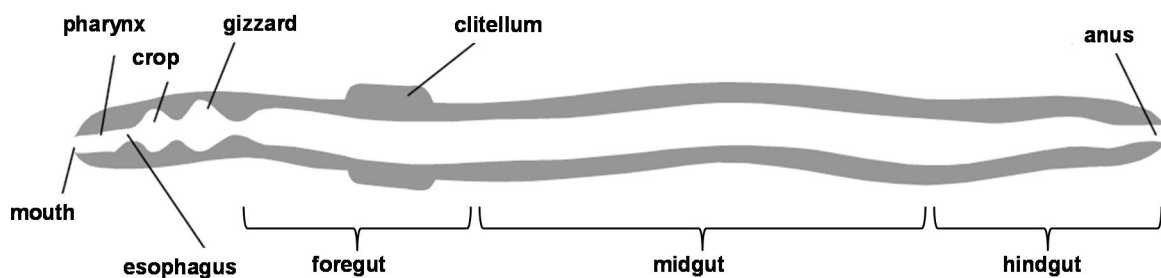
Figure 3   Model of the digestive tract of the earthworm *Lumbricus terrestris*.
Modified from refs [95] and [170].

L. terrestris ingest prokaryotes, fungi, algae, and protozoa that live in the mineral soil or are attached to the plant litter that the earthworm feeds on [36, 74]. The ingested microbes can be essential for the earthworm´s nutrition [27, 36, 110, 295]. Earthworms often prefer soil material rich in microbes like the plant rhizosphere [36, 67, 68, 303, 415, 484]. Large microbial cells may get disrupted by the grinding activity in the gizzard [35, 333, 348, 391, 484]. Energy rich and easily degradable organics (e.g., proteins and nucleic acids) are released when microbial cells get disrupted.   These microbial cell-derived organic polymers may be metabolized alongside with the sugars from the mucus, and plant-derived polymers by ingested and activated fermenting prokaryotes (1.2.3). These fermenters produce soluble organic acids that can be easily absorbed and used as carbon and energy source by the

earthworm [490]. Thus, ingested microbes might serve earthworms a dual purpose as food and feeders.

1.2.3.   Activation of anaerobic soil microbes during gut passage

Culture-dependent and culture-independent studies showed that the earthworm gut microbiota is predominantly transient and derived from the ingested soil, and is not endogenous [109, 113, 130, 167, 170, 404, 489]. The conditions ingested soil microbes experience during gut passage are contrasting to that of the soil. Soil is mainly oxic, relatively dry, often acidic, and poor in easily degradable carbon sources whereas the gut of earthworms is anoxic, has a high water content, neutral pH, and is rich in mucus-derived easily degradable carbon sources [16, 76, 95, 170, 234, 442, 488]. The conditions in the gut are beneficial especially for facultative aerobes and obligate anaerobes. Those prokaryotes that can deal with anoxia are activated during gut passage. As a result of this activation, the culturability of soil microbes can be up to 1,000-fold higher in the gut of earthworms compared to the surrounding soil [41, 95, 181, 192, 193, 325]. The activation of ingested anaerobes by the beneficial conditions in the alimentary canal of earthworms is called the 'priming effect' and might be essential for the live cycle of obligate anaerobes in aerated soils [22, 35]. Thus, the gut of earthworms represents an anoxic microzone that is a hotspot for anaerobic microbial activity [95, 167, 170, 488, 490].

Mucus-derived sugars are probably among the major substrates for ingested fermenters in the gut of *L. terrestris* [490]. As a result of mucus degradation by fermenters, the concentration of sugar equivalents decreases from the crop/gizzard to the hindgut region from 110 mM to less than 10 mM [488]. The fermenters produce high amounts of organic acids, CO_2 and H_2, and the concentrations of organic acids and H_2 is the highest in the midgut region [488]. The earthworm may absorb part of the fermentation products as source of carbon and energy, resulting in a lower concentration of organic acids towards the hindgut region [365, 366, 488]. The earthworm may also reabsorb part of the mucus-derived sugars as part of its nutrition. However, the earthworm needs a positive energy balance to survive and cannot exclusively feed on its own mucus and organic acids that are derived from mucus-fermenting microbes. Organic acids, on which the earthworm could feed on, might also be produced from microbes that ferment plant litter-derived biopolymers or organics derived from disrupted microbial cells that were grinded in the gizzard [35, 74, 316, 339, 442]. This symbiosis between the earthworm that provides a high water content, anoxia, mucus, grinded microbial and plant cells and the ingested microbes that feed the earthworm (e.g., with organic acids, amino acids, and nucleotides) is called the mutualistic digestive system of the earthworm [16, 35, 236, 442].

1.3. Microbes involved in the anaerobic degradation of organic matter in peat and the gut of earthworms

1.3.1. Primary fermenters

Fermentation is an anaerobic chemoorganoheterotrophic metabolism that is widespread among the three domains of life (*Eukarya*, *Bacteria*, *Archaea*), is catalyzed by facultative aerobes (e.g., *Enterobacteriaceae*) and obligate anaerobes (e.g., *Clostridiaceae*), and is not restricted to anoxic conditions [26]. Fermenters disproportionate energy-rich organic carbon compounds (e.g., glucose), do not need external electron acceptors, and conserve energy in the form of ATP primarily by substrate level phosphorylation (SLP) [215, 432]. Substrates for primary fermentations are sugars (e.g., from polymeric carbohydrates), amino acids (from proteins), and glycerol (from lipids) (Table 1). H_2 is a major fermentation product of primary fermentations [398]. Other important fermentation products include organic acids (e.g., acetate, formate, lactate, succinate, butyrate, and propionate), alcohols (e.g., ethanol), and CO_2 (Table 1).

Table 1   **Examples for primary fermentations**

Fermentation	Substrates → Products[a]	Organism	Ref
Mixed acid	glucose → ethanol + succinate + lactate + acetate + formate + H_2 + CO_2	*Escherichia coli*	[301]
Butyric acid	glucose → butyrate + acetate + H_2 + CO_2	*Clostridium saccharobutylicum*	[75]
Propionic acid	glucose → propionate + acetate + CO_2	*Propionibacterium*	[75]
Glutamate	glutamate → acetate + butyrate + NH_4^+ + H_2 + CO_2	*Clostridium tetanomorphum*	[14]
Glycerol	glycerol → ethanol + H_2 + CO_2	*Escherichia coli*	[91]

[a]Stoichiometries of fermentation reactions are not balanced.

Primary fermenters are confronted with a deficiency of their substrates as a result of slow rates of biopolymer hydrolysis in peatlands [208]. However, primary fermenters have a high metabolic capacity in peatlands and develop rapidly when easily degradable carbohydrates, free sugars, or peptides are supplemented [151, 176, 212, 487]. H_2 is one of the major fermentation products but only accumulates to high concentrations in peat soil when easily degradable carbon sources are supplemented [151, 176, 212, 487].

In contrast to the substrate deficiency for primary fermenters in peatlands, easily degradable carbon sources are readily available in the gut of earthworms [95, 488]. These carbon sources fuel distinct fermentation processes that are supposed to occur spatially and consequently in temporal sequence along the alimentary canal of the earthworm [366, 488]. This cascade of fermentations is probably related with the contrasting O_2-tolerance of the

different fermenters: Lactic acid fermentation and propionic acid fermentation are commonly performed by aerotolerant anaerobes [59, 397] and occurred in the crop/gizzard and foregut region; mixed acid fermentation is performed by facultative aerobic *Enterobacteriaceae* [490] and occurred in the foregut, midgut, and hindgut region; butyrate fermentation performed by O_2-sensitive *Clostridia* [490] occurred predominantly in the midgut and hindgut region [488]. H_2 is a stable end product of the fermentation processes in the gut of earthworms and is emitted by *Lumbricus terrestris* [192, 488, 490].

1.3.2. Secondary and syntrophic fermenters

Secondary fermenters use primary fermentation products like succinate, lactate, ethanol, butyrate, and propionate to grow on (Table 1). Succinate, lactate, and ethanol are relatively energy rich substrates and can be fermented by pure cultures of secondary fermenters [378, 377]. Other secondary fermenters (e.g., those that oxidize propionate or butyrate) perform a metabolism that is endergonic under standard conditions (Table 1). Those fermenters form symbiotic metabolic cooperations with partner organism (e.g., methanogens, sulfate reducer, or acetogens) that keep the pool size of the shuttling intermediate low, which is necessary to overcome the thermodynamic constraints of the secondary fermenter [376]. This symbiotic relationship is called syntrophy and the secondary fermenters of such cooperations are called syntrophic fermenters or just syntrophs [284, 376, 379]. Methanogens that cannot utilize ethanol, butyrate or propionate by themselves are considered as dominant partners of syntrophic fermenters in peatlands whereas sulfate reducer dominate in habitats with sufficient supply of sulfate (e.g., marine sediments) [100, 379]. H_2 and formate are the most important shuttling intermediates that are formed by the syntrophs. These intermediates are effectively scavenged by the partner organism to maintain exergonic conditions for the syntroph. This process of electron shuttling between syntrophs and their partner organisms is called interspecies transfer of H_2 or formate [29, 108]. Effective scavenging of acetate in addition to that of H_2 or formate is also beneficial especially for the syntrophic degradation of propionate and benzoate [95, 129, 469].

In the gut of earthworms, secondary fermenters are supposed to convert succinate and lactate according to reactions 1 and 2 in Table 2, respectively [395, 488]. Secondary fermenters might also use ethanol that is produced during mixed acid fermentation and was formed in glucose-supplemented gut contents [490]. However, syntrophic secondary fermentations are unlikely to occur since the high concentrations of H_2, formate, and acetate render them thermodynamically impossible in the gut of earthworms. Furthermore, a gut passage time of approximately half a day [153, 490] is just too short for the development of syntrophic consortia, a process that needs stable anoxic conditions [376].

Peatlands are characterized by relatively stable anoxic conditions [475], and the limited availability of easily degradable carbon sources circumvents H_2 or formate accumulation to concentrations that are thermodynamically unfavorable for syntrophs on the long run [208]. Because of these beneficial conditions, syntrophs are supposed to be the dominant sink for ethanol, butyrate, and propionate, and a major source of methanogenic substrates (H_2, formate, and acetate) in peatlands [100, 168, 289, 290, 445].

Table 2   Examples for secondary fermentations

No.	Reaction	$\Delta G^{0'}$ ($kJ \cdot mol^{-1}$)	Organism	Ref
Non-syntrophic secondary fermenters				
1	succinate + $H_2O \rightarrow$ propionate + HCO_3^-	-20.6	*Propionigenium modestum*	[378]
2	3 lactate $\rightarrow$ 2 propionate + acetate + HCO_3^- + H^+	-165.0	*Pelobacter propionicus*	[377]
3	3 ethanol + 2 $CO_2 \rightarrow$ 2 propionate + acetate + 3 H^+ + H_2O	-114.6	*Pelobacter propionicus*	[377]
Syntrophic secondary fermenters[a]				
4	butyrate + 2 $H_2O \rightarrow$ 2 acetate + 2 H^+ + 2 H_2	+48.2	*Syntrophomonas wolfei*	[376]
5	propionate + 2 $H_2O \rightarrow$ acetate + CO_2 + 3 H_2	+71.7	*Syntrophobacter wolinii*	[376]
6	2 propionate + 2 $H_2O \rightarrow$ 3 acetate + 1 H^+ + 2 H_2	+48.3	*Smithella propionica*	[82]
7	formate + $H^+ \rightarrow H_2$ + CO_2	-3.4	*Desulfovibrio* sp. G11	[94]
8	ethanol + $H_2O \rightarrow$ acetate + H^+ + 2 H_2	+9.6	*Pelobacter carbinolicus*	[376]
9	benzoate + 6 $H_2O \rightarrow$ 3 acetate + CO_2 + 2 H^+ + 3 H_2	+49.5	*Syntrophus aciditrophicus*	[376]

[a]Formate might be used instead of H_2 for the interspecies transfer of electrons.

1.3.3.   Methanogens

Methanogens are a phylogenetically diverse group of strictly anaerobic *Euryarchaeota* that grow on a narrow range of substrates (most importantly H_2-CO_2, formate, acetate, methanol, and methylamines) and form methane as a reduced end product [434]. Globally, methanogens form 1 giga ton of methane per year, which approximates 2% of the net CO_2 that is fixed into biomass by photosynthesis [431, 434]. Methanogenesis is the terminal step of anaerobic organic matter mineralization when electron acceptors others than CO_2 are absent [60, 100, 475]. Biochemically, two major groups of methanogens that are characterized by ecologically relevant differences in their energy metabolism can be differentiated: methanogens with and without cytochromes [434]. Methanogens without cytochromes (*Methanopyrales*,

Methanococcales, *Methanobacteriales*, and *Methanomicrobiales*) are more ancient, with few exceptions grow exclusively on H_2-CO_2 or formate, and have relatively low growth yields and ATP gains; methanogens with cytochromes (*Methanosarcinales*) have a relatively broad substrate spectrum (e.g., H_2-CO_2, acetate, methanol, methylamines, carbon monoxide [CO]), cannot grow on formate, and have relatively high growth yields and ATP gains [434]. Because of the higher ATP gains, methanogens with cytochromes require more negative ΔG values compared to methanogens without cytochromes when they are growing on the same substrate [434]. As an example, *Methanosarcina barkeri* (+ cytochromes) conserves ~1.5 mol ATP per mol CH_4 formed from H_2-CO_2 whereas *Methanothermobacter marburgiensis* (- cytochromes) conserves ~0.5 mol of ATP per mol CH_4 formed from H_2-CO_2 [434]. The ecological relevance of the biochemical differences is that *Methanosarcina* has much higher H_2 thresholds (i.e., the minimal H_2 concentration that is required to conserve energy) compared to methanogens without cytochromes [194]. In a balanced system, in which methanogenic syntrophy is not the rate limiting step of organic matter degradation, H_2 steady state concentrations are usually low and therefore *Methanosarcina* will be outcompeted by methanogens without cytochromes whereas *Methanosarcina* outgrows methanogens without cytochromes under H_2-rich conditions [499]. *Methanocella* that has cytochromes is an exception because it uses a metabolic pathway similar to that of methanogens without cytochromes and therefore is able to grow on very low H_2 concentrations [434]. Interestingly, *Methanocella* is also able to convert formate indicating that the capability of using formate is linked to the thermodynamic constraints of the metabolic pathway of a methanogen [434].

Table 3   Methanogenic reactions (modified after ref [499])

No.	Reaction	$\Delta G^{0\prime}$ (kJ·mol^{-1})	Organism
1	$4\ H_2 + CO_2 \rightarrow CH_4 + 2\ H_2O$	-131	Most methanogens
2	$4\ formate + H^+ + H_2O \rightarrow CH_4 + 3\ HCO_3^-$	-145	Many methanogens without cytochromes[a]
3	$4\ CO + 5\ H_2O \rightarrow CH_4 + 3\ HCO_3^- + 3\ H^+$	-196	*Methanobacterium* and *Methanosarcina*
4	$acetate + H^+ \rightarrow CH_4 + CO_2$	-36	*Methanosarcina* and *Methanosaeta*
5	$1\frac{1}{3}\ methanol \rightarrow CH_4 + \frac{1}{3}\ HCO_3^- + \frac{1}{3}\ H_2O + \frac{1}{3}\ H^+$	-105	Many methanogens with cytochromes
6	$1\frac{1}{3}\ methylamine + 2\ H_2O \rightarrow CH_4 + \frac{1}{3}\ CO_2 + 1\frac{1}{3}\ NH_3$	-77	Many methanogens with cytochromes
7	$methanol + H_2 \rightarrow CH_4 + H_2O$	-113	Few methanogens without and many with cytochromes

[a]*Methanocella* has cytochromes but can use formate [434].

A similar competition for low substrate concentrations between methanogens is known for *Methanosaeta* and *Methanosarcina* when growing solely on acetate. Both genera have evolved different mechanisms for acetate activation that result in a higher ATP gain for *Methanosarcina* (~0.5 mol ATP per mol acetate consumed) compared to *Methanosaeta* (~0.3 mol ATP) [184, 411]. The lower ATP gain allows *Methanosaeta* to grow on low steady state concentrations of acetate that are not thermodynamically favorable for *Methanosarcina* [184]. As a result of the lower acetate threshold, *Methanosaeta* outcompetes *Methanosarcina* for acetate in acetate-limited environments whereas *Methanosarcina* outgrows *Methanosaeta* on acetate-rich conditions [184]. In general, *Methanosarcina* is more of a generalist that can adapt to changing substrate availabilities whereas Methanosaeta and methanogens without cytochromes are specialists for the usage of acetate and H_2-CO_2, respectively [184, 434, 499].

Despite the fact that the gut of earthworms provides an ideal transient habitat for ingested methanogens (anoxia, high concentrations of H_2 and acetate, high water content, near nutria pH), methanogenesis is generally considered as metabolically insignificant in the gut of earthworms [95]. This assumption is based on the observation that methane was neither emitted by living individuals nor formed from gut homogenates of different earthworm species [166, 192, 428, 488]. Recently, CH_4 emissions by living individuals and CH_4 production in gut homogenates were observed for the epigeic earthworm *Eudrilus eugeniae* that was fed on composted cow manure, which was probably rich in active methanogens [89, 395]. Thus, methane emission by earthworms seems to be depend on the number of active methanogens in the substrate. *Lumbricus terrestris*, the model organism used here, feeds on aerated soil and the organic litter layer on the surface of the soil [95] and normally it might not take up a significant number of methanogens.

In peatlands, methanogenesis is generally assumed to be the major terminal process in the complete mineralization of organic matter, and numerous studies from different peatlands have analyzed methanogenic processes and/or the associated archaeal taxa [168, 176, 178, 212, 289, 290, 445]. However, other redox processes might co-occur or even dominate over methanogenesis when electron acceptors other than CO_2 are frequently available [105, 249]. Theoretically, aceticlastic and hydrogenotrophic methanogenesis should make up 67% and 33% of the total CH_4 formed during anaerobic degradation of carbohydrate polymers like cellulose [60]. However, if acetogens are involved in sugar degradation or compete successfully with methanogens for H_2 (this can be observed especially at low temperatures) than the contribution of aceticlastic methanogenesis increases [60, 61, 208, 210]. On the other hand, the contribution of hydrogenotrophic methanogenesis increases when acetate is syntrophically oxidized to H_2 and CO_2 or if there are additional sinks for acetate [60, 72, 168, 189, 228].

1.3.4.   Acetogens

Acetogens are a phylogenetically diverse group of strictly anaerobic bacteria that are able to reduce CO_2 to acetate during dissimilation using the acetyl-CoA pathway [96, 101, 102, 103, 253, 483]. These bacteria can oxidize various substrates to gain electrons for the reduction of CO_2 to acetate (Table 4) [96, 97, 375]. Dependent on the growth conditions, acetogens form lactate, ethanol, and succinate in addition to acetate, and should therefore not be called 'homoacetogens' [222, 298]. Acetogens are not restricted to a dissimilatory metabolism based on the acetyl-CoA pathway, and are capable of using alternative electron acceptors others than CO_2 (e.g., fumarate, nitrate, nitrite, and thiosulfate) [102]. Acetogens are also able to reverse the formation of acetate from H_2 and CO_2 (Reaction 1 in Table 4) if thermodynamically feasible. This process is called syntrophic anaerobic acetate oxidation, requires low H_2 concentrations, and is favored especially at elevated temperatures (e.g., thermophilic anaerobic bioreactor) [500]. Acetogens have evolved several strategies to cope with O_2 and can be frequently found in habitats that are not permanently anoxic [140, 141, 175, 220, 221, 222, 224, 329, 463]. The metabolic versatility and O_2 tolerance of acetogens allows them to adapt quickly to changing environmental conditions, and explains why acetogens can persist in ecosystem, in which they are outcompeted for single substrates by specialists (e.g., methanogens without cytochromes outcompete acetogens under H_2 limitation) [98, 102].

Acetogens, like methanogens, are considered metabolically not significant in the gut of earthworms despite the fact that the conditions in the gut are highly beneficial for them [192, 488]. However, H_2 stimulated the production of acetate when gut homogenates from the earthworm *Eudrilus eugeniae* were incubated for 14 d (an incubation time that is far longer than the gut passage time of 6 h [279]), and 16S rRNA sequences related to the acetogen *Clostridium glycolicum* (phylogenetically belongs to the *Peptostreptococcaceae*) were enriched in gut homogenates of *Lumbricus terrestris* and *E. eugeniae* when supplemented with glucose and incubated anoxically for 51 h and 24 h, respectively [395, 490]. Thus, acetogens, in addition to primary and secondary fermenters, might contribute to the production of acetate in the gut of earthworms.

The contribution of acetogens to the degradation of organic matter in peatlands is not well resolved and is probably highly variable on a temporal and regional (or local) scale. However, the metabolic flexibility [102] and an increasing competitiveness of hydrogenotrophic acetogenesis (i.e., acetogenesis from H_2-CO_2) versus hydrogenotrophic methanogenesis with decreasing temperatures [61, 208, 210,] suggest that acetogens are crucial for the anaerobic mineralization in peatlands and other cold ecosystems [317]. Acetogenesis was stimulated by supplemental H_2 and formate in soil slurries of the Fen Schlöppnerbrunnen indicating the potential of fen acetogens to convert both substrates [178, 487]. However, the contribution of

acetogens to the flow of reductant and carbon in unsupplemented soil slurries of the fen remains unclear.

Table 4   **Examples for acetogenic reactions**

No.	Reaction	$\Delta G^{0\prime}$ $(kJ \cdot mol^{-1})$	Ref
1	$4\,H_2 + 2\,CO_2 \rightarrow$ acetate $+ H^+ + H_2O$	-95	[96]
2	4 formate $+ 3\,H^+ \rightarrow$ acetate $+ 2\,CO_2 + 2\,H_2O$	-109	[96]
3	$1\frac{1}{3}$ methanol $+ \frac{2}{3}\,CO_2 \rightarrow$ acetate $+ H^+ + \frac{2}{3}\,H_2O$	-71	[96]
4	$\frac{2}{3}$ ethanol $+ \frac{2}{3}\,CO_2 \rightarrow$ acetate $+ H^+$	-25	[96]
5	$\frac{2}{3}$ lactate $\rightarrow$ acetate $+ \frac{1}{3}\,H^+$	-38	[243]
6	$\frac{1}{3}$ glucose $\rightarrow$ acetate $+ H^+$	-104	[96]
7[a]	$1\frac{1}{3}$ uric acid $+ 7\frac{1}{3}\,H_2O + 4\frac{1}{3}\,H^+ \rightarrow$ acetate $+ 4\frac{2}{3}\,CO_2 + 5\frac{1}{3}\,NH_4^+$	-192	[467]

[a]The glycine and the glycine-serine-pyruvate pathway are involved in the degradation of purines rather than the classical acetyl-CoA pathway [155, 467].

1.3.5.   Alternative anaerobic respiratory processes

Under anoxic conditions, facultative aerobes and obligate anaerobes can couple the mineralization of organic matter with several alternative electron acceptors others than CO_2 (Figure 2). In the Fen Schlöppnerbrunnen, nitrate, sulfate, and Fe^{3+} are important alternative electron acceptors that are constantly supplied at low concentrations with the catchment water and by rain [5, 326, 487]. Alternative electron acceptors are generally assumed to underlay a sequential reduction chain in which electron acceptors with a higher redox potential are consumed first: O_2 (used first) > nitrate > Fe^{3+} > sulfate > CO_2 (used last) [495]. However, several studies indicate that different reduction processes co-occur in the Fen Schlöppnerbrunnen [5, 205, 326]. Fe^{3+}-reduction, sulfate reduction, and denitrification are important processes that contribute to anaerobic organic matter mineralization in the fen [219, 257, 321, 327, 328, 350, 351, 382]. The fen denitrifiers have a high affinity for nitrate and cause a constant depletion of the nitrogen pool in the peat, thereby affecting the whole microbial community as well as the peat soil covering plant vegetation [321, 326, 328]. Supplemental H_2 stimulated Fe^{3+}-reduction and denitrification but not sulfate reduction in peat soil slurries of the fen indicating that some but not all of the alternative anaerobic respiratory processes might function as H_2-sinks in situ [350, 384].

Denitrification and Fe^{3+}-reduction are anaerobic respiratory processes that occur in the gut of earthworms [87, 88, 99, 169, 170, 181, 193, 488, 489]. Aerated soils can harbor high amounts of Fe^{3+} [372], which can serve ingested soil microbes as electron acceptor in the gut of earthworms. High concentrations of ferrous iron (Fe^{2+}) in the crop/gizzard of the earthworm *Lumbricus terrestris* indicate that Fe^{3+}-reduction occurs during the initial ingestion phase [488].

Denitrifiers are active especially in the crop/gizzard and hindgut region of *L. terrestris*, and different living earthworms emit N_2O and/or N_2 [87, 88, 169, 181, 193, 488, 489]. Thus, denitrifiers in the gut of earthworms contribute to the emission of the greenhouse gas N_2O and the depletion of nitrogen sources in soils [99, 258]. Certain denitrifiers and Fe^{3+}-reducers can use H_2 as a source of reductant [256, 410] but it is not yet resolved whether or not denitrifiers or Fe^{3+}-reducers convert H_2 produced during fermentation in the gut of earthworms.

1.3.6.   Aerobic processes

The significant contribution of Fe^{3+}- and sulfate reduction to the mineralization of organic matter (1.3.5) is eventually linked to the high reoxidation potential of these electron acceptors in the Fen Schlöppnerbrunnen [219, 328, 351]. The prerequisite for the biotic or abiotic oxidation of Fe^{2+} and reduced sulfur compounds is the availability of O_2. However, the presence of O_2 in peatland soils is commonly restricted to the uppermost cm of the soil, and the diffusion of O_2 into deeper soil layers is impaired in water-saturated soils [197, 198]. Strong rain events can saturate the fen with fresh oxygenated water deep into the peat soil [326]. Seasonal droughts can cause a lowering of the groundwater table and thus enhance O_2 diffusion into the peat soil, which results in a high contribution of aerobic degradation processes to the annual organic matter mineralization [105, 225]. The Fen Schlöppnerbrunnen is completely overgrown with sedges that are known to facilitate diffusion of O_2 to the rhizosphere in which electron acceptors are recycled and CH_4 is oxidized (1.1.2) [38, 326, 422]. Steep O_2-gradients exist at the oxic-anoxic interface and the microbes that inhabit the surface soil and rhizosphere in peatlands like the Fen Schlöppnerbrunnen have to cope with changing redox conditions [5, 38, 326, 479]. In summary, anoxic conditions in peatlands are not always stable, and temporarily available O_2 is used for (i) the reoxidation of terminal electron acceptors, (ii) aerobic organic matter mineralization, and (iii) the oxidation of CH_4.

The digestive tract of earthworms is free of O_2 right from the beginning (i.e., the crop/gizzard) [488]. Thus, O_2 does not effect the microbial activity in the gut but the earthworm itself and the active anaerobes in the gut effect aerobic processes in the soil. Fresh casts (<24 h old) that are excreted by the earthworm have a higher water content and a higher concentration of soluble organic carbon compared to the bulk soil [35]. Under those beneficial conditions aerobic microbes in and around casts are activated, multiply, and contribute to the breakdown of plant polymers that could not be digested during the short anoxic gut passage [35]. High amounts of H_2 are formed by H_2-evolving fermenters in the gut of earthworms [395, 488, 490]. This H_2 is partially emitted by the earthworm, which constitutes a mobile source of reductant for H_2-oxidizing aerobes (knallgas bacteria) in the soil [7, 488].

1.4. Hydrogenases and their contribution to the energy metabolism of H₂ producers and H₂ consumers

Hydrogenases catalyze the reversible reduction of protons to H_2 ($2H^+ + 2e^- \leftrightarrow H_2$) and are the central enzymes of H_2 metabolizers [398, 461]. Three groups of hydrogenases are distinguished according to their active sites in the catalytical subunit: [Fe]-, [FeFe]-, and [NiFe]-hydrogenases [430, 460, 461]. [Fe]-hydrogenases are present in some methanogens, are expressed under Ni-limited conditions, and catalyze the reversible reduction of methenyl-tetrahydromethanopterin to methylene-tetrahydromethanopterin [430]. Most presently known hydrogenases belong either to the [FeFe]- or [NiFe]-hydrogenases [460, 461]. [NiFe]-hydrogenases are widely spread among bacteria and archaea and are divided into five subgroups: group 1, periplasmic respiratory uptake hydrogenases; group 2, cyanobacterial uptake hydrogenases and H_2-sensors; group 3, cytoplasmic bidirectional heteromultimeric hydrogenases; group 4, energy-converting (ion-translocating), membrane-associated cytoplasmic hydrogenases; group 5, high-affinity uptake hydrogenases [66, 461]. [FeFe]-hydrogenases are found in phylogenetically diverse bacteria, in chloroplasts and hydrogenosomes of lower eukaryotes, and potentially also in anaerobic CH_4-oxidizing archaea [171, 172, 461].

In this study, PCR primers specific for [FeFe]-, group 1, and group 4 [NiFe]-hydrogenases were designed and therefore these groups are introduced in detail below and their physiological functions are summarized in Table 5. Group 1 [NiFe]-hydrogenases can be found in respiratory H_2 oxidizers like knallgas bacteria, fumarate reducers, denitrifiers, Fe^{3+}-reducers, sulfate reducers, and methanogens [461]. These hydrogenases catalyze H_2-oxidation in the periplasm and transfer the electrons via a membrane-integral cytochrome subunit to the quinone pool of the membrane (Figure 4A). This process is linked to the generation of a proton or sodium motive force (pmf or smf) which can be used to fuel ATP synthesis [227, 461]. Group 4 [NiFe]-hydrogenases are H^+- (or sodium ion-) translocating enzymes that are associated to the cytoplasmic site of the membrane in methanogens, acetogens, carboxydotrophs, and fermenters [158, 291, 368, 393, 412, 450]. The direction of H^+-translocation depends on the thermodynamics of the process to which H_2 production/consumption is linked: For example, the methanogen *Methanosarcina barkeri* couples the reoxidation of reduced ferredoxin ($Fd^{2)-}$ and the production of H_2 to the build up of a pmf during growth on acetate whereas it has to consume part of the pmf (generated by other reactions) to reduce oxidized ferredoxin (Fd) during growth on H_2 (Figure 4B) [158, 434].

[FeFe]-hydrogenases are predominantly cytoplasmic and their relation to the energy metabolism of the host microbes is mostly indirect, which is in contrast to group 1 and 4 [NiFe]-hydrogenases that are directly coupled to the generation of a pmf [393, 461]. Some [FeFe]-

Table 5   Physiological function of hydrogenases[a]

Class	Physiological function[b]	Organism
H₂ evolution[c]		
[FeFe]	Bifurcating; reoxidation of Fd^{2-} and NADH during fermentation; allows for enhanced ATP_{SLP} generation during acetate formation	*Thermotoga maritima* [396]
[FeFe]	Reoxidation of Fd^{2-} during fermentation; NADH has to be reoxidized during formation of butyrate, lactate, ethanol, or succinate which maybe coupled to ATP_{SLP} and/or ATP_{ETP}	*Clostridium pasteurianum* [42]
[FeFe]	Part of FHL; oxidation of formate derived from fermentation or exogenous sources; potentially coupled to ATP_{ETP}	*Eubacterium acid-aminophilum* [142]
[NiFe] 4	Part of FHL; oxidation of formate derived from fermentation or exogenous sources; potentially coupled to ATP_{ETP}	*Escherichia coli* [443]
[NiFe] 4	Reoxidation of Fd^{2-} during fermentation; coupled to ATP_{ETP}; allows for additional ATP_{SLP} and ATP_{ETP} during butyrate formation	*Pseudobutyvibrio ruminis* [147]
[NiFe] 4	Reoxidation of Fd^{2-} during acetogenesis and aceticlastic methanogenesis; coupled to ATP_{ETP}	*Moorella thermoacetica* [393]
[NiFe] 4	Oxidation of CO; coupled to ATP_{ETP}	*Rhodospirillum rubrum* [158]
H₂ uptake[c]		
[FeFe]	$NADP^+$ reducing; recycling of H₂ (e.g., formed from nitrogenase) or providing NADPH for acetogenesis	*Moorella thermoacetica* [393]
[FeFe]	Bifurcating; reduces Fd and NAD^+ for acetogenesis; coupled to ATP_{ETP} via the Rnf complex	*Clostridium ljungdahlii* [393]
[FeFe]	Part of FHL; reduces CO_2 to formate during acetogenesis	*Acetobacterium woodii* [335]
[NiFe] 4	Fd reducing; needed for activation of CO_2 during methanogenesis; coupled to pmf consumption	*Methanosarcina barkeri* [434]
[NiFe] 1	Contains a cytochrome subunit; reduces the quinone pool of respiratory H₂ oxidizers	*Wolinella succinogenes* [461]

[a]Only classes of hydrogenases to which PCR primers were designed in this study are listed.

[b]Abbreviations: $ATP_{SLP/ETP}$, Adenosine triphosphate generated via substrate level phosphorylation / electron transport phosphorylation; FHL, formate hydrogenlyase; $NADP^+$/NADPH, oxidized/reduced nicotineamide adenine dinucleotide phosphate; Rnf, ferredoxin:NAD^+-oxidoreductase.

[c]Hydrogenases are principially reversible and might in vivo function in both directions dependent on the actual concentrations of H₂, formate, and reduced/oxidized electron carriers.

hydrogenases are electron bifurcating and can use Fd/Fd^{2-} and oxidized/reduced nicotinamide adenine dinucleotide (NAD^+/NADH) simultaneously to consume/produce H₂ [393, 396]. H₂ production with a bifurcating [FeFe]-hydrogenase is thermodynamically feasible only at decreased H₂ concentrations and enables the fermenter to generate up to 4 mol ATP_{SLP} from the conversion of acetyl-CoA to acetate during glucose fermentation [396]. At high H₂ concentrations, non bifurcating [FeFe]-hydrogenases can be used to reoxidize Fd^{2-} [42]. The loss in ATP_{SLP} that is associated with the use of a non bifurcating hydrogenase may be compensated partially by additional ATP_{ETP} derived from the formation of reduced fermentation products (e.g. butyrate) [147]. In acetogens, the H₂ uptake can be performed by bifurcating or
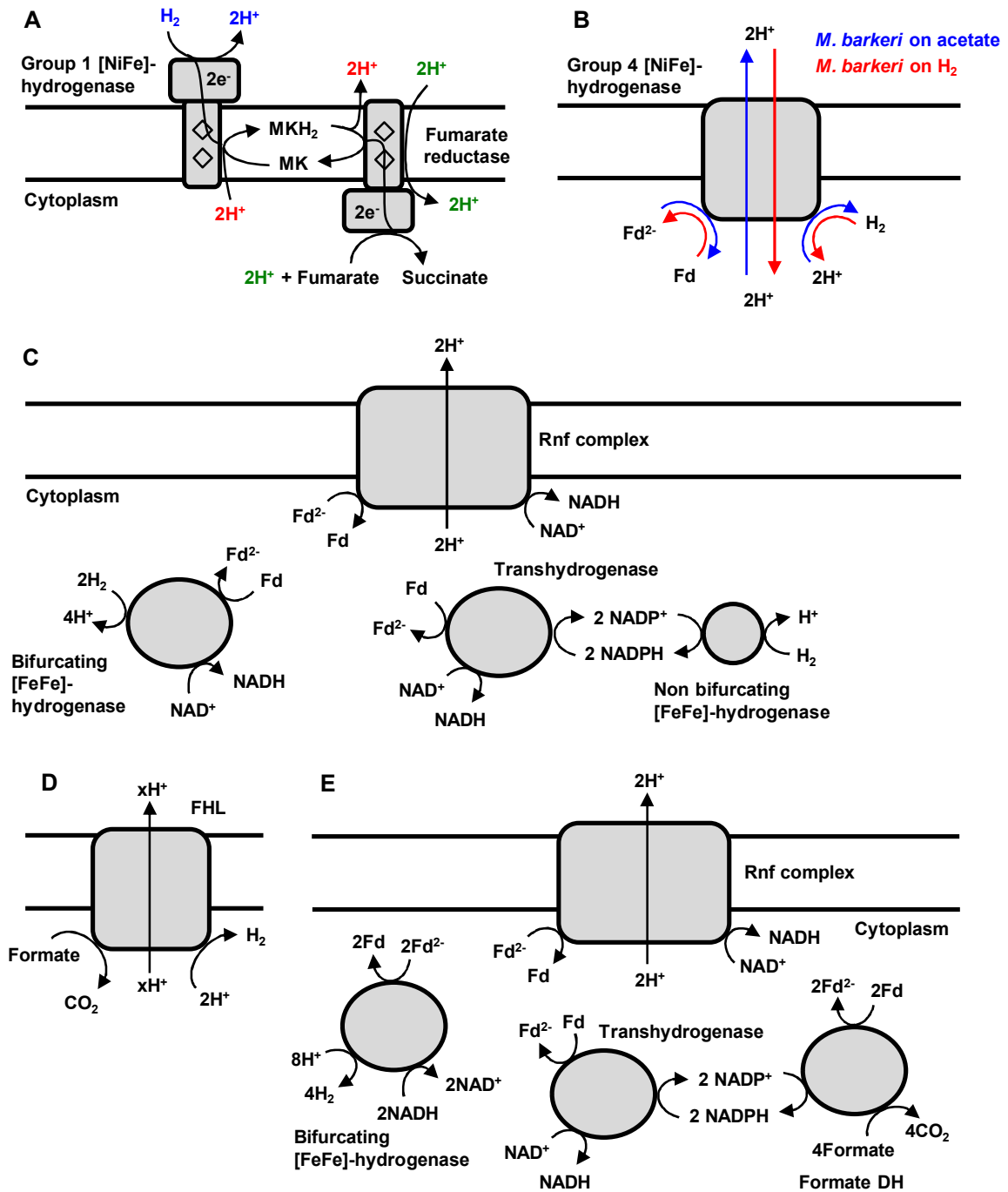
Figure 4   Contribution of different hydrogenases to the generation of a pmf in H_2 metabolizers.
A: H^+ and e^- transfer during fumarate respiration by *Wolinella succinogenes*. Diamonds represent cytochromes. Blue, H^+ released during H_2 oxidation; red, H^+ translocated during menaquinone (MK) reduction and menaquinol (MKH_2) oxidation; green, H^+ that are translocated to compensate the H^+ that are bound during fumarate reduction. B: Activity of the H^+-translocating hydrogenase of *Methanosarcina barkeri* during growth on acetate (blue) and H_2 (red). C: H^+ translocation during Fd^{2-} oxidation by the Rnf complex. Fd^{2-} is provided by a bifurcating hydrogenase (left) or by the combined activity of a $NADP^+$-reducing hydrogenase and a transhydrogenase (right). D: Group 4 [NiFe]-hydrogenase containing FHL complex of *Escherichia coli*. E: Proposed H^+ translocation during formate oxidation and H_2 production by the combined activity of a formate dehydrogenase (DH), a transhydrogenase, a Rnf complex, and a bifurcating hydrogenase. Models were modified after refs [40, 158, 227, 393, 443, 466].

non bifurcating [FeFe]-hydrogenases, and the build up of a pmf (or smf) is linked to the H^+ or Na^+ translocating Rnf complex and a bifurcating transhydrogenase (Figure 4C) [393].

Group 4 [NiFe]- or [FeFe]-hydrogenases together with formate dehydrogenases can form FHL complexes (FHL; Figure 4D and E) [142, 335, 443]. Microbes that harbor such a FHL complex are hereafter referred to as FHL-containing taxa [178]. The FHL complex catalyzes the conversion of formate into H_2 and CO_2, which is almost energy neutral under standard conditions (Reaction 7 in Table 2). However, this reaction can be coupled to energy conservation in both directions if the thermodynamics are favorable [75, 94, 246]. During mixed acid fermentation in which formate is produced during pyruvate oxidation, formate oxidation can be coupled to the build up of a pmf and thereby enhance the total ATP gain of the fermentative pathway [6, 149, 158, 443].

H_2 metabolizers often have multiple genes that encode for hydrogenases and formate dehydrogenases, and in combination with the transhydrogenase and the Rnf complex they can easily interconvert H_2, formate, Fd, NAD^+, and $NADP^+$. The capability to catalyze these interconversions enhances the metabolic flexibility of these microbes, and enables them to rapidly optimize their energy metabolism in response to changing environmental conditions.

1.5.   Hypotheses and objectives

Peatland soils are characterized by relatively stable anoxic conditions and a limited availability of easily degradable carbon sources whereas earthworm guts represent transient anoxic microhabitats with a high availability of such compounds. These contrasting conditions might be the reason why H_2, which is a central metabolite during anaerobic degradation processes in both ecosystems [100, 488], is effectively scavenged in peatland soils whereas it accumulates in the gut of earthworms.

H_2 accumulation was observed in sugar supplemented peat soil slurries but not in unsupplemented control microcosms of the Fen Schlöppnerbrunnen, indicating that the potential for H_2 production in this fen is high but the availability of free sugars is low [151, 487]. Thus, either the low amount of readily degradable plant biomass or a general low hydrolyzing capacity of the fermenters might limit H_2 production during anaerobic degradation under the cold and acidic conditions in the fen. Root biomass and root exudates (e.g., formate) represent high value organic compounds [313], and O_2 leaking from roots is likely to effect the redox conditions in the rhizosphere of peatland soils [38]. Therefore, H_2 metabolizers attached to root surfaces probably experience conditions that are exclusive to this microhabitat and metabolic pathways might differ from that of the bulk peat soil. The low H_2 concentrations observed in unsupplemented peat soil slurries [487] are a prerequisite for syntrophs that thrive at the thermodynamic limit of life [376]. These processes and the associated taxa are not well

resolved in peatlands, but it is likely that previously unrecognized syntrophs in addition to well known syntrophic genera contribute to the conversion of primary fermentation products to methanogenic substrates under the cold, acidic, and substrate limited conditions.

Ingested and activated soil anaerobes may utilize organics derived from microbial cells that are disrupted by the grinding activity of the gizzard [35]. However, the identity of the anaerobes that are involved in the degradation of disrupted cells is not yet resolved although they might be crucial for the nutrition of the earthworm, which potentially might feed on their metabolic endproducts.

The following hypotheses were proposed based on the observations mentioned above:

(1) Peat fermenters are well adapted to low temperatures and low pH but are substrate limited in their habitat.

(2) The rhizosphere of sedges is a hotspot for H_2 producing fermenters and H_2 consuming acetogens in peatlands.

(3) Known and novel syntrophs and associated methanogens thrive at the thermodynamic limit and collectively prevent an accumulation of fermentation products in peatlands.

(4) Ingested soil anaerobes utilize organic compounds derived from disrupted microbial cells and potentially can feed the earthworm with fatty acids.

The objectives of this study were to resolve the different metabolic activities of H_2 metabolizers that eventually result in contrasting in situ H_2 concentrations in peatlands and earthworm guts. In order to address this objective and the above listed hypothesis, microcosms experiments were performed with (i) peat soil or root slurries and (ii) diluted earthworm gut homogenates. Peat soil samples were derived from the exploratory field site Fen Schlöppnerbrunnen (2.1) and gut contents were derived from the anecic earthworm *Lumbricus terrestris* (2.2). Physiological processes (e.g., the production of gases or soluble organic compounds) were analyzed and compared in microcosms supplemented with different substrates (treatments) or unsupplemented control microcosms (controls). Metabolic capabilities of the microbial community were resolved based on the differences in the physiological processes between treatments and controls. Molecular analyses were performed to identify taxa that might be linked to certain metabolic capabilities. Primers for the amplification of hydrogenase genes and transcripts were developed in this study in order to specifically identify H_2 metabolizers in complex environments. In addition, the phylogeny of hydrogenase genes was compared to the 16S rRNA gene based phylogeny of microbes harboring these genes to evaluate the suitability of hydrogenase gene sequences as phylogenetic marker for H_2 metabolizing microbes.

2. MATERIALS AND METHODS

2.1. Sampling site Fen Schlöppnerbrunnen

2.1.1. Location and Sampling

The Fen Schlöppnerbrunnen is located about 700 m above sea level in the Fichtelgebirge (50°7′53″N, 11°52′51″E; northeastern Bavaria, Germany) within the catchment of the Lehstenbach. The catchment with a highest elevation of 877 m has an area of 4.19 km² [134]. Soils have developed from weathered granitic bedrock, and 30% of the catchment is covered by fens or intermittent seeps [250, 326]. The annual precipitation in the catchment varies between 900 and 1160 mm·yr^{-1} and the average annual air temperature is 5°C [326]. The Fen Schlöppnerbrunnen is a clearing surrounded by spruce, has an area of 0.8 ha, and the average peat thickness is 0.5 m [351]. The total carbon content approximated 400 g·kg [soil$_{dw}$]$^{-1}$ in the top 10 cm layer of the peat and decreased to 150-200 g·kg [soil$_{dw}$]$^{-1}$ in 30-40cm depth [487]. The total nitrogen content likewise decreased with increasing depth from approximately 20 to 8 g·kg [soil$_{dw}$]$^{-1}$ [487]. The fen is located down slope in the catchment, close to the runoff, and thus, constantly supplied with inorganic ions from the moving catchment water (i.e., a soligenous fen) [326]. The mean groundwater table of the fen was 13 cm with a maximum depth of 76 cm (measured in 2002) [326]. Fe^{2+}, nitrate, and sulfate concentrations in the pore water varied between 0.4-91.1 µM, 4.9-67.2 µM, and 64-494 µM respectively [487]. The pH at the fen site approximates 4.5 [219]. Soil temperature at 10 cm depth ranges from 0.5 to 15°C with mean annual temperatures of about 5°C [278]. CH_4 emissions of up to 530·µmol·m^{-2}·h^{-1} were measured in the fen (Goldberg S, Knorr KH, Gebauer G, unpublished data). The vegetation in the catchment is dominated by Norway spruce (*Picea abies*) of different ages [135]. The Fen Schlöppnerbrunnen is completely overgrown with sedges of the genus *Carex, Molinia, Juncus,* and *Eriophorum* [326]. In addition, *Sphagnum* mosses are common at the fen site [205]. Fresh peat soil was sampled with a soil corer at dates listed in Table 6. Soil cores were transferred into airtight sterile plastic bags, cooled on ice and transported to the lab where they were processed within 5 h of sampling. Pore water was collected from the holes that resulted from the removal of peat soil cores.

Table 6   **Overview of sampling time points for experiments with peat soil**

Collection date	Moisture content of soil	Soil depth (cm)	Experiment
October 2010	88.0%	10-30	Cellulose degradation (3.2.1)
April 2012	89.7% (89.1%)[a]	0-20	Root microcosms (3.2.2)
May 2013	88.6%	10-30	Syntrophic oxidation (3.2.3)

[a]Moisture content of roots is shown in parenthesis.

2.1.2. Microcosms experiments with peat soil and roots of *Carex rostrata* derived from the Fen Schlöppnerbrunnen

2.1.2.1. Preparation and incubation conditions of anoxic microcosms in cellulose degradation experiments (3.2.1)

The covering grass vegetation and the top 10 cm of peat soil cores were detached. Sixty grams of the remaining peat soil (10 to 30 cm depth) was diluted with 140 ml of anoxic mineral medium (2.3.2) in sterile 0.5 l infusion flasks (Müller + Krempel, Bülach, Switzerland) that were sealed with screw caps and rubber stoppers (Glasgerätebau Ochs, Bovenden, Germany). Microcosms were flushed with 100% sterile dinitrogen (N_2) for 20 min. A total of 12 replicate microcosms were prepared. Six replicates were supplemented with 0.04 g microcrystalline [^{12}C] cellulose (yielding approximately 1.23 mM glucose equivalents) and another six replicates were kept unsupplemented. Three cellulose supplemented (cellulose treatments) and three unsupplemented replicates (controls) each were preincubated at either 15°C or 5°C for 17 d and 22 d, respectively. This preincubation was done to deplete residual O_2 and to fully reduce alternative electron acceptors (e.g., nitrate, Fe^{3+}, and sulfate). After the preincubation, 0.2 g microcrystalline [^{13}C]cellulose (yielding 6.17 mM of glucose equivalents; from maize, IsoLife, Wageningen, the Netherlands) was supplemented to cellulose treatments for stable isotope probing. Control treatments were kept unsupplemented. Liquid phases and headspace gas phases were sampled with sterile syringes. After each measurement gas phases were flushed with sterile N_2 for 20 min to prevent cross-feeding effects from [^{13}C]cellulose-derived [^{13}C]-CO_2.

2.1.2.2. Preparation and incubation conditions of anoxic root-free peat soil microcosms and soil-free root microcosms (3.2.2)

Soil cores from patches that were overgrown by *Carex rostrata* were used. Stems and leaves of the grass plants were cut. Roots and root-attached soil (i.e., rhizosphere soil) were further proceeded in an anoxic chamber (100% N_2 atmosphere; Mecaplex, Grenchen, Switzerland). Rhizosphere soil was separated from roots by sieving. Remaining roots were washed with sterile anoxic water to remove soil particels on the surface of the roots. One to two grams of fresh weight (g_{fw}) roots or rhizosphere soil were added to 120 ml infusion flasks and diluted 1:10 (w/v) with anoxic mineral medium (2.3.2). Microcosms were flushed with 100% sterile N_2 for 20 min and incubated in the dark on an end-over-end shaker. Liquid phases and headspace gas phases were sampled with sterile syringes. Formate was pulsed several times to treatments at a final concentration of 2 mM whereas anoxic water instead of formate was added to unsupplemented controls.

2.1.2.3.   Preparation and incubation conditions of anoxic microcosms in syntrophic oxidation experiments (3.2.2)

The grass vegetation and the top layer of peat soil cores were removed. Two hundred grams of fresh peat soil (88.6% moisture content) were mixed with 400 ml of fresh surface water (collected during sampling in the fen, 2.1.1) in sterile 1 l infusion flasks that were sealed with screw caps and rubber stoppers. Microcosms were flushed with 100% sterile N_2 for 20 min. A total of 30 replicate microcosms were prepared. 20 and 10 microcosms were preincubated for 28 d and 38 d at 15°C and at 5°C, respectively. This preincubation was done to establish fully anoxic conditions and to deplete easily degradable endogenous carbon sources. After the preincubation, the microcosms were divided into sets of five replicates and regularly pulsed with 300 to 750 µM of either [^{12}C]ethanol (at 15°C and 5°C), sodium [^{12}C]butyrate (at 15°C), or sodium [^{12}C]propionate (at 15°C). Controls (at 15°C and 5°C) were supplemented with anoxic water (2.3.1). After 88 d, one replicate of the ethanol and butyrate treatment at 15°C were pulsed with [^{13}C]ethanol and sodium [^{13}C]butyrate (Campro Scientific GmbH, Berlin, Germany), respectively, for the stable isotope probing (2.5.5). In total 24 and 18 mM ^{13}C were added in the [^{13}C]butyrate and [^{13}C]ethanol treatment, respectively. A [^{13}C]propionate treatment at 15°C and a [^{13}C]ethanol treatment at 5°C were not conducted due to financial constraints. Liquid phases and headspace gas phases were sampled with sterile syringes. Head space gas phases were exchanged regularly with 100% sterile N_2. The pH was regularly adjusted by adding 50 µl to 300 µl of a 2.5 M hydrogen chloride solution in butyrate and propionate treatments.

2.2.   Experiments with gut contents of the earthworm *Lumbricus terrestris*

2.2.1.   Source of samples used for the amplification of hydrogenase transcripts and genes (3.3.1)

RNA and DNA were extracted from samples of glucose-supplemented *Lumbricus terrestris* gut content microcosms described elsewhere (see ref [490] for details about the experimental design, process data, and a 16S rRNA-based analysis of the microbial community in the microcosms). Samples were collected at the end of the microcosm experiment (i.e., at 51 h) and stored at -80°C until they were used for nucleic acid extraction.

2.2.2.   Preparation and incubation conditions of anoxic *Lumbricus terrestris* gut content microcosms

2.2.2.1.   Earthworms

Earthworms of the species *L. terrestris* were purchased from ANZO (Bayreuth, Germany) and maintained in soil that was collected from the meadow Trafo Wiese (Bayreuth) [170]. The worms were kept on soil at 20°C for seven days. Fresh grass and decaying plant leaves were added as a feedstock for the earthworms.

2.2.2.2.   Preparation of *Saccharomyces cerevisiae* cell lysates

Cells of *S. cerevisiae* Sa-07140 were incubated in 4×500 ml oxic growth medium (2.3.6) for 48 h at 30°C. The cells were harvested by centrifugation (20 min, 7500 rpm; J2-HS-centrifuge, rotor JA 10, Beckmann, Fullerton, CA, USA). Cell pellets were washed three times with phosphate buffer (2.3.3). In total, 20 g cells (21.7% dry weight) were harvested and resuspended in 20 ml phosphate buffer (2.3.3). 400 µl DNase I (10 000 U·ml^{-1}; Sigma) was added. Cells were lysed with a french press (14 000-16 000 psi; FA-032-40K pressure cell, SLM Aminco, Urbana, IL, USA) three times. The suspension with the lysed cells was centrifuged (15 000 rpm, J2-HS-centrifuge, rotor JA 10, Beckmann) for 20 min. The pellet that most probably contained the cell wall fragments, the associated phospholipid membranes, and undisrupted cells was discarded. The supernatant was collected and centrifuged one more time. The resulting cell lysate had a volume of 27 ml and was diluted with 13 ml phosphate buffer (2.3.3) to make up a total volume of 40 ml. The diluted lysate was finally sterile filtered (0.2 µm pore size, cellulose-acetate membrane; Sartorius Stedim, Göttingen, Germany). The sterile lysate with a dry weight of 6.27% was transferred in 100 ml serum vials and the atmosphere was exchanged with 100% argon.

2.2.2.3.   *L. terrestris* gut content and control microcosms

Earthworms (2.2.2.1) were washed in sterile ddH$_2$O, dried with paper towel, anesthetized on ice with 100% CO$_2$ for 20 min and further proceeded in an anoxic chamber (100 % N$_2$ atmosphere; Mecaplex). Worms were cut at the posterior end with scissors and the gut content was manually squeezed out (approximately 0.5 g per individual). Foregut, midgut, and hindgut contents of 50 individuals were pooled. 1 g gut content (0.8 ml) was diluted with 8.2 ml phosphate buffer (2.3.3) in tubes (27 ml) that were sealed with rubber stoppers and aluminum caps. Tubes were flushed with 100% sterile N$_2$ for 20 min. Six Tubes were autoclaved (control treatments with autoclaved gut contents). 1 ml of lysed *S. cerevisiae* cells (2.2.2.2) was added

to tubes with autoclaved and not autoclaved anoxic gut content microcosms. 1 ml of phosphate buffer (2.3.3) was added instead of cell lysate to unsupplemented controls. The total volume of anoxic gut content microcosms was 10 ml and all treatments (gut content supplemented with cell lysate, unsupplemented gut content, autoclaved gut content supplemented with cell lysate, and unsupplemented autoclaved gut content) were set up in triplicats. In addition, control treatments with 1:10 diluted lysed *S. cerevisiae* cells (2.2.2.2) in phosphate buffer (2.3.3) without earthworm gut content were prepared in triplicates and either supplemented with 0.5 mM of glucose or kept unsupplemented. All microcosms were incubated at 23°C in the dark. Headspace gas phases and liquid phases were sampled with sterile syringes and samples for nucleic acid extraction were stored at -80°C.

2.3.   Solutions and growth media

All solutions and media were prepared with deionized double destilled water (ddH$_2$O). Modified Hungate techniques were used to prepare anoxic solutions and media [77, 174]. Sterilization of solutions and media was done either via autoclaving (Sanoclav, Wolf, Geislingen, Germany) or filtration (0.2 µm pore size, cellulose acetate membrane, Schleicher & Schuell MicroScience GmbH, Dassel, Germany).

2.3.1.   Anoxic water

ddH$_2$O was boiled for 30 min in Erlenmayer flasks and subsequently transferred in 1 l infusion flasks. Infusion flasks were sealed with screw caps and rubber stoppers and the water was purged with 100% N$_2$ for 20 min.

2.3.2.   Anoxic mineral medium

Mineral salt solution (2.3.2.1)	10 ml
Trace element solution (2.3.2.2)	10 ml
Vitamin solution (2.3.2.3)	10 ml
Anoxic ddH$_2$O (2.3.1)	970 ml
pH 5.0	

Mineral salt and trace element solutions were added to the anoxic water in 1 l infusion flasks. Afterwards, the pH was adjusted and the medium was autoclaved. The vitamin solution was sterile filtered and added to the medium when it was cooled down.

2.3.2.1. Mineral salt solution

$(NH_4)_2SO_4$	1.26 g
Na_2SO_4	1.35 g
$CaCl_2 \cdot 2H_2O$	1 g
$MgCl_2 \cdot 6H_2O$	1 g
KH_2PO_4	0.04 g
$FeCl_2 \cdot 4H_2O$	1 g
Anoxic ddH_2O (2.3.1)	ad 1000 ml

2.3.2.2. Trace element solution

Modified after ref [13].

Nitrilotriacetic acid	1.5 g
$MnSO_4 \cdot H_2O$	0.5 g
$FeSO_4 \cdot 7H_2O$	0.1 g
$CoCl_2 \cdot 6H_2O$	0.1 g
$CaCl_2 \cdot 2H_2O$	0.1 g
$ZnSO_4 \cdot H_2O$	0.1 g
$CuSO_4 \cdot H_2O$	0.01 g
$AlK(SO_4)_2 \cdot 12H_2O$	0.02 g
H_3BO_3	0.01 g
$Na_2MoO_4 \cdot 2H_2O$	0.01 g
Anoxic ddH_2O (2.3.1)	ad 1000 ml

2.3.2.3. Vitamin solution

Biotin	2 mg
Folic acid	2 mg
Pyridoxine-HCl	10 mg
Thiamine-HCl	5 mg
Riboflavin	5 mg
Nicotinic acid	5 mg
DL-Ca-Pantothenate	5 mg
Vitamin B_{12}	0.1 mg
p-aminobenzoic acid	5 mg
Liponic acid	5 mg
Anoxic ddH_2O (2.3.1)	ad 1000 ml

2.3.3. Phosphate buffer

NaH$_2$PO$_4$·H$_2$O	1.9 g
Na$_2$HPO$_4$·2H$_2$O	3.36 g
Anoxic ddH$_2$O (2.3.1)	ad 1000 ml
pH 7	

2.3.4. SOC medium

After ref [143].

Tryptone	2 g
Yeast extract	0.5 g
NaCl solution (1 M)	1 ml
KCl solution (1 M)	0.25 ml
MgCl$_2$ solution (2 M)	1 ml
Glucose solution (2 M)	1 ml
ddH$_2$O	ad 100 ml
pH 7	

All components but MgCl$_2$ and glucose solutions were filled up to approximately 95 ml and autoclaved. Afterwards, sterile filtered MgCl$_2$ and glucose solutions were added and the pH was adjusted using sterile filtered solutions.

2.3.5. LB (lysogeny broth) agar plates

After ref [143].

Tryptone	10 g
Yeast extract	5 g
NaCl	5 g
Agar	15 g
ddH$_2$O	ad 1000 ml
pH 7	

All components were filled up to approximately 980 ml. The pH was adjusted and ddH$_2$O was added to make up a final volume of 1 l. The medium was autoclaved and poured into sterile plastic Petri dishes.

2.3.5.1.   LB agar plates with ampicillin

LB medium was prepared as described (2.3.5). 1 ml of sterile-filtered ampicillin (100 mg·ml^{-1}) was added to the medium after it cooled down to approximately 60°C.

2.3.5.2.   LB agar plates with ampicillin/IPTG/X-Gal

LB medium was prepared as described (2.3.5). 1 ml of sterile-filtered ampicillin (100 mg·ml^{-1}), 1 ml isopropyl-β-D-galactopyranoside (IPTG; 0.5 M), and 1.6 ml 5-bromo-4-chloro-3-indolyl-β-D-galactopyranoside (X-Gal; 50 mg·ml^{-1} in N,N-dimethylformamide) solutions were added to the medium after it cooled down to approximately 60°C.

2.3.6.   Oxic *S. cerevisiae* growth medium

Yeast extract	7 g
Tryptic soy broth	7 g
Glucose	10 g
ddH$_2$O	1 l
pH 7	

All components but glucose were filled up to approximately 900 ml and autoclaved. Afterwards, sterile filtered glucose (100 ml of a 100 g·l^{-1} glucose solution) were added and the pH was adjusted using sterile filtered solutions.

2.4.   Analytical methods

2.4.1.   pH measurements

The pH of fen surface water, media, and microcosm samples was measured using a combination pH electrode (U457-S7/110, Ingold, Steinbach, Germany) and a digital pH meter (WTW pH 330, Wissenschaftlich-Technische Werkstätten, Weilheim, Germany).

2.4.2.   Dry weight and moisture content of soils

Dry weight and moisture contents of soils were determined by weighing four samples of fresh soil followed by drying at 105°C for several days and subsequent weighing.

2.4.3.   Gases

Gas samples were collected using sterile syringes (flushed with 100% sterile N_2) and injected into 5890 Series II gas chromatographs (Hewlett Packard, Palo Alto, CA, USA). The gas chromatographs were equipped with columns and detectors as listed in Table 7. Gas concentrations in % were quantified with a Knauer IF2 integrator using the software EuroChrom (Version V3.05, Knauer, Berlin, Germany) and external standards with known gas concentrations. Over pressure in incubation flasks was measured directly before sampling with a digital precision manometer (GHM 3111, GHM Messtechnik GmbH, Regenstauf, Germany).

Table 7   Parameters of gas chromatographs

Gases	CO_2	H_2/CH_4 (≥ 0,8 %)	CH_4 (< 0,8 %)
Detector	Thermal conductivity detector (TCD)	Thermal conductivity detector (TCD)	Flame ionisation detector (FID)
Column	Chromopsorb 102, 2 m x 1/8" (Alltech, Unterhaching, Germany)	Molecular sieve, 2 m x 1/8" (Alltech, Unterhaching, Germany)	Molecular sieve, 2 m x 1/2" (Alltech, Unterhaching, Germany)
Carrier gas	Helium	Argon	Helium
Flow rate	15 ml min^{-1}	33 ml min^{-1}	40 ml min^{-1}
Oven temp.	40°C	50°C	60°C
Injection temp.	150°C	150°C	120°C
Detector temp.	175°C	175°C	150°C
Injection volume	100 µl	100 µl	100 µl
Retention time	2.3 min	0.7 min (H_2) 3.0 min (CH_4)	1.4 min

The total molar amount of a gas (n_t) was calculated as shown in Equation 1 to Equation 5. n_t comprises the amount of a gas in the gas phase (n_g), the amount of gas physically dissolved in the liquid phase (n_{lp}) and the amount of gas chemically dissolved in the liquid phase (n_{lc}, for CO_2 only) according to Equation 1.

Equation 1   Total amount of gases

$$n_t = n_g + n_{lp} + (n_{lc})$$

n_g (mmol) was calculated using the ideal gas law (Equation 2).

Equation 2   Ideal gas law

$$n_g = \frac{p_i \times V_g}{R \times T}$$

p_i, the partial pressure of the gas (in mbar); V_g, the volume of the gas phase (in ml); R, the universal gas constant (83.145 mbar·ml·K^{-1}·mmol^{-1}); T, the actual temperature in K.

p_i was calculated from the measured gas concentration C (in %), the current atmospheric pressure p_a (in mbar), and the overpressure measured in the flasks p_o (in mbar) according to Equation 3.

Equation 3   Partial pressure of gases

$$p_i = \frac{C \times (p_a + p_o)}{100}$$

n_{lp} is dependent on the gas specific solubility coeffiecent (α) listed in Table 8 and was calculated according to Equation 4.

Equation 4   Physically dissolved gases in the liquid phase

$$n_{lp} = \frac{n_g \times V_l \times \alpha}{V_g}$$

V_l, volume of the liquid phase (in ml).

n_{lc} has to be included in the calculation of total amounts of a gas if it reacts chemically with the solvent. Thus, n_{lc} was calculated for CO_2, which reacts with water predominately to bicarbonate in the pH range of the experiments in this dissertation (Equation 5).

Equation 5   Chemically dissolved CO₂ (bicarbonate)

$$n_{lc} = n_{lp} \times 10^{pH - pKa}$$

pKa, the logarithmic acid dissociation constant for bicarbonate is 6.37.

Table 8   Bunsen solubility coefficients [25]

Gas	Bunsen solubility coefficients α (in water)			
	5°C	*15°*	*20°C*	*25°C*
CO₂	1.38	0.99	0.85	0.74
CH₄	0.046	0.036	0.032	0.029
H₂	0.020	0.018	0.018	0.017

2.4.4.   Soluble organic compounds

The concentration of alcohols, organic acids and sugars in microcosm experiments were measured with a high pressure liquid chromatograph (Hewlett Packard 1090 Series II) equipped with an autosampler, an UV detector (G1314B, Series 1200, Agilent Technologies, Böblingen, Germany), and a refractive index detector (G1362A, Series 1200, Agilent Technologies). Compounds were separated with an Aminex ion exclusion column (HPX-87H, 300 x 7.8 mm, BioRad, Richmond, CA, USA). The oven temperature was 60°C and a 4 mM phosphoric acid solution was used as mobile phase at a flow rate of 0.8 ml·min⁻¹.

Concentrations were quantified with the 2D ChemStation software (Agilent). Liquid samples were collected with sterile syringes, transferred in sterile 1.5 ml microcentrifuge tubes, and centrifuged for 10 min at 13000 × g (1-15K Sartorius microcentrifuge, Sigma Laborzentrifugen, Osterode am Harz, Germany). The supernatant was filtered (pore size 0.2 µM, nylon filter, Infochroma, Zug, Switzerland) and transferred into flange bottles with aluminum caps (VWR International, Darmstadt, Germany). External standards with known concentrations were used to identify and quantify the different compounds.

2.5. Molecular methods

2.5.1. Extraction of nucleic acids

The coextraction of RNA and DNA from samples of peat soil or earthworm gut content microcosms followed a modified protocol of Griffiths and colleagues [144]. Cells were disrupted by bead-beating lysis and the nucleic acids separated from proteins, cell fragments and soil particles by extraction with phenol, chloroform and isoamyl acohol and subsequent centrifugation. 0.5 g sample were added to 0.5 ml extraction buffer (5% CTAB, 0.35 M NaCl, 120 mM potassium phosphate buffer, pH 8), 0.5 ml phenol / chloroform / isoamyl alcohol (25:24:1), and 1 g of zirconia/silica beads (0.5 g of Ø 0.5 mm beads and 0.5 g of Ø 0.1 mm beads; BioSpec, Bartlesvill, OK, USA) in 2 ml screw-capped tubes (VWR International). Bead-beating was done at a speed of 5.5 m·s^{-1} for 30 s in a FastPrep FP120 bead beater (Thermo Savant, Holbrook, NY, USA). The liquid phase containing the nucleic acids was separated from soil particles, cell fragments and denatured proteins by centrifugation (10 min at 13000 × g, 4°C, 1-15K Sartorius microcentrifuge) and transferred in a new 1.5 ml microcentrifuge tube. 0.5 ml chloroform / isoamyl alcohol (24:1) were added, tubes were thoroughly mixed and centrifuged (10 min at 13000 × g, 4°C) to seperate the nucleic acids from residual proteins and phenol. Precipitation of the nucleic acids in the supernatant was done by the addition of two volumes precipitation buffer (0.1 M Hepes pH 7 - 30% PEG; Fluka, Neu-Ulm, Germany) and a 2 h incubation at room temperature. Precipitated nucleic acids were pelletized by centrifugation (10 min at 13000 × g, 4°C) and the supernatant was discarded. Pellets were washed with 0.5 ml ice cold ethanol (70%) to remove salts. Ethanol was removed by centrifugation and pellets were dried at room temperature. The pelletized nucleic acids were resuspended in 50 µl sterile ddH$_2$O.

RNA was removed from coextracts by enzymatic digestion with RNase A (10 µg·µl^{-1}, Fermentas, St. Leon-Roth, Germany) for 30 min at roomtemperature to obtain DNA. DNA was removed by enzymatic digestion with DNase I (1 U·µl^{-1}, Fermentas) for 45 min at 37°C to obtain RNA. Enzymatic digestions were stopped by isopropanol precipitation of nucleic acids (2.5.2.1).

2.5.2. Purification and precipitation of nucleic acids

2.5.2.1. Isopropanol precipitation

One volume of nucleic acid extracts treated with DNase I or RNase A (2.5.1) were precipitated with 0.7 volume of ice cold isopropanol and 0.1 volume of sodium chloride (5 mM) [143]. Nucleic acids were incubated for 12 h in a freezer (-20°C) and pelletized by centrifugation (40 min at 18000 × g, 4°C). Pellets were washed with 0.5 ml ice cold ethanol (70%), dried at room temperature, and dissolved in 20 µl DNase/RNase-free ddH$_2$O.

2.5.2.2. Gel extraction

PCR products of the desired size were purified from products of unspific size by agarose gel extraction (Montage gel extraction kit, Millipore, Bedford, USA) according to the manufacturer's protocol. Agarose gel electrophoresis was done as described (2.5.4). Ethidium bromide stained DNA was visualized by UV light (302 nm, Transilluminator UVT-20M, Herolab GmbH, Wiesloch, Germany). DNA-bands of the desired size were excised from the gel with a sterile knife and transferred to the Montage gel extraction columns. Final gel extracts were purified by isopropanol precipitation (2.5.2.1).

2.5.3. Quantification of nucleic acids

2.5.3.1. NanoDrop-based quantification

Concentrations and purity of nucleic acids were determined spectrophotometrically with a ND1000 (NanoDrop Technology, Wilmington, NC, USA). Absorption (A) at 230, 260, and 280 nm wavelength were measured. An A_{260}/A_{280} ratio between 1.6 and 2.0 and an A260/A230 ratio of above one are indicative of a pure nucleic acid extract with little protein/phenol and humic acid contaminations, respectively [143, 444].

2.5.3.2. Pico- and Ribogreen-based quantification

A fluorescence-based method, which is less sensitive to interferences by contaminants than NanoDrop (2.5.3.1), was used to quantify DNA or RNA concentrations of ≤ 10 ng·µl^{-1}. Quant-iT-PicoGreen (for DNA) and Quant-iT-RiboGreen (for RNA) were added to the samples in microtiter plates according to the manufacturer's protocol (Invitrogen, Carlsbad, CA, USA). Fluorescence was measured with a FLx800 Microplate fluorimeter (BioTek, Bad Friedrichshall, Germany). Concentrations were evaluated with external DNA/RNA standards delivered by the manufacturer and the software Gen5 (BioTek).

2.5.4.   Agarose gel electrophoresis

Nucleic acid extracts (2.5.1) and PCR products (2.5.7) were analyzed by horizontal agarose gel electrophoresis [1, 143]. Gels were prepared with 1% w/v low EEO standard agarose (AppliChem GmbH, Darmstadt, Germany) and 1 × TAE buffer (40 mM Tris-HCl, 20 mM acetate, 1 mM EDTA, pH 8). The mixture was heated in a microwave until the agarose completely melted. Ethidium bromide (3,8-diamino-5-ethyl-6-phenyl-phenenthridium bromide, BioRad) at a final concentration of 0.08 mg·ml^{-1} was added when the solution was cooled down to approximately 60°C. Gels were transferred into a migration chamber (BioRad Mini- or Maxi-Sub cell, BioRad) filled with 1 × TAE buffer. 5 µl sample were mixed with 1 µl 6 × Blue Orange loading dye (Promega, Madison, WI, USA) and transferred into the gel slots. 2 µl molecular weight marker (MWM 1, Bilatec, Viernheim, Germany) were transferred into gel slots adjacing those filled with samples. Electrophoresis was done for 20-60 min at 80-120 V (Power-Pak 3000, BioRad). Bands containing nucleic acids were visualized by UV light (302 nm, Transilluminator UVT-20M, Herolab GmbH, Wiesloch, Germany). The UV-illuminated gel was photographed with a Canon PowerShot G5 camera (Canon, Krefeld, Germany).

2.5.5.   16S rRNA-based stable isotope probing (SIP)

SIP identifies organisms that feed on substrates marked with heavy stable isotopes (e.g., ^{13}C-carbon labled [^{13}C]cellulose) and incorporate the heavy isotopes into biopolymers (e.g., RNA, DNA, or proteins) [273]. Assimilation therefore results in biopolymers with an increased buyont density compared to those of organisms not feeding on the labeled substrate [286]. 16S rRNA-based SIP was performed with [^{13}C]cellulose (2.1.2.1), [^{13}C]ethanol and [^{13}C]butyrate (2.1.2.2) according to a modified protocol after Whiteley and colleagues [477].

2.5.5.1.   Density gradient centrifugation

Nucleic acids were extracted from samples of anoxic peat soil microcosms (2.1.2.1 and 2.1.2.2) before and after the incubation with [^{13}C]substrates. DNA was digested to obtain RNA (2.5.1). 600 ng RNA was added to a gradient solution (buoyant density 1.79 g·ml^{-1}) consisting of 83.3% cesium trifluoroacetate (CsTFA; buoyant density 2.0 g·ml^{-1}, GE Healthcare, Buckinghamshire, UK), 13.5% gradient buffer (100 mM Tris; 100 mM potassium chloride; 1mM EDTA; pH 8) and 3.2% deionized formamide and filled into OptiSeal Tubes (Beckman, Fullerton, CA, USA). Tubes were closed with plugs and placed in an ultra-vertical VTi 65.2 Rotor (Beckman). Aluminum spacers and rotor screws were put on top of the tubes, and the screws were tightened with a torque wrench (200 inch-pounds, Beckman) to a bolting torque of 60 inch-pounds. 'Heavy', potentially ^{13}C-labeled RNA was separated from 'lighter' ^{12}C-labeled RNA by isopycnic centrifugation (130000 × g or 37800 rpm at 20°C for 67 h) in a

LE-70 ultra centrifuge (Beckman). A control tube ('blank') containing gradient solution but no RNA was added in each centrifugation run and the resulting gradient was used to determine the buoyant density of fractions (2.5.5.3). Three different centrifugation runs were conducted containg samples of the cellulose SIP experiment at 15°C (run 1), at 5°C (run 2), and of the butyrate and ethanol SIP experiments (run 3) (Figure 5).

2.5.5.2. Fractionation

After the centrifugation (2.5.5.1), tubes were fixed vertically in a rag. An Econo Pump 1 peristaltic pump (BioRad) was connected with a silicon tube (1.6 mm inner diameter) to a sterile needle (23G × 1''). The needle was inserted into the tube underneath the plug and a second needle was used to cut a hole into the bottom of the tube. Fractionation was done with brilliant blue colored sterile ddH_2O pumped at a flow rate of 0.45 ml·min^{-1}. Fractions (450 µl each) were collected in 1.5 ml microcentrifuge tubes.

2.5.5.3. Determination of the CsTFA buoyant density of fractions

The CsTFA buoyant density of the fractions from the 'blank' gradients (2.5.5.1) were determined for each centrifugation run by repeatedly weighing 100 µl of each fraction (tempered in a thermomixer [Thermomixer comfort, Eppendorf, Hamburg, Germany] to 25°C) on an analytical balance (Analytic AC 120 S, Sartorius, Garching, Germany). Linearly decreasing densities with ascending fraction numbers and comparable linear regressions in the three centrifugation runs (2.5.5.1) indicated that the establishment of CsTFA density gradients by isopycnic centrifugation was succesfull and reproducible (Figure 5).
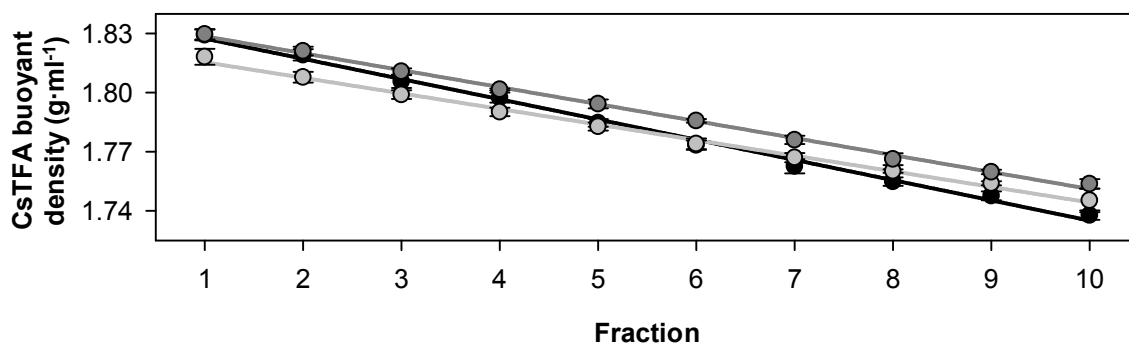
Figure 5   CsTFA buoyant density of gradient fractions.
A: black / light gray / dark gray circles, centrifugation run 1 (cellulose SIP at 15°C) / run 2 (cellulose SIP at 5°C) / run 3 (butyrate and ethanol SIP at 15°C) (2.5.5.1); lines represent linear regressions (R^2 ranged from 0.994 to 0.997); error bars indicate standard deviations (n=10).

2.5.5.4.   RNA precipitation

RNA precipitation was performed as described by Degelmann and colleagues [86]. 150 µl of each fraction were mixed with 97.5 µl sodium acetate solution (3 M, pH 5.2), 10.2 µl glycogen solution (10·mg ml^{-1}), and 750 µl ice cold ethanol (96%). The RNA was precipitated over night at -20°C and afterwards pelletized by centrifugation (13000 × g, 20 min, at 4°C). The supernatant was discarded and the pellet was washed with 500 µl ice cold ethanol (70%). Pellets were dried at room temperature and resuspended with 20 µl RNase-free ddH$_2$O. RNA in fractions was quantified by fluorescence based methods (2.5.3.2). RNA was finally transcribed into complementary DNA (cDNA, 2.5.6).
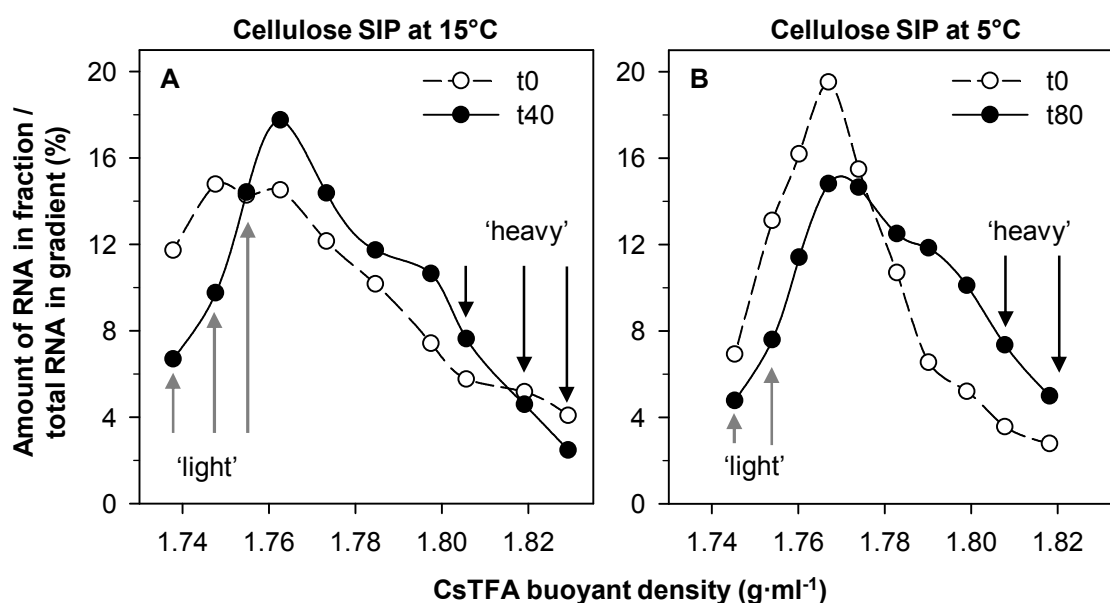
Figure 6   Distribution of RNA in gradient fractions of [^{13}C]cellulose supplemented anoxic peat soil microcosms (2.1.2.1) at 15°C (A) and at 5°C (B), respectively.
'Light' RNA from fractions with buoyant densities < 1.76 g·ml^{-1} (indicated by grey arrows) and 'heavy' RNA from fractions with buoyant densities > 1.80 g·ml^{-1} (indicated by black arrows) was pooled for the preparation of corresponding clone libraries (3.2.1.2 and 3.2.1.4), respectively. Symbols: empty circles, RNA extracted before the incubation with [^{13}C]cellulose; filled circles, RNA extracted after the incubation with [^{13}C]cellulose as indicated in Figure 9. Gradients contained 200 ng RNA of each triplicate of the [^{13}C]cellulose treatments. Modified from ref [387].

The RNA was distributed over all fractions in each gradient indicating that RNAs with different buoyant densities were successfully separated (Figure 6 and Figure 7). A clear separation of 'heavy' ^{13}C-labeled RNA from 'light' unlabeled (^{12}C-labeled) RNA resulting in two distinct peaks in RNA distribution curves, as found in SIP experiments with pure cultures [259], was not observed in any of the SIP experiments conducted here. Relatively low amounts of RNA in 'heavy' fractions (i.e., >1.80 g·ml^{-1} buoyant density) of gradients after the incubation

with [^{13}C]substrate suggest that only a subset of the taxa present in the peat soil assimilated ^{13}C-carbon.
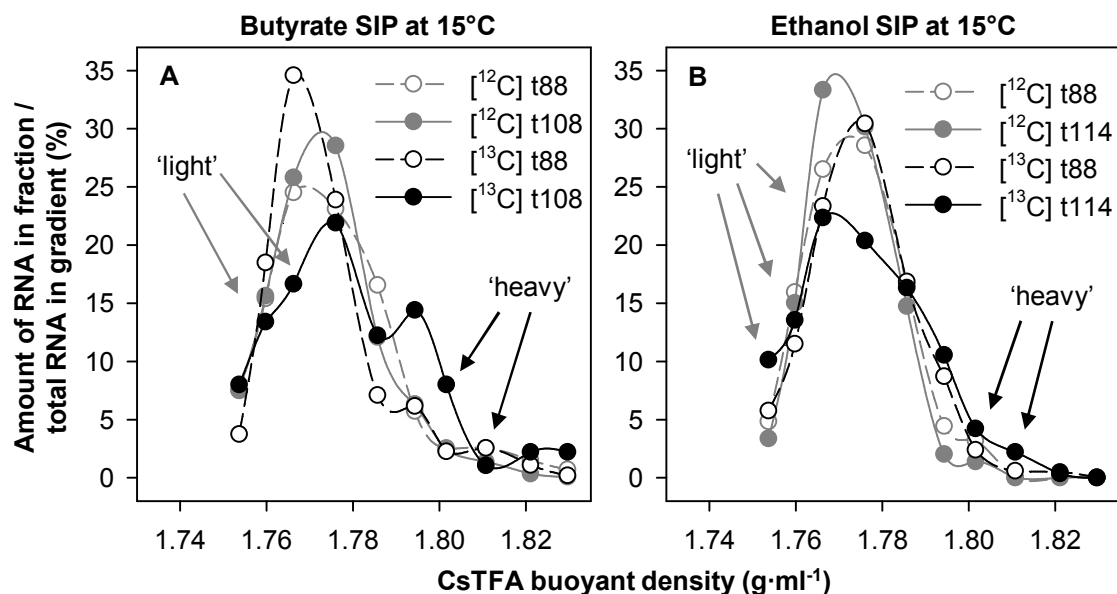
Figure 7   Distribution of RNA in gradient fractions of butyrate (A) and ethanol (B) supplemented anoxic peat soil microcosms at 15°C (2.1.2.2).
One of five replicates of the butyrate and ethanol supplemented microcosms was pulsed with [^{13}C]butyrate and [^{13}C]ethanol, respectively, after 88 d of the main incubation (black circles) while the other four replicates of either the butyrate or ethanol treatment were continously pulsed with [^{12}C]butyrate and [^{12}C]ethanol, respectively (grey circles) (see 2.1.2.2 for details).   Thus, t88 is the timpoint before (open circles) and t108/t114 is the timepoint after (closed circles) the incubation with [^{13}C]substrate in butyrate and ethanol treatments, respectively (see Figure 27 and Figure 29 to find when substrates were pulsed). Gradients of ^{12}C-treatments were loaded with pooled RNA from all four replicates whereas gradients of ^{13}C-treatments were loaded with RNA of the single replicate. Grey and black arrows indicate 'light' (8-9 for butyrate and 8-10 for ethanol treatments) and 'heavy' (3-4 for butyrate and ethanol treatments) fractions that were selected for preparing clone libraries from gradients of the [^{13}C]ethanol and [^{13}C]butyrate replicate at the end of the main incubation (filled black circles). Modified from ref [386].

2.5.6.   Reverse transcription of RNA into cDNA

RNA was reversely transcribed into cDNA with the SuperScript III RT kit (Invitrogen) according to the manufacturer's protocol. RNA (10 ng to 1 µg) was preincubated with 1 µl random hexamer primers (50 ng·µl^{-1}) and RNase-free ddH$_2$O (ad 13 µl) for 5 min at 25°C. Reverse transcription was performed after the addition of 4 µl 5 × First-Strand Buffer, 1 µl 0.1 M DTT and 1 µl SuperScript III RT enzyme (200 U·µl^{-1}) for 2 h at 42°C. The reaction was stopped by a 5 min incubation at 85°C.

2.5.7.   Polymerase chain reaction (PCR)

DNA fragments were amplified from DNA or cDNA templates using the polymerase chain reaction (PCR) [361]. A SensoQuest labcycler (SensoQuest GmbH, Göttingen, Germany) was used to perform cycles of denaturation, annealing, and elongation steps. Published PCR primers that were used are listed in Table 9 and newly designed primers targeting hydrogenase genes are listed in Table 16. Primers were synthesized by Microsynth (Balgach, Switzerland). Nucleotides were purchased from Eppendorf. PCR reactions (Table 10 to Table 13) were set up on ice in either single 0.2 ml PCR tubes or 96 well plates. Lids and heating blocks of thermocyclers were preheated to 95°C before PCR was started by placing the PCR tubes or plates into the cycler.

Table 9   Properties of published primers used in this study

Primer	Target gene/plasmid	Sequence (5'-3')[a]	Ref.
27F	16S rRNA gene (*Bacteria*)	AGA GTT TGA TCM TGG CTC	[229]
907R	16S rRNA gene (*Bacteria*)	CCG TCA ATT CMT TTR AGT TT	[229]
Bakt_341F	16S rRNA gene (*Bacteria*)	CCT ACG GGN GGC WGC AG	[163]
Bakt_805R	16S rRNA gene (*Bacteria*)	GAC TAC HVG GGT ATC TAA TCC	[163]
Arch21Fa	16S rRNA gene (*Archaea*)	TCC GGT TGA TCC YG SCR G	[168]
ARC915	16S rRNA gene (*Archaea*)	GTG CTC CCC CGC CAA TTC CT	[419]
M13uniF	pGEM-T vector plasmid	TGT AAA ACG ACG GCC AGT	[287]
M13uniR	pGEM-T vector plasmid	CAG GAA ACA GCT ATG ACC	[287]

[a]IUPAC nomenclature was used for mixed bases [70].

2.5.7.1.   Amplification of inserts in vector plasmids of (M13-PCR)

M13-PCR (Table 10) and subsequent agarose gel electrophoresis (2.5.4) was used to determine the length of DNA fragments ligated into vector plasmids of clones (2.5.8). Primers M13uniF and M13uniR (Table 9) target the flanking region of the multiple cloning site (MCS) of the pGEM-T vector plasmid [364]. The length of the ligated DNA fragment correlates to the length of the M13-PCR product substracted by approxmimately 150 bp. M13-PCR products of the desired length were selected for sequencing (2.5.9).

2.5.7.2.   Bacterial and archaeal 16S rRNA PCR for cloning

Fragments (of approximately 900 bp) of reversely transcribed bacterial and archaeal 16S rRNA from cDNA samples of peat soil microcosms (3.2.1 and 3.2.2) were amplified (Table 11) using the primer pairs 27F/907R and Arch21Fa/ARC915 (Table 9), respectively.

Table 10   PCR reaction mix and thermoprotocol for the M13-PCR

PCR reaction mix		Thermoprotocol		
Chemical[a] (conc. of stock)	Volume (final conc.)	Step	Temp.	Time[b]
10x PCR buffer	2 µl	Initial deanturation	95°C	5′
MgCl$_2$ (25 mM)	2 µl (2.5 mM)	Denaturation (D)	95°C	60″
Nucleotides (2 mM each)	2 µl (0.2 mM)	Annealing (A)	54°C	45″
M13uniF (10 µM)[c]	0.4 µl (0.2 µM)	Elongation (E)	72°C	90″
M13uniR (10 µM)[c]	0.4 µl (0.2 µM)	30 cycles of D/A/E		
Taq polymerase (5 U·µl^{-1})	0.1 µl (0.025 U·µl^{-1})	Final elongation	72°C	5′
PCR-H$_2$O	11.1 µl	Storage	8°C	∞
Template[d]	2 µl			

[a]CRYSTAL Taq-DNA-Polymerase kit (biola products GmbH, Gödenstorf, Germany) containing the Taq polymerase, the PCR buffer, and the MgCl$_2$ solution was used for M13-PCR.

[b]Minutes: ′; seconds: ″.

[c]See Table 9.

[d]Cell material from colonies of clones were resuspended in 50 µl of PCR-H$_2$O and 2 µl of the resulting cell suspension was used as template for M13-PCR.

Table 11   Conditions for bacterial or archaeal 16S rRNA PCR for cloning

PCR reaction mix		Thermoprotocol		
Chemical (conc. of stock)	Volume (final conc.)	Step	Temp.	Time[a]
2.5x 5 PRIME MasterMix[b]	10 µl	Initial deanturation	95°C	5′
MgCl$_2$ (25 mM)	0.5 µl (2 mM[c])	Denaturation (D)	95°C	60″
BSA (5 mg·ml^{-1})	0.5 µl (100 ng·µl^{-1})	Annealing (A)	50°C	30″
27F or Arch21Fa (10 µM)[d]	0.5 µl (0.2 µM)	Elongation (E)	72°C	90″
907R or ARC915 (10 µM)[d]	0.5 µl (0.2 µM)	35 cycles of D/A/E		
PCR-H$_2$O	12 µl	Final elongation	72°C	10′
Template[e]	1 µl	Storage	8°C	∞

[a]Minutes: ′; seconds: ″.

[b]5 PRIME GmbH, Hilden, Germany.

[c]1.5 mM Mg^{2+} was added with the 2.5x 5 PRIME MasterMix containing 3.75 mM Mg(OAc)$_2$.

[d]See Table 9.

[e]RT-PCR reaction mix (2.5.6) containing variable amounts of cDNA.

2.5.7.3.   Bacterial 16S rRNA PCR for Illumina sequencing

Primers Bakt_341F/Bakt_805R (Table 9) were selected to amplify fragments (460 bp) of bacterial 16S rRNA genes or reversly transcribed 16S rRNA from DNA or cDNA samples of earthworm gut contents (3.3.2). The amplified fragments cover the variable regions V3 and V4 of 16S rRNA genes and the selected primers cover a large diversity of known bacterial phyla [202]. Complementation of the mitochondrial 16S rRNA gene (KP263414) and the 18S

rRNA gene (NR_132222) of *Saccharomyces cerevisiae* with the selected primers was analysed. This was necessary to avoid amplification of substrate specific DNA fragments from DNA or cDNA samples of gut content microcosms that were supplemented with *S. cerevisiae* cell lysate (containing high amounts of nucleic acids) (2.2.2). The forward primer Bakt_341F had three mismatches to the 18S rRNA gene and six mismatches to the mitochondrial 16S rRNA gene. The reverse primer Bakt_805R had three mismatches to the 18S rRNA gene and two mismatches to the mitochondrial 16S rRNA gene. Thus amplification of *S. cerevisiae* cell lysate derived DNA fragments with the selected primers was unlikely. Indeed, no such sequences could be found in libraries of 16S rRNA and 16S rRNA gene sequences after Illumina sequencing (2.5.10). PCR for Illumina sequencing (Table 12) was conducted by Microsynth.

Table 12   Conditions for bacterial 16S rRNA PCR for Illumina sequencing

PCR reaction mix		Thermoprotocol		
Chemical (conc. of stock)	Volume (final conc.)	Step	Temp.	Time[a]
5x Kapa Reaction Buffer[b]	5 µl	Initial deanturation	95°C	3′
Nucleotides (10 mM each)[b]	0.8 µl (0.32 mM)	Denaturation (D)	98°C	20″
Bakt_341F (4 µM)[c]	2.5 µl (0.4 µM)	Annealing (A)	56°C	30″
Bakt_805R (4 µM)[c]	2.5 µl (0.4 µM)	Elongation (E)	72°C	30″
PCR-H$_2$O	8.7 µl	20 cycles of D/A/E		
Kapa DNA Polymerase (1 U·µl^{-1})[b]	0.5 µl	Final elongation	72°C	5′
Template (2.5 ng·µl^{-1} cDNA or DNA)	5 µl	Storage	10°C	∞

[a]Minutes: ′; seconds: ″.

[b]A KAPA HiFi HotStart PCR Kit (KapaBiosystems, Wilmington, USA) was used.

[c]See Table 9.

2.5.7.4.   Hydrogenase specific PCR

Optimal conditions for hydrogenase specific PCR with newly designed primers (Table 16) were determined by stepwise varying the following parameters: concentrations of Mg^{2+} and primers, annealing temperature, number of cycles. Environmental DNA samples (from peat microcosms) were used as template during PCR evaluation. Final PCR conditions and thermoprotocols that yielded the best compromise between quality (i.e., no or little unspecific products with fragment length differing from expected ones) and quantity (i.e., intensity of PCR product bands in agarose gels) are listed in Table 13 and Table 14. Hydrogenase specific PCR was conducted for root and gut content microcosms (3.2.2 and 3.3.1).

Table 13   Concentrations of chemicals for hydrogenase specific PCR

Hydrogenase target group	[FeFe]	Group 4 [NiFe] (Bac/Arc)	Group 4 [NiFe] (Gammaprot.)	Group 1 [NiFe] (Bacteria)
Primer pair[a]	HydH1f / HydH3r	NiFe-uniF(b) / NiFe-uniR	NiFe-gF / NiFe-gR	NiFe1-F / NiFe1-R
Chemical (conc. of stock)	Volume (final conc.)			
2.5x 5 PRIME MasterMix[b]	10 µl	10 µl	10 µl	10 µl
$MgCl_2$ (25 mM)	1.5 µl (3 mM[c])	1.5 µl (3 mM[c])	1.5 µl (3 mM[c])	1.5 µl (3 mM[c])
BSA (5 mg·ml^{-1})	0.5 µl (100 ng·µl^{-1})	0.5 µl (100 ng·µl^{-1})	0.5 µl (100 ng·µl^{-1})	0.5 µl (100 ng·µl^{-1})
each Primer (10 µM)	5 µl (2 µM)	1.25 µl (0.5 µM)	1 µl (0.4 µM)	2.5 µl (1 µM)
PCR-H_2O	2 µl	9.5 µl	10 µl	7 µl
Template[d]	1 µl	1 µl	1 µl	1 µl

[a]See Table 16.

[b]5 PRIME GmbH.

[c]1.5 mM Mg^{2+} was added with the 2.5x 5 PRIME MasterMix containing 3.75 mM $Mg(OAc)_2$.

[d]Either RT-PCR reaction mix (2.5.6) containing variable amounts of cDNA or DNA (50 ng·µl^{-1}).

Table 14   Thermoprotocols for hydrogenase specific PCR[a]

Hydrogenase target group	[FeFe]	Group 4 [NiFe] (Bac/Arc)	Group 4 [NiFe] (Gammaprot.)	Group 1 [NiFe] (Bacteria)
Initial deanturation	95°C / 5′	95°C / 5′	95°C / 5′	95°C / 5′
Denaturation (D)	95°C / 45″	95°C / 45″	95°C / 45″	95°C / 45″
Annealing (A)	55°C / 45″	50°C / 45″	52.5°C / 45″	59°C / 45″
Elongation (E)	72°C / 90″	72°C / 90″	72°C / 120″	72°C / 120″
Cycles of D/A/E	40x	40x	40x	35x
Final elongation	72°C / 5′	72°C / 5′	72°C / 5′	72°C / 5′
Storage	8°C / ∞	8°C / ∞	8°C / ∞	8°C / ∞

[a]Minutes: ′; seconds: ″.

2.5.8.   Construction of clone libraries

Cloning was performed to isolate single DNA fragments from PCR products that were derived from DNA or cDNA samples of peat, soil, or earthworm gut content microcosms (3.2.1, 3.2.2, 3.2.2, and 3.3.1). This isolation was done by insertion of the DNA fragments into vector plasmids via ligation (2.5.8.1) and subsequent transformation of the plasmids in competent cells of *Escherichia coli* (2.5.8.2). Plasmids containing the DNA fragments were than reproduced during growth of the transformed cells on agar plates (2.3.5.2). Cell material of colonies of clones was used to amplify inserted DNA fragments via M13-PCR (2.5.7.1). Resulting PCR products were used for Sanger sequencing (2.5.9).

2.5.8.1.   Ligation

PCR-derived DNA fragments were ligated into linearized vector plasmids of approximately 3 kbp length (pGEM-T Vector System II, Promega).   Vector plasmids had a 3′-thymidine-overhang at both ends within the multiple cloning site (MCS) (i) to prevent recirculazation and (ii) to provide a compatible overhang for PCR products generated by Taq DNA polymerase.   Ligation was optimized by performing the reaction at a molar insert to vector ratio of 1:1.   The amount of insert DNA that had to be added to the ligation reaction (Table 15) to achieve this ratio was calculated according to Equation 6.   The ligation reaction was set up in a water bath at room temperature and than placed in a refrigerator to allow the reaction mix to slowly cool down to 4°C and therby transcending the optimal temperature for the ligase.

Equation 6   Molar insert to vector ratio

$$insert\ (ng) = \frac{vector\ (ng) \times insert\ size\ (bp)}{vector\ size\ (bp)} \times (molar\ insert\ to\ vector\ ratio)$$

$insert\ (ng)$, amount of insert; $vector\ (ng)$, amount of vector used for ligation reaction (25 ng for 5 µl reaction); $insert\ size\ (bp)$, size of the insert; $vector\ size\ (bp)$, size of the pGEM-T vector (3000 bp).

Table 15   Composition of the ligation reaction

Component	Volume
2 × Rapid Ligation Buffer (Promega)	2.5 µl
pGEM-T vector (50 ng µl⁻¹)	0.5 µl
PCR product, i.e., insert	0.5 - 1.5 µl
T4 DNA ligase (3 Weiss units µl⁻¹)	0.5 µl
PCR-H_2O	ad 5 µl

2.5.8.2.   Transformation

50 µl of glyzerol cultures of competent *Escherichia coli* JM 109 cells (Promega) that were stored at -80°C were thawed on ice, gently mixed with 2 µl of circulized vector plasmids (2.5.8.1), and incubated for 30 min on ice.   Transformation was performed by a heat shock at exactly 42°C for 50 sec in a water bath.   Cells were placed back on ice for two minutes immediately after the heat shock.   950 µl SOC medium (2.3.4) were added and the cells were incubated for 90 min at 37°C.   Finally, cell suspensions were streaked out on agar plates (2.3.5.2) to perform blue/white screening (2.5.8.3).

2.5.8.3.   Blue/white screening

Blue/white screening was performed on agar plates (2.3.5.2) containing ampicillin [364]. The ampicillin prevented growth of plasmid-free cells while cells with vector plasmids (encoding

for β-lactamase, which hydrolyzes ampicillin) could grow. Cells containing self-ligated vector plasmids without inserts formed blue colonies while cells containing vector plasmids with inserts formed white colonies on the agar plates. Blue staining of colonies resulted from the conversion of the colorless X-Gal (an analogue of lactose) to a blue product. This reaction is catalyzed by the β-galactosidase that is encoded by *lacZ*. *lacZ* is located on the vector plasmid and is expressed in the presence of IPTG. The MCS of the vector plasmid is located within *lacZ*. Thus, *lacZ* is interrupted when an insert is ligated into the MCS. Cells that harbor vector plasmids with inserts had no β-galatosidase activity, could not convert X-Gal, and therefore formed white colonies as a result of *lacZ* interruption. Cells with self-ligated vectors had β-galatosidase activity, converted X-Gal, and therefore formed blue colonies. White colonies were picked and resuspended in 50 µl PCR-H_2O. This cell suspension was used as template for M13-PCR (2.5.7.1), which was done to check the length of inserts and to amplify inserts for Sanger sequencing (2.5.9).

2.5.9. Sequencing by chain-termination

Sequencing by chain-termination (also known as Sanger sequencing) [367] was performed to determine the sequence of M13-PCR products (2.5.7.1) derived from constructed clone libraries (2.5.8). Purification of PCR products and sequencing was done by Macrogen (Amsterdam, the Netherlands). M13-PCR products with fragment length lower than 1 kbp were sequenced with the primer M13uniF (Table 9). Cloned group 1 [NiFe]-hydrogenase gene fragments (approximately 1.5 kbp) were sequenced from both ends using primers M13uniF and M13uniR (Table 9).

2.5.10. Sequencing by synthesis

Sequencing by synthesis (also known as Illumina sequencing) [20] was performed for bacterial 16S rRNA and 16S rRNA gene sequences amplified from DNA and cDNA samples of earthworm gut content microcosms (2.5.7.3). Sequencing was done by Microsynth using Illumina MiSeq sequencing technology (Illumina, San Diego, USA).

2.6. Sequence analyses and phylogenetic calculations

2.6.1. Analyses of sequences derived from clone libraries

Residual vector sequences and sequences fragments of low quality at both ends of the Sanger sequenced (2.5.9) M13-PCR products (2.5.7.1) were removed using the MEGA

software (http://www.megasoftware.net; release 5.1. [429]). Trimmed nucleic acid sequences were aligned and than clustered within OTUs (Opperational taxonomic units) as explained below.

2.6.1.1.   Alignment of 16S rRNA sequences and check for chimeric sequences

Bacterial and archaeal 16S rRNA complementary DNA sequences (approximately 900 bp in length) were aligned with the SINA webaligner (http://www.arb-silva.de [340]), and imported into the latest 16S rRNA gene-based database available from the SILVA hompage [341] within ARB. Chimeric sequences were identified by comparing the phylogenetic position of the first and last 300 nucleotides of a sequence in the 16S rRNA gene-based tree from SILVA. Sequence fragments were added to the tree using the ARB parsimony tool "quick add marked." Sequences where the two 300 nucleotide fragments clustered differentially were regarded as chimeric sequences and excluded from further analyses.

2.6.1.2.   Clustering of 16S rRNA sequences into OTUs

Archaeal and bacterial 16S rRNA sequences were clustered into OTUs based on a similarity cutoff of 95% and 87.5%, respectively, using the DOTUR software [381]. Minimum 16S rRNA sequence similarities of 95% and 87.5% are considered conservative boundaries at the genus- and family-level, respectively [492]. Representative sequences of each OTU were compared with those in public databases using the Basic Local Alignment Search Tool (BLAST) [497]. Closest cultured organisms and accession numbers of the sequence with the highest identity for each bacterial OTU representative sequences are listed in Table A2 and Table A3. Closest cultured and uncultured BLAST-hits for archaeal OTU representative sequences are given in Figure 14 and Figure 37. OTUs were taxonomically assigned based on their position in the 16S rRNA tree from SILVA.

2.6.1.3.   Alignment of hydrogenase gene and transcript sequences

Initially, alignments for the different groups of hydrogenases were constructed from publicly available hydrogenase gene sequences (Table A1). These hydrogenase gene sequences were in silico translated in amino acid sequences with the ARB software (http://www.arb-home.de; version 2005 [264]), prealigned with the ClustalW algorithm [437], and the alignment was refined manually. Nucleic acid sequences were realigned according to the aligned amino acid sequences. Hydrogenase gene and transcript sequences obtained in

this study were in silico translated in ARB, prealigned using the integrated aligner tool and an aligned amino acid sequence as reference, and the alignement was refined manually.

2.6.1.4.   Calculation of similarity correlation plots

A total number of 229 [FeFe]-, 184 group 4 [NiFe]-, and 329 group 1 [NiFe]-hydrogenase genes from 496 species were retrieved from GenBank [19], in silico translated, and aligned as described above (2.6.1.3). Aligned 16S rRNA sequences of the 496 species were retrieved from the 16S rRNA gene database from the SILVA homepage (www.arb-silva.de) [341]. Hydrogenase amino acid sequences corresponding to regions amplified with primers listed in Table 16 and approximately 1300 bp (positions 122 to 1420 of the 16S rRNA gene from *Escherichia coli* [GenBank accession no. ANWG01000004]) from the 16S rRNA gene sequences were used for the calculation of similarity plots. Distance matrices for pairwise comparisions of the hydrogenase amino acid sequences and the 16S rRNA gene sequences were calculated with the MEGA software. Similarity was expressed as shown in Equation 7. This approach is similar to those of previous studies [320, 342].

Equation 7   Distance and Similarity of nucleic acid or amino acid sequences

$$S = 1 - D$$

S, similarity; D, dissimilarity obtained from distance matrices.

2.6.1.5.   Clustering of hydrogenase gene and transcript sequences into OTUs

In silico translated hydrogenase gene and transcript sequences were clustered based on the 80% amino acid sequence similarity cutoff evaluated in this study (3.1.2) using DOTUR. Representative sequences of each OTU were compared with those in public databases using protein BLAST [497]. OTUs were taxonomically assigned according to their position in hydrogenase amino acid sequence based phylogenetic trees.

2.6.2.   Analyses of Illumina sequencing-derived data

Primary analyses of sequence data derived from Illumina sequencing (2.5.10) were done by Microsynth using the QIIME software package [44]. A total of 1965642 demultiplexed, stitched, and quality filtered 16S rRNA sequences and 16S rRNA gene sequences were obtained from RNA and DNA samples of anoxic gut content microcosms (3.3.2). 76609 sequences were identified as chimeras using the ChimeraSlayer software [146] implemented in QIIME. Chimeric sequences were excluded from further sequence analyses. Non-chimeric

sequences were clustered into OTUs based on a nucleic acid sequence similarity cutoff of 99%, which is a conservative threshold similarity for assigning organisms to different species [417, 418]. Resulting OTUs were classified based on the SILVA [341] incremental aligner SINA [340]. 161650 singeltons (OTUs that occurred only once in the complete dataset) were excluded. 9251 sequences could not be assigned to any bacterial OTU (130 of these sequences were affiliated with *Archaea*) and were also excluded from further analyses. The remaining dataset comprised 1715804 sequences and was used for the calculation of rarefaction curves (Figure 41) and taxa level plots (Figure 42).

2.6.3.   Coverage and rarefaction analyses

The coverage was calculated according to Equation 8 and indicates the ratio of detected to expected OTUs [137].

Equation 8   Coverage

$$C = \left(1 - \frac{N_X}{n}\right) \times 100$$

C, coverage (%); N_X, number of OTUs that occur once; n, total number of sequences.

Rarefaction analyses enable to compare the observed richness in samples that have not been sampled equally. Rarefaction curves and 95%-convidence intervals were calculated according to the Hurlbert-rarefaction concept [157, 179] using the aRarefact-Win software available at http://strata.uga.edu/software/. Flat and plateauing curves indicate that sampling was sufficient and most of the expected diversity was covered by the sampling effort. Steeply increasing curves indicate that sampling was not sufficient and a more thorough sampling would be sufficient to cover most of the expected diversity in the sample.

2.6.4.   Calculation of phylogenetic trees

Phylogenetic trees were calculated using the maximum parsimony, neighbor joining, or maximum likelihood method in the ARB software [264]. Branch lengths are based on the maximum parsimony tree unless otherwise stated. Nodes congruent with all three treeing methods are indicated with filled circles. Nodes congruent with two treeing methods are indicated with open circles. Bootstrap values are averages from the maximum parsimony tree (1000 resamplings), the neighbor joining tree (1000), and the maximum likelihood tree (100). Bootstrap values were shown for nodes that were congruent with all three treeing methods.

2.6.5. Nucleotide sequence accession numbers

Sequences obtained during this study were submitted to the European Nucleotide Archive with the following accession numbers: FR715716-FR715893, FR717338-FR717357, FR717732-FR717817, HG324304-HG325724, LK024545-LK026322, LN555754-LN556287.

2.7. Calculations and statistical analyses

2.7.1. Carbon and electron balances

2.7.1.1. Recoveries of carbon and reductant in cellulose-supplemented peat soil microcosms (3.2.1)

Concentrations of a compound after the preincubation in cellulose supplemented and unsupplemented treatments (2.1.2.1) were subtracted from concentrations of this compound at the end of the incubation to calculate net amounts. Net amounts from controls were subtracted from that of cellulose treatments to calculate recoveries. Approximately 37 mM carbon and 148 mM reductant were supplemented by the addition of cellulose. The following numbers of electrons/carbon atoms per molecule were used to calculate net amounts of reductant/carbon: CH_4, 8/1; CO_2, 0/1; Acetate, 8/2; Butyrate, 20/4; Propionate, 14/3.

2.7.1.2. Recoveries of carbon and reductant in soil-free root and root-free soil microcosms (3.2.2)

Concentrations of a compound at the start of the incubation were subtracted from concentrations of this compound at the end of the incubation to calculate net amounts. Net amounts from controls were subtracted from that of formate treatments to calculate recoveries. A total of 5.6 and 5.9 mM formate were supplemented in formate treatments of soil-free root and root-free soil microcosms, respectively. The amount of carbon and reductant derived from formate was set to 100%. The following numbers of electrons/carbon atoms per molecule were used to calculate net recoveries of reductant/carbon: CH_4, 8/1; CO_2, 0/1; acetate, 8/2; butyrate, 20/4; propionate, 14/3; formate, 2/1; H_2, 2/0.

2.7.1.3. Recoveries of carbon and reductant in peat soil microcosms supplemented with ethanol, butyrate, or propionate (3.2.3)

Cumulative amounts of CH_4 and CO_2 were calculated from amounts of gases formed in the timeframe between two flushing events (i.e., when gasphases were exchanged with sterile

N_2 as indicated in Figure 31). Cumulative amounts of CO_2 were corrected as follows: When gas phases were flushed, CO_2 could not be removed completely since some CO_2 remained dissolved in the liquid phase. Those leftover concentrations of CO_2 could not be detected during the gas chromatographic measurments directly after flushing as CO_2 in gas and liquid phases were not yet in equilibrium. This resulted in very low CO_2 concentrations (close to the detection limit) measured directly after flushing. At the second measurement after each flushing event, gaseous and dissolved CO_2 were back in equilibrium, and relatively high concentrations of CO_2 were detected. As a result of the re-emergeing equilibrium, the increase in CO_2 per time interval was much higher between the first two CO_2 measurements after each flushing event compared to the increase in CO_2 in the same time interval before flushing and after the second measurement following a flushing event. To correct the CO_2 concentrations, linear CO_2 production was assumed after flushing of the gas phase with N_2. The correction of cumulative CO_2 concentrations influences carbon recoveries and overall stoichiometries but not the recoveries of reductant (Table 23). This correction was not necessary for CH_4 since the solubility of CH_4 is rather low compared to CO_2 (Table 8). Cumulative amounts of CH_4 and CO_2 in unsupplemented controls were subtracted from cumulative amounts of CH_4 and CO_2 formed in butyrate, ethanol, and propionate treatments between the end of the preincubation and the end of the main incubation (2.1.2.2). This resulted in net-amounts of CH_4 and CO_2. Finally, amounts of carbon atoms and electrons from net-amounts of CH_4 and CO_2 were divided by the amounts of carbon atoms and electrons supplemented as either butyrate, ethanol, or propionate. The following numbers of electrons/carbon atoms per molecule were used for the calculations: CH_4, 8/1; CO_2, 0/1; Ethanol, 12/2; Butyrate, 20/4; Propionate, 14/3.

2.7.1.4.   Recoveries of carbon and reductant in earthworm gut content microcosms supplemented with *S. cerevisiae* cell lysate

An elemental formula of $CH_{1.613}O_{0.557}N_{0.158}$ and a molar weight of 26.09 g·C-mol^{-1} for *S. cerevisiae* biomass [462] was used to calculate carbon recoveries for anoxic earthworm gut content microcosms supplemented with lysed *S. cerevisiae* cells (Table 27). The total carbon recovery was calculated according to Equation 9. Approximately 2400 µmol *S. cerevisiae*-derived carbon per gram of earthworm gut content fresh weight (g_{FW}) was supplemented to treatments with cell lysate. The average redox state of carbon was calculated to be 0 based on the elemental formula above. Thus, each C-mol may donate 4 mols of electrons if it is completely oxidized to the redox state of carbon in CO_2 (+4). This factor of 4 mols of electrons per mol of carbon was used to calculate the electron recovery according to Equation 10. Electrons derieved from the oxidation of organic nitrogen were not included into electron recoveries since nitrogen-containing compounds (e.g., N_2, N_2O or NH_4^+) were not measured.

Equation 9   Total carbon recovery

$$R_c = \frac{\sum(n_X \times C_X)}{n_c} \times 100$$

R_c, total carbon recovery in %; n_X, net molar amount of a compound X (CO_2, H_2, acetate, succinate, or propionate) that was formed during the incubation; C_X, number of carbon atoms per molecule of compound X (C_X for CO_2, H_2, acetate, succinate, and propionate is 1, 0, 2, 4, and 3, respectively); n_c, amount of *S. cerevisiae*-derived carbon supplemented (2400 µmol·g$_{FW}^{-1}$).

Equation 10   Total electron recovery

$$R_e = \frac{\sum(n_X \times e_X)}{n_e} \times 100$$

R_e, total electron recovery in %; e_X, number of electrons per molecule of compound X that can be transferred if the compound is completely oxidized (e_X for CO_2, H_2, acetate, succinate, and propionate is 0, 2, 8, 14, and 14, respectively); n_e, amount of electrons that can be transferred if the carbon of the supplemented *S. cerevisiae* cell lysate is completely oxidized (9600 µmol·g$_{FW}^{-1}$).

2.7.2.   Thermodynamic calculations

Gibbs free energies (ΔGs) were calculated for processes potentially linked to syntrophic methanogenesis (i.e., syntrophic fermentations, acetogenesis, and methanogensis) and for the FHL reaction (Figure 32 and Figure 16) to determine the likelihood of a certain process to contribute to the flow of carbon and reductant. ΔGs were calculated according to Equation 11 to Equation 16. This approach includes the temperature dependent effect of the entropy on the ΔG which is important for temperatures other than 25°C [65]. H_2, CO_2, and CH_4 were assumed as gaseous compounds and all other compounds were assumed as dissolved.

Equation 11   Standard Gibbs free energy

$$\Delta G^0 = \sum \Delta G_f{}^0 \,(products) - \sum \Delta G_f{}^0 \,(reactants)$$

ΔG^0, Gibbs free energy under standard conditions (298.15 K, 1 at partial pressure for gasous compounds, 1 M concentarions for dissolved compounds, pH = 0); $\Delta G_f{}^0$, Gibbs free energies of formation (listed in ref [432]).

Equation 12   Standard reaction enthalpy

$$\Delta H^0 = \sum \Delta H_f{}^0 \,(products) - \sum \Delta H_f{}^0 \,(reactants)$$

ΔH^0, reaction enthalpy under standard conditions; $\Delta H_f{}^0$, Gibbs free energies of formation (listed in refs [231, 425]).

Equation 13   Entropy change

$$\Delta S^0 = \frac{\Delta H^0 - \Delta G^0}{T_S}$$

ΔS^0, entropy change of a reaction; T_S, temperature under standard conditions (298.15 K).

Equation 14   Standard Gibbs free energy at a given temperature

$$\Delta G_T{}^0 = \Delta H^0 - \Delta S^0 \cdot T$$

$\Delta G_T{}^0$, temperature-corrected Gibbs free energy under otherwise standard conditions; T, actual temperature (e.g., 278.15 K or 288.15 K).

Equation 15   Gibbs free energy

$$\Delta G = \Delta G_T{}^0 + R \cdot T \cdot lnK$$

ΔG, enthalpy- and entropy-corrected Gibbs free energy at actual concentrations of products and reactants, actual pH, and the actual temperature; R, universal gas constant ($8.314 \cdot 10^{-3}$ kJ·mol^{-1}·K^{-1}); K, equilibrium constant.

Equation 16   Equilibrium constant

$$K = \frac{[C]^c \cdot [D]^d}{[A]^a \cdot [B]^b}$$

$[A]$ / $[B]$ and $[C]$ / $[D]$, concentrations of reactants and products (in M for dissolved compounds and at for gaseous compounds), respectively; a / b and c / d represent the stoichiometries of reactants and products in a reaction, respectively. A concentration of 10 µM was assumed when a certain substance could not be detected but its concentration was needed for the calculation of the ΔG.

2.7.3.   Average and standard deviation

All incubation experiments were conducted in variable numbers of replicates. Averages and standard deviations were calculated based on the concentrations of compounds detected in the different replicates according to Equation 17 and Equation 18.

Equation 17   Average

$$\bar{x} = \frac{1}{n} \times \sum_{i=1}^{n} x_i$$

$\bar{x}$, average; n, number of replicates; i, continuous index that runs from 1 to n; x_i, concentration of a compound measured for a certain replicate.

Equation 18   Standard deviation

$$S = \sqrt{\frac{1}{n-1} \times \sum_{i=1}^{n} (x_i - \bar{x})^2}$$

S, standard deviation.

2.8.   Chemicals, gases, and labware

A Seralpur Pro 90 CN ultrapure water purification system (Seral Erich Alhäuser, Ransbach-Baumbach, Germany) was used to produce ddH_2O with a conductivity of less than 0.055 µS·cm^{-1}. ddH_2O was sterile filtered and autoclaved to produce PCR-H_2O. Syringes with 14- to 20-gauge needles (BD Biosciences, Heidelberg, Germany) were used to take samples from gas and liquid phases in microcosm experiments. All chemicals, gases, and labware were obtained from Sigm Aldrich (Steinheim, Germany), Fluka (Buchs, Switzerland), Applichem (Darmstadt, Germany), Rießner (Lichtenfels, Germany), Eppendorf (Hamburg, Germany), BioRad (Hercules, USA), and Carl Roth (Karlsruhe, Germany) unless otherwise noted.

2.9.   Contribution of other workers to this dissertation

Samplings, set-up of experiments, measurements, data analyses, and interpretation of data were conducted by myself unless otherwise noted below. Most of the data that is presented in this dissertation was published already or will be published soon in peer-reviewed journals [177, 386, 387, 388]. That data is presented and discussed here in a manner that is similar to how the information was presented in these publications.

2.9.1.   Hydrogenase primer design and hydrogenase gene and transcript sequence analyses

Set-up of hydrogenase amino acid sequence alignments, primer design and calculation of correlation plots were conducted by myself. PCR optimization for the amplification of [FeFe]-hydrogenase gene sequences was performed by myself [385]. PCR optimization for the amplification of group 1 and group 4 [NiFe]-hydrogenase gene sequences was performed by Maik Hilgarth and Katharina Borst, respectively.

2.9.2.   Experiments with peat soil microcosms

2.9.2.1.   Cellulose degradation experiments

The experimental design was conceptionalized by Harold L. Drake, Marcus Horn and myself. Sampling of peat soil, set-up of microcosms, all molecular work as well as data analyses and interpretation of the data were conducted by myself. Sampling of gas and liquid phases from microcosms as well as GC and HPLC measurements were performed by Ralf Mertel.

2.9.2.2.   Syntrophic oxidation experiments

Conceptionalization of the experimental design was conducted by myself. Linda Hink performed sampling of peat soil, set up of microcosms, sampling of gas and liquid phases, and all molecular work. Thermodynamic calculations, sequence data analyses, and interpretation of the results were conducted by myself.

2.9.2.3.   Experiments with root-free soil and *Carex* roots

Microcosm experiments were conceptionalized and performed by Sindy Hunger and Anita Gößner. Sindy Hunger provided DNA samples of *Carex* root microcosms for the amplification of hydrogenase gene fragments, which was conducted by Maik Hilgarth. Thermodynamic calculations, hydrogenase gene sequence analyses, and interpretation of thermodynamic calculations and hydrogenase gene sequence data were performed by myself.

2.9.3.   Experiments with earthworm gut contents

2.9.3.1.   Glucose supplemented gut content microcosms

Physiological data and 16S rRNA sequence analyses of experiments with glucose-supplemented *L. terrestris* gut content microcosms were published in ref [490]. Pia Wüst, who conducted the above mentioned experiments, provided DNA and RNA samples from these experiments. These DNA and RNA samples were used for the amplification of [FeFe]-hydrogenase transcripts (conducted by Susanne Hellmuth) and group 4 [NiFe]-hydrogenase genes and transcripts (conducted by Katharina Borst). Hydrogenase gene and transcript sequence analyses and interpretation of the data were performed by myself.

2.9.3.2.   Gut content microcosms supplemented with *S. cerevisiae* cell lysate

Experiments were conceptionalized by Harold L. Drake and myself. Peter Depkat-Jakob cultured cells of *S. cerevisiae* and produced the cell lysate. Lydia Zeibich performed the set-up of gut content microcosms, GC and HPLC analyses, and the extraction of DNA and RNA. PCR-amplification, Illumina sequencing, and clustering of sequences into OTUs was performed by Microsynth. Sequence analyses and interpretation of the data were conducted by myself.

3. RESULTS

3.1. Hydrogenases as molecular markers for H₂-producing and H₂-consuming prokaryotes

3.1.1. Design of PCR primers specific for hydrogenase genes

[FeFe]-hydrogenases differ in the composition of subunits and domains but all known [FeFe]-hydrogenases contain at least the so called H-cluster domain that harbors the active site of these enzymes [460]. Three characteristic and unique amino acid sequence signatures (designated as FeFe_P1, FeFe_P2, and FeFe_P3 [461]) are conserved within the H-cluster domains of [FeFe]-hydrogenases. The nucleic acid sequences of the signatures FeFe_P1 and FeFe_P3 from 188 publicly available [FeFe]-hydrogenases genes (Table A1) were screened for suitable primer binding sites. The design of degenerate primers followed the principals of the consensus degenerate hybrid oligonucleotide primer strategy [356]. Thus, primers were constructed with a degenerate 11-12 bp 3'-core region followed by a 5'-consensus clamp. A higher number of ambiguities was included in the 3'-core region to allow for an efficient binding of the primers to variable positions at the primer binding sites and therefore a specific amplification during the initial PCR-cycles. A viewer number of ambiguities was included in the 5'-consensus clamp region of the primers and none or little destabilizing mismatches [330] were accepted. In addition, inosine as a less destabilizing base [470] was used at positions with a very high variability in order to decrease the degeneracy of the primers. The length of the 5'-consensus clamp region determine the melting temperature of the degenerate primers.

[NiFe]-hydrogenases consist of at least a small and a large subunit [460]. The large subunits harbor two characteristic amino acid sequence motifs designated as L1 and L2 [461]. The amino acids of L1 and L2 form the direct protein environment of the active center in [NiFe]-hydrogenases similar as do the amino acids of the signatures FeFe_P1, FeFe_P2, and FeFe_P3 for the [FeFe]-hydrogenases (see text above). Primers specific for the genes encoding the large subunits of [NiFe]-hydrogenases were designed according to the nucleic acid consensus sequences of L1 and L2 from 184 and 329 aligned group 1 and group 4 [NiFe]-hydrogenase genes, respectively (Table A1). Primer design was according to the strategy explained for [FeFe]-hydrogenase primers. Primer specific for group 4 [NiFe]-hydrogenases of the *Gammaproteobacteria* (NiFe-gF/gR) were constructed in addition to universal group 4 [NiFe]-hydrogenase primers (NiFe-uniF/Fb/R). All newly designed hydrogenase primers are listed in Table 16.

Table 16   Sequences and properties of designed hydrogenase primers

Primer	Target group	Sequence (5'-3')[a]	Position	Deg.[b]
HydH1f	[FeFe] (*Bacteria*)	TIACITSITGYWSYCCIGSHTGG	524[c]	192
HydH3r	[FeFe] (*Bacteria*)	CAICCIYMIGGRCAISNCAT	1126[c]	64
NiFe-uniF	Group 4 [NiFe] (*Bacteria*)	GAIMGIRTITGYGGIATHTGY	715[d]	48
NiFe-uniFb[e]	Group 4 [NiFe] (*Bacteria*)	GARMGIGTITGYTCICTGTGY	715[d]	16
NiFe-uniR	Group 4 [NiFe] (*Bacteria*)	GTRCAISWIWIRCAIGGRTC	1585[d]	64
NiFe-gF	Group 4 [NiFe] (*Gammaproteobacteria*)	GAYCGIRTITGYGGIATYTGYGG	715[d]	32
NiFe-gR	Group 4 [NiFe] (*Gammaproteobacteria*)	GTRCAIGARTARCAIGGRTC	1585[d]	16
NiFe1-F	Group 1 [NiFe] (Bacteria)	GAGCGIATYTGYGGNGTNTGYAC	217[f]	128
NiFe1-R	Group 1 [NiFe] (Bacteria)	GMGCAGGCIAKGCANGGRTCRAA	1739[f]	128

[a]I, inosine. IUPAC nomenclature was used for mixed bases [70].

[b]Deg., degeneracy, i.e., the number of combinations for the degenerate primers.

[c]The 5' end in the nucleic acid sequence of the *Desulfovibrio vulgaris* [FeFe]-hydrogenase gene (GenBank accession no. AAS96246).

[d]The 5' end in the nucleic acid sequence of the *Escherichia coli* group 4 [NiFe]-hydrogenase gene (GenBank accession no. AAC75763).

[e]Primer NiFe-uniFb was designed to cover group 4 [NiFe]-hydrogenase genes that were not covered by primer NiFe-uniF.

[f]The 5' end in the nucleic acid sequence of the *Escherichia coli* group 1 [NiFe]-hydrogenase gene (GenBank accession no. AAC74058).

3.1.2.   Criteria for establishing hydrogenase OTUs

Hydrogenase amino acid sequence similarities did not correlate linearly to the corresponding 16S rRNA gene similarities. Multitudinous dots in the lower right corner of the plots in Figure 8 indicate that closely related organisms often harbor distantly related hydrogenases. In addition, one microorganism may have several homologous hydrogenase genes in its genome (Table A1), and these homologs often share little sequence similarities. This is reflected by the multiple dots at 100% 16S rRNA gene sequence similarity that have hydrogenase amino acid sequence similarities of less than 50% (Figure 8). While closely related microorganisms may have distantly related hydrogenases, distantly related microorganisms generally do not have closely related hydrogenases. A noticeable exception is found within the phylum *Thermotogae* where the [FeFe]-hydrogenases from *Thermotoga maritima* and other *Thermotoga* species share 98%-100% amino acid sequence similarity to the [FeFe]-hydrogenase of *Marinitoga piezophila* although *M. piezophila* and *T. maritima* do have only 83% 16S rRNA sequence similarity.
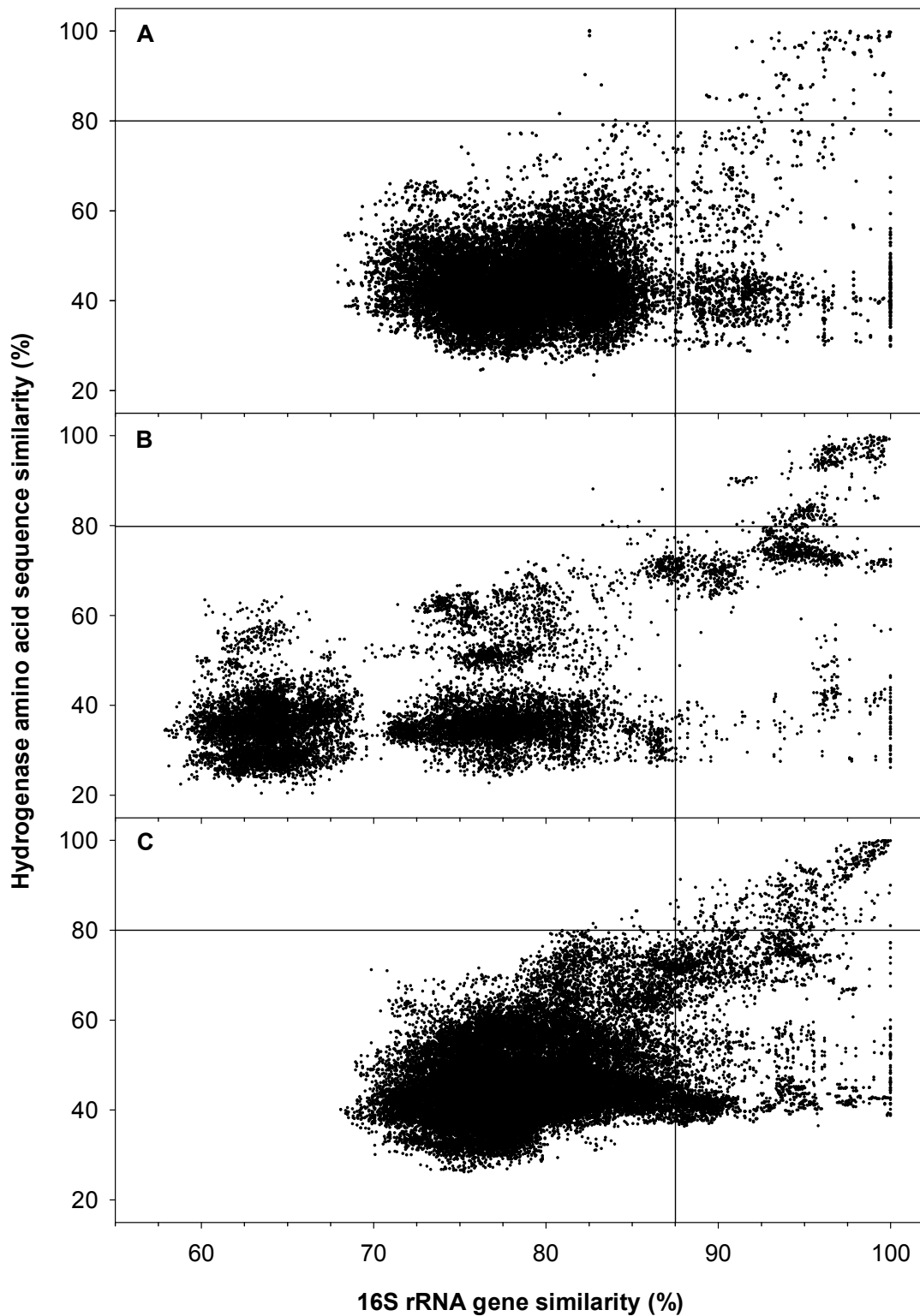
Figure 8   Correlation plot of hydrogenase amino acid sequence similarities versus 16S rRNA gene sequence similarities.

The vertical line at 87.5% 16S rRNA gene sequence similarity indicates a conservative family-level cutoff for 16S rRNA gene sequence based OTU assignment [492]. The horizontal line at 80% hydrogenase amino acid sequence similarity indicates the similarity cutoff for in silico-translated hydrogenase gene sequence based OTU assignment used in this study. Modified from refs [177] and [388].

Despite the abovementioned exception, the nonexistence of closely related [FeFe]-, group 1, and group 4 [NiFe]-hydrogenases in distantly related organisms underscore the idea that homologous hydrogenases originated from gene duplication and subsequent diversification and only to a minor extent from horizontal gene transfer [292, 460]. Homologous hydrogenases may differ in their structural compositions as well as enzyme characteristics, and they may get stabilized in the genome by performing different functions in vivo [11, 396]. Drawing accurate phylogenetic inferences for host organisms can be optimized if only hydrogenases with related functions are considered for amino acid sequence comparisons. A reclassification of hydrogenases based on the in vivo function would be helpful but is presently hard to achieve since no functional information is available for most of the hydrogenase gene sequences in the databases.

Similarity correlation plots between structural gene markers and corresponding16S rRNA genes can be used to calculate cutoffs for the assignment of environmental gene and transcript sequences to OTUs based on species, genus, family and phylum level [178, 200, 320, 342]. However, the non-linear correlation between hydrogenase amino acid sequences and corresponding 16S rRNA gene sequences as displayed in Figure 8 rendered such a classical stepwise taxa level based OTU assignment impossible. Nevertheless, the observation that closely related hydrogenases generally belong to microorganisms that share high 16S rRNA sequence similarities enabled an alternative standardized assignment of hydrogenase sequence OTUs. 90% of microorganism with hydrogenases that shared at least 80% amino acid sequence similarity showed 16S rRNA gene sequence similarities of ≥ 90.7%, ≥ 90.4%, and ≥ 93.4% for [FeFe], group 1, and group 4 [NiFe]-hydrogenases, respectively. In other words, all hydrogenase amino acid sequences that cluster within one OTU (based on a hydrogenase similarity cutoff of 80%) most probably belong two microorganisms of the same family (a conservative family-level cutoff for 16S rRNA gene sequences is 87.5% [492]).

Thus, in silico translated [FeFe]-, group 1 and group 4 [NiFe]-hydrogenase gene sequences obtained from environmental samples that share ≥ 80% similarity to publicly available hydrogenase amino acid sequences of pure cultures can be assigned to the family of the corresponding microorganism. In addition, all amplified environmental hydrogenase gene or transcript sequences that share ≤ 80% similarity to known hydrogenases can be assigned as one ('novel') family if they share ≥ 80% similarity to each other. Nevertheless, such 'novel' hydrogenases might still belong to organisms of known families since microorganisms that share high 16S rRNA sequence similarities can harbor distantly related hydrogenases (Figure 8). Furthermore, usage of the 80% hydrogenase amino acid sequence similarity cutoff for family level based OTUs can result in the overestimation of the diversity of hydrogen metabolizers in an environmental sample since several OTUs might belong to only one organism and represent homologous hydrogenases.

3.2. Anaerobic mineralization of plant-derived organic carbon and associated prokaryotic taxa in peatlands

3.2.1. Degradation of cellulose by peat soil anaerobes

Biomass of peat soil-covering plants (sedges and *Sphagnum* mosses) is the single most abundant source of carbon for the microbiota in peatlands [100, 208, 313], and cellulose is the dominant polymer in peatland plant-derived biomass [214, 305]. Thus, cellulose was chosen as model substrate for the analysis of hydrolytic fermentation processes at 5°C (annual mean temperature) and 15°C (a temperature reached in the peat soil during summer) in the exploratory field site Fen Schlöppnerbrunnen. 16S rRNA-based SIP was performed to identify key microbes that are associated to cellulose hydrolysis and the degradation of cellulose-derived sugars.

3.2.1.1. Effect of cellulose on the flow of carbon and reductant in anoxic peat soil microcosms at 5°C and 15°C

After an anoxic preincubation (2.1.2.1) of 17 d, CH_4 and CO_2 accumulated linearly during the subsequent 40 d of incubation in unsupplemented controls at 15°C (Figure 9A and B). Organic acids that were detected after the preincubation did not accumulate and were consumed during the 40 d of incubation (Figure 9D-F). CH_4 production was lower in unsupplemented controls at 5°C compared to 15°C (Figure 9A and G). This result is consistent with the finding that temperatures below 15°C greatly limited methanogenesis in lake sediments [498] and rice paddies [64]. Acetate, propionate, and (to a lesser extent) butyrate accumulated in unsupplemented controls at 5°C but not at 15°C, which suggests that aceticlastic methanogensis and syntrophic oxidation of propionate and butyrate were rate limiting at 5°C whereas hydrolysis of endogenous carbon sources was rate limiting at 15°C.

Table 17   Effect of cellulose on hydrogen partial pressures in anoxic microcosms

	15°C			5°C	
	Hydrogen partial pressure (Pa)			*Hydrogen partial pressure (Pa)*	
Time (d)	*Control*	*+ Cellulose*	*Time (d)*	*Control*	*+ Cellulose*
25	2.5	4.2	29	1.3	12.5
32	2.7	3.5	57	1.6	22.6
40	1.8	2.4	78	0.9	5.3

[a]Hydrogen partial pressures were measured in one of three replicates. Modified from ref [387].

15ºC

5ºC

● + cellulose   ○ unsupplemented
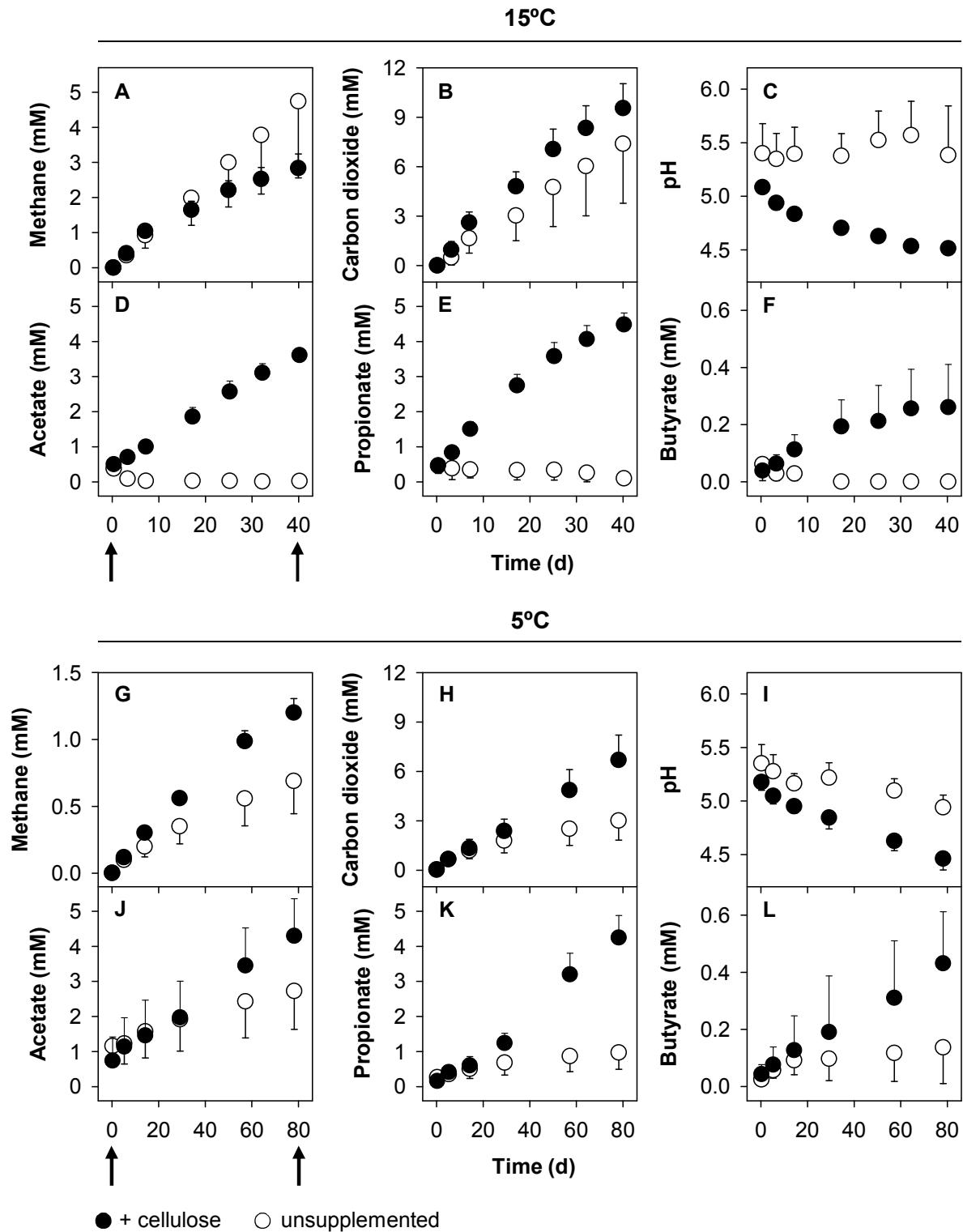
Figure 9   Effects of cellulose on the accumulation of gases, organic acids, and pH of preincubated anoxic microcosms.

A-F and G-L: microcosms incubated at 15°C and 5°C, respectively. Symbols: filled circles, treatments supplemented with [^{13}C]cellulose; open circles, unsupplemented control treatments. Gas concentrations are cumulative. Values are means of triplicates; error bars indicate standard deviations. Arrows indicate when samples were taken for RNA SIP analyses. Modified from ref [387].

15°C

5°C

■ + cellulose □ unsupplemented
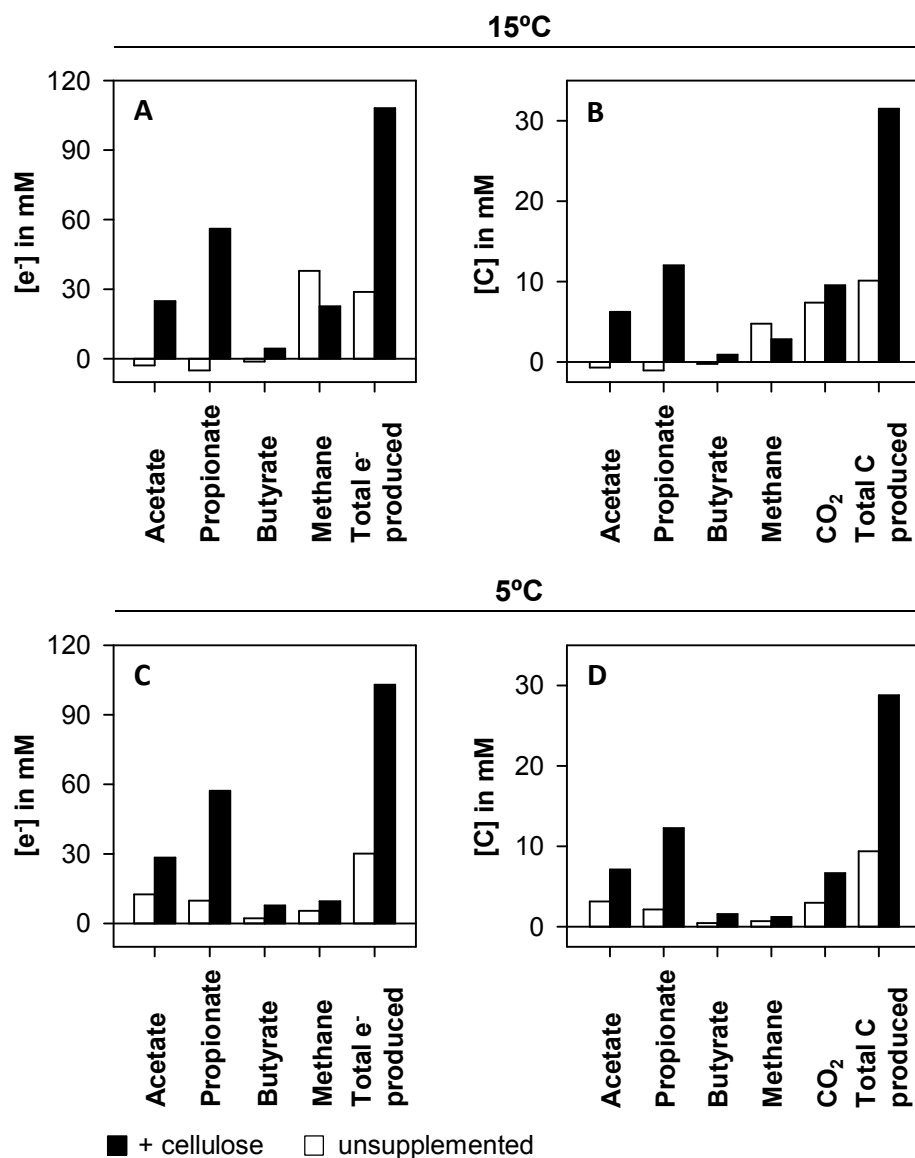
Figure 10   Amount of reductant (A and C) and carbon (B and D) produced or consumed in anoxic microcosms at 15°C after 40 d (A and B) and at 5°C after 80 d (C and D).

Black bars, treatments supplemented with [^{13}C]cellulose; white bars, unsupplemented control treatments. Negative values indicate consumption of a substance. Modified from ref [387].

Table 18   Recoveries of carbon/reductant (%) in [^{13}C]cellulose-supplemented microcosms

Temperature[a]	CO$_2$	CH$_4$	Acetate	Propionate	Butyrate	Sum
5° (78 d)	10/0	1/3	11/11	27/32	3/4	53/49
15° (40 d)	6/0	-5/-10[b]	19/19	35/41	3/4	58/54

[a]Recoveries were calculated for net amounts of a compound formed during 78 and 40 d of incubation for microcosms incubated at 5°C and 15°C, respectively.

[b]Negative values indicate that more CH$_4$ was produced in controls compared to cellulose treatments.

The enhanced production of CO_2 and organic acids and an overall increased turnover of carbon and reductant in cellulose treatments at 5°C and 15°C (Figure 9 and Figure 10) suggests a stimulatory effect of supplemental cellulose on the peat fermenters. This stimulatory effect endorsed the assumption that the capacity for cellulose hydrolysis exceeds cellulose availability in peat soil of the Fen Schlöppnerbrunnen. A stimulatory effect of supplemental cellulose was also observed in anoxic microcosms of tundra wetland soil, taiga pond sediment, agricultural soil, and oxic bog peat [211, 212, 323, 372], indicating that a limited availability of accessible cellulose is common to various habitats. Cellobiose and Glucose were not detected reinforcing that soluble breakdown products of cellulose hydrolysis were effectively consumed by cellulolytic fermenters and satellite microbes (i.e., non-cellulolytic sugar-degrading anaerobes like saccharolytic fermenters and acetogens) [244, 267]. CO_2, propionate and acetate were the main fermentation products and accumulated twice as fast at 15°C compared to 5° (Figure 9). Butyrate also accumulated but its concentrations were significantly lower than that of propionate and acetate. Traces of other fermentation products (H_2, ethanol, lactate, succinate, and formate) were occasionally detected. This fermentation profile indicates that different types of fermentation were ongoing in parallel.

During the first week of incubation, CH_4 production was slightly stimulated in cellulose treatments compared to unsupplemented controls at 15°C (Figure 9A). However, afterwards CH_4 production slowed down in the cellulose treatments whereas it was stable in the unsupplemented controls (Figure 9A). This decrease of the methanogenesis rate was likely due to the lower pH observed in cellulose treatments because methanogens are generally less active at acidic pH (even those that inhabit acidic environments) [481]. The inhibitory effect of the acidic pH was probably increased by high concentrations of undissociated organic acids that may have uncoupled part of the proton motife force and therby decreased energy conservation and growth of methanogens [168, 265, 359]. However, methanogenesis was stimulated despite higher concentrations of organic acids and a lower pH in cellulose treatments compared to unsupplemented controls at 5°C. It is likely that the inhibitory effect of pH and undissociated organic acids on methanogens was counter balanced by up to tenfold higher H_2 concentrations, which is stimulatory for methanogenesis [499], in cellulose compared to control treatments (Table 17).

Approximately half of the carbon and reductant that was supplemented as cellulose could be recovered at the end of the incubation at 5°C (78 days) and 15°C (40 days). Most of this carbon and reductant was stored in propionate, acetate, and CO_2 reinforcing that those were the predominant fermentation products. 'Negative recoveries' for CH_4 at 15°C indicate that CH_4 production was inhibited as discussed above.

3.2.1.2. Active bacterial taxa linked to the degradation of [^{13}C]cellulose

A total of 989 bacterial 16S rRNA sequences were analyzed and assigned to 94 family-level OTUs from 'light' and 'heavy' fractions of [^{13}C]cellulose treatments at 15°C and 5°C (Table 19). Family-level coverages ranged between 85-94% in the different clone libraries indicating sufficient sampling. Rarefaction curves were lower in clone libraries from 'heavy' fractions at the end of the incubation with [^{13}C]cellulose at 15°C and 5°C compared to clone libraries of 'light' and 'heavy' fractions at the start of the incubation or in 'light' fractions at the end of the incubation (Figure 11). This indicates that the RNA of only a subset of bacterial families was labeled with ^{13}C-carbon derived from [^{13}C]cellulose during the incubation.

High amounts of propionate, acetate and CO_2 were produced during cellulose degradation (Figure 9). Certain *Bacteroidetes* species can hydrolyze cellulose and produce the observed fermentation products [23, 173, 353], and this phylum was involved in cellulose degradation in anoxic incubated agricultural soil [372] and in the human gut [48]. In this regard, OTU4a, which was enriched in 'heavy' fractions at 15°C, was closely related (96% maximum identity to FN434002; Figure 12) to sequences of unclassified *Prolixibacteraceae* that were labled in [^{13}C]cellulose but not in [^{13}C]glucose treatments of agricultural soil [372]. OTU4a had 95% maximum identity to the rice soil bacterium PB90-2, which was highly abundant in its habitat and could hydrolyze xylan and pectin but not cellulose [51, 162]. OTU4b was labeled at 5°C and 15°C and was closely related to an uncultured bacterium from a paper pulp degrading consortia (EF562547; Figure 12). Recently, *Mangrovibacterium diazotrophicum*, a cellulolytic facultative aerobe of the *Prolixibacteraceae* was isolated (91% and 90% identity to OTU4a and 4b, respectively) [173], validating that this family indeed harbors cellulolytic fermenters. The hydrolytic nature of cultured relatives, the presence of uncultured relatives in various cellulose-degrading environments, and the incorporation of [^{13}C]cellulose derived ^{13}C-carbon in peat soil microcosms indicate that members of a novel genus within the *Prolixibacteraceae* are likely to contribute to cellulose degradation and propionate production in contrasting ecosystems.

Table 19   Number of sequences, OTUs, and coverages of bacterial 16S rRNA clone libraries

Clone library[a]	15°C				5°C		total
	t_0 L	t_0 H	t_{40} L	t_{40} H	t_{80} L	t_{80} H	
No. of Sequences	150	165	171	170	174	168	989
No. of OTUs[b]	45	54	43	25	45	19	94
Coverage [%]	85	85	91	94	90	94	98

[a]t_0 and t_{40}, 0 d and 40 d of incubation, respectively, after 17 d of preincubation at 15°C; t_{80}, 80 d of incubation after 22 d of preincubation. L and H; 'light' and 'heavy' fractions, respectively (Figure 6).
[b]OTUs were calculated based on 87.5% similarity cutoff ('family level' [492]). Modified from ref [387].

The highly novel OTU1 was abundant in 'heavy' fractions of [^{13}C]cellulose treatments at 5°C and 15°C and could only be distantly affiliated to the *Fibrobacteres* (79% maximum identity to *Fibrobacter succinogenes*) (Figure 12). Taxa assigned to the *Fibrobacteres* were abundant cellulose degraders in the digestive tract of ruminants, anaerobic digesters, and municipal waste landfill sites [281, 360, 455], but this phylum was previously not recognized in peatlands. *F. succinogenes* is the type species and represents one of only two cultured species of the *Fibrobacteres*. This microbe is a well studied hydrolytic fermenter that produces succinate and acetate exclusively from the breakdown products of cellulose [302, 426]. Based on the affiliation (although distinct) to a cellulose degrader, the accumulation of high amounts of propionate and acetate, and the high abundance of OTU1, on may suggest that this taxon was important for cellulose hydrolysis and contributed to propionate and acetate formation in the microcosms at 5°C and 15°C.

The *Acidobacteria* belong to the dominant phyla in peatlands, are metabolically highly versatile, and are repeatedly characterized as well adapted to cold and acidic environments [84, 176, 468]. Relative abundances of *Acidobacteriaceae* in the different clone libraries were more balanced and did not show a clear labeling from [^{13}C]cellulose (Figure 12). However, within the *Acidobacteriaceae*, there are two subfamily-level OTUs (OTU3b and 3e) that are enriched in 'heavy' fractions compared to 'light' fractions at the end of the incubation at 15°C and 5°C (Table A2). OTU3e was closely related to the slowgrowing microaerophil *Telmatobacter bradus* (98% maximum identity), which was isolated from a peatland and was the first cultured member of the *Acidobacteria* that could grow anaerobically on cellulose [324]. OTU3b was was distantly related to *Koribacter versatillis* (93% maximum identity), which was isolated as an aerobe (anerobic growth was not tested) and harbors cellulase genes in its genome [468]. The agricultural soil isolate KBS 83, is another cellulolytic facultative aerobe of the *Acidobacteriaceae* [112], and *A. capsulatum* (the type species of the *Acidobacteriaceae*) is also a facultative aerobe and harbors cellulase genes in its genome but could not grow on cellulose [199, 324, 468]. The collective data suggest that the capability to grow anaerobically on cellulose is spread among the *Acidobacteriaceae*, and genera within this family are likely to contribute to cellulose hydrolysis in peatlands and might especially adapted to changing redox conditions. However other subfamily OTUs within the Acidobacteriaceae (OTUs 3a and 3c) were abundant but not labled in the [^{13}C]cellulose treatments and may be capable of cellulose hydrolysis under aerobic conditions or may contribute to the degradation of polymers like xylan or pectin [112, 322, 323, 468].

The *Holophagaceae* represent a family that are only distantly related to other members of the *Acidobacteria*. None of the two currently available isolates (both are strict anaerobes) have been shown to grow on cellulose [57, 245]. However, 16S rRNA gene sequences affiliated to the *Holophagaceae* were frequently detected in peatlands [84] and this family constituted 11%

of the 16S rRNA sequences in 'heavy' fractions of the [^{13}C]cellulose treatment at 15°C (OTU8b; Figure 12). Thus, the *Holophagaceae* may contribute to the mineralization of cellulose in peatlands at moderate temperatures.
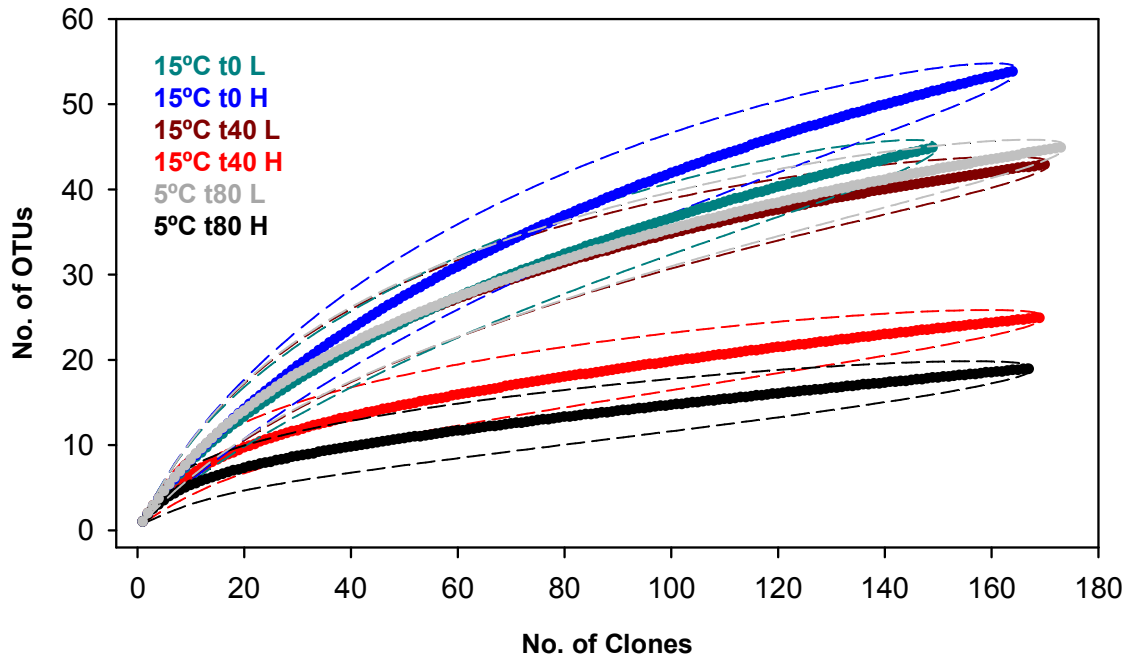
Figure 11   Rarefaction analyses and 95% confidence intervals of bacterial 16S rRNA sequences obtained from cellulose supplemented microcosms.
OTUs were calculated based on 87.5% similarity cutoff ('family level' [492]). t_0 and t_{40}, 0 d and 40 d of incubation, respectively, after 17 d of preincubation at 15°C; t_{80}, 80 d of incubation after 22 d of preincubation. L and H; 'light' and 'heavy' fractions, respectively (Figure 6). Modified from ref [387].

Ruminococcaceae are important cellulose degraders in the digestive tracts of animals and humans, agricultural soil, swamp soil, and municipal wastes [48, 244, 281, 372, 449]. This family was also labled in [^{13}C]cellulose treatments in this study but the relative abundance was considerably lower than that of other potential cellulose degraders (e.g., *Fibrobacter*-related unclassified Bacteria and *Prolixibacteraceae*; Figure 12), indicating that novel hitherto unrecognized rather than well studied hydrolytic fermenters were the drivers of cellulose degradation under the experimental conditions.

Saccharolytic fermenters compete with cellulolytic fermenters for sugars released during cellulose hydrolysis [17, 241] but may also enhance cellulose hydrolysis by keeping the concentrations of soluble sugars low, which prevents product inhibition of the cellulase systems [254, 336]. OTU9, and 12 were labled in [^{13}C]cellulose treatments (Figure 12) and were closely related to saccharolytic fermenters of the *Porphyromonadaceae*, and *Spirochaetaceae*, respectively, indicating that saccharolytic fermenters contribute to the degradation of cellulose derived sugars. OTU9 had 99% maximum identity to the propionate

producing strictly anaerobic non-hydrolyzing fermenter *Paludibacter propionicigenes* (isolated from rice paddy soils) [446] and therefore, might have contributed to the high amounts of propionate detected during cellulose degradation (Figure 9). The closest cultured relative of OTU12 (96% maximum identity) was *Spirochaeta zuelzerae*, which was isolated from freshwater mud and ferments glucose to H_2, CO_2, acetate lactate and succinate [458]. Saccharolytic fermenters of the genus *Spirochaeta* are known to enhance the rate of cellulose hydrolysis when grown in coculture with hydrolytic fermenters [336] and might fulfill a similar role in peatlands.
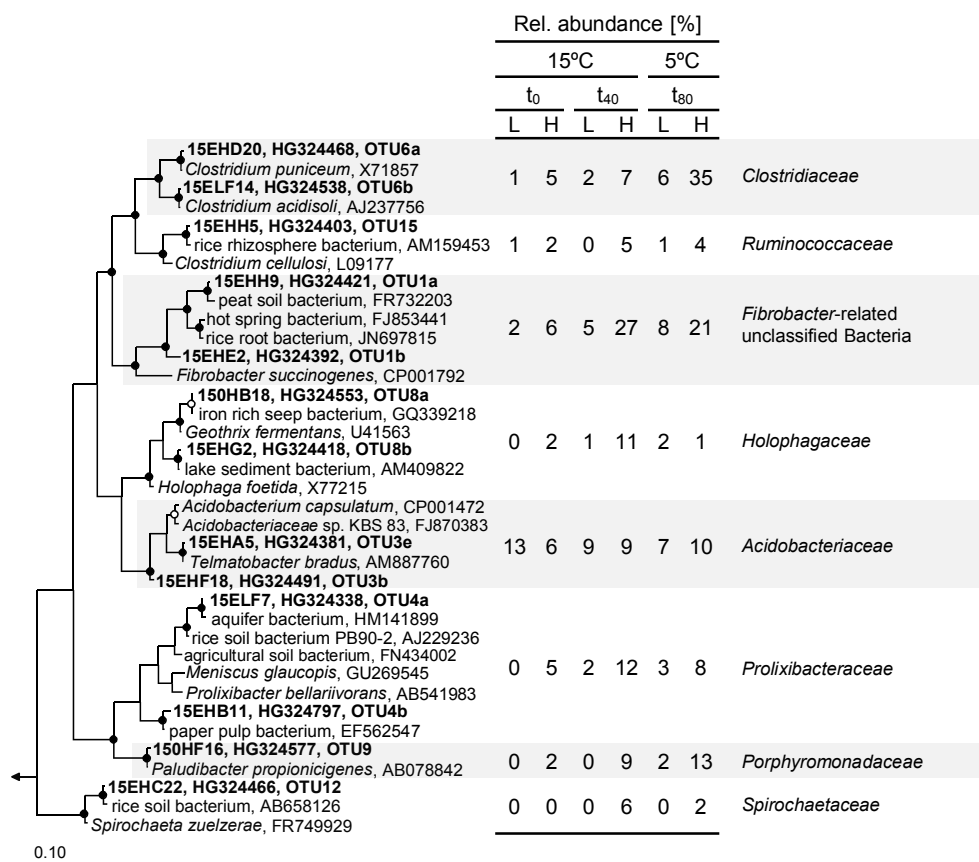
Figure 12 Phylogenetic tree of bacterial 16S rRNA sequences retrieved from [^{13}C]cellulose treatments (bold) and reference sequences.

Shown are potentially labeled OTUs that displayed increased relative abundances in 'heavy' (H) compared to 'light' (L) fractions at the end of the incubation. See Table A2 for the sequence descriptor code and a complete list of all bacterial family-level OTUs. The phylogenetic tree was calculated as described in (2.6.4). Branch length are based on the neighbor-joining tree. Filled circles at nodes indicate congruent nodes in the maximum-likelihood, maximum parsimony, and neighbor-joining tree. Open circles indicate congruent nodes in two of the three trees. The bar indicates 0.1 change per nucleotide. *Methanosarcina mazei* (AE008384) was used as outgroup. 't0' was after 17 or 22 days of anoxic preincubation at 15°C and 5°C, respectively (2.1.2.1). L and H; 'light' and 'heavy' fractions, respectively (Figure 6). Modified from ref [387].

Sequences within OTU6b were closely related to *Clostridium acidisoli* (Table A2). *C. acidisoli* was isolated from a bog site close to the Fen Schlöppnerbrunnen, ferments a broad range of soluble sugars to acetate, butyrate, lactate, formate, H_2, and CO_2, growths well under cold and acidic conditions, and is characterized by fast growth rates (at least at 30°C) [218]. Unfortunately, hydrolytic growth on cellulose, xylan, and pectin was not tested. However, the outstanding feature of this microbe is the capability to fix N_2 at a pH as low as 3.7, which is not known from other acid tolerant *Clostridia*. OTU6b was especially abundant at 5°C and might have cooperated with cellulose hydrolyzers in a synergistic relationship in which the hydrolyzer provides soluble sugars and the *C. acidisoli*-related OTU6b provides the nitrogen source for growth.

OTU6a was not as abundant as OTU6b and was closely related to *C. puniceum* (Table A2). *C. puniceum* is pectinolytic, acido- and psychrotolerant, and produces butyrate, acetate, and butanol during fermentation [165, 266]. *C. puniceum* was the dominant consumer of [^{13}C]glucose and [^{13}C]xylose in microcosms of the Fen Schlöppnerbrunnen [151]. This suggests that *C. puniceum* might be more competitive for high concentrations of soluble sugars whereas *C. acidisoli* might be more competitive for the low sugar concentrations released during cellulose hydrolysis.

3.2.1.3.   Active but not labeled bacterial taxa

Unlabeled bacterial taxa were dominated by *Proteobacteria*, a phylum that can be dominant in peatlands [84], at 15°C and 5°C (Table A2). Most of the *Alphaproteobacteria* were affiliated with methanotrophs, aerobic chemoorganotrophs, and anoxygenic phototrophs of the orders *Rhizobiales* and *Rhodospirillales*, and some of the family-level OTUs within the *Rhizobiales* and *Rhodospirillales* were only distantly related to described species. These uncultured *Alphaproteobacteria* are common in peatlands but their biology remains unclear [84, 323]. Detected *Deltaproteobacteria* affiliated with iron and sulfate reducers of the *Geobacteriaceae*, *Desulfovibrionaceae*, and *Desulfobulbaceae* as well as with syntrophic bacteria of the *Syntrophobacterales* (Table A2). Iron and sulfate reduction are ongoing processes in the peatland, and members of the *Geobacteraceae* and *Syntrophobacterales* have been repeatedly detected in this ecosystem [151, 175, 219, 257, 350, 382]. Relatively little is known of the syntrophic bacteria in this or other peatlands, and their involvement in the intermediary ecosystem metabolism and links to methanogenesis remain mostly conceptional for these ecosystems [100]. *Actinobacteria* and *Planctomycetes* were enriched during anoxic incubation in 'light' fractions at 15°C and 5°C, respectively (Table A2), suggesting that these phyla are capable of utilizing endogenous organic compounds in the peatland. Because the affiliations of these 16S rRNA sequences to those of physiologically described species were

relatively low, the biology of the detected members of the *Actinobacteria* and *Planctomycetes* remains unclear.

3.2.1.4.   Active archaeal taxa in cellulose-supplemented anoxic peat soil microcosms at 5°C and 15°C

A total of 422 archaeal 16S rRNA sequences were analyzed and assigned to 13 genus-level OTUs from 'light' and 'heavy' fractions of [^{13}C]cellulose treatments at 15°C and 5°C (Table 20). Genus-level coverages ranged between 91-100% in the different clone libraries suggesting that the majority of archaeal genus-level taxa could be detected. Rarefaction analyses indicated higher diversities for clone libraries at 5°C compared to 15°C (Figure 13).

Aceticlastic methanogens of the genera *Methanosarcina* and *Methanosaeta* were highly abundant at 15°C and 5°C in cellulose treatments (Figure 14). This finding (i) is in accordance with the occurrence of acetate in soil slurries (Figure 9) as well as the earlier detection of aceticlastic methanogens in this peatland [151, 175, 487] and (ii) indicates that aceticlastic methanogensis contributes to the overall production of methane in this peatland. Interestingly, *Methanosaeta* was more abundant at 5°C whereas the abundance of *Methanosarcina* decreased at 5°C. A similar shift in the community composition of aceticlastic methanogens was also observed in paddy rice soil slurries incubated at 15°C and 30°C [53], suggesting that *Methanosaeta* might be more tolerant than *Methanosarcina* to low temperatures. *Methanosarcina* is also able to use H_2-CO_2 for methanogenesis. However, *Methanosarcina* is characterized by higher H_2-threshold concentrations compared to methanogens that lack cytochromes (e.g., *Methanobacterium*, *Methanoregula*; [434]), and detected H_2 concentrations (Table 17) were lower than the H_2-threshold for *Methanosarcina barkeri* [194]. Thus, the contribution of *Methanosarcina* to hydrogenotrophic methanogenesis might have been minimal under the experimental conditions.

Methanoregula was the single abundant obligatory hydrogenotrophic methanogenic genus detected after 17 d of preincubation at 15°C ("t_0" in Figure 14). The relative abundance of *Methanoregula* decreased after incubation with [^{13}C]cellulose at 15°C while *Methanoregula* was abundant at the end of incubation at 5°C, especially in 'heavy' fractions. *M. boonei*, a slow growing methanogen that grows at 10°C and requires acetate, was isolated from an acidic peatland [31]. The 16S rRNA sequence of *M. boonei* displayed up to 99% identity to *Methanoregula*-related 16S rRNA sequences from cellulose treatments. These results indicate that *Methanoregula* (i) is abundant in the fen, (ii) is well adapted to low in situ temperatures, and (iii) assimilated [^{13}C]cellulose-derived [^{13}C]acetate. In contrast to *Methanoregula*, *Methanocella*, another obligate hydrogenotrophic methanogenic genus that requires acetate for growth [362], displayed a relatively low abundance after 17 d of

preincubation ("t_0" in Figure 14) but was enriched in 'heavy' fractions during subsequent 40 d of incubation with [^{13}C]cellulose at 15°C. This finding indicates that *Methanocella* was able to outgrow *Methanoregula* at moderate temperatures whereas *Methanoregula* dominated hydrogenotrophic methanogenesis at 5°C. *Methanocella* was previously found to dominate over *Methanoregula* in soil samples of this peatland incubated at 15°C [175]. Furthermore, a methanogenic enrichment culture derived from a siberian peatland sample incubated at 28°C was dominated by a *Methanocella*-affiliated archaeon (AF524853 in Figure 14; [407]). These collective results demonstrate that the composition and activities of aceticlastic as well as hydrogenotrophic methanogens in peat are strongly influenced by temperature.

Table 20   Number of sequences, OTUs, and coverages of archaeal 16S rRNA clone libraries

Clone library[a]	15°C				5°C		total
	t_0 L	t_0 H	t_{40} L	t_{40} H	t_{80} L	t_{80} H	
No. of Sequences	87	87	83	78	45	42	422
No. of OTUs[b]	6	4	6	6	10	9	13
Coverage[c] [%]	97	100	98	99	91	93	100

[a]t_0 and t_{40}, 0 d and 40 d of incubation, respectively, after 17 d of preincubation at 15°C; t_{80}, 80 d of incubation after 22 d of preincubation. L and H; 'light' and 'heavy' fractions, respectively (Figure 6).
[b]OTUs were calculated based on 95% similarity cutoff ('genus level' [492]). Modified from ref [387].
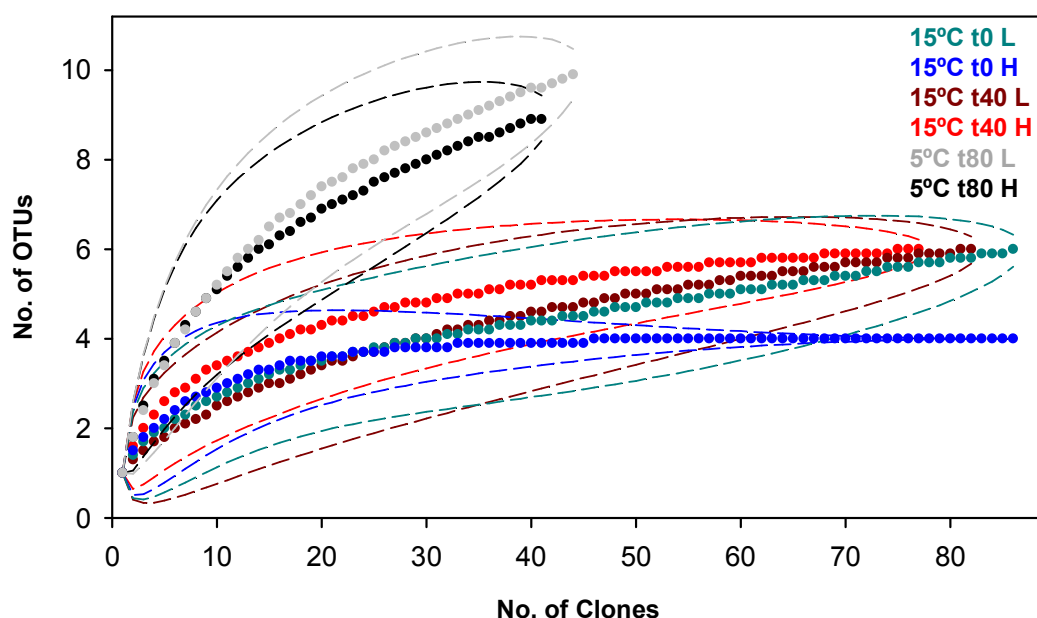
Figure 13   Rarefaction analyses and 95% confidence intervals of archaeal 16S rRNA sequences obtained from cellulose supplemented microcosms.

OTUs were calculated based on 95% similarity cutoff ('genus level' [492]). t_0 and t_{40}, 0 d and 40 d of incubation, respectively, after 17 d of preincubation at 15°C; t_{80}, 80 d of incubation after 22 d of preincubation. L and H; 'light' and 'heavy' fractions, respectively (Figure 6). Modified from ref [387].

	Rel. abundance [%]						
	15°C				5°C		
	t$_0$		t$_{40}$		t$_{80}$		
	L	H	L	H	L	H	
15AEHG4, HG325539, OTU2 peat soil archaeon, JN649107 *Methanosaeta concilii*, CP002565 **15AEHE2, HG325519, OTU2** peat soil archaeon, JN649251	9	13	10	5	9	17	*Methanosaeta*
Methanosarcina barkeri, AJ012094 *Methanosarcina vacuolata*, FR733661 **15AELH11, HG325628, OTU1** peat soil archaeon, AY175383	76	69	82	58	42	24	*Methanosarcina*
15AEHA7, HG325485, OTU4 peat soil archaeon, FR744950 peat soil archaeon K-5a2, AF524853 **15AEHB1, HG325488, OTU4** peat soil archaeon, EU155966 *Methanocella paludicola*, AP011532	1	4	0	26	9	12	*Methanocella*
15A0LF8, HG325453, OTU5 peat soil archaeon, JN649231	1	0	0	0	2	2	Unclassified *Methanomicrobia* (RCII)
15A0LA11, HG325391, OTU3 peat soil archaeon, AB364925 *Methanoregula boonei*, DQ282124 **15A0LC10, HG325413, OTU3** peat soil archaeon, JN649288 *Methanoregula formicicum*, AB479390	12	14	4	9	9	31	*Methanoregula*
5AELH03, HG325717, OTU10 peat soil archaeon, JN649294, *Methanolinea mesophila*, AB447467 *Methanolinea tarda*, AB162774	0	0	0	0	2	0	*Methanolinea*
pit mud archaeon, JX576140, *Methanomassiliicoccus luminyensis*, HQ896499 **15A0LG6, HG325463, OTU6** **15AELB6, HG325572, OTU6** peat soil archaeon, FR745001	1	0	1	2	2	2	*Methanomassiliicoccus*
15AELC1, HG325575, OTU7 acidic spring archaeon, AB600345	0	0	2	0	0	0	Unclassified *Euryarchaeota*
5AEHD09, HG325676, OTU8 peat soil archaeon, JN649126 *Methanobacterium lacus*, HQ110085	0	0	0	0	2	5	*Methanobacteriun*
5AEHB01, HG325646, OTU11 lake archaeon, HE589674 "*Candidatus* Nitrosotalea devanaterra", JN227488	0	0	0	0	16	5	*Nitrosotalea*
"*Candidatus* Nitrosocaldus yellowstonii", EU239960 **15AELH7, HG325635, OTU9** aspen rhizosphere archaeon, EF020900,	0	0	1	0	0	0	Unclassified *Thaumarchaeota* I
5AEHD11, HG325678, OTU12 peat soil archaeon, EU155993 *Ignisphaera aggregans*, CP002098	0	0	0	0	7	2	Unclassified *Thaumarchaeota* II

0.10

Figure 14 Phylogenetic tree of archaeal 16S rRNA sequences retrieved from [^{13}C]cellulose treatments (bold) and reference sequences.

Relative abundances are given for genus-level OTUs [492]. The phylogenetic tree was calculated as described in (2.6.4). Branch length are based on the maximum parsimony tree. Filled circles at nodes indicate congruent nodes in the maximum-likelihood, maximum parsimony, and neighbor-joining tree. Open circles indicate congruent nodes in two of the three trees. The bar indicates 0.1 change per nucleotide. *Escherichia coli* (CP000948) was used as outgroup. 't0' was after 17 days of anoxic preincubation. L and H; 'light' and 'heavy' fractions, respectively (Figure 6). Modified from ref [387].

Thaumarchaeota-related sequences were almost absent in gene libraries derived from incubations at 15°C (Figure 14).   In contrast, *Thaumarchaeota*-related sequences were abundant at the end of incubation with [^{13}C]cellulose at 5°C, especially in 'light' fractions. Most thaumarchaeal sequences were closely related (99% maximum identity) to "*Candidatus* Nitrosotalea devanaterra", an aerobic obligate acidophilic chemolithoautotrophic ammonium oxidizer [242]. However, the presence of these thaumarchaeal sequences in long-term anoxic incubations suggest a physiological function other than aerobic ammonium oxidation for the organism associated with these sequences.   In this regard, heterotrophic growth was hypothesized for *Thaumarchaeota* in a wastewater treatment plant [309], and a potential role of *Thaumarchaeota* in syntrophic fatty acid oxidation was proposed in deep layers of arctic peat soil [248]. Thus, *Thaumarchaeota* likely contribute to anaerobic mineralization processes in the fen especially at low temperatures.

3.2.2. Effect of roots from the peat soil covering sedge *Carex rostrata* on H_2 metabolizers in the rhizosphere

Mesotrophic peatlands like the Fen Schlöppnerbrunnen are often completely overgrown with sedges (e.g., *Carex rostrata*) [118, 326]. In the uppermost peat layers, plant litter (leaves and stems) of these vascular plants is degraded mainly (i) aerobically when the groundwater level is below the peat surface or (ii) anaerobically when the groundwater level is above the peat surface [313]. In deeper peat layers, in which the remains of the leaves and stems are of low quality, root-derived organic compounds (i.e., root exudates and root biomass) are the most important energy and carbon source for the microbes [313]. In the experiments here, roots of *C. rostrata* were separated from the surrounding peat soil to analyze root-independent and root-dependent mineralization processes in root-free peat soil and soil-free root microcosms, respectively. Formate is one of the most important organic acids that are released from roots of sedges [206], and was therefore used to mimic the effect of root-exudates on the rhizosphere inhabiting microbiota. Hydrogenase gene analyses were performed to identify H_2 metabolizers that were attached to roots and potentially linked to H_2 production or H_2 consumption.

3.2.2.1. H_2-metabolizing processes in formate-supplemented and unsupplemented root-free soil and soil-free root microcosms

The rapid accumulation of large amounts of CO_2 in unsupplemented soil-free root microcosms during the initial six days of incubation was indicative of ongoing respiratory processes (Figure 15). The accumulation of acetate and H_2 during this initial phase suggests that fermenters were active in addition to respiratory microbes, and therefore CO_2 accumulation likely resulted from both processes. Between day 6 and 21, CO_2 accumulation slowed down and H_2 concentrations decreased whereas acetate, propionate, and butyrate concentrations increased steadily. Electron acceptors for respiratory processes were probably depleted, and CO_2 production may have been limited to fermentation processes during this time. Furthermore, H_2-dependent acetogenesis, which was thermodynamically feasible (Figure 16), likely was a sink for CO_2 and H_2 between day 6 and 21. Remarkably, acetate concentrations decreased at the end of the incubation although CO_2 and H_2 concentrations were still high enough to support acetogenesis. Butyrate and propionate production increased at the end of the incubation, and one may speculate that acetate and H_2 were consumed by butyrate- and propionate-producing fermenters. In this regard, butyrate fermenters (e.g., *Roseburia intestinalis*) can take up acetate and propionate fermenters (e.g., *Selenomonas ruminantium*) can take up H_2 for an enhanced production of butyrate and propionate during

fermentation of sugars, respectively [107, 160]. CH_4 production was almost not observed in unsupplemented soil-free root microcosms, suggesting that methanogensis was not a sink for H_2 or acetate although hydrogenotrophic and aceticlastic methanogenesis were thermodynamically feasible. Thus, methanogens were not present or their activity was inhibited in unsupplemented soil-free root microcosms.
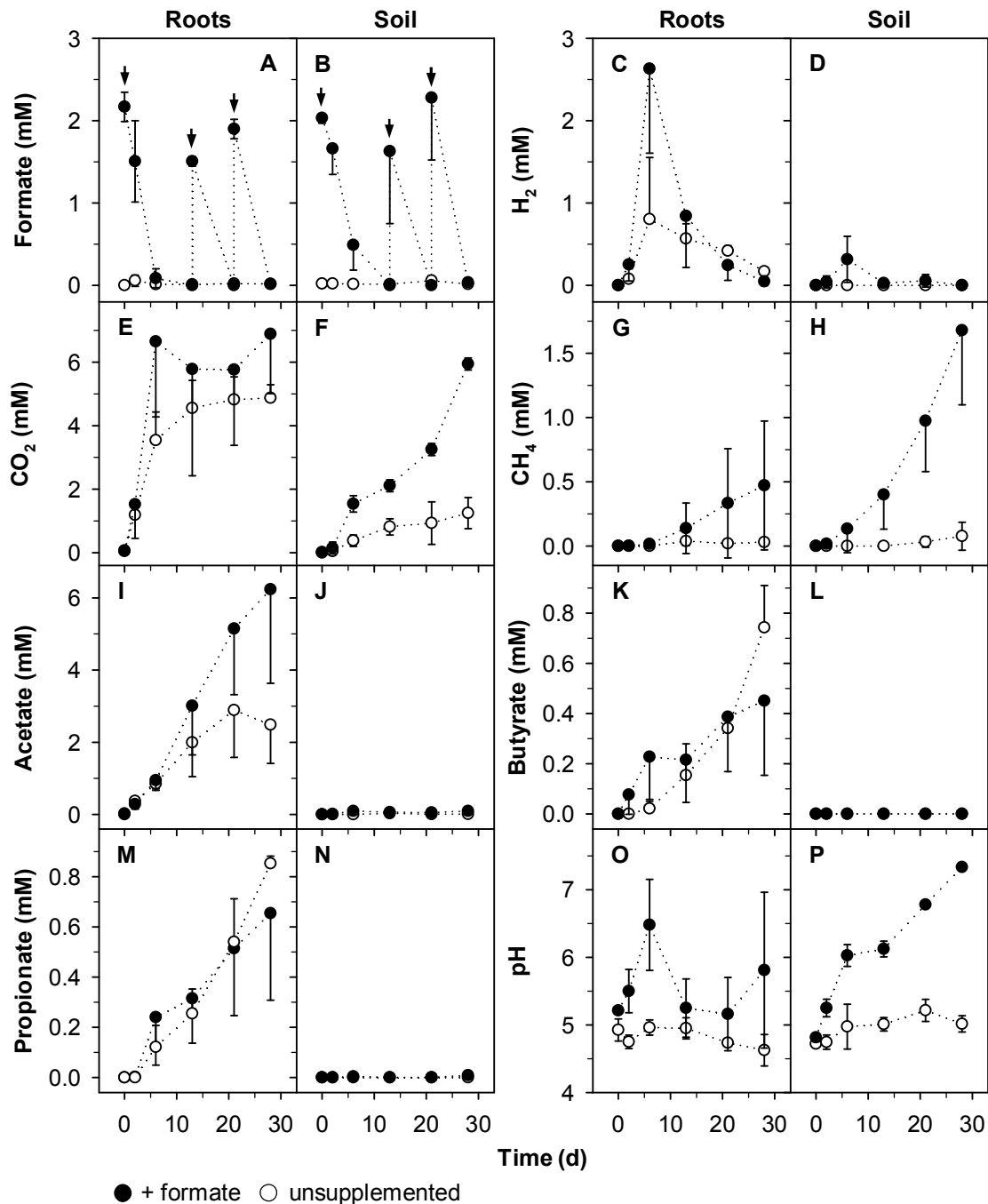
Figure 15   Product profiles in anoxic soil-free root and root-free soil microcosms.

Values are means of triplicates and duplicates for formate treatments and unsupplemented controls, respectively. Error bars indicate standard deviations. Arrows indicate the supplementation of formate. Modified from ref [177].

Table 21   Recoveries of reductant and carbon in soil-free root and root-free soil microcosms[a]

Microcosm	Recovery [%]	Acetate	Propionate	Butyrate	CH_4	H_2	CO_2	∑
Roots	Reductant	270.8	-25.0	-52.3	31.7	-2.2	0.0	223.0
	Carbon	135.4	-10.7	-20.9	7.9	0.0	36.5	148.2
Soil	Reductant	5.6	1.0	0.0	109.0	0.0	0.0	115.6
	Carbon	2.8	0.4	0.0	27.2	0.0	79.7	110.1

[a]Recoveries were calculated for the 28 d of incubation as described in 2.7.1.2. Negative values of butyrate, propionate, and H_2 indicate that these compounds accumulated to a lesser extent in formate treatments compared to unsupplemented controls.

● + formate   ○ unsupplemented
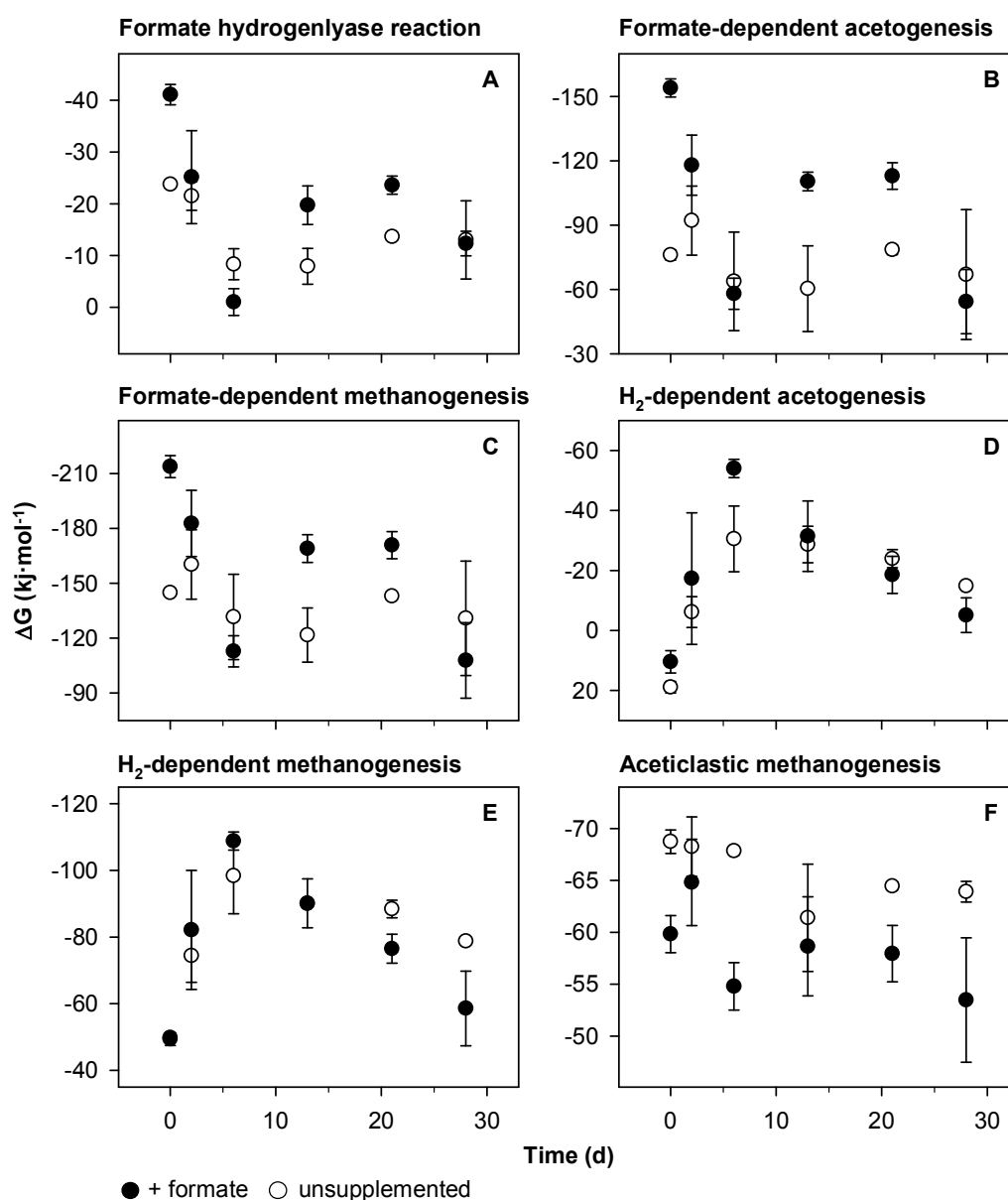
Figure 16   Gibbs free energies of anaerobic processes in anoxic soil-free root microcosms.

See Figure 15 for concentrations of organic acids and gases. ∆Gs were calculated as described (2.7.2). Values are means of triplicates and duplicates for formate treatments and unsupplemented controls, respectively. Error bars indicate standard deviations. Modified from ref [177].
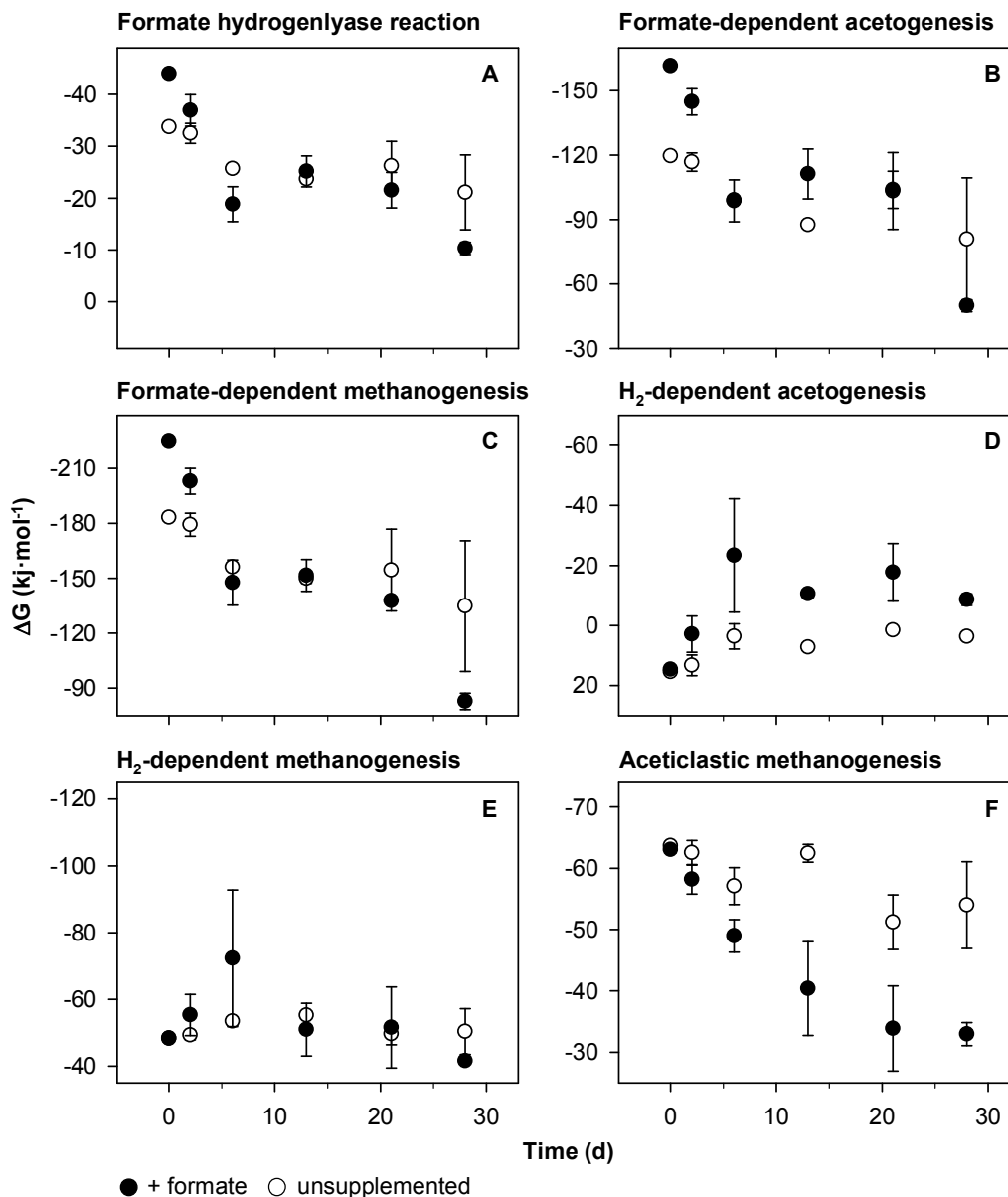
Figure 17   Gibbs free energies of anaerobic processes in anoxic root-free soil microcosms.

See Figure 15 for concentrations of organic acids and gases. ΔGs were calculated as described (2.7.2). Values are means of triplicates and duplicates for formate treatments and unsupplemented controls, respectively. Error bars indicate standard deviations. Modified from ref [177].

Low amounts of CO_2 and no H_2, acetate, propionate, or butyrate accumulated in unsupplemented root-free soil microcosms (Figure 15). This is in sharp contrast to the unsupplemented soil-free root microcosms in which a higher respiratory rate (i.e., more CO_2 accumulated initially) and a higher fermentation activity was observed. Thus, the low overall activity in root-free soil microcosms suggests that the peat soil microbiota is largely dependent on root-derived organic compounds, and by removing the roots the microbes were substrate limited. This underscores the assumption that the organic carbon in the bulk peat soil is of low quality and that the root-derived organic compounds represent a readily degradable source of

carbon. Thus, the rhizosphere of sedges is a hot spot for respiratory organisms and fermenters in predominantly substrate limited peatlands.

Formate was supplemented to soil-free root microcosms and root-free soil microcosms to mimic the stimulatory effect of root exudates on the microbial community in the rhizosphere of peat soil-covering sedges. H_2 and CO_2 concentrations increased nearly equimolar to the consumption of initially supplemented formate in soil-free root microcosms during the first six days (Figure 15). The decrease of formate concentrations parallel to the production of H_2 and CO_2 indicated that FHL-containing taxa (1.4), which are known to be present in the investigated fen [178], split formate to H_2 and CO_2 (Reaction 7 in Table 2) under the experimental conditions in the root microcosms. ΔGs for the FHL reaction were < -20 kJ·mol^{-1} when formate was supplemented (Figure 16A) and therefore, formate consumption could have been coupled to the generation of ATP by the FHL-containing taxa. Subsequent consumption of the initially accumulated H_2 and CO_2 yielded increased accumulation of acetate and CH_4, which is indicative of hydrogenotrophic acetogenesis and methanogenesis, respectively. Transient H_2 accumulation was not observed after a second and third pulse of formate but acetate and CH_4 production were stimulated, indicating that (i) formate-derived H_2 was effectively scavenged by acetogens and methanogens, or (ii) formate was directly converted during acetogenesis and methanogenesis in soil-free root microcosms (Figure 15). In this regard, ΔGs for acetogens and methanogens were exergonic enough to allow growth on H_2 and formate (Figure 16). Total carbon and reductant recoveries calculated for the complete incubation time considerably exceeded 100% (Table 21), which suggests that the supplemental formate had a priming effect [124] on the consumption of root-derived carbon sources. Such a priming effect of formate was reported earlier for root-containg peat soil microcosms of the fen [171]. However, in the earlier study propionate production was stimulated by supplemental formate (butyrate was not reported) whereas propionate and butyrate accumulated to a lesser extent in formate treatments compared to unsupplemented controls in this study. This and the high amounts of carbon and reductant recovered in acetate (Table 21) suggest that acetogens, which were activated from formate-derived reductant and carbon, competed successfully with butyrate and propionate producing fermenters for root-derived organic carbon and therefore, acetogens may have decreased the activity of fermenters.

The transient accumulation of H_2 after the intial formate supplementation was less pronounced, and H_2 concentrations during the whole experiment were considerably lower in root-free soil microcosms compared to soil-free root microcosms (Figure 15). This indicates that (i) FHL activity was lower or (ii) formate-derived H_2 was more effectively scavenged in the bulk soil compared to the roots. In this regard, high amounts of reductant were recovered in CH_4 (Table 21), suggesting that it was the terminal sink for formate-derived reductant. Methanogenesis from formate, H_2, and acetate was exergonic (Figure 17), and therefore all

three processes may have contributed to the accumulation of CH_4. Remarkably, formate supplementation did not stimulate acetate accumulation in root-free soil microcosms although this was observed in soil-free root microcosms (this study) and soil microcosms containing roots [171]. There are several potential reasons that might explain why acetate did not accumulate although formate-dependent acetogenesis was highly exergonic in root-free soil microcosms: (i) acetogens were only attached to roots but not present in the bulk peat soil; (ii) acetogens were present and consumed formate but produced acetate was effectively scavenged by aceticlastic methanogens; (iii) acetogens were present but performed only the FHL reaction and did not produce acetate [94]; (iv) acetogens were present and had the capability to grow on H_2-CO_2 but not on formate. If (iii) is correct than acetogens might have been outcompeted for H_2 by methanogens, which is supported by the ΔGs for H_2-dependent acetogenesis (Figure 17D) that were close to the thermodynamic limit for acetogens (-15 $kJ \cdot mol^{-1}$ [393]).

In summary, formate-derived reductant stimulated mainly acetogenesis in soil-free root microcosms whereas it stimulated methanogenesis in root-free soil microcosms. FHL-containing taxa are likely involved in the formate oxidation in soil-free root microcosms and may also be involved in the formate oxidation in root-free soil microcosms.

3.2.2.2. H_2-metabolizing taxa associated with *Carex* roots

H_2 transiently accumulated in unsupplemented and formate-supplemented soil-free root microcosms (Figure 15). Production of H_2 was probably linked to fermentation and formate oxidation whereas respiratory microbes (e.g., acetogens, methanogens, and Fe^{3+}-reducers) and maybe some fermenters consumed H_2 (3.2.2.1). Hydrogenase gene diversity analyses were performed with samples of fresh *Carex* roots as well as with samples of the unsupplemented and the formate supplemented soil-free root microcosms after the 28 days of anoxic incubation to identify potential H_2-producing and H_2-consuming taxa. In this regard, [FeFe]- and group 4 [NiFe]-hydrogenases can be involved in H_2 production from fermentable carbon sources and formate, but can also be used as H_2 uptake enzymes whereas group 1 [NiFe]-hydrogenases in vivo exclusively function as uptake enzymes (Figure 4 and Table 5). Because of the multiple functions of some classes of hydrogenases and the presence of multiple hydrogenases in one genome, an unambiguous assignment of hydrogenase-containing taxa as H_2 consumers or H_2 producers was not always possible.

A total of 533 hydrogenase gene sequences were in silico translated and clustered into 'family-level' OTUs based on the 80% amino acid sequence similarity cut-off established in 3.1.2. Coverages for the different clone libraries ranged between 71% and 99% (Table 22). Thus, most of the 'family-level' hydrogenase gene diversity was probably covered but a more

Table 22   Coverages of in silico-translated hydrogenase gene sequences

Clone library[a]	[FeFe]-hydrogenases				Group 1 [NiFe]-hydrogenases				Group 4 [NiFe]-hydrogenases			
	all	*R*	*UR*	*FR*	*all*	*R*	*UR*	*FR*	*all*	*R*	*UR*	*FR*
No. of seq.[b]	196	38	46	112	135	38	46	51	203	44	48	111
No. of OTUs[c]	46	9	16	31	31	19	14	23	11	3	5	10
Coverage	89	89	89	84	93	71	87	76	99	98	96	97

[a]R, fresh roots; UR, unsupplemented root microcosms; FR, formate supplemented root microcosms.

[b]seq, sequences

[c]OTUs were calculated based on 80% similarity cut-off (3.1.2). Modified from ref [177].
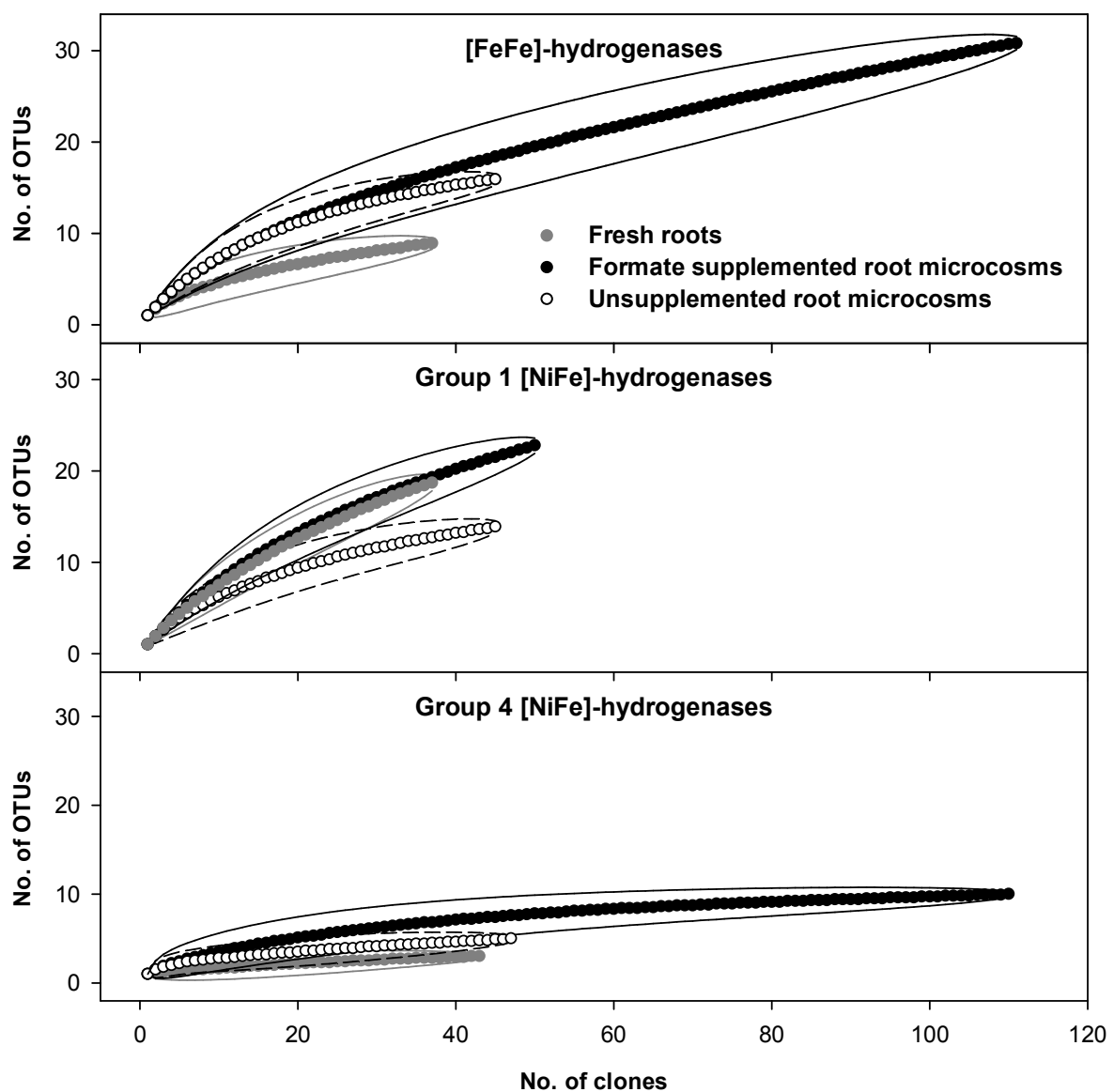
Figure 18   Rarefaction analyses of in silico translated hydrogenase gene sequences.
95% confidence intervals are shown. OTUs were calculated based on 80% similarity cut-off (3.1.2). Modified from ref [177].

extensive sequencing might have resulted in the detection of additional rare OTUs. Rarefaction analyses showed that the detected diversity of [FeFe]-hydrogenase and group 4 [NiFe]-hydrogenase genes increased during the anoxic incubation and was highest in formate-supplemented treatments (Figure 18). In contrast, the diversity of group 1 [NiFe]-hydrogenases was similar in fresh root samples and formate supplemented treatments but lower in unsupplemented treatments. A higher number of OTUs and more rampant rarefaction curves indicated a overall higher diversity of [FeFe]- and group 1 [NiFe]-hydrogenases compared to group 4 [NiFe]-hydrogenases for fresh roots and soil-free root microcosms (Table 22 and Figure 18).
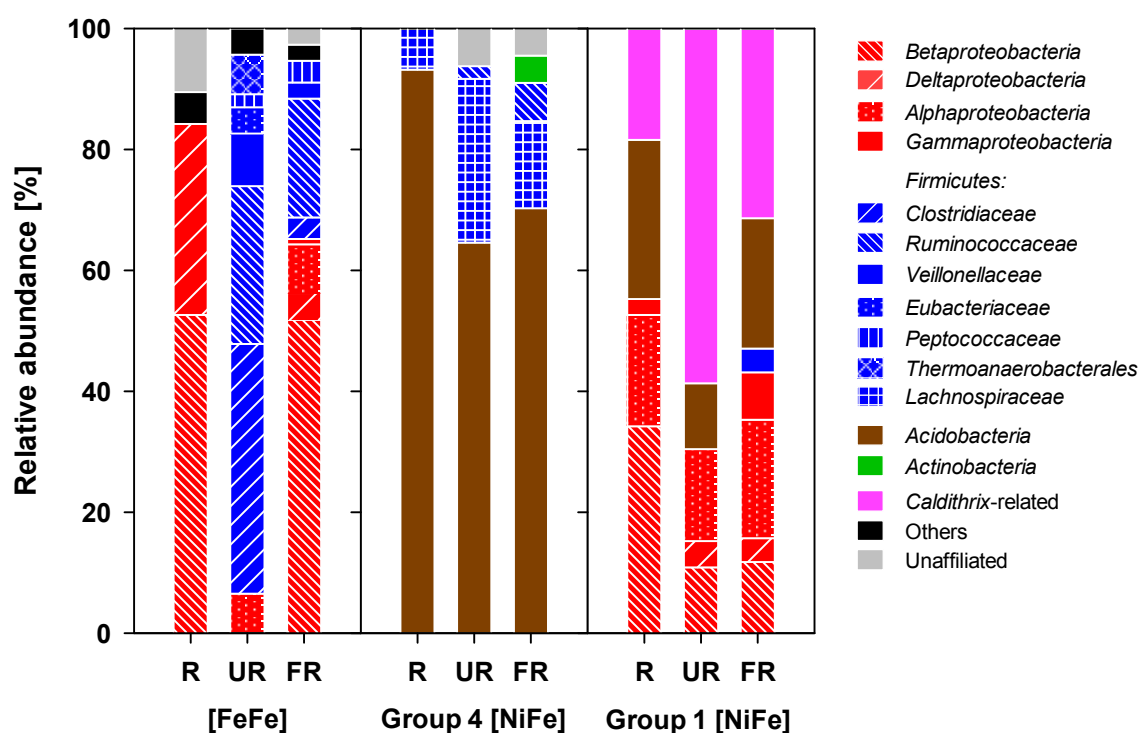
Figure 19   Relative abundancies of taxa in hydrogenases gene libraries of fresh *Carex* roots (R), unsupplemented (UR) and formate-supplemented (FR) soil-free root microcosms.
UR and FR are after 28 days of anoxic incubation. Unaffiliated: less than 60% identity to publicly available hydrogenase gene sequences of cultured organisms.

[FeFe]-hydrogenase gene sequences in unsupplemented microcosms were affiliated mainly to saccharolytic fermenters of the *Clostridiaceae* (41% relative abundance), cellulolytic fermenters of the *Ruminococcaceae* (26%), and other families within the *Firmicutes* (22%) (Figure 19 and Figure 20). OTUs that affiliated with hydrogenases of saccharolytic *Clostridiaceae* were less abundant in formate treatments whereas that of cellulolytic *Ruminococcaceae* were similarly abundant in the presence and absence of formate. This suggests that cellulolytic fermenters were not affected by supplemental formate whereas saccharolytic *Clostridiaceae* were replaced by other taxa in the presence of formate. In this
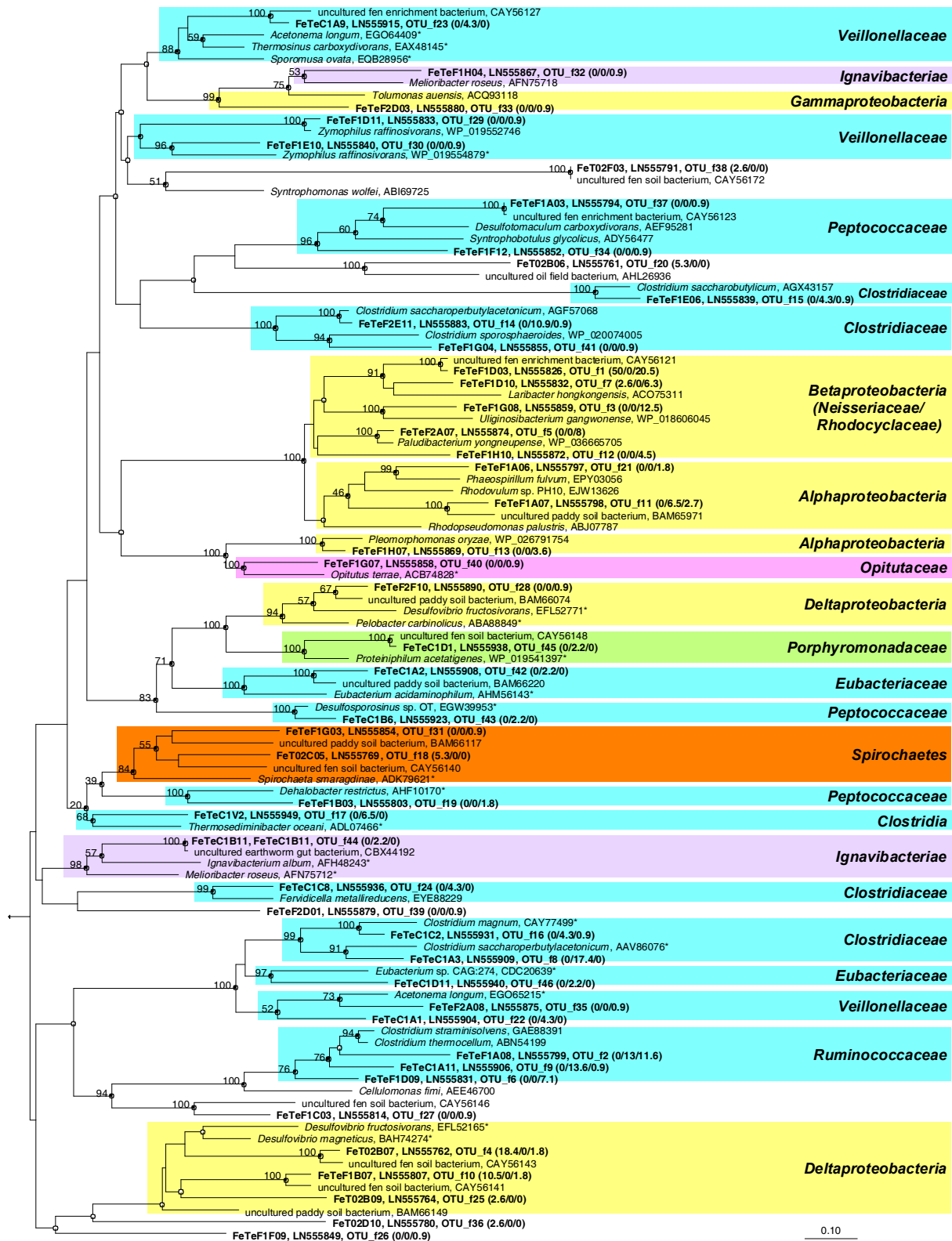
Figure 20 Phylogentic tree of in silico translated [FeFe]-hydrogenase gene sequences (bold) and related sequences.

Legend of Figure 20:

GenBank accession numbers are shown. Relative abundancies of OTUs in clone libraries from fresh roots / unsupplemented root microcosms / formate supplemented microcosms are given in parenthesis. *, these [FeFe]-hydrogenases are potentially bifurcating (based on their flanking genes that encode for subunits similar to those of the trimeric bifurcating enzyme of *Thermotoga maritima* [396]. Sequences correspond to residues 183 to 375 of the *Desulfovibrio vulgaris* hydrogenase (GenBank accession no. AAS96246). Branch lengths are based on the maximum parsimony tree. Filled circles at nodes indicate congruent nodes in the maximum-likelihood, maximum parsimony, and neighbor-joining tree. Open circles indicate congruent nodes in two of the three trees. Bootstrap values are averages from the maximum parsimony tree (1000 resamplings), the neighbor joining tree (1000), and the maximum likelihood tree (100) and are only displayed at nodes congruent in all three trees. The bar indicates 0.1 change per amino acid. The hydrogenase of *Thermotoga maritima* (AAD36496) was used as outgroup. Color code: blue, *Firmicutes*; yellow, *Proteobacteria*; green, *Bacteroidetes*; orange, *Spirochaetes*; pink, *Verrucomicrobia*; purple, *Chlorobi*; uncolored, unaffiliated (less than 60% identity to publicly available [FeFe]-hydrogenase gene sequences of cultured organisms). Modified from ref [177].

regard, OTUs f1, f3, f5, f7 and f12, which affiliated to [FeFe]-hydrogenase genes of facultative aerobic *Betaproteobacteria* and were not detected in unsupplemented controls, made up more than 50% of the sequences in formate treatments. Thus, facultative aerobic *Betaproteobacteria* were more competitive in the presence of formate whereas the *Clostridiaceae* dominated when formate was not supplemented. Formate, which is released by roots of living *Carex* plants [206], may also stimulate *Betaproteobacteria* in situ. This assumption is reinforced by the finding that [FeFe]-hydrogenase genes affiliating with *Betaproteobacteria* were abundant whereas [FeFe]-hydrogenase genes of the *Firmicutes* were not detected in samples of fresh roots (Figure 19).

In contrast to the pronounced effect of formate on the community composition of [FeFe]-hydrogenase-containing taxa, only minor differences were observed with group 4 [NiFe]-hydrogenase genes in fresh roots and unsupplemented or formate-supplemented microcosms, in which *Acidobacteriaceae* and *Lachnospiraceae* were most dominant (Figure 19). Nevertheless, the minor OTUs 4n4, 4n5, 4n6, 4n8, and 4n11, which affiliated with group 4 [NiFe]-hydrogenase genes of *Ruminococcaceae*, *Coriobacteriaceae*, and *Acidobacteriaceae*, were only detected in formate treatments (Figure 21), suggesting that these taxa were involved in H_2-production from formate.

Minor differences in group 1 [NiFe]-hydrogenase gene abundancies were observed on the phylum level between fresh roots, unsupplemented and formate supplemented microcosms (Figure 19). These differences could be largely attributed to the *Caldithrix*-related OTUs 1n2, 1n3, and 1n4 that increased in abundance during the anoxic incubation in unsupplemented and formate-supplemented microcosms compared to fresh roots (Figure 22). The above mentioned OTUs were distantly related (64-66% identity) to *Caldithrix abyssi* that is able to

perform dissimilatory nitrate reduction to ammonium (DNRA) with hydrogen as electron donor [297]. Furthermore, members of the genus *Caldithrix* are able to form hydrogen during fermentation of proteins or sugars [296, 297]. Thus it is possible that the detected *Caldithrix*-related hydrogenase gene sequences belong to bacteria that are able to either evolve or consume hydrogen in situ.
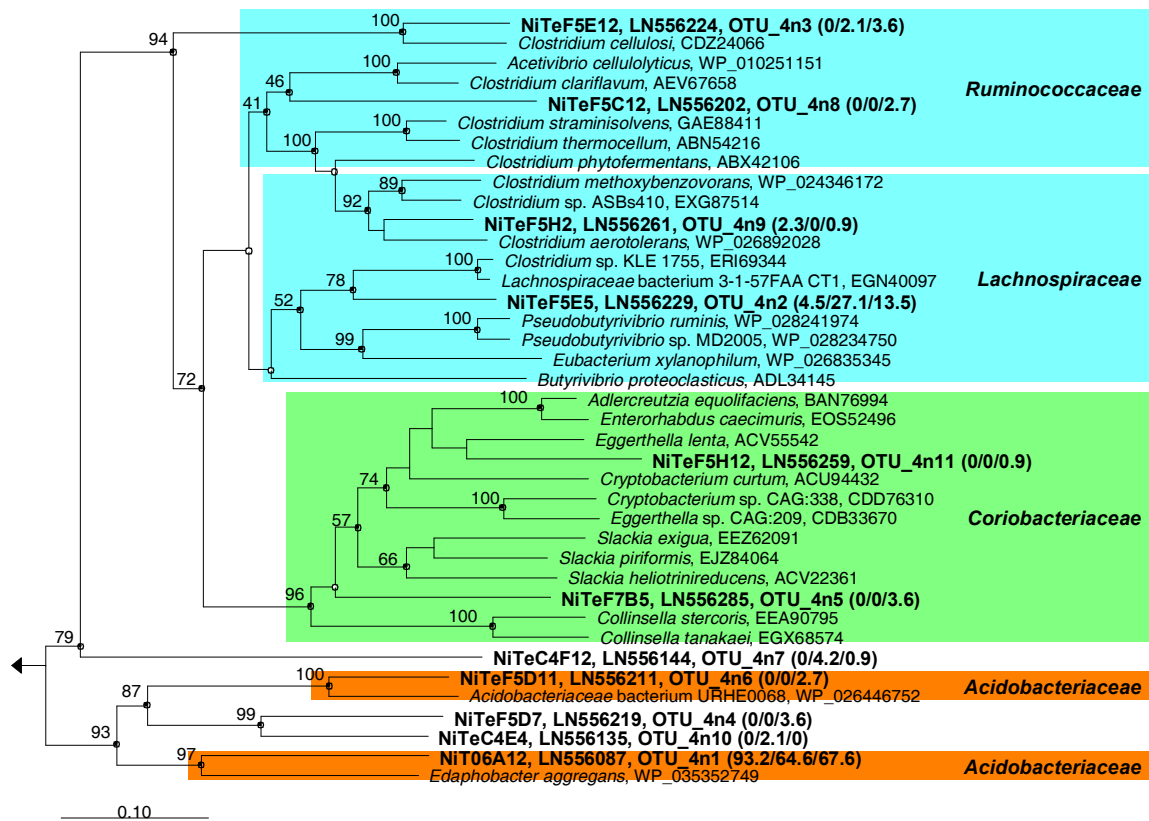
Figure 21 Phylogentic tree of in silico translated group 4 [NiFe]-hydrogenase gene sequences (bold) and closely related sequences.

GenBank accession numbers are indicated. Relative abundancies of OTUs in clone libraries from fresh roots / unsupplemented root microcosms / formate supplemented microcosms are given in parenthesis. Sequences correspond to residues 246 to 528 of the *E. coli* hydrogenase 3 HycE protein (GenBank accession no. AAC75763). Branch lengths are based on the neighbor joining tree. Filled circles at nodes indicate congruent nodes in the maximum-likelihood, maximum parsimony, and neighbor-joining tree. Open circles indicate congruent nodes in two of the three trees. Bootstrap values are averages from the maximum parsimony tree (1000 resamplings), the neighbor joining tree (1000), and the maximum likelihood tree (100) and are only displayed at nodes congruent in all three trees. The bar indicates 0.1 change per amino acid. The hydrogenase of *Methanocaldococcus jannaschii* (AAB99031) was used as outgroup. Color code: blue, *Firmicutes*; orange, *Acidobacteria*; green, *Actinobacteria*; uncolored, unaffiliated (less than 60% identity to publicly available [FeFe]-hydrogenase gene sequences of cultured organisms). Modified from ref [177].
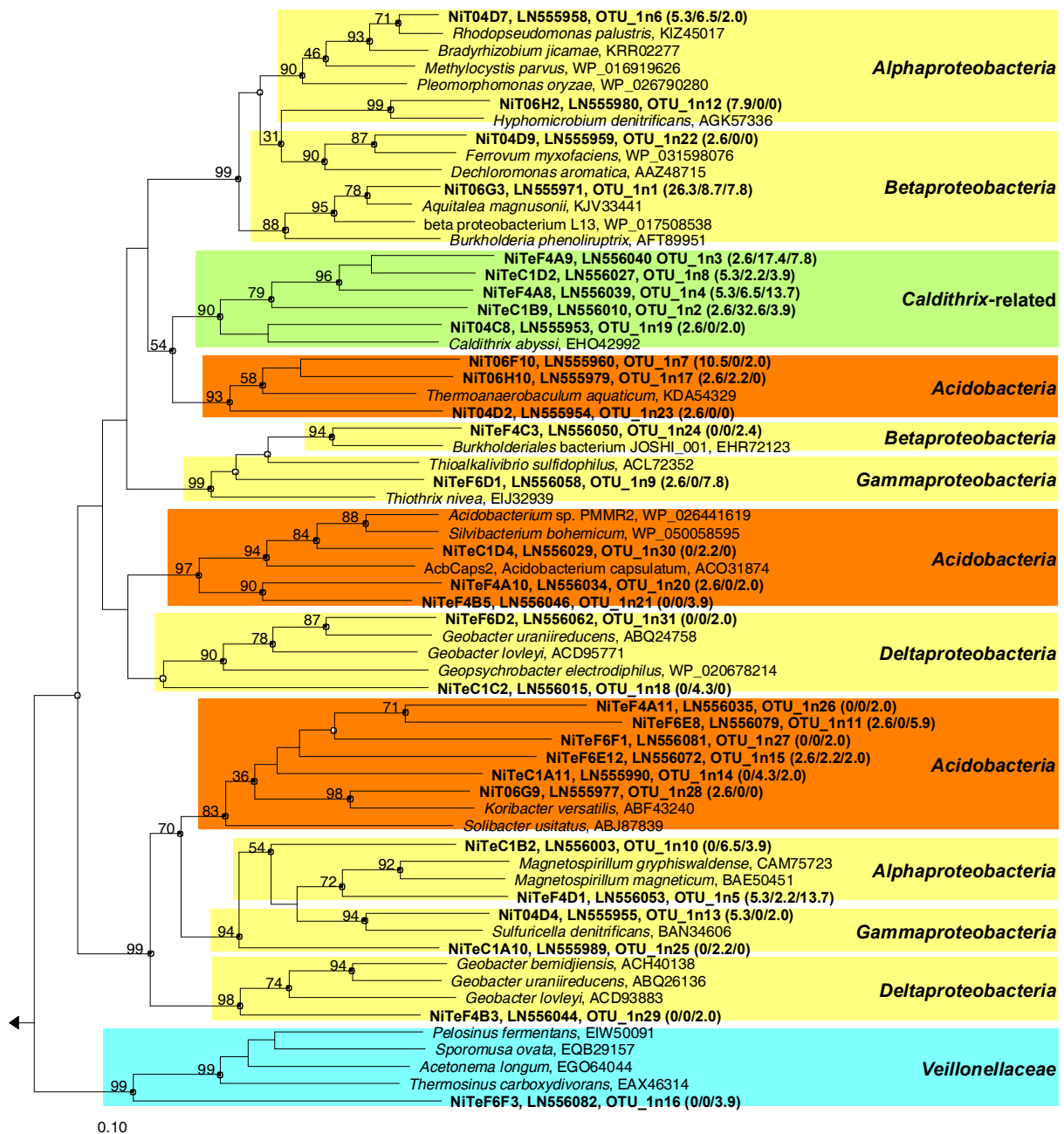
Figure 22   Phylogentic tree of in silico translated group 1 [NiFe]-hydrogenase gene sequences (bold) and closely related sequences.

GenBank accession numbers are indicated. Relative abundancies of OTUs in clone libraries from fresh roots / unsupplemented root microcosms / formate supplemented microcosms are given in parenthesis. Sequences correspond to residues 81 to 572 of the *E. coli* hydrogenase 1 (HyaB, GenBank accession no. AAC74058). Branch lengths are based on the neighbor-joining tree. Filled circles at nodes indicate congruent nodes in the maximum-likelihood, maximum parsimony, and neighbor-joining tree. Open circles indicate congruent nodes in two of the three trees. Bootstrap values are averages from the maximum parsimony tree (1000 resamplings), the neighbor joining tree (1000), and the maximum likelihood tree (100) and are only displayed at nodes congruent in all three trees. The bar indicates 0.1 change per amino acid. The hydrogenase of *Methanosarcina mazei* (AAM31872) was used as outgroup. Color code: blue, *Firmicutes*; yellow, *Proteobacteria*; green, *Caldithrix*-related; orange, *Acidobacteria*.

Several OTUs (especially OTUs 1n1, 1n12, 1n13) were more abundant in fresh root samples compared to anoxic microcosms which is in contrast to the *Caldithrix*-related OTUs that increased in abundance during the anoxic incubation (Figure 22). This indicates that the conditions in the anoxic microcosms differentially stimulated growth of group 1 [NiFe]-hydrogenase gene containing taxa. OTUs 1n1, 1n12 and 1n13 were related to facultative aerobic *Alpha-* and *Betaproteobacteria* that are able to denitrify [207, 235, 447]. The relatively high abundance of group 1 [NiFe]-hydrogenase genes related to that of denitrifying facultative aerobes indicate a potential contribution of such prokaryotes to the hydrogen uptake under the changing redox conditions prevailing in the fen rhizosphere.

OTUs 1n18, 1n29, and 1n31 were affiliated with group 1 [NiFe]-hydrogenase genes of ferric iron reducers of the genus *Geobacter*. *Geobacter* sp. have been detected in the fen before and ferric iron reduction is known to contribute to hydrogen oxidation in this fen [219, 350]. *Acidobacteria* were potentially involved in Fe^{3+} reduction in arctic peat soil [249], and the high abundance of group 1 [NiFe]-hydrogenase genes of *Acidobacteria* in fresh roots and anoxic root microcosms (Figure 19) suggests that this phylum is involved in H_2 consumption and Fe^{3+} reduction in addition to *Geobacter*.

OTUs f4 and f10, which were affiliated with [FeFe]-hydrogenases of sulfate reducing *Deltaproteobacteria*, were abundant in the gene library of fresh roots suggesting that sulfate reduction might occur in close proximity to the roots (Figure 19 and Figure 20). Sulfate reduction is an important respiratory process in the fen and is limited by the availability of sulfate [327, 328]. However, sulfur oxidizers may use O_2 leaking from roots to oxidize reduced sulfur compounds, and therefore the sulfate pool might be replenished faster in the rhizosphere compared to the bulk peat soil. In this regard, OTU_1n13, which afiliated with a group 1 [NiFe]-hydrogenase of the facultative aerobic sulfur oxidizer *Sulfuricella denitrificans* [207], was detected in fresh roots (Figure 22) and therefore, this phylotype might represent a sulfur oxidizer that is active in the rhizosphere. In addition to an enhanced availability of electron acceptors, sulfate reducers are likely provided with suitable electron donors like acetate, propionate, and H_2 that are produced by fermenters that convert root-derived organic compounds (Figure 15). Thus, the rhizosphere is likely a hotspot for sulfate reducing bacteria.

OTUs f16, f22, f29, f35 and 1n16 were affiliated with [FeFe]- and group 1 [NiFe]-hydrogenase genes of acetogens from the families *Clostridiaceae* and *Veillonellaceae* (Figure 20 and Figure 22). These OTUs were observed in unsupplemented and formate-supplemented microcosms, reinforcing the assumption that acetogens contributed to the H_2 uptake at the relatively high concentrations of H_2 that were measured throughout the experiment (Figure 15). Hydrogenase genes of acetogens were not detected in samples of fresh roots, suggesting that the abundance of acetogens was low in the rhizosphere of *Carex* plants at the timepoint of sampling.

Methanogens use [NiFe]-hydrogenases of group 1, 3 and 4 for hydrogen oxidation [433]. However, group 1 and group 4 [NiFe]-hydrogenase specifc primers used in this study were not designed to cover hydrogenase genes of methanogens and thus no hydrogenase genes affiliated to methanogens could be detected. Nevertheless, CH_4 was produced in formate supplemented microcosms and therefore, methanogens likely contributed to H_2 consumption (Figure 15).

The collective data indicate that physiologically and phylogenetically divers H_2 metabolizers are associated to *Carex*-roots in the fen. *Proteobacteria*, *Firmicutes*, *Acidobacteria*, and the *Caldithrix*-related taxa seem to be dominant H_2-metabolizing taxa and made up at least 85% of the sequences in each hydrogenase gene library. Fermenters of the *Ruminococcaceae*, *Clostridiaceae*, and *Lachnospiraceae* are likely important fermentative H_2 producers and denitrifiers (of the *Alpha*-, *Beta*-, and *Gammaproteobacteria*), Fe^{3+}-reducers (*Geobacter* and *Acidobacteria*), sulfate reducers (*Deltaproteobacteria* and *Peptococcaceae*), acetogens (*Veillonellaceae* and *Clostridiaceae*), and methanogens are involved in H_2 consumption in the rhizosphere of sedges in the fen.

3.2.3.   Syntrophic oxidation of ethanol, butyrate, and propionate by peat soil anaerobes

Propionate, butyrate, and ethanol were important fermentation products in glucose- and cellulose-supplemented peat soil microcosms ([151, 176, 384, 487] and 3.2.1) and in soil-free root microcosms (3.2.2) of the Fen Schlöppnerbrunnen. In the absence of electron acceptors other than CO_2, these compounds are generally mineralized by syntrophic methanogenic consortia [376], but the members of such consortia are not resolved for peatlands. Here, 16S rRNA-based SIP and SIP-independent 16S rRNA analyses were performed with samples of ethanol-, butyrate-, propionate- and unsupplemented (root-containing) peat soil microcosms incubated at 5°C and 15°C to identify taxa associated to syntrophic processes. Due to financial constraints, SIP experiments were limited to the ethanol and butyrate treatments at 15°C and no propionate and butyrate treatments were conducted at 5°C.

3.2.3.1.   Preincubation of anoxic peat soil microcosms

A preincubation (28 d and 38 d at 5°C and 15°C), in which the microcosms were kept unsupplemented, was done to establish fully anoxic conditions and to deplete easily degradable endogenous carbon sources (e.g., root-derived carbon) (2.1.2.3). CO_2 accumulation started immediately and was approximately twice as fast at 15°C compared to 5°C; in contrast, only minor amounts of acetate and propionate were formed, and methane

production did not start before 10 and 20 days at 15°C and 5°C, respectively (Figure 23 and Figure 24). The production of CO_2 without an appreciable production of methane or fermentation products (such as acetate or propionate) during the preincubation period suggested that the mineralization of endogenous sources of carbon was linked to the consumption of residual electron acceptors other than CO_2, such as oxygen, nitrate, sulfate, or Fe^{3+} [5, 100, 219, 321, 326, 327, 350]. The consumption of acidic anionic electron acceptors (nitrate and sulfate) likely caused the observed increase in pH from 4.5 to 5.2 during the initial preincubation. The average CO_2 production rate during the initial 7 days at 15°C was 10.1 $\mu mol \cdot g_{dw}^{-1} \cdot d^{-1}$, which was slightly higher compared to that in root-free soil microcosms (6.1 $\mu mol \cdot g_{dw}^{-1} \cdot d^{-1}$) but considerably less than in soil-free root microcosms (53.1 $\mu mol \cdot g_{dw}^{-1} \cdot d^{-1}$). The higher rates in root-containing compared to root-free soil microcosms underscored the importance of roots as endogenous carbon sources for the microbes in peat soil. On the other hand, the 80% lower rates in root-containing soil compared to soil-free root microcosms indicates that the availability of root-derived carbon sources limits the microbial activity in peat soil.

Partial pressures of H_2 increased to 10 and 7 Pa at 15°C and 5°C, respectively, but did not increase any further (Figure 23C and Figure 24C). Formate concentrations were close to the detection limit (1-10 µM) and could therefore not be quantified adequately (data not shown). Steady low concentrations of H_2 and formate were a thermodynamic prerequisite for the syntrophic degradation of ethanol, butyrate, and propionate [376], and therefore these processes could be analyzed after the preincubation.
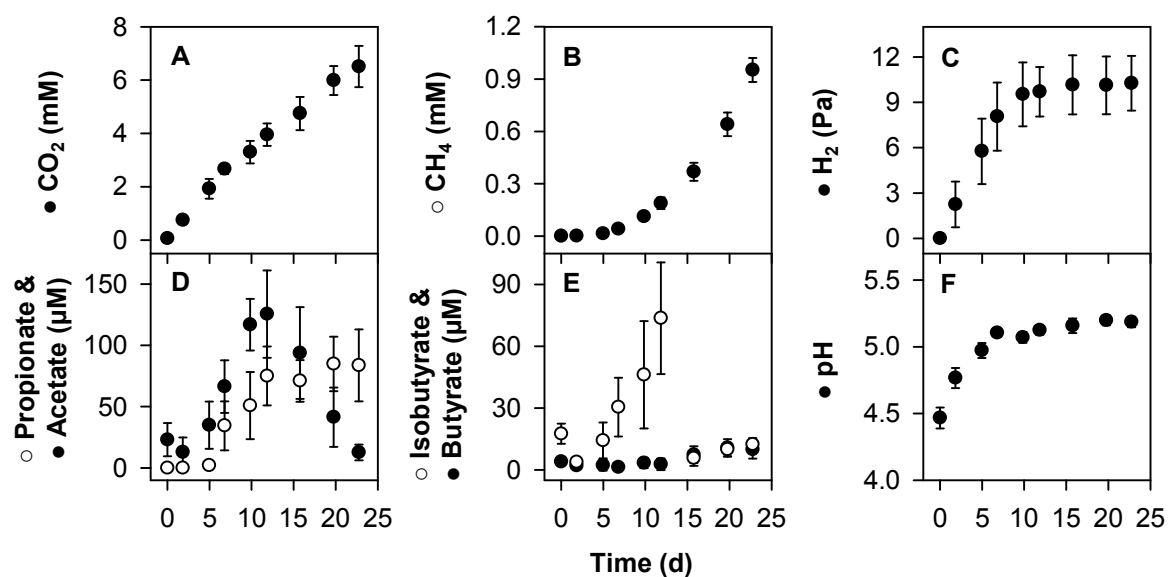
Figure 23   Concentrations of organic acids, gases, and pH of unsupplemented microcosms during the preincubation at 15°C.

Values are means of 20 replicates. Error bars indicate standard deviations. A H_2 partial pressure of 10 Pa correlates to approximately 4.5 µM H_2. Modified from ref [386].
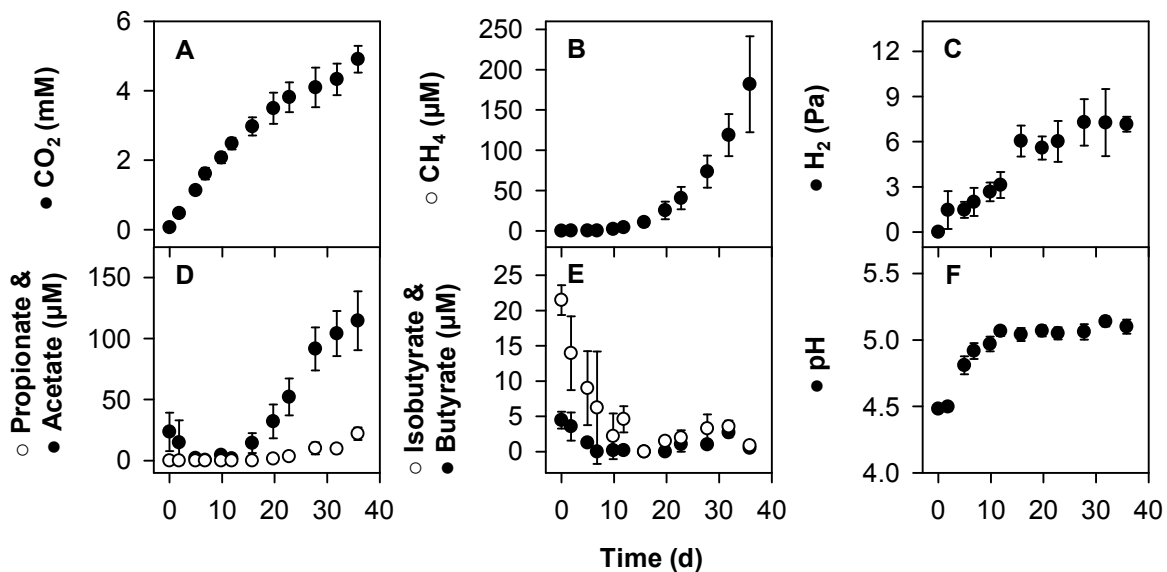
Figure 24 Concentrations of organic acids, gases, and pH of unsupplemented microcosms during the preincubation at 5°C.

Values are means of 10 replicates. Error bars indicate standard deviations. A H_2 partial pressure of 10 Pa correlates to approximately 4.5 μM H_2. Modified from ref [386].

3.2.3.2.   Anaerobic flow of endogenous carbon and reductant in unsupplemented anoxic peat soil microcosms

After the preincubation, CO_2 and methane were the only detected end products that accumulated at both 15°C and 5°C in unsupplemented controls (Figure 25 and Figure 26). This result is in contrast to other studies where acetate, ethanol, butyrate, or propionate were detected at mM concentrations in anoxic microcosms of unsupplemented peat at the end of anoxic incubation, especially at lower temperatures [289, 445].   The low steady state concentrations of organic acids and alcohols observed in unsupplemented controls at 5°C and 15°C in this study indicate that the hydrolysis of organic matter rather than syntrophic methanogensis was rate limiting. Average methane production rates were 2.9 μmol·g_{dw}^{-1}·d^{-1} at 15°C and 0.89 μmol·g_{dw}^{-1}·d^{-1} at 5°C, respectively.   Slightly lower rates were observed with subarctic peat soil (1.5 μmol·g_{dw}^{-1}·d^{-1} at 15°C and 0.75 μmol·g_{dw}^{-1}·d^{-1} at 4°C; [290]). CO_2:CH_4 ratios at the end of the incubation were 2.0 and 2.4 at 15°C and 5°C, respectively. That the CO_2:CH_4 ratios were greater than 1 indicated that methanogenesis was not the sole terminal process (this conclusion assumes that CO_2 and CH_4 were derived from carbon at the oxidation state of carbon in glucose). Nevertheless, methanogenesis contributed to about half of the CO_2 produced during organic matter mineralization at 15°C and only slightly less at 5°C according to the CO_2:CH_4 ratios. These results support the hypothesis that methanogenesis is one of several anaerobic processes that contribute to the overall mineralization of organic matter in this fen [205].
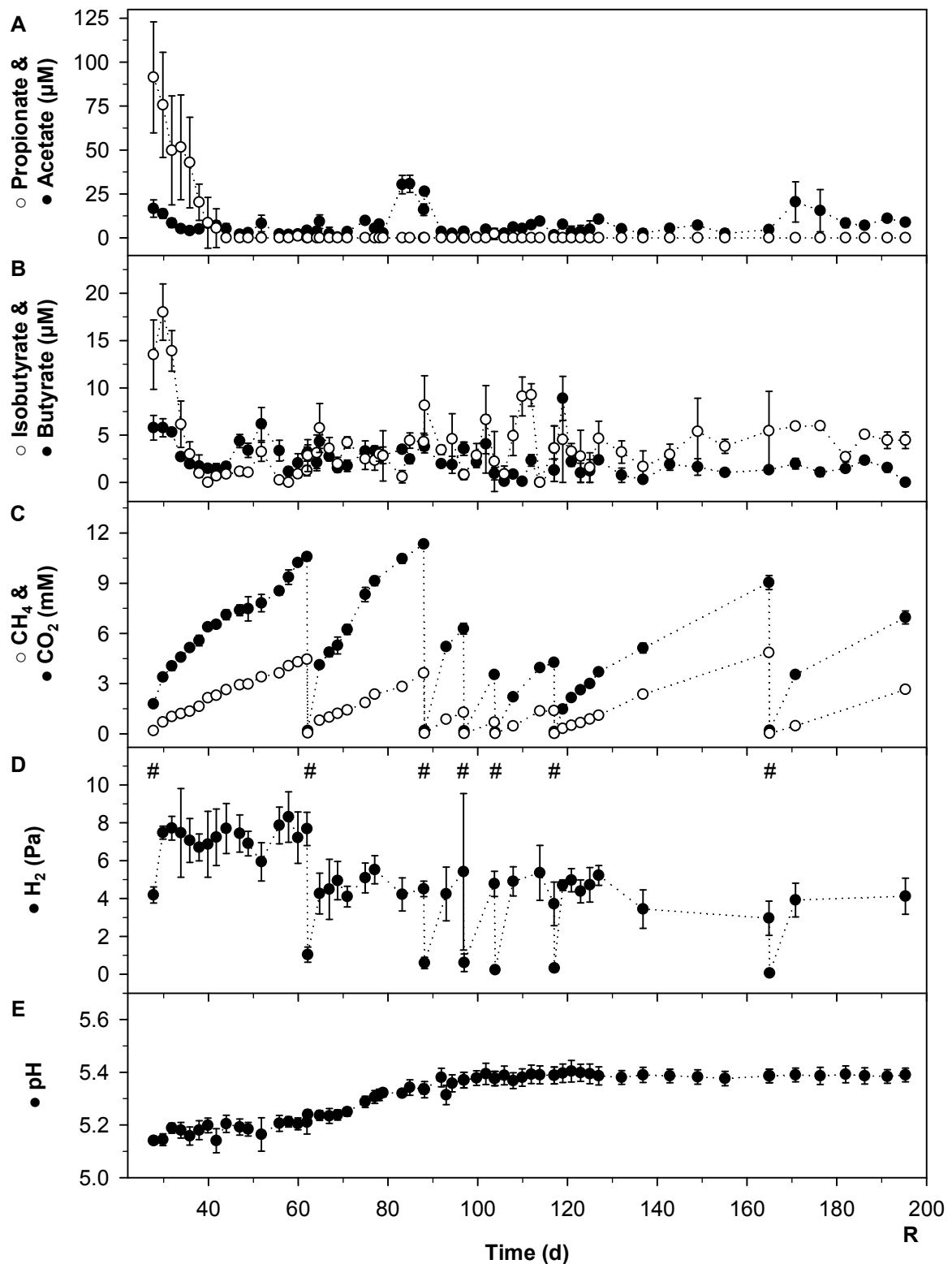
Figure 25   Concentrations of acids, gases, and pH of unsupplemented controls at 15°C.

#, gas phases were flushed with sterile N_2; R, sampling for RNA extraction. Anoxic microcosms were preincubated (2.1.2.2 and 3.2.3.1). Values are means of five replicates and error bars indicate standard deviations. A H_2 partial pressure of 10 Pa correlates to approximately 4.5 µM H_2. Modified from ref [386].
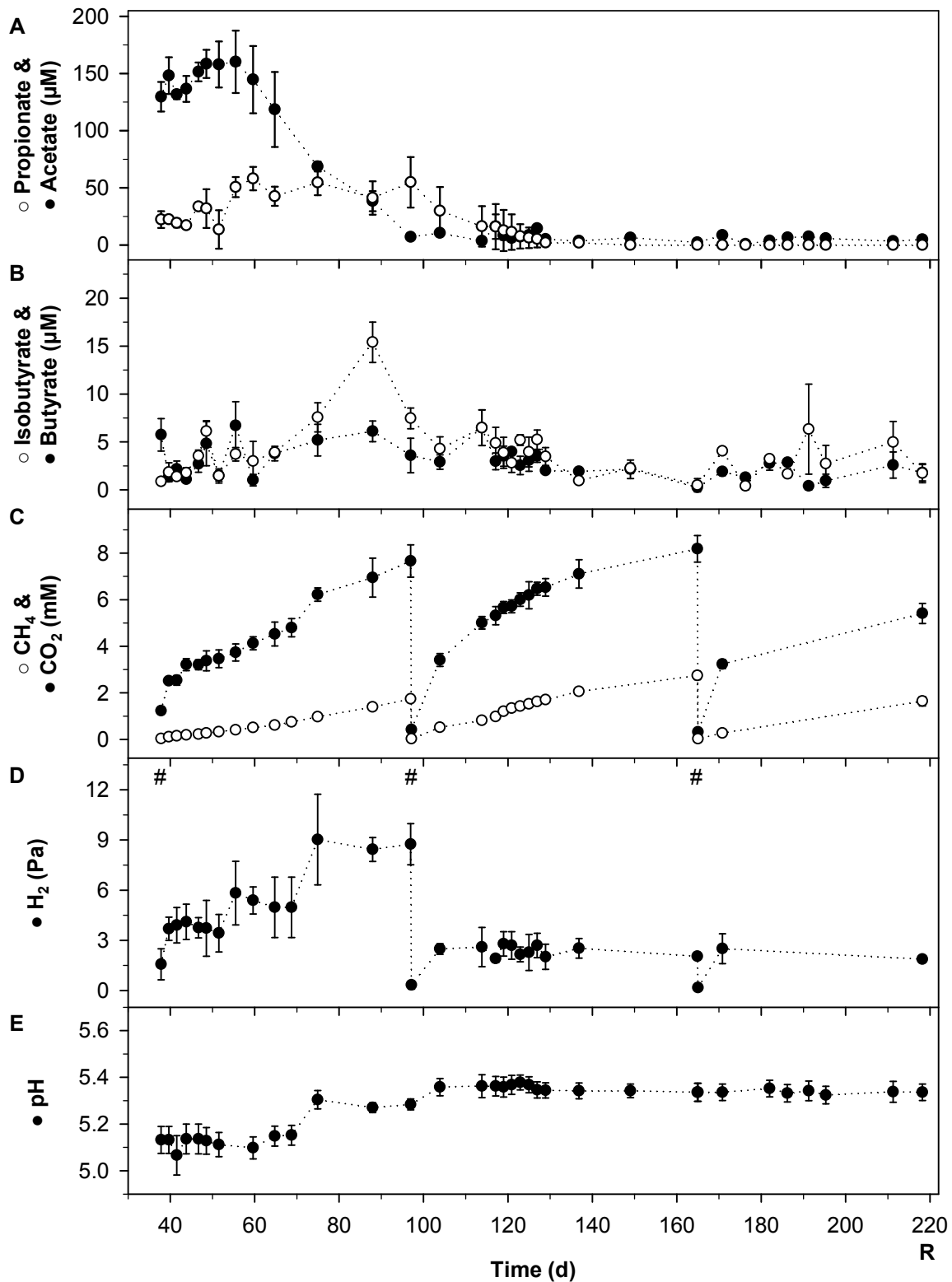
Figure 26   Concentrations of acids, gases, and pH of unsupplemented controls at 5°C.

#, gas phases were flushed with sterile N_2; R, sampling for RNA extraction (2.5.1). Anoxic microcosms were preincubated (2.1.2.2 and 3.2.3.1). Values are means of five replicates and error bars indicate standard deviations. A H_2 partial pressure of 10 Pa correlates to approximately 4.5 µM H_2. Modified from ref [386].

Partial pressures of H_2 approximated 7-9 Pa until day 60 and decreased to 4-6 Pa afterwards at 15°C (Figure 25D). Partial pressures of H_2 increased slowly to 9 Pa and decreased to 2-3 Pa after the gas phase was exchanged on day 96 at 5°C (Figure 26D). Decreasing H_2 partial pressures suggested that H_2 was scavenged more efficiently by H_2-consumers (e.g., hydrogenotrophic methanogens) at the end compared to the beginning of the main incubation. Formate concentrations were low and could not be adequately quantified at 15°C and 5°C (data not shown). Thus, formate was probably effectively scavenged by formate consuming microbes. The pH increased slowly from 5.2 to 5.4 at 15°C and 5°C (Figure 25E and Figure 26E).

3.2.3.3. Effect of supplemental ethanol, butyrate, and propionate in anoxic peat soil microcosms

Preincubated anoxic microcosms were pulsed with low concentrations (300-750 µM) of ethanol, butyrate, or propionate and incubated at 15°C to identify processes that lead to the oxidation of these three fermentation products. The utilization of ethanol at 5°C was also evaluated.

Initially supplemented ethanol was consumed rapidly and without delay, whereas initially supplemented butyrate and propionate were consumed more slowly (Figure 27-Figure 30). Subsequent pulses of substrates resulted in faster consumption of substrates, indicating that syntrophic consortia developed with time resulting in an incresead efficiency of syntrophic processes. Acetate accumulated transiently and was subsequently consumed in ethanol and butyrate treatments. Hardly any transient accumulation of acetate was observed in propionate treatments in which detected acetate concentrations never exceeded 40 µM (this is in the range of what was detected in unsupplemented controls; Figure 25). Isobutyrate transiently accumulated in butyrate treatments and was subsequently consumed parallel to butyrate consumption (Figure 29), indicating an isomerization of butyrate to isobutyrate as observed in syntrophic methanogenic cultures (Wu *et al.*, 1994). Low concentrations of formate could be detected but could not be adequately quantified (data not shown). H_2 concentrations in headspace gas phases were relatively low and ranged between 3 Pa (ethanol treatments at 5°C) and 17 Pa (ethanol treatments at 15°C) (Figure 27-Figure 30). Low concentrations of formate and H_2 indicated that either (a) these compounds were not important intermediates or (b) formate- and H_2-scavaging was efficient in all treatments. Effective hydrogen- and formate-scavanging is supported by the finding that H_2 and formate were formed in glucose-, xylose-, or N-acetylglucoseamine-supplemented microcsosms and both stimulated acetogenesis and methanogenesis in hydrogen- or formate-supplemented microcosms of the fen [151, 175, 487].
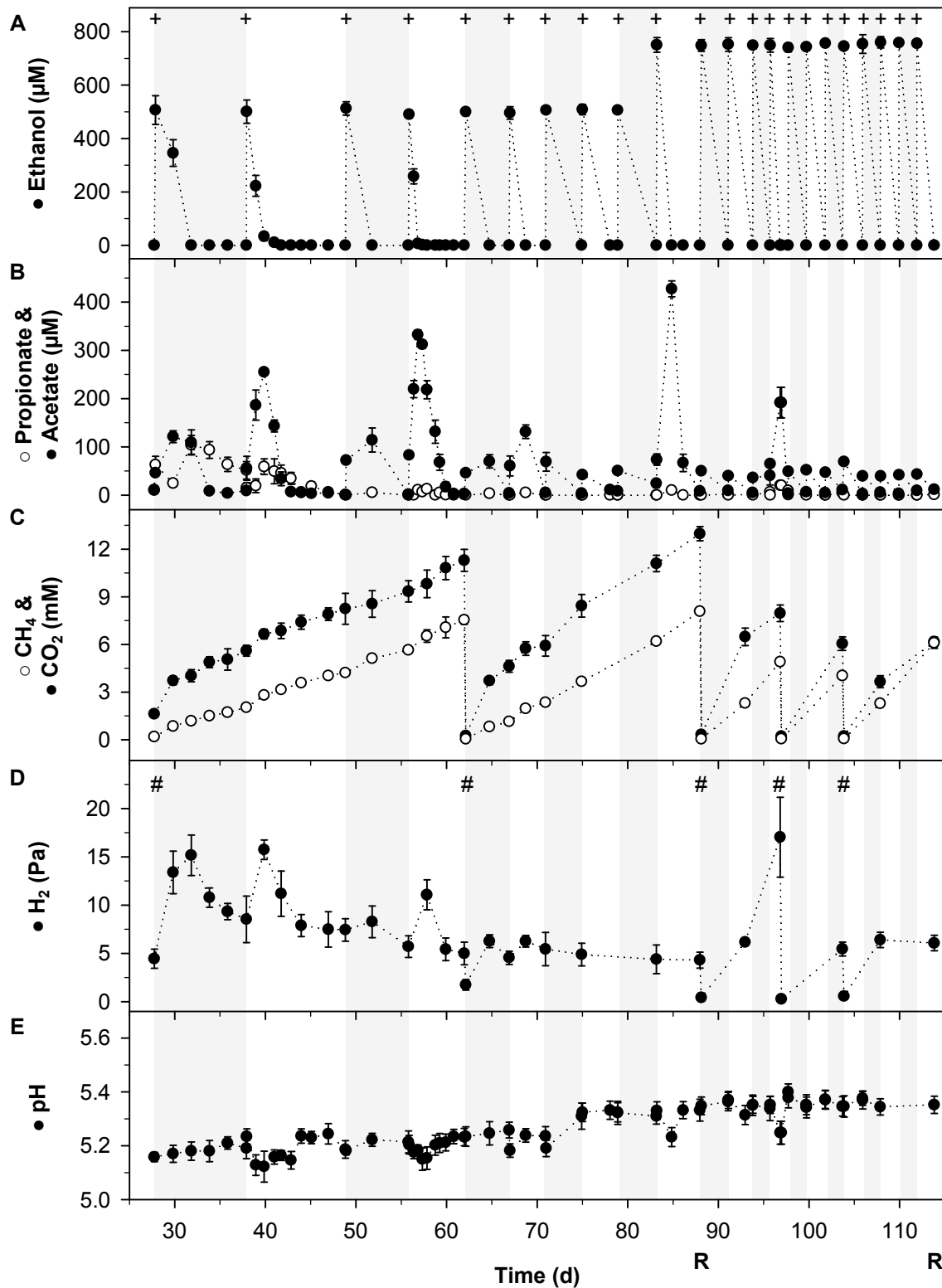
Figure 27 Concentrations of ethanol, acids, gases, and pH of ethanol treatments at 15°C.
+, supplementation of [^{12}C]ethanol (one replicate was supplemented with [^{13}C]ethanol after day 88; 2.1.2.3); #, gas phases were flushed with N_2; R, sampling for RNA extraction (2.5.1). Anoxic microcosms were preincubated (2.1.2.3 and 3.2.3.1). Values are means of five replicates and error bars indicate standard deviations. A H_2 partial pressure of 10 Pa correlates to approximately 4.5 µM H_2. Modified from ref [386].
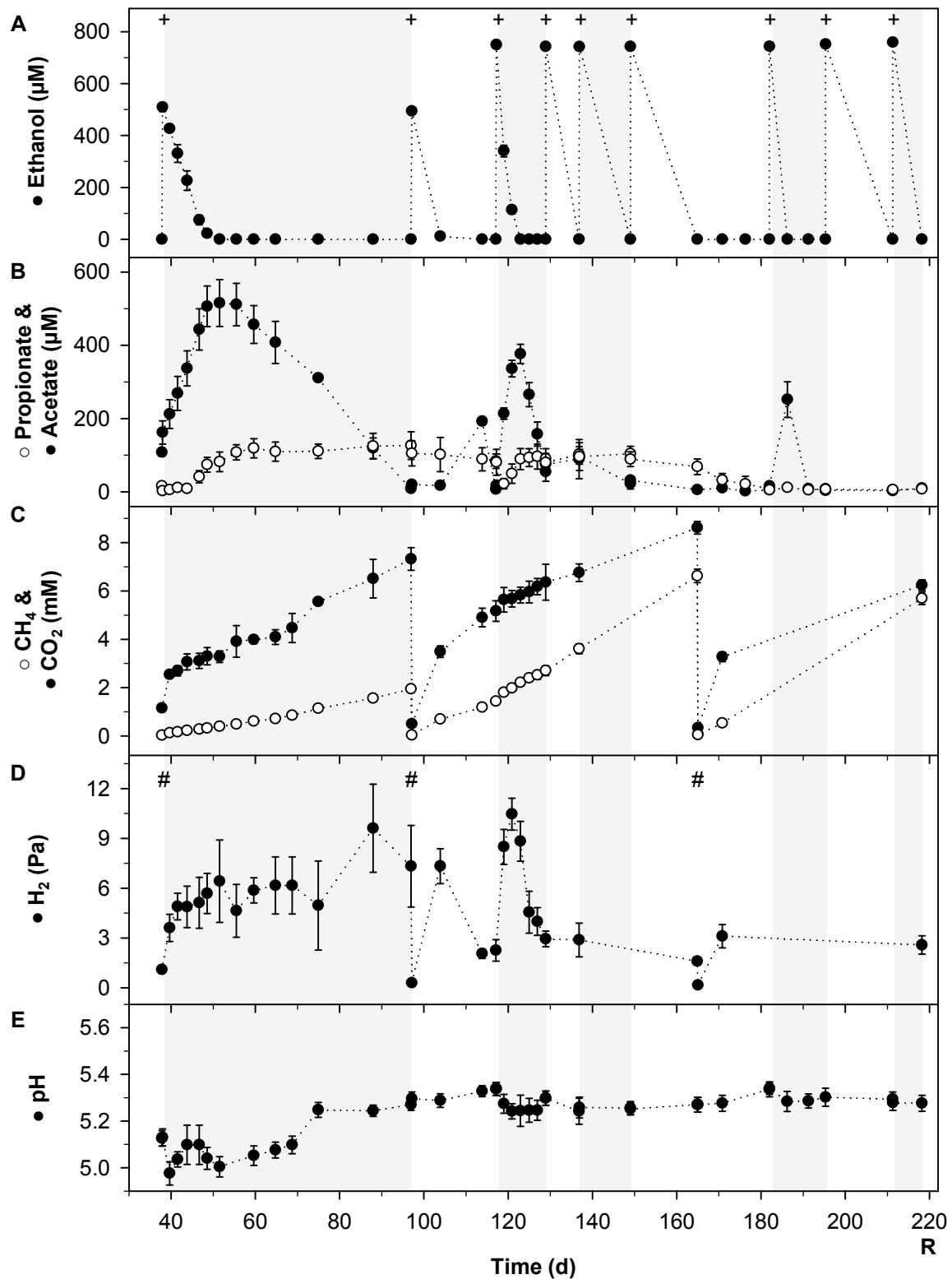
Figure 28   Concentrations of ethanol, acids, gases, and pH of ethanol treatments at 5°C.

+, supplementation of [^{12}C]ethanol; #, gas phases were flushed with sterile N$_2$; R, sampling for RNA extraction (2.5.1). Anoxic microcosms were preincubated (2.1.2.3 and 3.2.3.1). Values are means of five replicates and error bars indicate standard deviations. A H$_2$ partial pressure of 10 Pa correlates to approximately 4.5 µM H$_2$. Modified from ref [386].
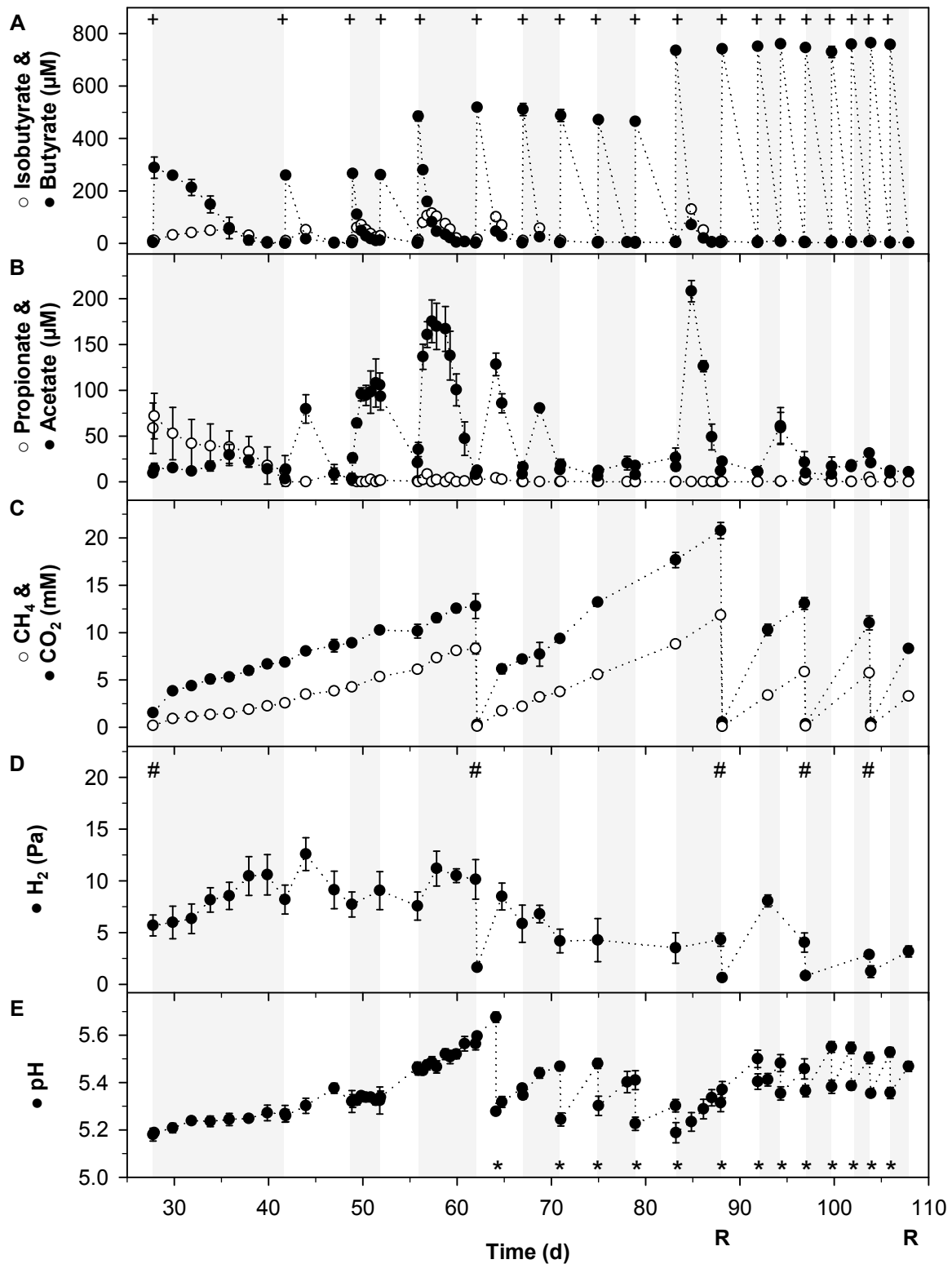
Figure 29   Concentrations of acids, gases, and pH of butyrate treatments at 15°C.

+, supplementation of [^{12}C]butyrate (one replicate was supplemented with [^{13}C]butyrate after day 88; 2.1.2.3); #, gas phases were flushed with sterile N_2; *, pH was readjusted; R, sampling for RNA extraction (2.5.1). Anoxic microcosms were preincubated (2.1.2.3 and 3.2.3.1). Values are means of five replicates and error bars indicate standard deviations. A H_2 partial pressure of 10 Pa correlates to approximately 4.5 µM H_2. Modified from ref [386].
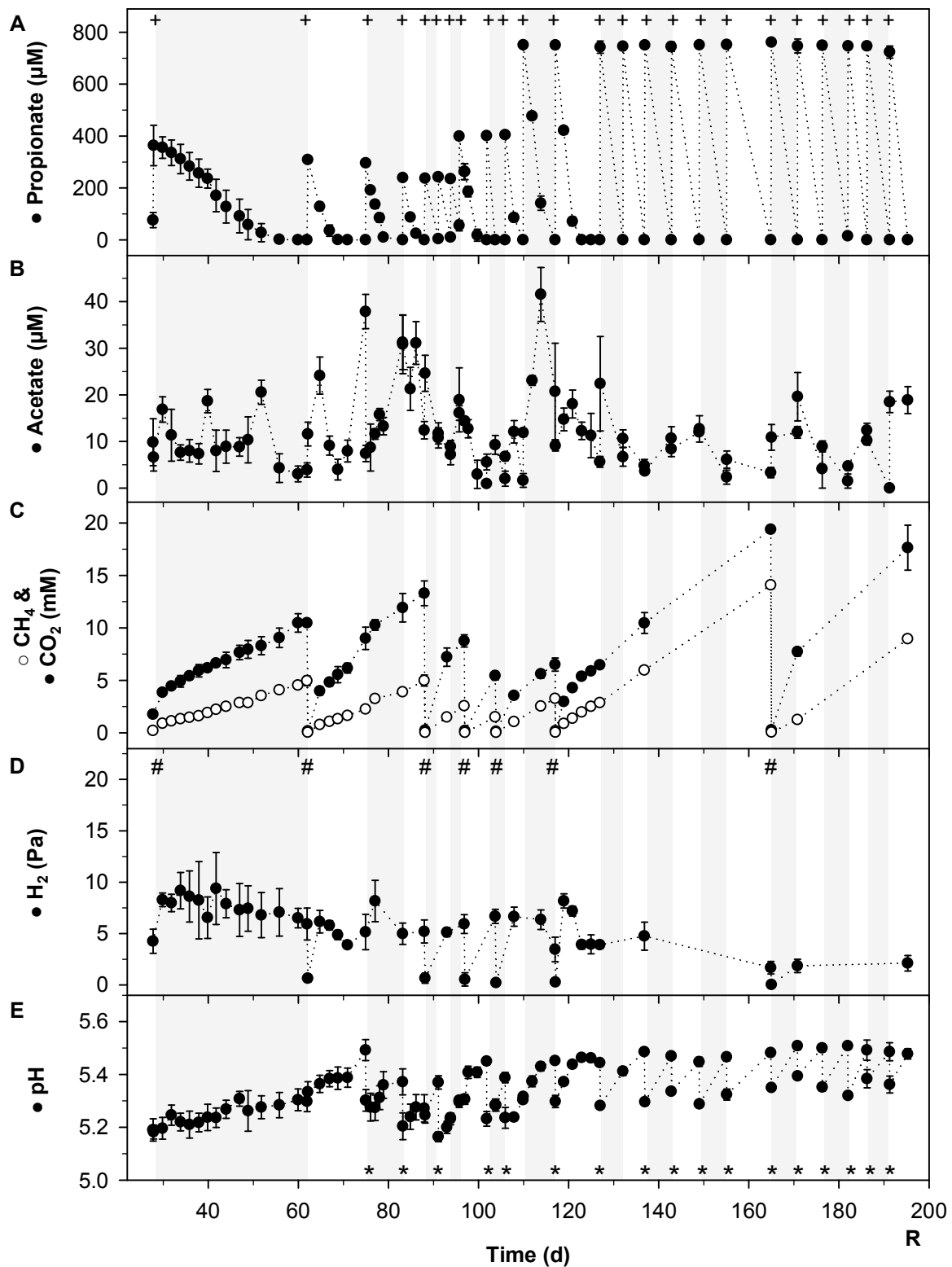
Figure 30 Concentrations of acids, gases, and pH of propionate treatments at 15°C.

+, supplementation of [^{12}C]propionate; #, gas phases were flushed with sterile N_2; *, pH was readjusted; R, sampling for RNA extraction (2.5.1). Anoxic microcosms were preincubated (2.1.2.3 and 3.2.3.1). Values are means of five replicates and error bars indicate standard deviations. A H_2 partial pressure of 10 Pa correlates to approximately 4.5 µM H_2. Modified from ref [386].
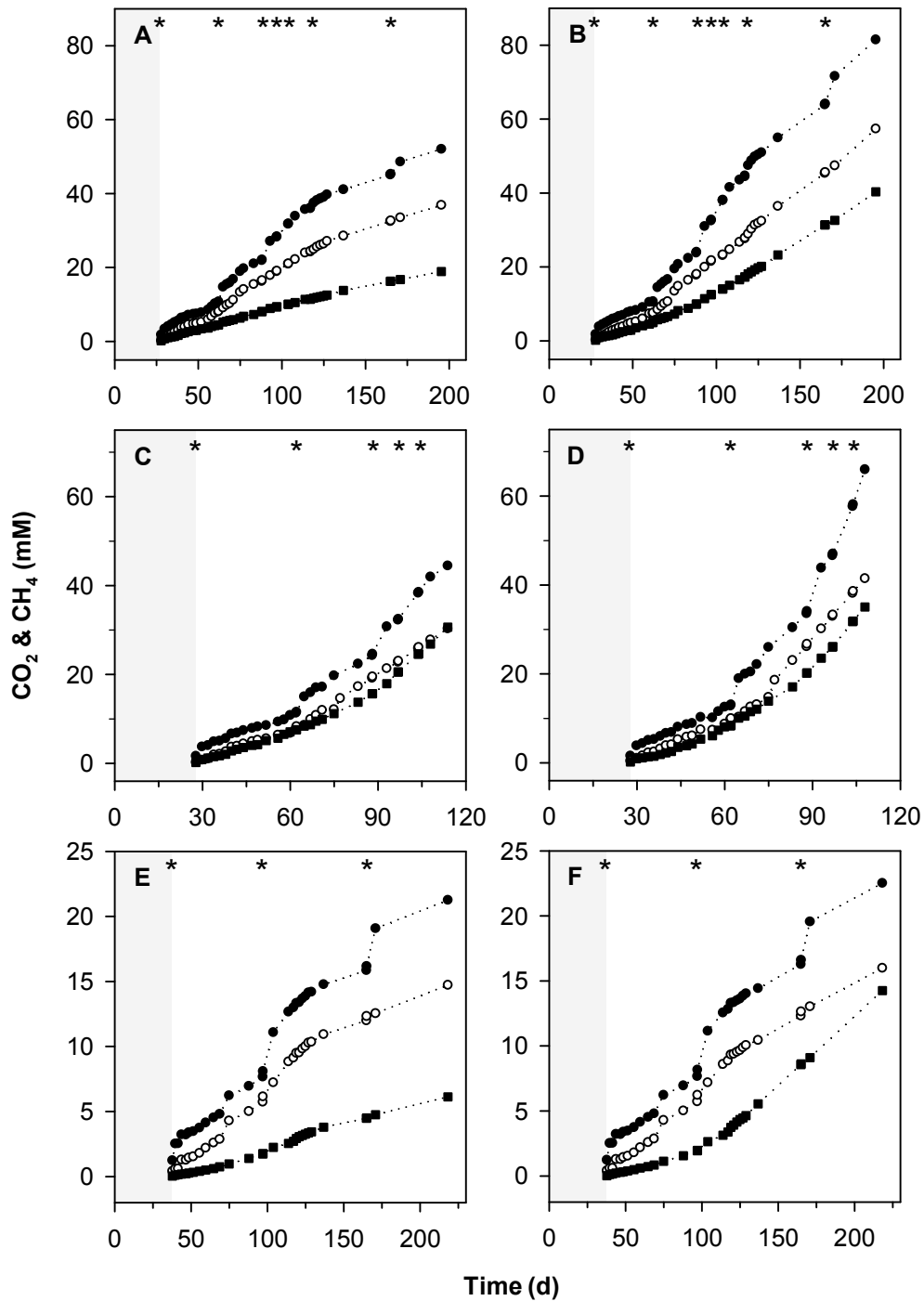
Figure 31   Cumulative CO₂ and CH₄ concentrations of peat soil microcosms.

A and E, unsupplemented controls at 15°C and 5°C, respectively; B, propionate treatments at 15°C; C and F, ethanol treatments at 15°C and 5°C, respectively; D, butyrate treatments. Gray boxes indicate the preincubation (2.1.2.3 and 3.2.3.1). Values are means of five replicates. Symbols: ●, CO₂ (uncorrected); ○, CO₂ concentrations were corrected after each flushing of the gas phase with N₂ (indicated by *) as described (2.7.1.3); ■, CH₄. Modified from ref [386].

CH₄ and CO₂ were the sole detected accumulating end products in ethanol, butyrate, and propionate treatments (Figure 27-Figure 30). The production of both gases was stimulated by

the addition of substrates compared to unsupplemented controls (Figure 31). Observed substrate:CH_4:CO_2 ratios were close to theoretical ratios for complete substrate conversion to methane and CO_2 (Table 23). Electron recoveries of about 90% and carbon recoveries ranging from 75% to 104% also reflect the near stoichiometric conversion of substrates to methane and CO_2 (Table 1). The missing 10% in electron recoveries might reflect assimilation of biomass and thus growth of syntrophs and methanogens [183].

The pH was relatively stable in ethanol treatments but increased in butyrate and propionate treatments (Figure 27-Figure 30). This increase in pH could be attributed to sodium ions that were added since the substrate solutions were prepared with the sodium salts of butyrate and propionate, respectively (2.1.2.3). Hydrogen chloride was added to readjust the pH in butyrate and propionate treatments (2.1.2.3).

Table 23   Conversion of substrates to CH_4 and CO_2, and recoveries of anoxic peat soil microcosm[a]

Treatment	Incubation time frame	Substrate : CH_4 : CO_2 ratio		Electron recovery (%)	Carbon recovery (%)
		observed	theoretical		
Ethanol (15°C)	d 28-114	1:1.35:0.44	1:1.5:0.5[b]	90	89
Ethanol (5°C)	d 38-218	1:1.31:0.20	1:1.5:0.5[b]	87	75
Butyrate (15°C)	d 28-108	1:2.28:1.77	1:2.5:1.5[c]	91	101
Propionate (15°C)	d 28-195	1:1.60:1.53	1:1.75:1.25[d]	92	104

[a]Concentrations of unsupplemented controls were subtracted from that of ethanol, butyrate, and propionate treatments to calculate ratios and recoveries (2.7.1.3).

[b,c,d]Complete oxidation of substrate to CH_4 and CO_2 according to the following reactions: [b], 2 ethanol → 3 CH_4 + 1 CO_2; [c], 2 butyrate + 2 H^+ + 2 H_2O → 5 CH_4 + 3 CO_2; [d], 4 propionate + 4 H^+ + 2 H_2O → 7 CH_4 + 5 CO_2. Modified from ref [386].

3.2.3.4.   Thermodynamics of processes potentially linked to syntrophic methanogenesis

ΔGs for hydrogenotrophic methanogenesis approximated -50 kJ·mol^{-1} and were always far more exergonic compared to the ΔGs for acetogenesis (Figure 32). However, acetogenesis became thermodynamically favorable if transiently accumulated acetate was consumed especially in unsupplemented controls at 5° where ΔGs for acetogenesis decreased down to -26 kJ·mol^{-1} (Figure 26A and Figure 32C). Thus, acetogens and methanogens may have competed for the low concentrations of H_2 detected in the anoxic peat soil microcosms. Aceticlastic methanogenesis was more exergonic at the start of the main incubation (-40 kJ·mol^{-1} at 15°C and -50 kJ·mol^{-1} at 5°C) and eventually became less exergonic (> -30 kJ·mol^{-1}) when CH_4 and CO_2 increased (see also Figure 25 to Figure 30).
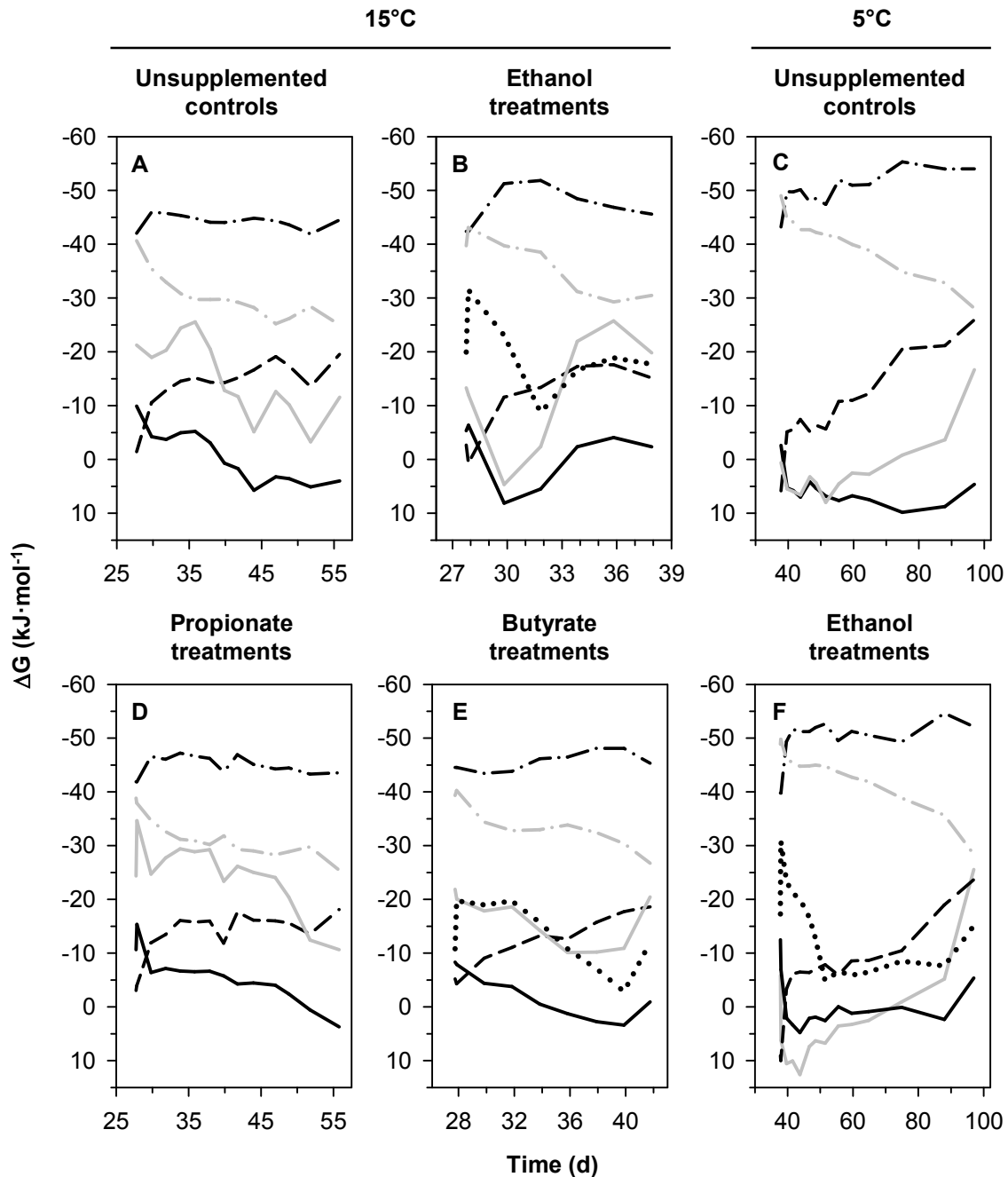
Figure 32   Gibbs free energies of syntrophic processes in anoxic peat soil microcosms.

Shown is the time frame between the first and second substrate supplementations after the preincubation (2.1.2.3 and 3.2.3.1). See Figure 25 to Figure 30 for concentrations of ethanol, acids, and gases. ΔGs were calculated as described (2.7.2). Lines: black and grey solid lines, syntrophic oxidation of propionate according to Reaction 5 and 6 in Table 2, respectively; black dotted line, syntrophic oxidation of ethanol (Reaction 8 in Table 2) in B and F, and syntrophic oxidation of butyrate (Reaction 4 in Table 2) in E; black dashed dotted lines, hydrogenotrophic methanogenesis (reaction 1 in Table 3); grey dashed dotted lines, aceticlastic methanogenesis (reaction in Table 3); black dashed line, acetogenesis (reaction 1 in Table 4). Modified from ref [386].

Syntrophic ethanol oxidation (-31 kJ·mol^{-1}) was more exergonic compared to syntrophic butyrate oxidation (-20 kJ·mol^{-1}) after the initial substrate supplementation. Thermodynamics of syntrophic ethanol and butyrate oxidation became less favorable when the supplemented substrate was consumed and acetate transiently accumulated (Figure 27, Figure 28, Figure 32B, E and F). ΔGs for both syntrophic processes became more exergonic again when acetate was subsequently consumed. Endogenously formed or supplemented amounts of propionate were consumed in unsupplemented controls at 15°C and 5°C, and in propionate treatments at 15°C (Figure 25A, Figure 26A, and Figure 30A) in which ΔGs for syntrophic propionate oxidation ranged from -17 to +10 kJ·mol^{-1} (Figure 32A, C, and D). Those relatively endergonic ΔGs suggest that propionate was consumed primarily in microbial aggregates where the thermodynamics for syntrophic propionate oxidation may have been more favorable compared to the bulk soil slurry (details are discussed in 4.1.2.4).

3.2.3.5. Microbial community of fresh peat

179 bacterial 16S rRNA sequences were obtained from fresh peat. Those sequences clustered into 60 family-level OTUs (85% coverage), which were affiliated with 15 different phyla (Table 24 and Table A3). Almost 50% of the sequences were affiliated with the *Proteobacteria*. The *Alphaproteobacteria* (33.5% relative abundance) were more abundant than were the *Beta-* (5%), *Delta-* (4.5%), and *Gammaproteobacteria* (3.9%). Within the *Alphaproteobacteria* well known genera of anoxygenic phototrophs (e.g., *Rhodoblastus* and *Rhodomicrobium*), chemo-organotrophs (e.g., *Acidisphaera*), and methylotrophs (e.g., *Methylosinus* and *Methylocella*) were detected. *Alphaproteobacteria* have been frequently detected in several peatlands, and they are important for the carbon- and nitrogen cycling because of their collective capacity to fix N_2, oxidize CH_4, and mineralize organic matter [84].

The *Firmicutes* (13.4% relative abundance) were identified as the second most abundant phylum in fresh peat (Table A3) and sequences were mainly affiliated to either families of obligate anaerobes (e.g., *Ruminococcaceae*, *Clostridiaceae*, and *Veillonellaceae*) or *Paeni-bacillaceae*, a family that comprises many facultative aerobes [83, 345, 346, 478]. Members of those families are often hydrolytic or saccharolytic fermenters and sequences related to them were detected in cellulose supplemented microcosms (3.2.1.2). Firmicutes might therefore contribute to the anaerobic degradation of cellulosic organic matter in the fen.

Acidobacteria (8.9% relative abundance), which was the dominant phylum in peatlands in the USA, Slovenia, and northern Russia [9, 154, 323], were also abundant in fresh peat of the fen (Table A3). Acid tolerant, slow-growing, and metabolically versatile heterotrophic members of the Acidobacteria were repeatedly isolated from peatlands and may play a key role in the oxidation of organic matter in cold and temperate peatlands [84].

Additional bacterial phyla present in fresh peat comprised *Actinobacteria* (6.1% relative abundance), *Planctomycetes* (4.5%), *Verrucomicrobia* (3.9%), *Bacteroidetes* (3.4%), *Cyanobacteria* (2.8%), and *Chloroflexi* (2.2%). Sequence identities to cultured species of these taxa were often below 90% and the in situ function of the detected uncultured taxa remains unclear.

The 92 archaeal 16S rRNA sequences obtained from fresh peat clustered into 6 genus-level OTUs (100% coverage) (Table 24). Most of the sequences (97% relative abundancies) were affiliated to genera of methanogenic *Euryarchaeota* and the remaining sequences were closely related (99% identity) to *Nitrosotalea devanaterra*, which is a thaumarchaeal ammonium oxidizer [242]. *Methanosarcina* (51% relative abundance) and *Methanosaeta* (34%) that are both aceticlastic methanogens were the two dominant archaeal genera in fresh peat. Thus acetate might have been an important source of methane at the sampling time point. Hydrogenotrophic methanogens were less abundant and were affiliated to the genera *Methanocella* (7% relative abundance), *Methanosphaerula* (3%), and *Methanoregula* (2%).

Table 24   No. of OTUs and coverages of bacterial/archaeal 16S rRNA sequences

Clone library[a]	*Fresh peat*	15°C						5°C		*Total*
		E_H	*E_L*	*B_H*	*B_L*	*P*	*C*	*E*	*C*	
No. of Sequences	179/ 92	118/ 70	133/ 67	119/ 60	135/ 108	136/ 65	113/ 65	112/ 60	84/ 62	1129/ 649
No. of OTUs[b]	60/ 6	30/ 5	36/ 8	38/ 3	40/ 5	46/ 6	44/ 7	44/ 4	36/ 8	116/ 11
Coverage[c] (%)	85/ 100	86/ 99	89/ 97	84/ 100	85/ 99	89/ 97	87/ 97	85/ 98	86/ 94	97/ 100

[a]E, B, P: ethanol, butyrate, or propionate treatments. C: unsupplemented controls. H and L are 'heavy' and 'light' fractions, respectively (Figure 7).
[b]OTUs were calculated based on 87.5% similarity cut-off (family level) for bacterial and 95% similarity cut-off (genus level) for archaeal 16S rRNA sequences. Modified from ref [386].

3.2.3.6.   Bacteria involved in the anaerobic mineralization of endogenous carbon sources in unsupplemented controls

Alphaproteobacteria, which made up one third of the 16S rRNA sequences in fresh peat, were also abundant in unsupplemented controls at the end of the anoxic incubation at 15°C (31% relative abundance) and 5°C (25%) (Table A3). *Alphaproteobacteria* that are known to be metabolically diverse (e.g., some can ferment or reduce ferric iron under anoxic conditions [84, 185, 349, 406]) therefore might have contributed to the mineralization of endogenous carbon sources during the prolonged anoxic incubation period in the unsupplemented controls (Figure 25 and Figure 26). Approximately 8.8% and 3.6% of the 16S rRNA sequences at 15°C

and 5°C, respectively, were closely related (99% identity) to *Rhodoblastus acidophilus*, an anoxygenic phototrophic alphaproteobacterium [196]. This suggests that *Rhodoblastus* was active under the incubation conditions by either growing via (a) photosynthesis when the flasks were illuminated during sampling, or (b) fermentation, which is known for other phototrophic *Alphaproteobacteria* [394].

Additional abundant phyla that might have contributed to the mineralization of endogenous carbon sources under the prolonged anoxic conditions were *Actinobacteria* (10.6% and 9.5% relative abundances at 15°C and 5°C, respectively), *Verrucomicrobia* (10.6% and 8.3%), *Chloroflexi* (7.1% and 8.3%), *Acidobacteria* (7.1% and 8.3%), and *Bacteroidetes* (4.4% and 4.8%). Identities of the 16S rRNA sequences of these phyla to cultured relatives were often low (Table A3) indicating that heretofore uncultured anaerobes might have been involved in the mineralization of peat derived carbon sources. *Firmicutes* are considered to be classical anaerobes and were the second most abundant phyla in fresh peat. However, at the end of the anoxic incubation the *Firmicutes* seemed to be of minor importance (Table A3).

3.2.3.7.   Bacterial taxa potentially linked to syntrophic processes

Relative abundancies of 16S rRNA sequences from 'light' and 'heavy' fractions of [^{13}C]butyrate and [^{13}C]ethanol treatments (Figure 7) were compared to identify butyrate- and ethanol-oxidizing syntrophs, respectively. Rarefaction analyses revealed a lower diversity of bacterial family-level OTUs if 'heavy' or 'light' fractions of RNA were used compared to total RNA extracts (Figure 33), indicating a successful separation of populations with different RNA buoyant densities. Thus, unlabeled (i.e., 'light') RNA originating from taxa that assimilated carbon from endogenous sources was probably separated from that labeled (i.e., 'heavy') RNA of taxa that assimilated ^{13}C-labled carbon derived from [^{13}C]butyrate and [^{13}C]ethanol, respectively.

OTU35a, which was closely related to the ethanol oxidizer *Pelobacter propionicus* (98% identity) [377], was the dominant OTU in 'heavy' fractions but was clearly less abundant in 'light' fractions of the [^{13}C]ethanol-supplemented microcosm at 15°C (Table A3). No other OTU was considerably enriched in 'heavy' compared to 'light' fractions. OTU35a was also detected in ethanol-supplemented microcosms but not in unsupplemented controls at 5°C (Figure 34). Thus, OTU35 appeared to represent an important taxon associated with the consumption of ethanol at low and moderate temperatures.

OTU79a and OTU26a were abundant in 'heavy' fractions but could not be detected in 'light' fractions of the [^{13}C]butyrate-supplemented microcosm at 15°C (Figure 34 and Table A3). OTU79a was related to *Syntrophomonas zehnderi* (up to 95% identity) (Figure 35), which is a syntrophic butyrate oxidizer [414]. OTU 26a was related to the facultative aerobic

alphaproteobacterium *Telmatospirillum siberiense* (up to 95% identity), which is not known for a syntrophic metabolism [406]. Thus, known (*Syntrophomonas*) and novel (*Telamtospirillum*) syntrophic butyrate oxidizers might be important for the anaerobic butyrate oxidation in the fen.
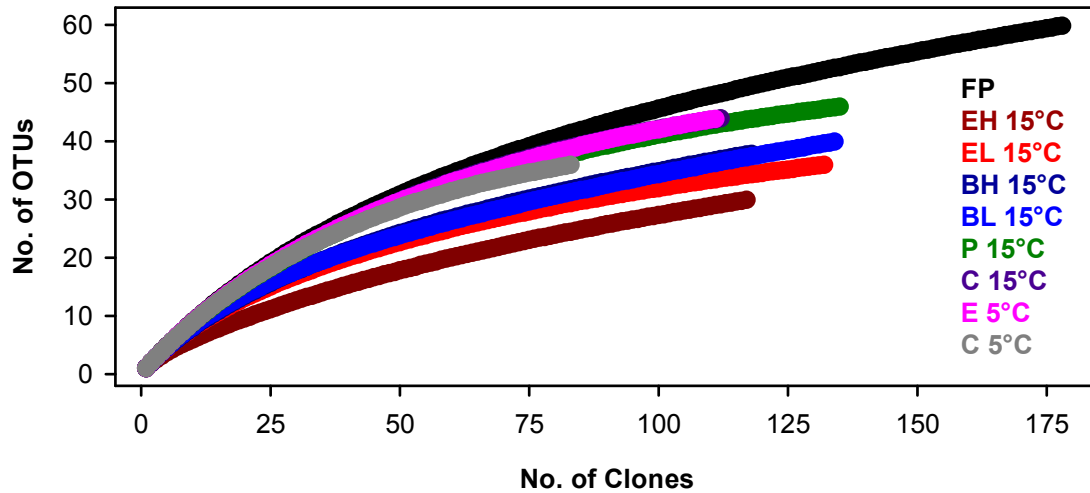
Figure 33   Rarefaction analyses of bacterial 16S rRNA sequences obtained from fresh peat and anoxic microcosms.

OTUs were calculated based on 87.5% similarity cutoff ('family level' [492]). No 95% confidence intervals are displayed to enhance clarity of the graph. E, B, P: Ethanol, butyrate, propionate treatments. C: unsupplemented controls. FP: fresh peat. L and H are 'light' and 'heavy' fractions, respectively (Figure 7). Modified from ref [386].
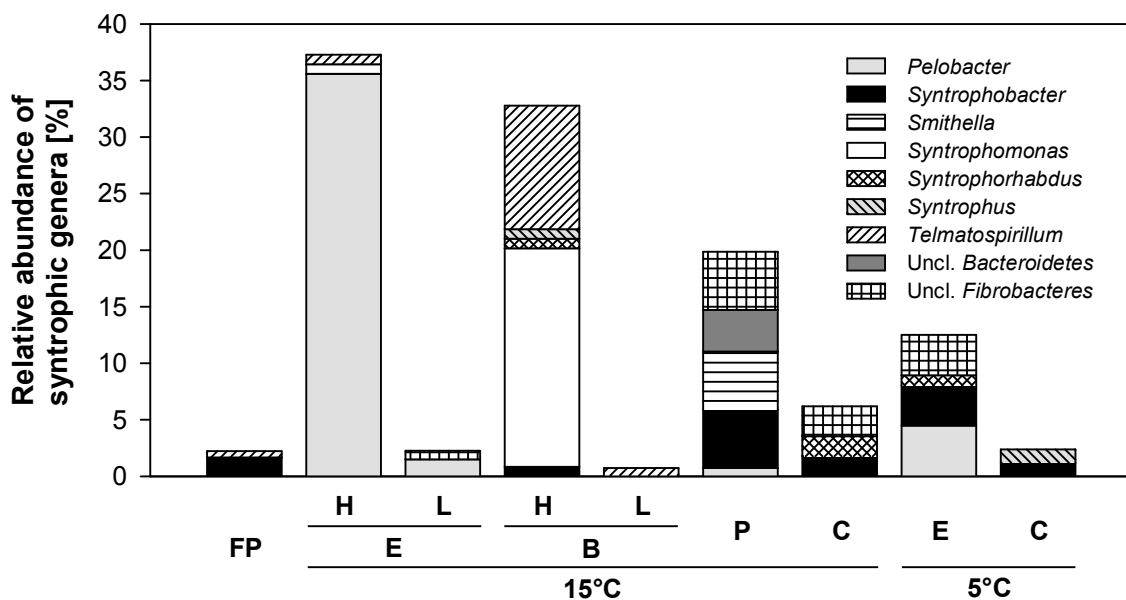
Figure 34   Relative abundances of genera potentially linked to syntrophic processes.

See Table A3 for a complete overview of all detected bacterial taxa. Abbreviations: FP, fresh peat; E, B, or P, ethanol, butyrate, or propionate treatments, respectively; C, unsupplemented controls; H or L, derived from 'heavy' or 'light' fractions, respectively. Modified from ref [386].
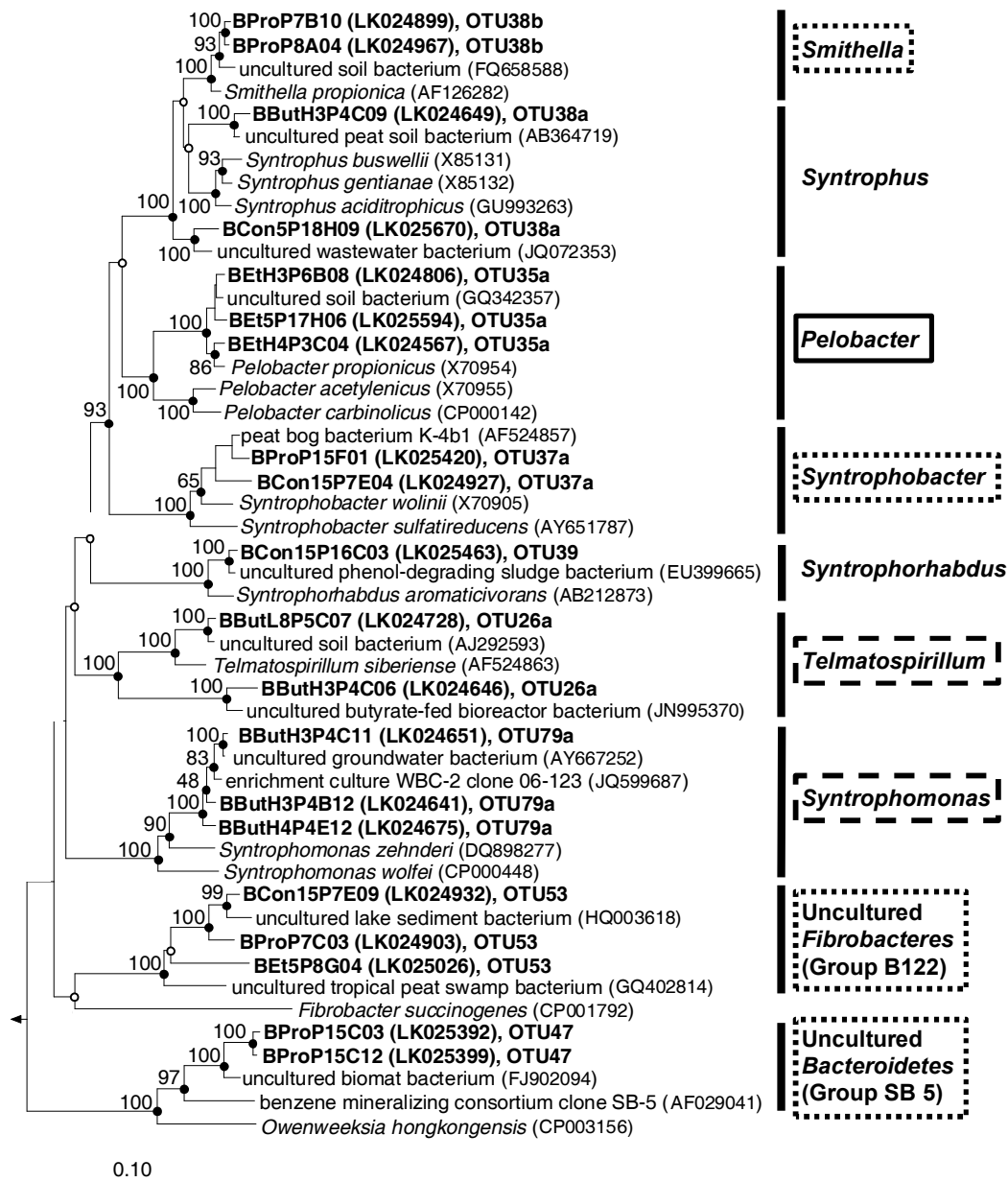
Figure 35 16S rRNA-based phylogenetic tree of potentially syntrophic taxa (bold).

Taxa responded to the supplementation of propionate (dotted boxes), butyrate (dashed boxes), or ethanol (solid boxes). OTUs potentially linked to syntrophic degradation of aromatic compounds are included (without boxes). The phylogenetic tree was calculated using the neighbor-joining, maximum parsimony and maximum likelihood method. Empty and solid circles at nodes indicate congruent nodes in two and three trees, respectively. Branch length and bootstrap values (1,000 resamplings) are from the neighbor-joining tree. The bar indicates 0.1 change per nucleotide. *Methanosarcina mazei* (AE008384) was used as outgroup. Sequence descriptor code: B, Bacteria; Et, But, Pro, or Con, sequences obtained at the end of the incubation with ethanol, butyrate, propionate, or unsupplemented control, respectively; H3 or H4, derived from 'heavy' fraction 3 or 4, respectively; 5 or 15, incubated at 5°C or 15°C, respectively; the last 5-6 characters represent the clone identifier (e.g., P15F01 is from plate 15 position F01). See Table A3 for complete overview of all detected bacterial taxa. Modified from ref [386].

Two OTUs (OTU37a and OTU38b) that were affiliated with known syntrophic propionate oxidizers were more abundant in propionate-supplemented microcosms compared to fresh peat or unsupplemented controls (Figure 34). OTU37a was related to *Syntrophobacter wolinii* (Figure 35). Known *Syntrophobacter* species syntrophically oxidize propionate to acetate, hydrogen, and CO_2 according to Reaction 5 in Table 2. OTU37a was also detected in ethanol treatments at 5°C as well as in unsupplemented controls at 15°C and 5°C, suggesting that OTU37a might have been associated with the consumption of the transiently formed propionate (Figure 25, Figure 26, and Figure 28). Furthermore, OTU37a was the only OTU in fresh peat that was affiliated with any known syntroph (Figure 34). This finding as well as the finding that propionate and acetate were dominant products of cellulose fermentation (3.2.1.1) suggests that syntrophic oxidation of propionate is important during the anaerobic mineralization of plant-derived organic matter in this fen. OTU38b was related to *Smithella propionica* (Figure 35) and was only detected in propionate treatments (Figure 34). *S. propionica* uses a propionate-degrading pathway that yields high amounts of acetate, very little hydrogen, and no CO_2 (Reaction 6 in Table 2). Thus, propionate oxidizers with different metabolic pathways are likely involved in propionate oxidation in the fen. OTU53 and OTU47 (affiliated to the *Fibrobacteres* and *Bacteroidetes*, respectively; Figure 35) had increased abundancies in propionate treatments (Figure 34) and might thus represent unrecognized propionate oxidizers.

Sequence similarities within OTUs that were enriched by substrate addition and could be affiliated to known syntrophic genera (OTU35a, 37a, 79a, 38b) ranged between 95% and 99%. Thus, these OTUs represent a population of closely related but not identical species (Figure 35).

In Summary, some OTUs responded to supplemental ethanol, butyrate, and propionate, suggesting that these taxa were involved in syntrophic degradation processes. The response of potentially syntrophic taxa on the supplemented substrates was more pronounced for the SIP experiments (ethanol and butyrate treatment at 15°C), but known and novel syntrophs were successfully identified with SIP-indipendent treatments (propionate treatment at 15°C and ethanol treatment at 5°C) also.

3.2.3.8.   Archaeal taxa linked to syntrophic processes

A total of 649 archaeal 16S rRNA sequences were obtained from fresh peat or anoxic microcosms (Table 24). High coverages (94%-100%) for genus-level OTUs of the different clone libraries indicated that sampling was sufficient and most of the archaeal genera were detected. Rarefaction analyses showed that the diversity of archaeal genus-level OTUs were generally low (Figure 36).
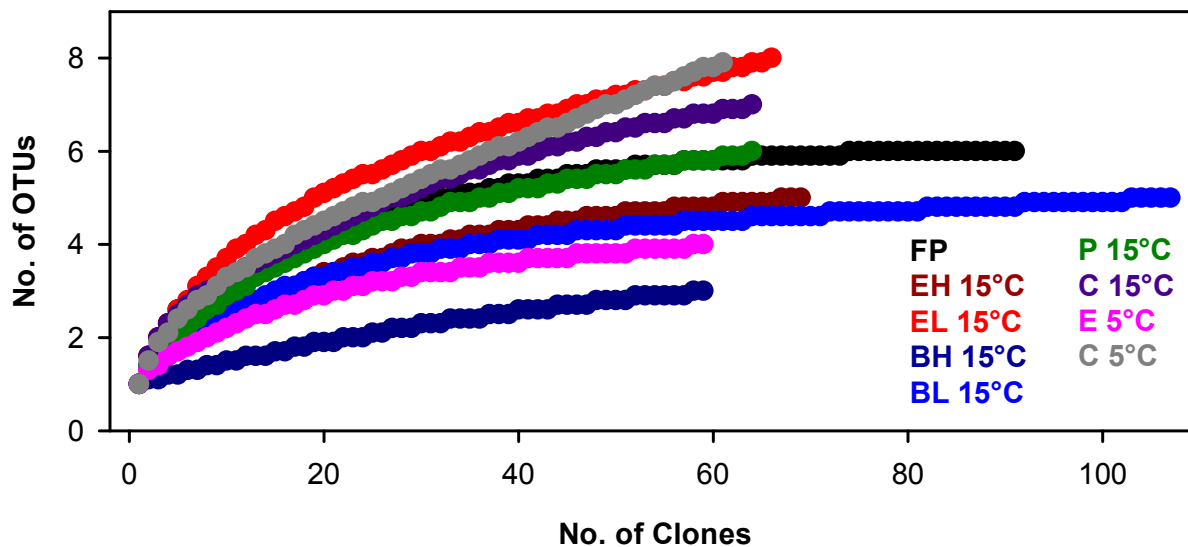
Figure 36 Rarefaction analyses of archaeal 16S rRNA sequences obtained from fresh peat and anoxic microcosms.
OTUs were calculated based on 95% similarity cutoff ('genus level' [492]). No 95% confidence intervals are displayed to enhance clarity of the graph. E, B, P: Ethanol, butyrate, propionate treatments. C: unsupplemented controls. FP: fresh peat. L and H are 'light' and 'heavy' fractions, respectively (Figure 7). Modified from ref [386].

All archaeal clone libraries were dominated by the aceticlastic methanogens *Methanosarcina* and *Methanosaeta*, and the sum of the relative abundancies of both genera ranged between 84%-97% in fresh peat and anoxic microcosms (Figure 37). It is therefore likely that aceticlastic methanogenesis was an important source of methane. Aceticlastic methanogensis was also the dominant methanogenic pathway in other peat soils [290, 445] whereas hydrogenotrophic methanogenesis contributed to most of the methane production in other studies with peat soil [168, 289]. Within the aceticlastic methanogens, *Methanosarcina* was more abundant than *Methanosaeta* in fresh peat and in almost all microcosms. The relative abundance of *Methanosaeta* was higher than that of *Methanosarcina* only in unsupplemented controls at 15°C. *Methanocella* and *Methanoregula* were the most abundant obligate hydrogenotrophic (i.e., not able to dissimilate acetate) methanogens in unsupplemented controls and ethanol, butyrate, or propionate treatments. Few sequences were affiliated to the methanogenic genera *Methanosphaerula*, *Methanobacterium,* and *Methanomassiliicoccus*. OTUs 9-11 clustered within the *Thaumarchaeota* and represented heretofore uncultivated genera (OTUs 10 and 11) or were closely related to *Nitrosotalea devanaterra*.

	Rel. abundance [%]								
	F P	15°C						5°C	
		E		B		P	C	E	C
		H	L	H	L				
100 *Methanosarcina vacuolata* (FR733661) / 99 AEtH3P1A09 (LK026043), OTU1	51	83	63	95	80	77	35	85	68
100 AEtH3P1B03 (LK026048), OTU2 / 100 uncultured fen archaeon (EU155954) / *Methanosaeta concilii* (CP002565)	34	7	15	2	4	8	51	8	16
100 AEtL10P1H11 (LK026122), OTU5 / 100 uncultured fen archaeon (EU155965) / *Methanocella paludicola* (AP011532)	7	3	8	0	5	5	3	5	8
100 *Methanoregula boonei* (DQ282124) / 100 AEtH4P1C07 (LK026084), OTU3 / 51 *Methanoregula formicicum* (AB479390)	2	6	8	3	11	8	3	0	2
At0P19D10 (LK026275), OTU4 / 100 uncultured bog archaeon (JN649301) / *Methanosphaerula palustris* (CP001338)	3	0	2	0	0	0	0	0	0
Methanomicrobium mobile (M59142) / 96 *Methanoculleus bourgensis* (AB065298) / 100 *Methanolinea tarda* (AB162774) / *Methanospirillum hungatei* (CP000254)									
100 AEtL9P1F05 (LK026151), OTU6 / 100 uncultured peat soil archaeon (AB364939) / 100 *Methanomassiliicoccus luminyensis* (HQ896499)	0	0	3	0	0	0	2	0	2
100 ACon5P22G09 (LK025954), OTU7 / uncultured acidic spring archaeon (AB600367)	0	0	0	0	0	0	0	0	2
100 *Methanobacterium lacus* (HQ110085) / AButL10P11H05 (LK025738), OTU8	0	1	0	0	1	0	0	0	0
100 ACon15P21C05 (LK025868), OTU11 / 100 uncultured fen archaeon (EU155993)	0	0	0	0	0	2	5	0	2
ACon15P21E08 (LK025892), OTU10 / 96 uncultured river archaeon (HQ532941)	0	0	2	0	0	2	2	2	0
100 *Nitrosotalea devanaterra* (JN227488) / ACon5P22G12 (LK025868), OTU9	3	0	2	0	0	0	0	0	2

0.10

Figure 37 Phylogenetic tree of archaeal 16S rRNA sequences obtained from fresh peat and anoxic microcosms (bold), and reference sequences.

Relative abundances are given for genus-level OTUs [492]. The phylogenetic tree was calculated as described in (2.6.4). Branch length are based on the maximum parsimony tree. Filled circles at nodes (bootstrap values are attached) indicate congruent nodes in the maximum likelihood, maximum parsimony, and neighbor-joining tree. Open circles indicate congruent nodes in two of the three trees. The bar indicates 0.1 change per nucleotide. *Escherichia coli* (CP000948) was used as outgroup. E, B, P: Ethanol, butyrate, propionate treatments. C: unsupplemented controls. FP: fresh peat. L and H are 'light' and 'heavy' fractions, respectively (Figure 7). Sequence descriptor code: A, Archaea; Et, But, or Con, ethanol, butyrate treatments, or unsupplemented controls, respectively; H3 or H4, derived from 'heavy' fraction 3 or 4, respectively; L10, derived from 'light' fraction 10; 5 or 15, incubated at 5°C or 15°C, respectively; t0, fresh peat; the last 5-6 characters represent the clone identifier (e.g., P22G12 is from plate 22 position G12). Modified from ref [386].

3.3. Fermentation processes and associated taxa in the gut of the earthworm *Lumbricus terrestris*

3.3.1. Hydrogenase transcript analyses in glucose supplemented anoxic gut content microcosms

Glucose is an abundant component of the mucus in *Lumbricus* sp. [343] and occurred in hydrolyzed alimentary canal contents of *L. terrestris* [488]. In a previous study, glucose was supplemented to diluted gut contents of *Lumbricus terrestris* to analyze fermentative processes and to identify active saccharolytic ferementers [490]. H_2, lactate, ethanol, butyrate, acetate and CO_2 were the major products of glucose fermentation, and *Clostridiaceae* and *Enterobacteriaceae* were identified as major glucose-fermenting taxa based on 16S rRNA analyses [490]. RNA samples of gut content microcosms from the above mentioned study were used to analyze the diversity of [FeFe]- and group 4 [NiFe]-hydrogenase transcripts in order to resolve H_2 metabolizing taxa in the gut.

3.3.1.1. [FeFe]-hydrogenase gene transcript diversity

The 178 transcript sequences that were obtained yielded 13 different OTUs based on an amino acid sequence threshold similarity of 80% (Figure 38). The majority of the in silico translated sequences clustered in OTUs 1-3 and displayed similar identities to hydrogenase amino acid sequences from the *Clostridiales* families *Lachnospiraceae*, *Clostridiaceae*, and *Ruminococcaceae* (Table 25). Furthermore, some of the sequences within each of the three most abundant OTUs (i.e., OTUs 1-3) displayed a high degree of dissimilarity (e.g., sequences H36 and H63 in OTU 1 were 14.7% dissimilar), indicating that OTUs 1-3 harbored sub-OTU-level [FeFe]-hydrogenase diversity (Figure 38 and Table 25). OTUs 4-9, 11, and 12 were less abundant and were affiliated with hydrogenases of the *Clostridiaceae*, *Lachnospiraceae*, *Peptostreptococcaceae*, and *Ruminococcaceae* (Figure 38). OTU 13 displayed the lowest identity to a known hydrogenase (61% to *Alkaliphilus oremlandii*) (Table 25). Sequence H178 (OUT 10) had the highest identity to a known [FeFe]-hydrogenase gene (84% to that of *Pelobacter carbinolicus*) (Table 25). Furthermore, sequence H178 was the only sequence that could be affiliated to the *Deltaproteobacteria* but not to the *Clostridia*. A coverage of 97% at 80% sequence threshold similarity indicated that the 178 sequences provided good coverage of the [FeFe]-hydrogenase diversity in the gut content microcosms. However, additional less abundant hydrogenases might be present in gut contents.
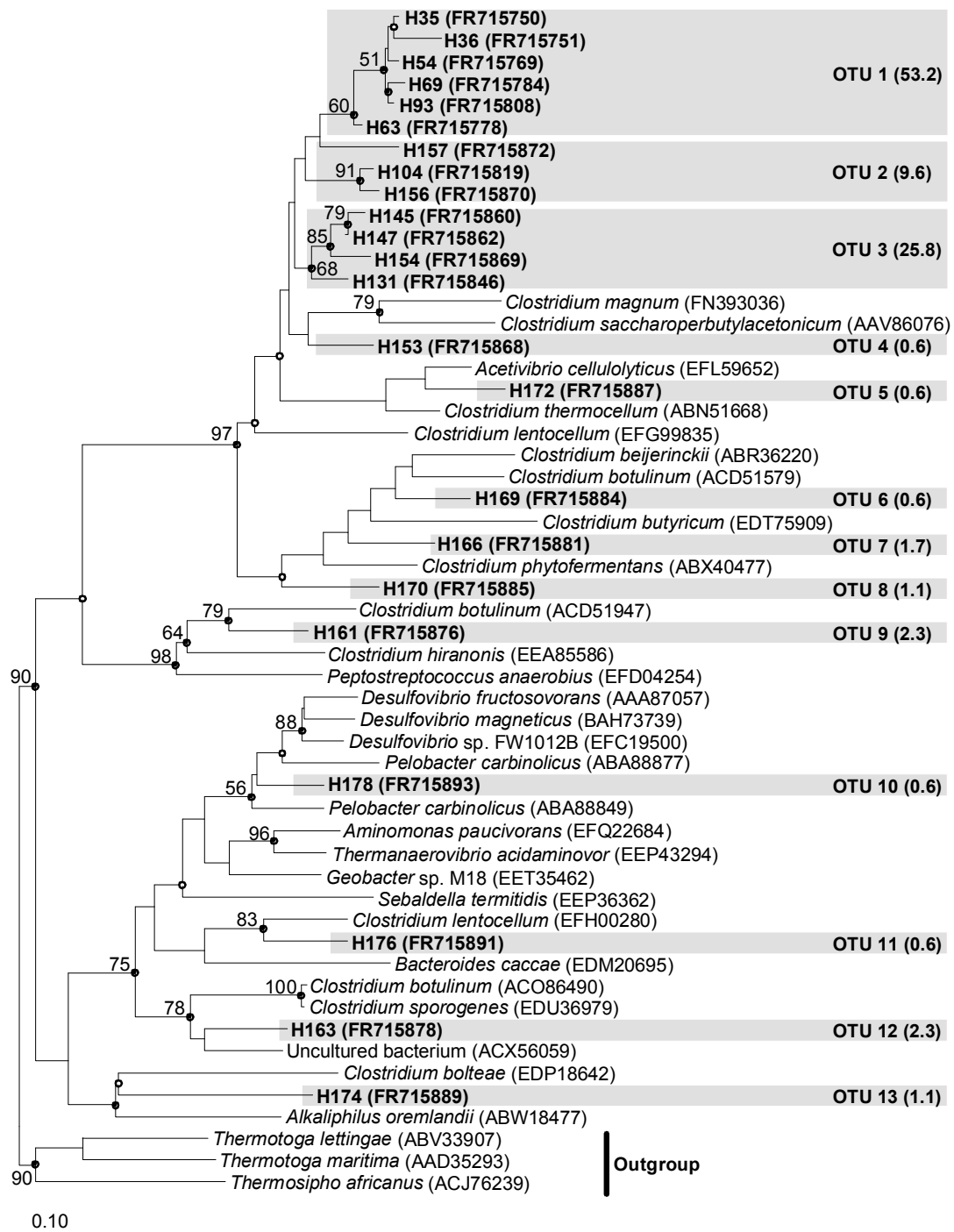
Figure 38 Phylogenetic tree of in silico translated [FeFe]-hydrogenase gene transcripts (bold) and closely related sequences.

Relative abundancies of OTUs (%) are given in parenthesis. OTUs were calculated based on an amino acid sequence similarity cutoff of 80% (3.1.2). Sequences correspond to residues 183 to 375 of the *D. vulgaris* hydrogenase (GenBank accession no. AAS96246). Branch length are based on the maximum parsimony tree. Filled circles at nodes indicate congruent nodes in the maximum-likelihood, maximum parsimony, and neighbor-joining tree. Open circles indicate congruent nodes in two of the three trees. Bootstrap values are averages from the maximum parsimony tree (100 resamplings) and the neighbor-joining tree (1000), and are only displayed at nodes congruent in all three trees. The bar indicates 0.1 change per amino acid. Modified from ref [388].

Table 25 Phylogenetic affiliations of [FeFe]-hydrogenase gene transcripts obtained from glucose-supplemented earthworm gut microcosms (2.9.3.1)

OTU	MSS (%)[a]	Organism with the closest related sequence (Acc. no.)	Identity range (%)	Affiliation
1	85.3	Clostridium lentocellum (EFG99835)	65-72	Lachnospiraceae
		C. magnum (FN393036)	65-72	Clostridiaceae
		C. thermocellum (ABN51668)	64-70	Ruminococcaceae
		C. saccharoperbutylacetonicum (AAV86076)	63-68	Clostridiaceae
2	80.2	C. lentocellum (EFG99835)	70-72	Lachnospiraceae
		C. magnum (FN393036)	69-70	Clostridiaceae
		C. thermocellum (ABN51668)	66-70	Ruminococcaceae
3	86.9	C. lentocellum (EFG99835)	70-72	Lachnospiraceae
		C. magnum (FN393036)	69-72	Clostridiaceae
		C. thermocellum (ABN51668)	64-67	Ruminococcaceae
4	NA	C. magnum (FN393036)	75	Clostridiaceae
5	NA	Acetivibrio cellulolyticus (ABN51668)	81	Ruminococcaceae
6	NA	C. botulinum (ACD51579)	79	Clostridiaceae
7	98.9	C. phytofermentans (ABX40477)	76-77	Lachnospiraceae
8	100	C. phytofermentans (ABX40477)	74	Lachnospiraceae
9	96.8	C. botulinum (ACD51947)	74-76	Clostridiaceae
10	NA	Pelobacter carbinolicus (ABA88849)	84	Desulfuromonadaceae
11	NA	C. lentocellum (EFH00280)	80	Lachnospiraceae
12	98.9	C. sporogenes (EDU36979)	75-76	Clostridiaceae
13	99.5	Alkaliphilus oremlandii (ABW18477)	61	Clostridiaceae

[a]MSS, minimal sequence similarity within an OTU (obtained from a distance matrix calculated with the ARB software [264]). NA, not applicable. Modified from ref [388].

3.3.1.2. Group 4 [NiFe]-hydrogenase gene and transcript diversity

[NiFe]-hydrogenase transcript analyses were performed with the primer pair NiFe-gF/R, targeting only group 4 [NiFe]-hydrogenases of the *Gammaproteobacteria* (Table 16). 74% of the 86 *in silico* translated amino acid sequences clustered with hydrogenases of diverse *Enterobacteriaceae* species and were related to HycE of *E. coli* (Figure 39). HycE is the catalytical subunit of hydrogenase 3 isoenzyme (HYD3) [369]. HYD3 together with the formate dehydrogenase H (Fdh-H) form a formate hydrogenlyase complex (FHL-1) that oxidizes formate derived from mixed acid fermentation and produces H_2 via the reduction of cytoplasmic H^+, thus minimizing acidification [11, 370]. Five percent of the sequences were in a cluster that was related to HyfG (Figure 39). In *E. coli*, HyfG is the large subunit of a putative H_2-producing [NiFe]-hydrogenase, namely HYD4 [6]. HYD4 together with Fdh-H is proposed to form a second formate hydrogenlyase (FHL-2) that might be involved in (i) energy conservation during intracellular H_2 cycling in the presence of nitrate, nitrite, or fumarate, (ii) cometabolization of formate during fermentation, or (iii) delivering CO_2 for carboxylation-linked processes in biosynthesis [6, 10]. Highest identities (87%) of *hyfG*-like clone sequences was

to a hydrogenase of *Pectobacterium atrosepticum* (Table 26). 21% of the sequences were affiliated to the *Aeromonadaceae* and the closest related sequence (98-99% identity) was to a hydrogenase of *Aeromonas salmonicida* (Figure 39 and Table 26). Overall high identities to group 4 [NiFe]-hydrogenases of the *Gammaproteobacteria* verified that primers NiFe-gF/R were specific for these hydrogenases. At a threshold similarity of 80%, a coverage of 100% indicated that the 86 clones provided good coverage of the diversity of *Gammaproteobacteria* group 4 [NiFe]-hydrogenases in the earthworm gut content microcosms.

Table 26   Phylogenetic affiliations of group 4 [NiFe]-hydrogenase gene transcripts and genes obtained from glucose-supplemented earthworm gut microcosms (2.9.3.1)

Affiliation (Abundance [%])	MSS (%)[a]	Organism with the closest related sequence (Acc. no.)	Identity range [%]
Transcripts[b]			
Enterobacteriaceae			
hycE-like (74)	91.5	*Enterobacter cancerogenus* (ZP_0597002)	94-98
hyfG-like (5)	99.3	*Pectobacterium atrosepticum* (CAG74151)	87
Aeromonadaceae (21)	96.0	*Aeromonas salmonicida* (ABO89889)	98-99
Genes[c]			
Enterobacteriaceae			
hycE-like (50)	93.4	*Enterobacter cancerogenus* (ZP_0597002)	94-98
Aeromonadaceae (10)	99.3	*Aeromonas salmonicida* (ABO89889)	98-99
Ruminococcaceae (5)	NA	*Clostridium thermocellum* (ABN54216)	70
Thermoanaerobacterales Family III Incertae Sedis (5)	NA	*Caldicellulosiruptor saccharolyticus* (ABP67131)	65
Opitutaceae (30)	73.7	*Opitutus terrae* (ACB77392)	73-78

[a]MSS, minimal sequence similarity within an OTU (obtained from a distance matrix calculated with the ARB software [264]). NA, not applicable.

[b]Total number of transcript sequences: 86. Primers NiFe-gF/R (Table 16) were used for PCR amplification.

[c]Total number of gene sequences: 20. Primers NiFe-uniF(b)/R (Table 16) were used for PCR amplification. Modified from ref [388].

Primers NiFe-uniF(b)/R (Table 16) have a higher degree of degeneracy than primers NiFe-gF/R and should therefore cover a broader range of group 4 [NiFe]-hydrogenases and were used to detect hydrogenases that belonged to not only the *Gammaproteobacteria* but all other known group 4 [NiFe]-hydrogenases. However, amplification of transcript-dervied cDNA from gut content microcosms failed. The huge background of ribosomal RNA may have hindered a proper annealing of the highly degenerated primers NiFe-uniF(b)/R to the hydrogenase template transcripts. Nonetheless, amplification was successful with DNA of the microcosms. 60% of 20 clone sequences were affiliated to the families *Enterobacteriaceae* and *Aeromonadaceae* of the *Gammaproteobacteria* (Figure 39). These sequences were also

amplified at the transcript level with primers NiFe-gF/R (see above). One sequence was most closely related to [NiFe]-hydrogenase of *Clostridium thermocellum* (70% identity) and another to that of *Caldicellulosiruptor saccharolyticus* (65%) (Table 26). Six sequences that had an amino acid sequence dissimilarity of up to 26% to each other clustered next to a hydrogenase of *Opitutus terrae* (Table 26). Although the 20 sequences were insufficient for obtaining a good coverage of group 4 [NiFe]-hydrogenase-containing taxa in the gut content microcosms, the primers NiFe-uniF(b)/R were effective in detecting novel group 4 [NiFe]-hydrogenase genes not resolved with primers NiFe-gF/R.
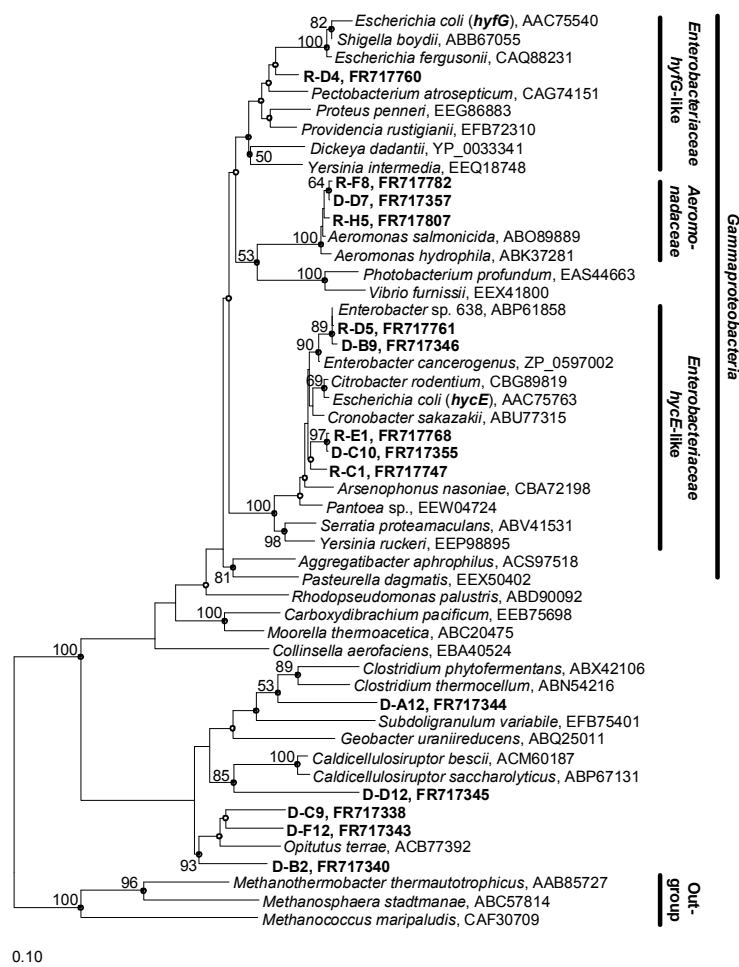
Figure 39 Phylogenetic tree of in silico translated group 4 [NiFe]-hydrogenase transcript or gene sequences (bold) and closely related sequences.

OTUs were calculated based on an amino acid sequence similarity cutoff of 80% (3.1.2). Sequences correspond to residues 341 to 710 of the *E. coli* hydrogenase 3 HycE protein (GenBank accession no. AAC75763). Branch length are based on the maximum parsimony tree. Filled circles at nodes indicate congruent nodes in the maximum likelihood, maximum parsimony, and neighbor-joining tree. Open circles indicate congruent nodes in two of the three trees. Bootstrap values are averages from the maximum parsimony tree (500 resamplings), maximum likelihood (10 resamplings), neighbor joining tree (1000), and are only displayed at nodes congruent in all three trees. The bar indicates 0.1 change per amino acid. Modified from ref [388].

3.3.2.   Bacterial taxa involved in the degradation of microbial cells in the gut of *L. terrestris*

Earthworms ingest microbial cells (prokaryotes, fungi, algae, and protozoa) that are present in the soil or attached to the plant litter on which the earthworms feed [36, 74]. It is assumed that part of the ingested cells, especially larger ones, are disrupted by the grinding activity of the gizzard [35, 333, 348, 391, 484]. The breakdown products of disrupted microbial cells may be metabolized alongside with the sugars from the mucus, and plant-derived polymers by ingested and activated fermenting prokaryotes that produce soluble organic acids which the earthworm probably reabsorbs as part of its nutrition [490]. In the following experiment lysed cells of the yeast *Saccharomyces cerevisiae* (2.2.2.2) were supplemented to *L. terrestris* gut content microcosms (2.2.2.3) to stimulate taxa that are potentially involved in the degradation of organic compounds that are derived from disrupted cells in situ. The formation of fermentation products was measured and active taxa were identified based on 16S rRNA gene and transcript analyses.

3.3.2.1.   Fermentation profile of anoxic earthworm gut content microcosms supplemented with lysed *S. cerevisiae* cells

Supplemental *S. cerevisiae* cell lysate rapidly stimulated the production of gases and organic acids in anoxic gut content microcosms (Figure 40), indicating that ingested soil anaerobes were active and were not saturated for organics derived from the cell lysate (e.g., proteins, amino acids, nucleic acids, and sugars [230]). Acetate, succinate, and formate were the dominat fermentation products that accumulated during the initial 6 h of incubation (Table 27). Subsequently, formate concentrations decreased parallel to an enhanced accumulation of acetate and CO_2. This suggests that formate-dependent acetogenesis (Reaction 2 in Table 4), which was thermodynamically favorable in treatments with cell lysate and unsupplemented controls during the whole experiment (ΔGs ranged between -110 to -65 kJ·mol^{-1}), was ongoing. In addition, acetogens may have used H_2 and CO_2 (Reaction 1 in Table 4) at the end of the incubation in treatments with cell lysate in which the ΔGs approximated -50 kJ·mol^{-1}. This assumption is based on the observation that the accumulation of H_2 and CO_2 slowed down after 20 h whereas acetate was still produced in high quantities. Propionate accumulated after 6 h and at the same time the rate of succinate production (i.e., accumulation) was lower compared to that during the initial incubation (Table 27). Succinate decarboxylation to propionate (Reaction 1 in Table 2) is a likely explanation for the observed phenomenon and ΔGs of this process ranged between -57 to -36 kJ·mol^{-1}. Alternatively, propionate was produced during carbohydrate or amino acid fermentation [301, 409]. In total, 33.9% and

30.0% of carbon and electrons supplemented as lysed cells could be recovered in the aforementioned products (Table 27), indicating that approximately one third of the organic substrates derived from the cell lysate were consumed during the 30 h incubation time.

Table 27 Production rates, ratios of products, and recoveries of anoxic gut content microcosms supplemented with lysed *S. cerevisiae* cells

| Products | Rates ($\mu mol \cdot g_{FW}^{-1} \cdot h^{-1}$)[a] | | Ratios of products[a] | Recoveries (%)[a] | |
	Initial 6 h	Subsequent 24 h		Carbon	Electron
CO_2	1.65	3.67	1.00	4.1	0.0
H_2	1.04	0.93	0.29	0.0	0.6
Acetate	6.45	7.98	2.35	19.2	19.2
Succinate	3.63	1.23	0.52	8.6	7.5
Propionate	0.00	0.86	0.21	2.6	3.0
Formate	3.74	-1.47	-0.13	-0.5	-0.3
Total ($\sum$)				33.9	30.0

[a]Concentrations of unsupplemented controls were subtracted from treatments supplemented with lysed cells to calculate initial (0 to 6 h) and subsequent (6 to 30 h) production rates as well as product ratios and recoveries during the whole incubation (0 to 30 h).

Initial formate concentrations were higher in treatments with lysed cells compared to unsupplemented controls (Figure 40E). Similar initial formate concentrations were observed in autoclaved gut content microcosms supplemented with lysed cells as well as in controls that contained lysed cells but no gut content (data not shown). This suggests that formate was present in *S. cerevisiae* cell lysate.

Lactate, butyrate and ethanol, which were major products in anoxic gut content microcosms supplemented with glucose [490], were hardly detected in treatments with or without lysed cells (data not shown), suggesting that these fermentation products were either not formed or turned over rapidly. Furthermore, no glucose was detected at the start of the incubation in treatments with or without cell lysates (data not shown). This is in contrast to similar experiments with gut content microcosms conducted in the past, in which approximately 1 mM of glucose was found to be present at the start of the incubation in unsupplemented controls [490]. Thus, the in situ availability of free sugars seems to be variable in the gut of earthworms.

A series of controls (autoclaved gut content with/without lysed cells, lysed cells with/without glucose; 2.2.2.3) were conducted to proof wheter or not the activity observed in microcosms of gut content supplemented with lysed cells is derived from enzymes of the cell lysate or the microbes in the gut. Only trace amounts of CO_2 and organic acids could be detected in these controls (data not shown), indicating that the microbes of the gut content

rather than the enzymes in the cell lysate contributed to the production of gases and organic acids.
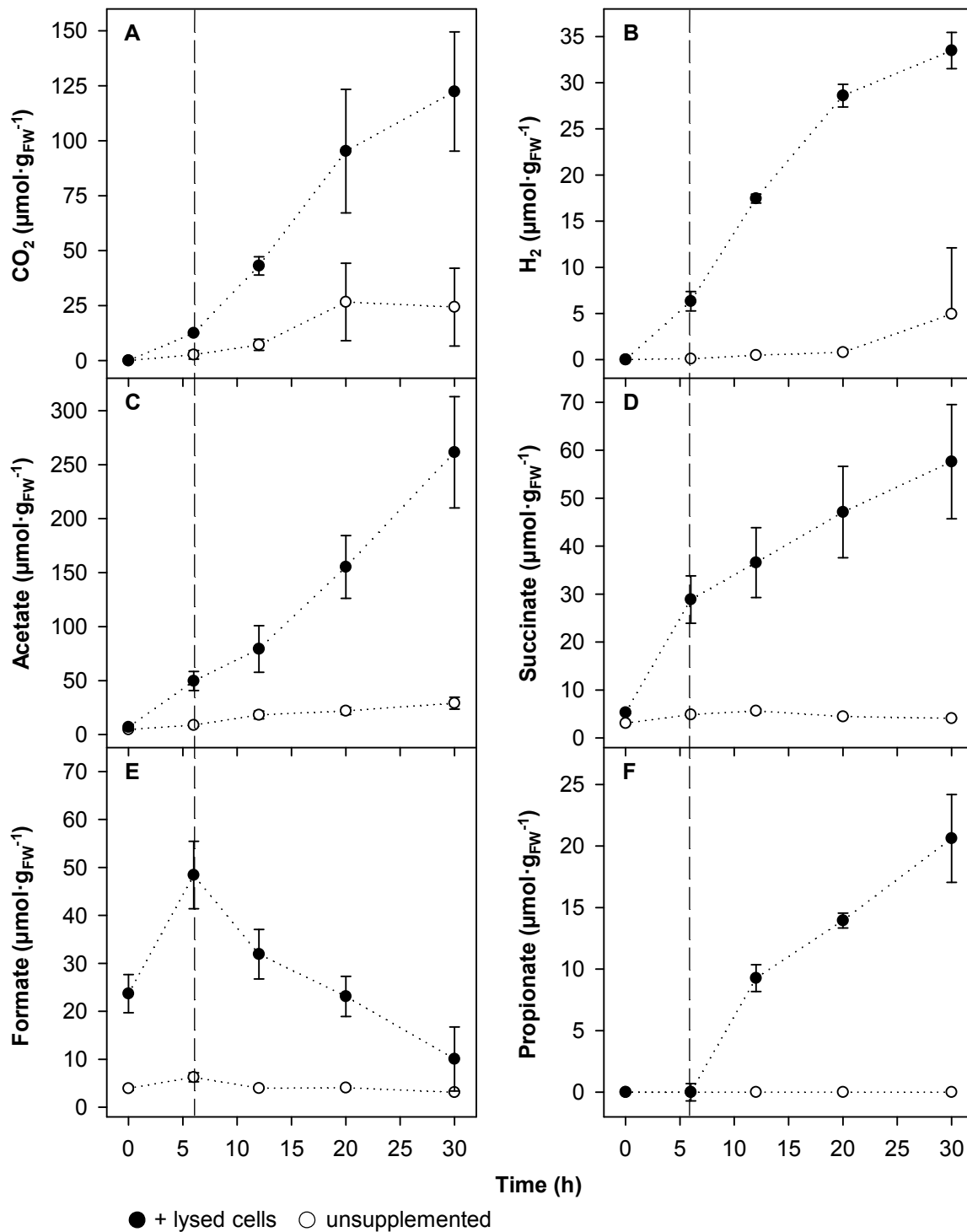
Figure 40 Effect of lysed *S. cerevisiae* cells (2.2.2.2) on the product profile of anoxic earthworm gut content microcosms (2.2.2.3).

Symbols: filled circles, treatments supplemented with lysed *S. cerevisiae* cells; open circles, unsupplemented control treatments. Values are means of triplicates; error bars indicate standard deviations. Dashed lines separate initial (0 to 6 h) and subsequent processes (6 to 30 h).

3.3.2.2. Effect of lysed *S. cerevisiae* cells on the composition and activity of the bacterial community in gut content microcosms

16S rRNA gene and transcript analyses were conducted to target both activity and community composition of the *Bacteria* present in anoxic gut content microcosms [122, 144, 473]. A total of 1715804 bacterial 16S rRNA gene and transcript sequences were obtained from DNA and RNA samples. The sequences were clustered in 19763 OTUs (99% sequence similarity threshold) and assigned to 26 different phyla (inclusive candidate phyla). Rarefaction analyses indicated that the sampling effort was sufficient to cover most of the diversity present in the different samples (Figure 41). However, more exhaustive sampling would most likely result in the detection of additional rare OTUs. Interestingly, the number of detected OTUs at a distinct number of sequences (e.g., 70000 sequences) was lower for RNA and DNA samples from microcosms supplemented with lysed cells compared to samples from unsupplemented controls or samples collected prior to the incubation (Figure 41). This suggests a lower bacterial diversity in treatments with lysed cells compared to unsupplemented controls and thus a stimulation of only a subset of the microbial community by the supplemented lysed cells.
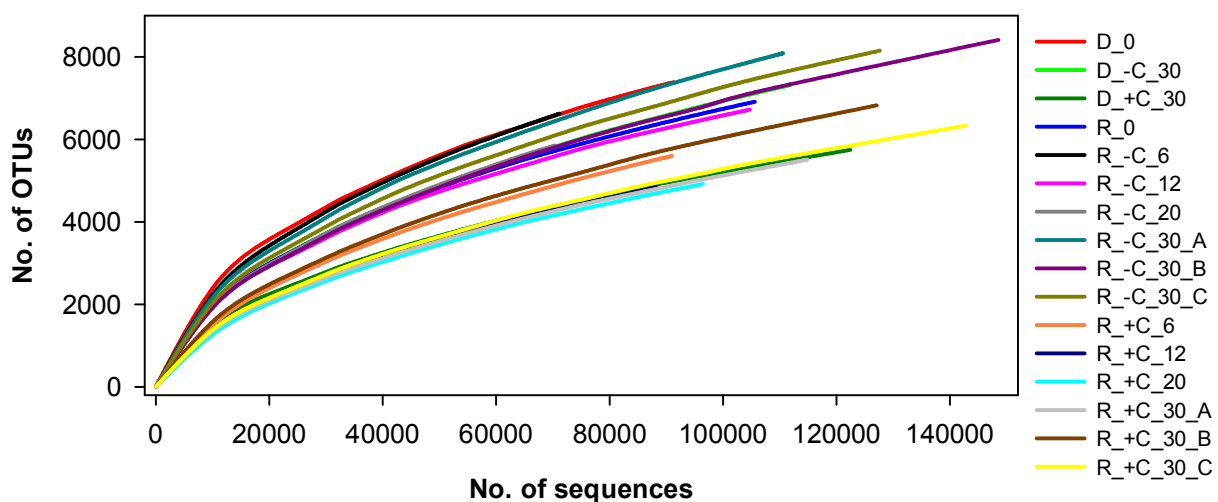
Figure 41 Rarefaction analyses of of bacterial 16S rRNA transcript and gene sequences obtained from RNA and DNA samples of anoxic earthworm gut content microcosms.
OTUs were calculated based on 99% sequence similarity cutoff. Legend: D / R, DNA / RNA; +C / -C, microcosms supplemented with lysed *S. cerevisiae* cells / unsupplemented controls (2.2.2); 0 / 6 / 12 / 20 /30, incubation time in hours; A / B / C, identifies the triplicate. See also legend of Figure 42 for details on how samples were pooled for molecular analyses.

16S rRNA gene analyses revealed that *Actinobacteria* and *Proteobacteria* (of the alpha and gamma subgroup) dominanted the bacterial community in earthworm gut contents prior to the incubation in microcosms (Figure 42). *Planctomycetes*, *Verrucomicrobia*, and *Tenericutes* of the family *Mycoplasmataceae* were also abundant. Similar taxa were detected on RNA level

but 16S rRNA transcripts of the *Mycoplasmataceae* were more abundant and those of the *Actinobacteria* were less abundant compared to 16S rRNA genes, suggesting that the *Mycoplasmataceae* were more active than the *Actinobacteria* in the freshly collected gut content material. The *Mycoplasmataceae* were represented by a single species level OTU that shared 99% similarity to *Lumbricincola* sp. LR-B2. Representatives of the candidatus genus *Lumbricincola* were detected in tissues, gut contents, and casts of earthworms and a symbiotic relationship between these microbes and their hosts was suggested [311]. However, no cultured representatives of this genus are available so far and their physiological role is not resolved yet. In unsupplemented gut content microcosms, the microbial community changed marginally over time, indicating that the conditions in the microcosms resembled the in situ conditions. Solely the *Peptostreptococcaceae* increased on RNA and DNA level.

Distinct changes in the relative abundancies of 16S rRNA transcripts between the fresh gut content material and the samples taken after 6 hours of anoxic incubation in microcosms supplemented with lysed cells suggested that the bacterial community immediately responded to the substrate addition (Figure 42). Especially, *Peptostreptococcaceae* and *Aeromonadaceae* rapidly increased while the *Actinobacteria* and *Mycoplasmataceae* decreased in relative abundance. The rapid increase of the *Peptostreptococcaceae* and *Aeromonadaceae* could be largely attributed to single species level OTUs that were closely related to *Clostridium bifermentans* (99% identity) and several *Aeromonas* sp. (e.g., 99% identity to *A. media* and *A. hydrophila*), respectively (Figure 43). Both, the obligate fermenter *Clostridium bifermentans* and the facultative aerobic species of *Aeromonas*, can ferment proteinaceous substrates as well as sugars [2, 46] and therefore, these taxa may profit from various organic compounds that will be released when cells get disrupted by the grinding activity of the gizzard. Subsequently, *Clostridiaceae*, *Enterobacteriaceae*, and *Lachno-spiraceae* partially replaced the initially responding taxa at later timepoints. The majority of the *Clostridiaceae* were represented by specialiced proteolytic species (e.g., *C. peptidovorans*, *C. sulfidigenes*, and *C. frigidicarnis* [34, 285, 363]). In contrast, the single most abundant OTU of the *Enterobacteriaceae* was 100% similar to different species (e.g., *Enterobacter aerogenes*, *Buttiauxella agrestis*, and *Klyvera intermedia*) that are not proteolytic (i.e., do not liquefy gelatin and therefore do not excrete proteases) but are saccharolytic [33]. The most abundant OTU of the *Lachnospiraceae* was not closely related to any cultured organism (94% identiy to *Epulopiscium fishelsoni*) and may therefore represent a novel genus. However, the physiology of this taxa is unknown.

OTUs Y5 and Y18 were closely related to *C. glycolicum* and *C. magnum*, two species that comprise acetogenic strains [28, 175, 222]. Both OTUs were abundant predominantly in treatments with cell lysate and at later time points. This is in accordance with the assumption that formate- and (at the end of the incubation) H_2-dependent acetogenesis were ongoing

processes. Some strains of *C. glycolicum* could grow by succinate decarboxylation to propionate [45], and this process may have been a source for propionate in the treatments with cell lysate. Thus, *C. glycolicum* may have consumed various fermentation products derived from cell lysates.

In summary, fermenters that can degrade sugars and proteins were rapidly stimulated by cell lysates and these taxa were partially replaced by more specialized fermenters with time. Acetogens likely profit from the accumulation of acetogenic substrates (formate and H_2) and some may also utilize succinate.
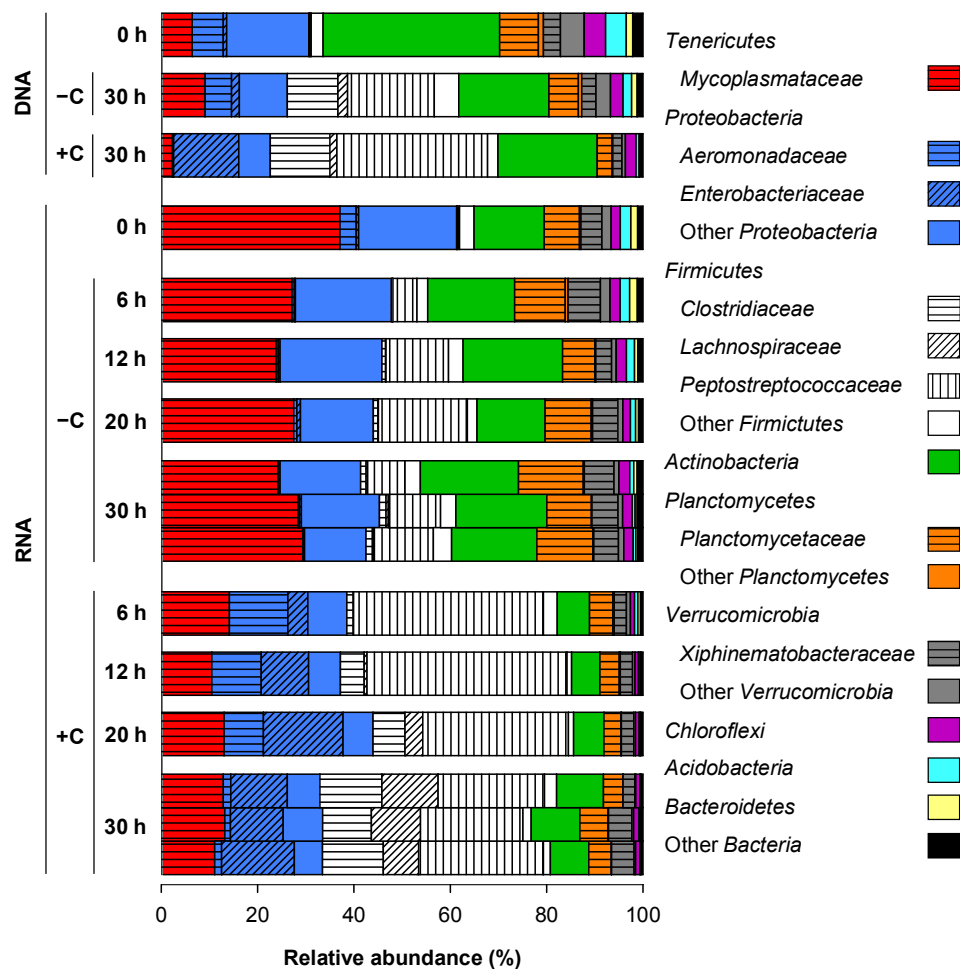
Figure 42 Relative abundace of bacterial phyla and dominant families in earthworm gut content microcosms over time based on 16S rRNA transcript and gene sequence analyses.

+C / -C, microcosms supplemented with lysed *S. cerevisiae* cells / unsupplemented controls (2.2.2). 0 h, samples from triplicates of the lysed cell treatments and unsupplemented controls were pooled prior to the incubation; 6 h / 12 h / 20 h, samples from triplicates of the lysed cell treatments or unsupplemented controls were pooled at given time points; 30 h, samples from each triplicate of the lysed cell treatments and unsupplemented controls at the end of the incubation were prepared separately and each bar represents one replicate (the high similarity between different replicates indicates that the results of the microbial community analyses were reproducible).

	RNA					DNA		
Taxon	**0**	**6**	**12**	**20**	**30**	**0**	**30**	
Clostridium carnis, M59091 (47)								
Clostridium tertium, Y18174 (67)	0	0	0.1	0.3	0.5	0	1.3	+
OTU_Y32	0	0	0.1	0.3	0.5	0	4.0	−
Clostridium butyricum, AB075768								
Clostridium pascui, X96736								
Clostridium peptidivorans, AF156796	0	0	0.2	1.1	4.9	0	1.2	+
OTU_Y8 (81)	0	0	0	0.1	0	0	0.5	−
Clostridium carboxidivorans, FR733710 (81)								
Clostridium drakei, Y18813 (72)								
Clostridium magnum, X77835 (42)	0	0	0	0.4	2.0	0	0.9	+
OTU_Y18 (70)	0	0	0	0	0	0	0	−
Clostridium ljungdahlii, FR733688								
Clostridium frigidicarnis, AF069742	0	0.1	0.7	2.2	1.1	0	3.8	+
OTU_Y15	0	0	0	0	0	0	0	−
Clostridium hydrogeniformans, DQ196623 (67/64)								
Clostridium sulfidigenes, EF199998								
Clostridium subterminale, AB294137 (83)								
Clostridium thiosulfatireducens, AB294141	0	0.8	3.2	1.7	1.0	0	2.3	+
OTU_Y10 (99)	0	0.1	0.4	0.3	0.5	0	3.5	−
Clostridium bifermentans, AB075769 (87)	0.4	36	37	21	13	0.2	23	+
OTU_Y2 (95)	4.5	12	16	7.7			15	−
Clostridium glycolicum, X76750	0	0.6	1.3	6.5	7.2	0	5.9	+
OTU_Y5 (24)	0.1	0.2	0.6	1.4			1.2	−
Clostridium lentocellum CP002582 (90)	0	0	0.5	3.3	7.2	0	1.3	+
OTU_Y6	0	0	0	0	0	0	0	−
Buttiauxella agrestis, AJ233400								
OTU_Y4	0.4	3.5	8.6	15	11	0.6	12	+
Enterobacter aerogenes, AJ251468	0.2	0.3	0.6	0.2			1.4	−
Kluyvera intermedia, AB004747								
Klebsiella oxytoca, AB004754 (82/100)								
Aeromonas hydrophila, AB472953								
Aeromonas media, X60410 (97)	3.0	10	8.9	7.2	1.1	5.8	0.2	+
OTU_Y7	0.4	0.4	0.6	0.1			4.8	−
Lumbricincola sp. Lr-G2, FM165585 (100)	37	14	10	13	12	6.3	2.3	+
OTU_Y1	27	24	27	27			8.9	−
Xiphinematobacter rivesi, AF217461								
Xiphinematobacter americani, AF217460 (83)								
Xiphinematobacter brevicolli, AF217462	4.2	2.5	2.5	2.5	3.9	3.3	1.8	+
OTU_Y3 (100)	6.5	3.2	5.1	5.4			2.7	−

Family labels (left of tree): *Clostridiaceae*, *Peptostreptococcaceae*, *Lachnospiraceae*, *Enterobacteriaceae*, *Aeromonadaceae*, *Mycoplasmataceae*, *Xiphinematobacteraceae*. Scale bar: 0.10

Figure 43   16S rRNA phylogenetic tree of abundant species level OTUs from earthworm gut content microcosms (bold) and reference sequences.

The phylogenetic tree was calculated using the neighbor-joining, maximum parsimony and maximum likelihood method. Empty and solid circles at nodes indicate congruent nodes in two and three trees, respectively. Branch length and bootstrap values (1,000 resamplings) are from the maximum parsimony tree. The bar indicates 0.1 change per nucleotide. *Thermotoga maritima* (AE000512) was used as outgroup. Relative abundancies (in %) of the species level OTUs are shown for the different samplings after 0, 6, 12, 20, and 30 h of incubation. +/− indicates microcosms +/− supplemental yeast cell lysate.

4. DISCUSSION

4.1. Cooperation and competition: interactions between H$_2$-metabolizing and other microbes in peatlands

Various H$_2$-metabolizing microbes and those that do not metabolize it (e.g., obligate aceticlastic methanogens) interact during the anaerobic mineralization of plant-derived organic compounds in peatlands [100, 208]. Some may compete with each other: e.g., (i) cellulolytic fermenters with saccharolytic fermenters for soluble sugars, (ii) hydrogenotrophic methanogens with acetogens for H$_2$, and (iii) aceticlastic methanogens with Fe^{3+}- and sulfate reducers for acetate. Others may cooperate with/depend on each other: e.g., (i) syntrophs and methanogens, and (ii) acetogens and aceticlastic methanogens. These trophic interactions and the associated taxa are not well resolved in peatlands. Thus, one major objective of this study was to gain insights into the interwoven anaerobic food web, and to identify key players of potential bottleneck processes like polymer hydrolysis or syntrophic fatty acid degradation in a model peatland, the Fen Schlöppnerbrunnen.

4.1.1. Dynamics in fermenter community compositions and product profiles in respond to changing availabilities of plant-derived organic carbon in peatlands

Polymer hydrolysis is the initial step of the anaerobic organic matter mineralization in anoxic environments like peatlands [100]. All the subsequent degradation processes that follow polymer hydrolysis inevitably depend on the release of soluble monomers that can be taken up by microbial cells [208]. Thus, polymer hydrolysis can be rate-limiting for the complete anaerobic mineralization if sufficient amounts of accessible biodegradable polymers are not available or the activity of hydrolytic exoenzymes that are released by hydrolytic fermenters is low. The second seems to be the case for the degradation of aromatic polymers (mainly derived from *Sphagnum* biomass) that are readily available but are very slowly degraded under the anoxic conditions that prevail in peatlands [126, 313, 441].

In contrast to the slow hydrolysis rates for aromatic polymers, cellulose is degraded much faster under oxic and anoxic conditions [3, 267, 305]. As a result of rapid cellulose degradation, its availability (and accessibility) might become the limiting factor for cellulolytic and associated microbes in peatlands [208, 313, 441]. In this regard, no or only little accumulation of organic acids was observed in unsupplemented peat soil microcosms at 5°C and 15°C whereas supplemental cellulose considerably stimulated organic acid accumulation (Figure 9, Figure 23, and Figure 24). This stimulatory effect of supplemental cellulose on the accumulation of

fermentation products indicated that the capacity for cellulose hydrolysis exceeded cellulose availability in peat soil of the Fen Schlöppnerbrunnen at the timepoint of sampling, which was in late October. The observed high capacity for cellulose hydrolysis at low and moderate temperatures (i) reflects the ability of the peat microbial community to respond to an enhanced input of organic matter (e.g., during the growing season in spring and summer) and (ii) reinforces the hypothesis that peat fermenters are well adapted to the in situ conditions (e.g., low temperatures and low pH) in their habitat (*Hypothesis 1*, 1.5).

4.1.1.1.   Novel taxa replace model cellulolytic fermenters in cold, acidic, and substrate-limited peatland soils

[^{13}C]cellulose-based 16S rRNA SIP was performed to identify the utilizers of cellulose-derived carbon (3.2.1.2). Labeled OTUs partially had low identities to cultured relatives (Table 28) indicating a high degree of novelty among the peat fermenters. In this regard, OTU1, which was abundant at 5°C and 15°C, was only distantly affiliated to the phylum *Fibrobacteres* and therefore the members of this phylotype might represent a new class or phylum. Remarkably, only few publicly available sequences of uncultured bacteria had BLAST-identites of ≥ 90% to that of OTU1, which underscores the novelty of this phylotype. OTU4 and related sequences represent a novel lineage within the *Prolixibacteraceae* (*Bacteroidetes*), a family recently shown to comprise cellulolytic fermenters [173]. Members of this novel lineage were also detected in agricultural and rice paddy soil [51, 372], indicating a distribution in contrasting soil ecosystems. Known (OTU3e) and novel (OTU3b, OTU8a) members of the *Acidobacteriaceae* and *Holophagaceae* were labeled and therefore were likely involved in cellulose degradation. The presence of the slow-growing facultative microaerophilic cellulose decomposer *T. bradus* [324] implies that such taxa may be well adapted to low substrate concentrations and changing redox conditions that are characteristic for peatlands [313]. The collective data suggests that previously unrecognized and uncultured anaerobes of different phyla are present in the fen and likely dominated cellulose hydrolysis in the conducted microcosm experiments. In contrast, the *Ruminococcaceae* (OTU15) (this family comprises *Clostridium* Cluster III and IV [58, 262]) had low relative abundancies in this study although they were important/dominant during cellulose degradation in gut systems, various soil environments, and anaerobic digestor sludges [48, 51, 244, 281, 372, 449, 454]. This indicates that this family, which is considered to be well adapted to various substrate rich environments [241], may be not as competitive at the acidic, cold, nutrient- and substrate-limited conditions prevailing in peat soils. Under these conditions novel taxa seem to replace the well studied model cellulolytic fermenters.

Table 28 Characteristics of taxa labeled in [^{13}C]cellulose treatments

OTU	Relative abund. (%)[a]	Phylogenetic affiliation[b]	Other eco-systems[c]	C/G[d]	Closest cultured Relative[e]	Id. (%)[f]	Products[g]
Potential cellulolytic fermenters							
1a	0/11.8	*Fibrobacter*-rel.	WB/P	?	*Fibrobacter*	79	S/A/(F)
1b	20.8/15.3	Uncl. *Bacteria*	-	?	*succinogenes**	79	
3b	4.5/3.8	Uncl. *Acido-bacteriaceae*	P	?	*Koribacter versatillis***	93	?
3e	4.8/4.1	*Telmatobacter*	P	C	*T. bradus**	98	A/H/E/C
4a	1.8/7.6	*Prolixibacter*aceae	AS/RS	C	Strain PB90-2#	95	A/P
4b	5.4/4.1		P	?	*Mangrovibacterium diazotrophicum**	90	-
15a	3.6/5.3	*Ruminococcaceae* (III+IV)	AS/SP/LS / HG/R/B	C	*Clostridium cellulosi**	94	A/E/H/C
Potential saccharolytic fermenters							
6a	3.6/2.4	*Clostridium* (I)	AS/SP/LS	G	*C. puniceum*$	99	A/B/E/O/N
6b	31/2.9				*C. acidisoli*$	98	A/B/L/F/C/H
9	12.5/9.4	*Porphyro-monadaceae*	LS	G	*Paludibacter propionicigenes*#	99	A/P/(S)
12	1.8/5.9	*Spirochaetaceae*	LS	G	*Spirochaeta zuelzerae*#	96	A/L/H/C/(S)
Potential syntrophic acetate oxidizers							
8b	0/10.6	Uncl. *Holo-phagaceae*	LA	?	*Holophaga foetida*#	93	-

[a]Relative abundancies of the OTU in 'heavy' fractions of the [^{13}C]cellulose treatment at 5°C/15°C.

[b]Abbreviations: rel, related; uncl, unclassified. Numbers in parenthesis: *Clostridium* clusters [58].

[c]Examples of other ecosystems in which related sequences were detected: B, bioreactor [120, 454]; P, peat [175, 324, 386]; AS, agricultural soil [372]; RS, rice paddy soil; SP, swamp peat [449]; LS, landfill site [244, 281]; HG, human gut [48]; R, rumen [123]; LA, lake sediment (unpublished sequence: AM409822); -, no related sequences were detected thus far.

[d]Environmental sequences that were detected in other ecosystems were affiliated with cellulose (C) or glucose (G) metabolism; ?, not clear.

[e]Symbols: *, degrades cellulose anaerobically; **, genomic evidence for cellulose metabolism; #, does not use cellulose; $, use of cellulose was not tested.

[f]Id, maximum identity.

[g]Glucose or cellulose fermentation product profiles: A, acetate; B, butyrate; C, CO_2; E, ethanol; H, H_2; L, lactate; N, acetone; O, butanol; P, propionate; S, succinate. Parenthesis indicate minor products; -, does not use glucose.

4.1.1.2.   Cooperation instead of competiton: a model for synergism between cellulolytic and noncellulolytic fermenters in the fen

Glucose or cellobiose were not detected in cellulose treatments, indicating that soluble breakdown products of cellulose were limiting, and therefore one may assume that hydrolytic and saccharolytic fermenters competed for their substrates. In this regard, cellulolytic fermenters have strategic advantages in the competition for cellulose-derived sugars: (i) they tightly adhere to cellulose fibers thereby minimizing the loss of soluble breakdown products by diffusion, and (ii) they have evolved efficient uptake systems for cellodextrins (i.e., soluble glucose oligomers that are released during cellulose hydrolysis) [241, 358, 402]. However, OTUs that were closely related to the saccharolytic fermenters were highly abundant in 'heavy' fractions of [^{13}C]cellulose treatments and obviously not outcompeted (Table 28). Notice, it can not be excluded that members of OTU6 (closely related to *Clostridium puniceum* and *C. acidisoli*) that were assigned as saccharolytic fermenters are actually cellulolytic as this has not been tested thus far [218]. However, members of *Clostridium* cluster I, to which those *Clostridium* sp. phylogenetically belongs, are generally not cellulolytic (*C. cellulovorans* is an exception) [58, 281]. Thus *C. acidisoli* and *C. puniceum* will be considered noncellulolytic in the following discussion, but this has to be verified.

The co-occurence of cellulolytic and noncellulolytic fermenters might not necessarily be linked to the ability of the second to compete successfully for free sugars but may be explained by synergistic effects that are well described for the fermenter community in the digestive tract of ruminants [123, 267, 300] but not evaluated for peatlands. In the following, a model for potential synergistic relationships between cellulolytic and noncellulolytic fermenters is presented in order to explain the high abundancies of labled saccharolytic fermenters observed in the [^{13}C]cellulose supplemented peat soil microcosms (Figure 44). On the on side of the proposed relationship, cellulolytic fermenters like that of the highly novel and abundant *Fibrobacter*-related OTU1 may actively release sugars on which an associated saccharolytic partner could feed on. Such a crossfeeding is known for the hydrolytic fermenter *Fibrobacter succinogenes* that hydrolyzes hemicellulose, pectin, and cellulose but ferments only glucose but not xylose or other sugars that therefore become available for nonhydrolytic fermenters [426]. Furthermore, cellulolytic fermenter can actively excretes cellulose-derived sugars [371, 474, 482]. In this respect, such an active excretion of [^{13}C]cellulose-derived sugars would enhance the extent to which saccharolytic fermenters could receive a labeling which was observed in the conducted experiments. On the other side of the proposed relationship, (i) noncellulolytic fermenters may scavenge sugars that are not converted by the cellulolytic fermenter and thereby prevent an product inhibition of hydrolytic enzymes [17, 92, 254, 271], (ii) pectinolytic and xylanolytic fermenters may enhance the accessibility to cellulose fibres by actively hydrolyzing pectin and hemicellulose [123, 267, 426], or (iii) saccharolytic fermenters

may support growth of cellulolytic fermenters by providing essential amino acids and vitamins or by fixing N_2 [150, 306, 426, 457]. Of the labeled saccharolytic taxa listed in Table 28, *Clostridium acidisoli* would represent a suitable noncellulolytic partner organism as it metabolizes a variety of sugars and has the outstanding trait to fix N_2 at a pH as low as 3.7 [218]. Therefore *C. acidisoli* could provide the hydrolytic partner with a source of nitrogen (e.g., ammonium or amino acids). In the nitrogen limited acidic environment of peat soils, in which N_2 fixation of many microbes is impaired [161, 247, 315], this would be a valuable gift for the hydrolytic fermenter and such a synergistic relationship might be a selective advantage over other nonsynergistic hydrolytic fermenters. In this regard, *Acidobacteria* (like the cellulolytic fermenter *Telmatobacter bradus* [OTU3e]) are abundant carbohydrate utilizer in this and other peatlands but are not know to fix N_2 [84, 176, 324, 468], and therefore would benefit from such a synergism.
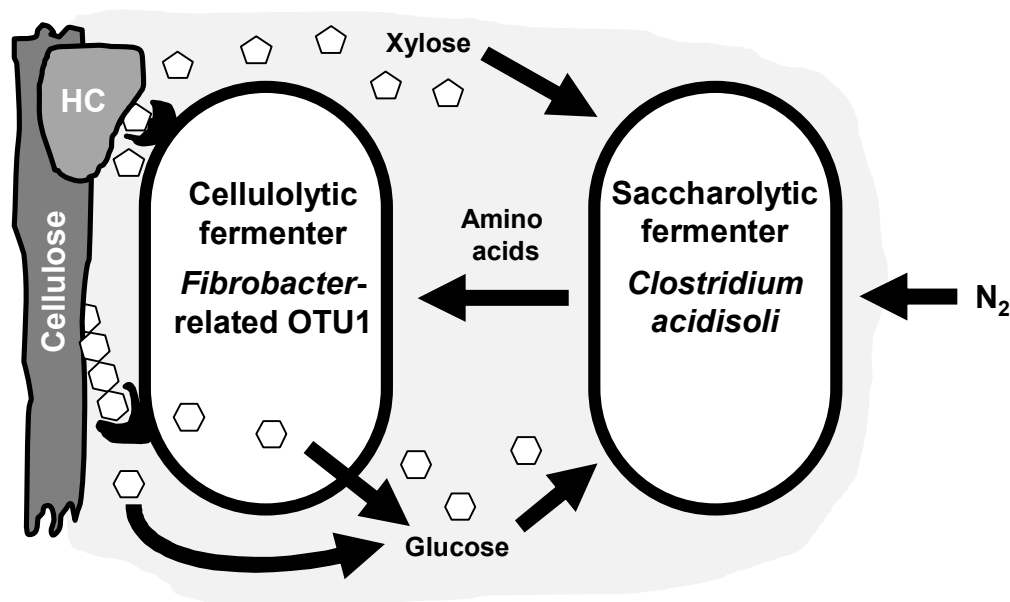
Figure 44 Model of the proposed synergistic relationship between cellulolytic and saccharolytic fermenters in the nitrogen-limited environment of peatlands.
Potential cellulolytic fermenters like the *Fibrobacter*-related unclassified *Bacteria* (OTU1) provide cellulose- and hemicellulose (HC)-derived soluble sugars (hexagons and pentagons represent glucose and xylose) for saccharolytic fermenters that are able to fix N_2 (e.g., *Clostridium acidisoli* [218]) and deliver amino acids for the partner microbe. A biofilm matrix is indicated as light grey background.

Synergistic fermenter communities in peatlands are likely organized in biofilms similar to those in the rumen [50, 123, 267]. In this respect, thick biofilms were observed in cellulose/pectin/xylan-supplemented liquid serial dilutions that were derived from peat soil of the investigated fen [384]. Unfortunately, the community composition of these biofilms was not evaluated. *Acidobacteria* (like *Telmatobacter*) might play a key role for biofilm formation in

peatlands because (i) they are abundant in these ecosystems, (ii) their culturability heavily increases when using biofilm based isolation procedures, (ii) they harbor genes that are crucial for biofilm formation, and (ii) they have been shown to contribute to biofilm formation in acidic mine drainage environments [84, 85, 176, 186, 468]. However, this needs to be verified.

In summary, saccharolytic fermenters were abundant and labeled in [^{13}C]cellulose-supplemented microcosms, and are likely to cooperate in synergistic relationships with cellulolytic fermenters in peatlands.

4.1.1.3.   Growth yield vs. growth rate: how the fermentation profile in peatlands is affected by substrate availability

Propionate, acetate, and CO_2 were the dominant accumulating fermentation products in cellulose-supplemented peat soil microcosms (Figure 9), and a similar product profile was observed during cellulose degradation in tundra wetland soil and taiga pond sediments [211, 212]. This product profile is indicative for propionate fermentation [301], and bacterial families known to comprise propionate fermenters were abundant in the heavy fractions of [^{13}C]cellulose treatments (OTUs 4 and 9; Table 28). Novel taxa (e.g., OTU1) may have contributed to propionate fermentation but their physiology is presently unknown and needs to be evaluated in the future. Nevertheless, the high amounts of propionate that were formed and the high abundance of known propionate fermenters indicates that propionate fermentation is crucial for the cellulose degradation in the fen.

The labled OTUs 3, 6, 12, and 15 were related to fermenters that produce butyrate, ethanol, lactate, and H_2 (Table 28) but these fermentation products accumulated only slightly if at all in cellulose treatments (Figure 9). Some of these fermentation products may have been formed in minor quantities while others were formed in high amounts but turned over quickly. In this regard, fermenters can alter their product profiles in order to achieve high ATP yields [268]. As an example, *C. butyricum* can generate more ATP from SLP when it forms acetate instead of butyrate [496]. However, enhanced acetate production is coupled to enhanced H_2 production and this is thermodynamically feasible only if the H_2 concentrations are low [376]. Similarily, more ATP can be generated when fermenters reduce the production of ethanol and lactate in favor for enhanced acetate and H_2 production as long as H_2 is effectively scavenged [268, 472]. However, the prerequisite for low H_2 concentrations implies the presence of H_2 sinks, but these sinks need to be evaluated for the cellulose treatments. Judged by the relative low amounts of reductant recoverd in CH_4 compared to acetate and propionate (Figure 10 and Table 18), hydrogenotrophic methanogenesis probably was a minor sink for cellulose-derived H_2 in cellulose treatments incubated at 5°C in which CH_4 production was stimulated compared to unsupplemented controls. In contrast, CH_4 production was inhibited in cellulose treatments

compared to controls at 15°C, and therefore methanogenesis was probably not a sink for cellulose-derived H_2 at 15°C. Acetogens can consume H_2 but the ΔGs for acetogenesis were unfavorable (most times > 0 kJ·mol⁻¹). The contribution of acetogens results in high acetate:propionate ratios as observed in cellulose-supplemented microcosms of agricultural and swamp soil [372, 449]. However, acetate and propionate accumulated in equimolar amounts at 5°C and 15°C, reinforcing that acetogenesis was not a sink for H_2.

Propionate fermenters can cometabolize glucose and H_2, and therefore they can function as H_2 sinks [160]. When propionate fermenters use external H_2 during glucose fermentation than more propionate but less acetate and CO_2 are produced (Figure 45). ΔGs for glucose fermentation +/- H_2 by propionate fermenters ranged between -300 to -280 kJ·mol⁻¹ in cellulose treatments and were most times slightly more exergonic for glucose fermentation without H_2. At first glance, one might conclude that H_2 oxidation therefore would be irrational for propionate fermenters. However, the thermodynamics merely 'decide' wheter a biochemical pathway is feasible or not whereas the ATP yield (i.e., how many molecules of ATP can be conserved per molecule of substrate) is solely dependent on the pathway itself [432, 434]. In this regard, the ATP yield is higher when propionate fermenters convert glucose + H_2 compared to -H_2 because of the additional ATP from ETP (during fumarate respiration) [160, 432]. The additional ATP_{ETP} that is coupled to propionate production more than compensates the lower ATP yields from SLP that can be conserved when acetate is produced instead of propionate (Table 29). In summary, propionate fermenters that were abundant and produced high amounts of propionate in cellulose treatments, likely scavenged H_2 produced by H_2-evolving fermenters (e.g., *Clostridium* sp.). As a consequence of the maintenance of low H_2 concentrations in the system, H_2-evolving fermenters redirected their own fermentation profile away from the production of ethanol, lactate, and butyrate towards the production of acetate and H_2. Such a H_2-transfer increases the ATP yield and therefore the growth yields of both types of fermenters (Table 29) [160, 472]. Similar relationships can be found in the rumen were fumarate respiration (in addition to methanogenesis) is a sink for fermentation-derived H_2 [180].

Accumulation of propionate, acetate, and CO_2 was relatively slow in the cellulose-supplemented microcosms (Figure 9) compared to glucose-supplemented microcosms of the investigated fen [151, 178, 487]. Furthermore, the product profile differed considerably between cellulose and glucose supplementation: Propionate, acetate, and CO_2 were the dominant accumulating products in cellulose treatments whereas acetate, H_2, CO_2, butyrate, and ethanol were the major fermentation products in glucose treatments in which only minor amounts of propionate accumulated. This indicated that H_2 production exceeded the capacity for H_2 consumption in glucose treatments but not in cellulose treatments. As a result of H_2 accumulation in glucose treatments, H_2-evolving fermenters were forced to produce butyrate and ethanol to dispose excess reductant which is linked to a reduced growth yield [376].

However, in the presence of relatively high amounts of glucose, growth rates and not growth yields are pivotal for the competitiveness of fermenters [240]. Thus, it is likely that in glucose treatments, fast-growing "copiophiles" (i.e., microbes preferring substrate-rich conditions) outcompeted slow-growing "oligophiles" (i.e., microbes preferring substrate-poor conditions) due to a higher metabolic flux whereas the slow-growing fermenters were favored under the more substrate-limited conditions in cellulose treatments due to an enhanced energy output. In fact, the microbial community in cellulose treatments (Figure 12 and Table A2) and glucose treatments [151, 176] of the fen soil differed considerably: Taxa with high growth rates (*Clostridium puniceum*-related taxa, *Enterobacteriaceae*, and *Aeromonadaceae*) dominated in [^{13}C]glucose treatments [151] but were considerably less abundant in the [^{13}C]cellulose treatments (OTUs 6a and 92 in Table A2). Furthermore, the dominant taxa in 'heavy' fractions of [^{13}C]cellulose treatments (Table 28), that were partially affiliated with known slow-growing oligophiles (e.g., *Acidobacteriaceae* [43] and *Prolixibacteraceae* [173]) were not labeled in [^{13}C]glucose treatments [151]. This reinforces the assumption that slow-growing fermenters that were involved in cellulose degradation were outcompeted by fermenters with high growth rates in glucose treatments.

Table 29   Energetics of fermentations potentially involved in H$_2$ transfer

Fermentation	$\Delta G_{15}{}^a$	$\Delta G_5{}^a$	ATP^b (SLP + ETP)	$\Delta G_M{}^c$
Butyrate fermenter				
Glucose + 0.6 H$_2$O → 0.7 Butyrate + 0.6 Acetate + 1.3 H$^+$ +2 CO$_2$ + 2.6 H$_2{}^d$	-303	-279	3.3+0.0	-167
Glucose → 2 Acetate + 2 H$^+$ +2 CO$_2$ + 4 H$_2{}^e$	-298	-265	4.0+0.0	-200
Propionate fermenter				
Glucose → 1.3 Propionate + 0.7 Acetate + 2 H$^+$ + 0.7 CO$_2$ + 2 H$_2$O^d	-286	-283	2.7+1.8	-222
Glucose + 2 H$_2$ → 2 Propionate + 2 H$^+$ + 2 H$_2$O^e	-280	-293	2.0+2.7	-233

[a]ΔGs were calculated for concentrations measured at day 32 and 57 at 15°C and 5°C, respectively.
[b]Amounts of ATP$_{SLP}$ were obtained from ref [301] and amounts of ATP$_{ETP}$ were calculated based on ⅔ ATP per involved electron [216, 227].
[c]ΔG$_M$ is the minimum Gibbs free energy that is required for the pathway. ΔG$_M$ was calculated by multiplication of ATP$_{SLP+ETP}$ with 50 kJ mol that is assumed to be required for ATP synthesis [432].
[d]Fermentation without H$_2$ transfer.
[e]Fermentation with H$_2$ transfer.

The fermentation profiles and the microbes labled in [^{13}C]cellulose and [^{13}C]glucose supplemented microcosms of the Fen Schlöppnerbrunnen suggests that (i) slow-growing propionate- and H$_2$-evolving fermenters are involved in cellulose hydrolysis and cooperate via interspecies H$_2$ transfer in order to achieve higher growth yields under substrate-limited

conditions, whereas (ii) fast-growing fermenters compete for exogenous sugars under non substrate-limited conditions that are indicated by the accumulation of H_2, butyrate and ethanol.
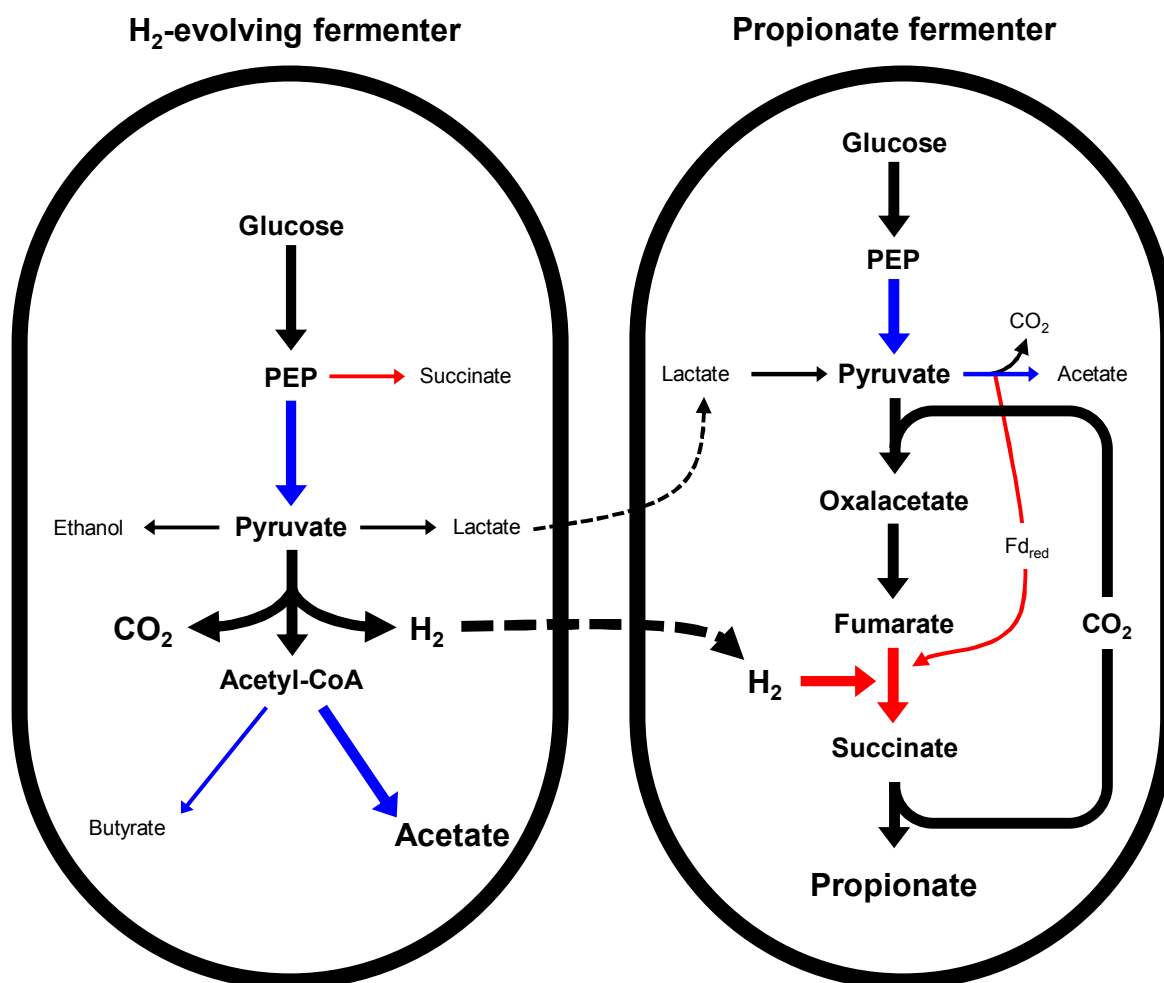
Figure 45 Model for the H_2 transfer between H_2-evolving fermenters and H_2-consuming propionate fermenters under substrate-limited conditions (e.g., during cellulose hydrolysis).
H_2-evolving fermenters produce enhanced levels of acetate and H_2 and less ethanol, succinate, lactate, and butyrate. The H_2 is used by propionate fermenters to reduce glucose-derived fumarate. As a result of this cooperation, CO_2 and acetate formed from H_2-evolving fermenters and propionate formed from propionate fermenters accumulates during growth on (cellulose-derived) glucose. During H_2 transfer, both fermenters benefit from higher ATP yields (Table 29), which is more important under substrate-limited conditions; but the fermenters probably suffer from lower growth rates [240], which is more important under substrate-rich conditions (e.g., glucose treatments). Lactate can also be converted by propionate fermenters (dashed thin arrow) [301]. Ethanol, succinate, and butyrate may have been degraded by syntrophic and non syntrophic secondary fermenters (Reactions 1,3, and 4 of Table 2). The proposed model is based on observations in pure and defined mixed cultures of fermenters [160, 472] and the findings in the cellulose treatments of this study (3.2.1). Thick arrows indicate major pathways when H_2 transfer is involved. Colors: red, reactions involved in ETP; blue, reactions involved in SLP. Fd_{red} is reduced ferredoxin.

4.1.1.4.   The rhizosphere of sedges: a hotspot for H_2-metabolizing fermenters in peatlands

High amounts of relative easily degradable organic carbon sources in the form of root cell biomass, low molecular weight exudates (e.g., formate), and mucilage (high molecular weight exudates [204]) are available for fermenters in the rhizosphere of sedges [206, 313, 332], and therefore this microzone around the roots is a potential hotspot for fermenters in peatlands (*Hypothesis 2*, 1.5). In fact, the accumulation of H_2, acetate, butyrate, and propionate that was observed in unsupplemented microcosms of sedge roots but not in unsupplemented root-free soil microcosms (Figure 15) indicated that fermenters were highly active when roots were present whereas they were severly substrate limited when roots were absent. Especially the considerably higher levels of H_2 that were observerd in soil-free root microcosms (up to 650 Pa) compared to root-free soil microcosms (<5 Pa) underscore the high activity of root-attached fermenters in the fen. Hydrogenase gene diversity analyses were performed to identify H_2-metabolizing fermenters that were attached to sedge roots (3.2.2.2). *Firmicutes* were identified as important fermentative H_2 producers in unsupplemented soil-free root microcosms. *Ruminococcaceae* and *Clostridiaceae* were especially abundant in [FeFe]-hydrogenase gene libraries whereas *Lachnospiraceae* were exclusively detected in group 4 [NiFe]-hydrogenase gene libraries (Figure 19). The contrasting set of hydrogenase genes may reflect differential roles of the hydrogenases in the fermentative pathways of these families. Observed [FeFe]-hydrogenase genes of the *Clostridiaceae* clustered to potential bifurcating (e.g., OTU_f8) and non bifurcating (e.g., OTU_f14) enzymes (Figure 20) [42]. The bifurcating hydrogenases allow the *Clostridiaceae* an enhanced ATP_{SLP} gain when H_2 concentrations are low, and the non bifurcating hydrogenases could be used when H_2 production with bifurcating hydrogenases is thermodynamically not feasible (1.4). Thus, the *Clostridiaceae* present in the rhizosphere of sedges can probably adapt H_2 production to the H_2 concentration and thereby optimize ATP_{SLP} generation. Observed group 4 [NiFe]-hydrogenases that were affiliated with the *Lachnospiraceae* clustered to hydrogenases of the *Butyvibrio / Pseudobutyvibrio* subgroup (Figure 21). Members of this subgroup are assumed to use there group 4 [NiFe]-hydrogenase for Fd^{2-} reoxidation coupled to proton translocation whereas NADH is reoxidized during butyrate formation, which is coupled to ATP_{SLP} and ATP_{ETP} [147]. At elevated H_2 concentrations, these *Lachnospiraceae* produce formate (at the expense of ATP_{ETP}) and therefore do not need an alternative hydrogenase that is not coupled to ATP generation (i.e., such as non bifurcationg [FeFe]-hydrogenases) [147]. OTUs that affiliated with a hydrogenase gene from the propionate fermenter *Caldithrix abyssi* [121] dominated in the group 1 [NiFe]-hydrogenase gene library of unsupplemented root microcosms (Figure 19). Thus, propionate fermenters, which were proposed to take up H_2 in cellulose-supplemented root-containing soil microcosms (Figure 45), may have been involved in H_2 take up in the soil-free root microcosms.

In summary, *Ruminococcaceae*, *Clostridiaceae*, *Lachnospiraceae*, and *Caldithrix*-related taxa probably dominated fermentation processes in unsupplemented soil-free root microcosms. These dominant fermenters had functionally distinct hydrogenase genes that likely reflect the H_2 metabolism in the fermentative pathway of these taxa.

Formate, which is a quantitatively abundant compound in root exudates of living sedges [206], was converted into H_2 and CO_2 in formate-supplemented soil-free root microcosms (Figure 15) indicating FHL activity. In these formate treatments, [FeFe]-hydrogenase-containing facultative aerobic *Betaproteobacteria* (OTUs f1, f3, f5, f7, and f12 in Figure 20) and group 4 [NiFe]-hydrogenase-containing *Coriobacteriaceae* (OTUs 4n5 and 4n11 in Figure 21), *Ruminococcaceae* (OTUs 4n3 and 4n8), *Acidobacteriaceae* (OTU 4n6), and *Acidobacteria*-related unaffiliated taxa (OTU 4n4) were more abundant compared to unsupplemented controls. The higher abundance in formate treatments and the finding that [FeFe]- and group 4 [NiFe]-hydrogenases are part of biochemically characterized FHL-complexes [6, 142, 443, 466] suggests that the above mentioned taxa may represent FHL-containing taxa that were attached to sedge roots. These taxa may have cometabolized root-derived organic compounds and supplemented formate to increase the total ATP gain. In this regard, formate oxidation to H_2 and CO_2 was exergonic (Figure 16) and group 4 [NiFe]-hydrogenase could be used to transform the released energy into a pmf which would subsequently drive ATP synthesis [443]. The genenration of a pmf in [FeFe]-hydrogenase containing taxa may be realized by a Rnf-complex (Figure 4E) and such a complex is present in *Laribacter hongkongensis* [73], to which the abundant OTU_f1 was affiliated (Figure 20). Summarized, potential FHL-containing taxa that use different hydrogenases were stimulated in formate-supplemented soil-free root microcosms whereas other taxa (e.g., *Clostridiaceae* and *Lachnospiraceae*) likely dominated fermentative H_2 production in unsupplemented controls.

In situ, formate and O_2 are released by living roots [206, 422, 424] and therefore FHL-containing facultative aerobes have selective advantages over obligately fermenters in the rhizosphere of sedges: (i) FHL-containing facultative aerobes can increase their ATP yield by cometabolizing formate and other root-derived carbon compounds under anoxic conditions [6, 443], and (ii) they can grow aerobically under oxic conditions. These selective advantages were reflected by the high abundance of potentially FHL-containing facultative aerobic *Betaproteobacteria* in [FeFe]-hydrogenase gene libraries of fresh roots in which the obligately anaerobic *Clostridiaceae* were not detected (Figure 19). Dead roots that are disconnected from the atmosphere (e.g., by high water tables) will not release formate and O_2 and might represent a niche for obligately fermenters (e.g., *Ruminococcaceae*, *Clostridiaceae*, *Lachnospiraceae*) that were observed in high numbers in unsupplemented soil-free root microcosms (Figure 19).

The collective results indicate that contrasting fermenter communities are probably highly active on living and dead roots in peatlands whereas the fermenters in the bulk soil suffer from a limited availability of degradable carbon compounds.

4.1.2. Trophic interactions between novel syntrophs and acetate- and H$_2$-scavenging methanogens at 5°C and 15°C

Peat soil microcosm studies with the focus on primary fermentations indicated that ethanol, butyrate, and propionate are important intermediates of the anaerobic mineralization processes in the Fen Schlöppnerbrunnen and other peatlands [151, 176, 384, 487]. The syntrophic conversion of these fermentation products to methanogenic substrates is regarded as a potential bottle neck process of the intermediary ecosystem metabolism in cold and anoxic environments like peatlands [208, 445]. However, the fast consumption of supplemental ethanol, butyrate, and propionate especially after several substrate pulses revealed a high capacity for syntrophic conversions in the peat soil (Figure 27-Figure 30) and suggested that syntrophic secondary fermentation processes were not rate limiting for the anaerobic mineralization of organic matter. Carbon and reductant derived from supplemental ethanol, butyrate, and propionate were recovered in CH$_4$ (Table 23), indicating trophic links between syntrophic fermenters and methanogens. 16S rRNA analyses revealed new strains/species of known syntrophic genera and methanogenic archaea as well as taxa previously not considered as syntrophic. In the following, potential trophic interactions between syntrophs and methanogens in the fen and the ecological consequences of the involved energy metabolism of model microbes that were related to observed taxa are discussed to address *Hypothesis 3* (1.5).

4.1.2.1. Indications for seasonal differences in the rate-limiting steps of syntrophic methanogensis in peatlands

CH$_4$ and CO$_2$ were the sole observed endproducts in unsupplemented microcosms that were prepared with fresh peat soil collected in October 2010 (Figure 9) or May 2013 (Figure 25) and incubated at 15°C, indicating that (i) methanogenesis was an important terminal process of the mineralization of endogenous carbon sources, and (ii) neither syntrophic fermentation processes nor methanogenesis was rate limiting at this temperature. Similar results were observed with Arctic and Siberian peat soil [290, 445] in which polymer hydrolysis was assumed to be the rate-limiting step at moderate temperatures.

At 5°C, acetate, propionate, and butyrate were effectively scavenged in unsupplemented microcosms with peat soil collected at the beginning of the vegetation period in May (Figure

26). In contrast, acetate, propionate, and to a lesser extent butyrate accumulated in unsupplemented microcosms at 5°C with peat soil collected in October (Figure 9). The latter time point represents the end of the vegetation period, and more endogenous carbon sources might have been available compared to the sampling in May at which growth of plants was ongoing for only 1 or 2 month. Aceticlastic methanogenesis was likely the rate limiting process with the October samples, and propionate and butyrate accumulation were the results of the thermodynamic constraints of the syntrophs at the elevated acetate concentrations. In this regard, 16S rRNA sequences of aceticlastic methanogens outnumbered that of hydrogenotrophic methanogens by 7:1 in fresh peat soil of the fen collected in May (Figure 37) whereas the ratio for transcripts of the methyl coenzyme M reductase of aceticlastic and hydrogenotrophic methanogens was 2:3 in fresh soil samples collected in October [176]. Thus, aceticlastic methanogenesis may have been rate limiting at the end of the vegetation period because of a relatively low number (or activity) of aceticlastic methanogens. In contrast to this findings, syntrophic propionate oxidation was rate limiting in Arctic peat soil in which propionate accumulated to mM concentrations whereas acetate was effectively scavenged by *Methanosarcina* at low temperatures [445].

These results indicate that the rate-limiting step in syntrophic minaralization varies between different peatlands and may also vary between different seasons that are characterized by different soil temperatures and a different availability of fresh plant organic matter. H_2 concentrations were always low (≤ 10 Pa) in unsupplemented peat soil microcosms of the investigated fen as well as Arctic [445] and Siberian [290] peatlands at moderate and low temperatures, suggesting that hydrogenotrophic methanogenesis is not rate-limiting in these peatlands.

4.1.2.2. A new strain – a new trait: indications of syntrophic ethanol oxidation by *Pelobacter propionicus*

Ethanol accumulated only transiently when peat soil microcosms were supplemented with a mixture of cellulose, xylan, and pectin, and it did not accumulated at all in cellulose-supplemented soil microcosms and soil-free root microcosms whereas propionate and butyrate accumulated in all of these experiments ([384], 3.2.1.1 and 3.2.2.1). It was discussed above (4.1.1.3) that fermenters may have redirected their fermentative pathways away from ethanol and towards acetate and H_2. An alternative explanation is that ethanol was produced (parallel to propionate and butyrate) by primary fermenters but was effectively consumed by secondary fermenters that prevented its accumulation. That the microbial community in the investigated fen had the capacity to oxidize ethanol at low and moderate temperatures was shown with the ethanol-supplemented microcosms, in which the substrate was consumed with-
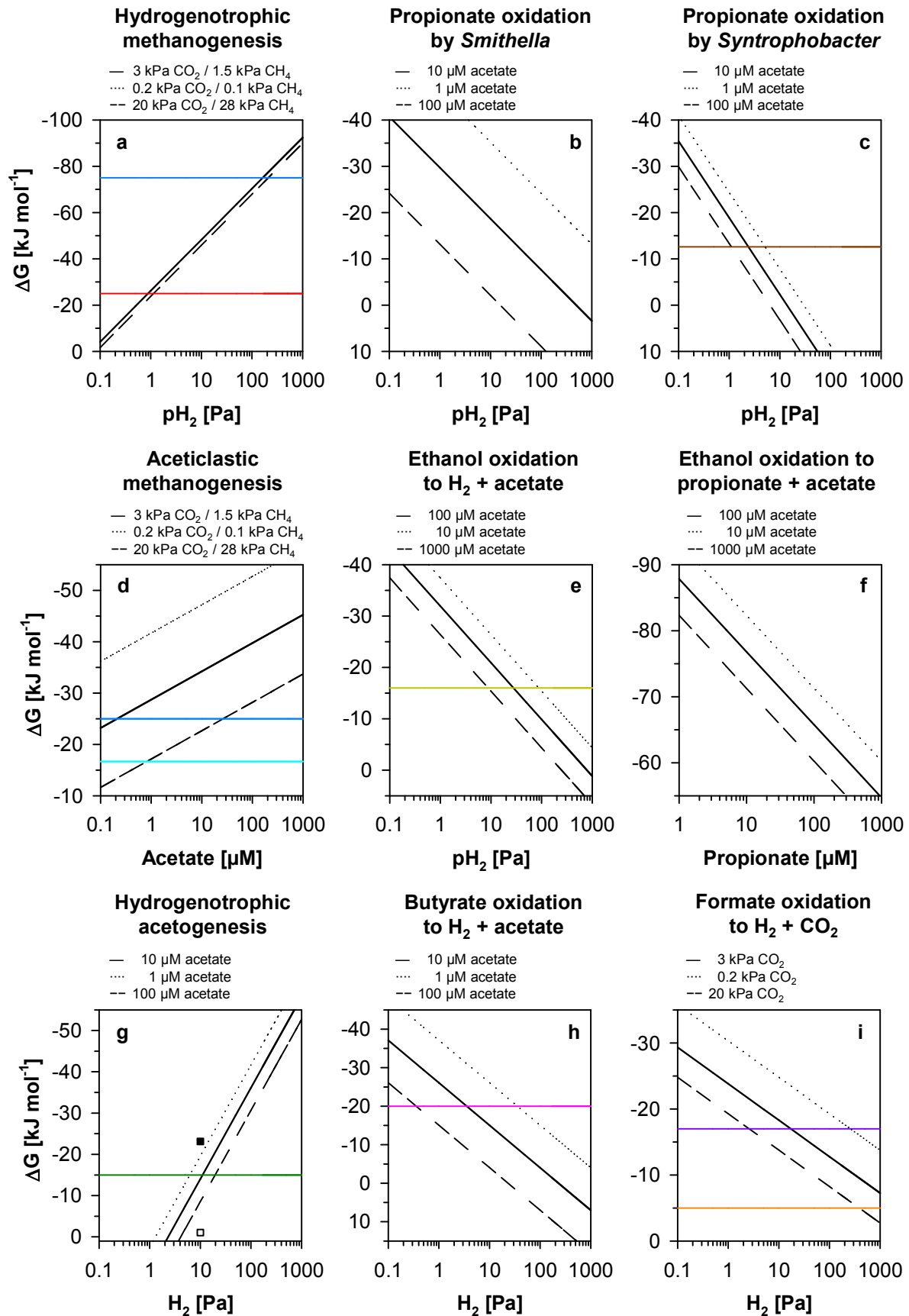
Figure 46 ΔGs of important intermediary processes at variable concentration of products and substrates at moderately acid pH (5.3) and moderate temperatures (15°C).

Find the figure legend on page 130.

Figure 47 ΔGs of important intermediary processes at variable concentration of products and substrates at moderately acid pH (5.3) and low temperatures (5°C).

Find the figure legend on page 130.
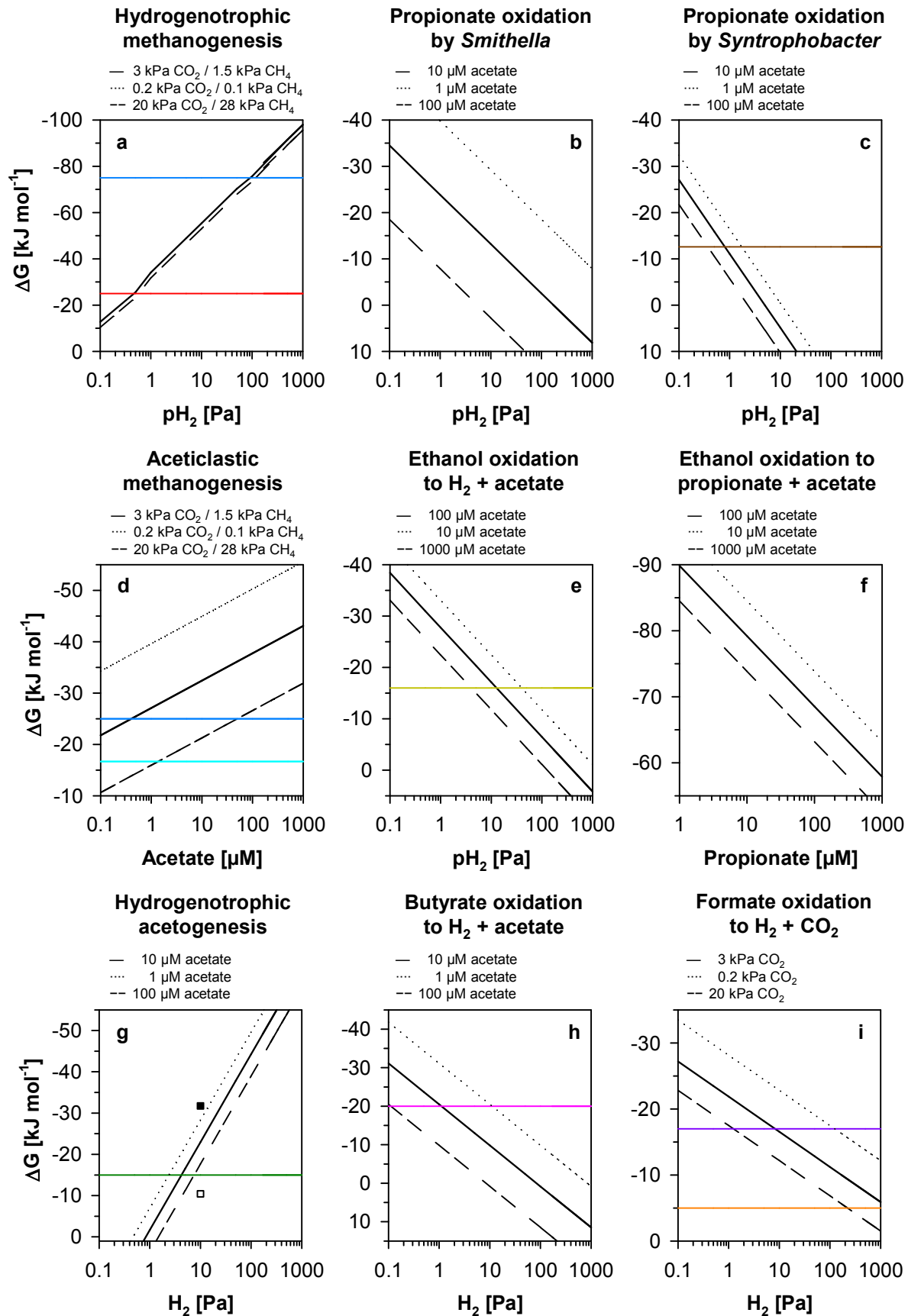
Legend of Figure 46 and Figure 47: Plots: a, hydrogenotrophic methanogenesis (Reaction 1 in Table 3); b, propionate oxidation by *Smithella* (Reaction 6 in Table 2); c, propionate oxidation by *Syntrophobacter* (Reaction 5 in Table 2); d, aceticlastic methanogenesis (Reaction 4 in Table 3); e, syntrophic ethanol oxidation (Reaction 8 in Table 2); f, ethanol oxidation to propionate and acetate (Reaction 3 in Table 2); g, hydrogenotrophic acetogenesis (Reaction 1 in Table 4); h, syntrophic butyrate oxidation (Reaction 4 in Table 2); i, formate oxidation by FHL (Reaction 7 in Table 2). Horizontal lines represent estimates of the theoretical ΔG limits for ATP synthesis of the respective organisms: blue in a and d, *Methanosarcina* on H_2-CO_2 (-75 kJ·mol^{-1} [434]) and acetate (-25 kJ·mol^{-1} [411]), respectively; red in a, methanogens without cytochromes or *Methanocella* (-25 kJ·mol^{-1} [434]); cyan in d, *Methanosaeta* (-16.7 kJ·mol^{-1} [184]); green in g, *Acetobacterium* (-15 kJ·mol^{-1} [393]); dark yellow in e, *Pelobacter* (-16 kJ·mol^{-1} [399, 400]); pink in h, *Syntrophomonas* (-20 kJ·mol^{-1} [383]); brown in c, *Syntrophobacter* (-12.6 kJ·mol^{-1} [390]); purple in i, *Desulfovibrio* (-17 kJ·mol^{-1} [94]); orange in i, *Thermococcus* (-5 kJ·mol^{-1} [246]). These ΔG limits were either observed (for *Syntrophobacter*, *Pelobacter*, *Thermococcus*, and *Desulfovibrio*) or estimated from theoretical ATP gains of the respective biochemical pathway (given that at least -50 kJ·mol^{-1} phosphorylation potential are required to form ATP [432]). No such data is available for the propionate oxidation via the *Smithella* pathway and the ethanol oxidation to propionate and acetate. Further concentrations used for calculations (diagonal lines): pCO_2 in c, f, and g was 3 kPa; propionate in b and c, ethanol in e and f, butyrate in h, and formate in i was 50 µM. Symbols: ■, acetogenesis at 20 kPa CO_2, 10 µM acetate, and 10 Pa H_2; □, acetogenesis at 0.2 kPa CO_2, 10 µM acetate, and 10 Pa H_2. 3 kPa CO_2 and 1.5 kPa CH_4 represents the average composition of the head spaces in the microcosm experiments. 20 kPa CO_2 and 28 kPa CH_4 were the highest partial pressures of both gases observed before exchanging the gas phase with N_2. 0.2 kPa CO_2 and 0.1 kPa CH_4 were the lowest partial pressures of these gases observed directly after exchanging the gas phase with N_2.

out delay (Figure 27 and Figure 28). Ethanol consumption was also observed in several other peatlands [168, 289, 290, 445], suggesting that this compound is turned over fast in such environments.

Several pathways for the consumption of ethanol under methanogenic conditions are known: (i) cometabolization of ethanol and acetate to butyrate by *Clostridium kluyveri* [40]; (ii) acetogenesis on ethanol (Reaction 4 of Table 4); (iii) conversion of ethanol to propionate and acetate (Reaction 3 of Table 2); (iv) syntrophic ethanol oxidation to acetate and H_2 (Reaction 8 of Table 2); (v) direct methanogenesis on ethanol [127, 182]. So far only two methanogenic species that were able to grow on ethanol are known (*Methanogenium organophilum* and *Methanofollis ethanolicus*), and the deposited culture of *M. ethanolicus* was recently found to be contaminated [http://jcm.brc.riken.jp/en/ announcement_e/ann20150928jcm15103_e]. However, the ecological relevance of direct methanogenesis on ethanol is unclear and this possible ethanol sink is not discussed further in this dissertation. Butyrate was formed in ethanol-supplemented serial dilutions of the investigated fen [384] and in ethanol containing microcosms of a mire in northern Finnland [289], suggesting that ethanol oxidation by the *C. klyveri*-like pathway can occur in peatlands. However, (transient) butyrate accumulation was

not observed in this study (Figure 27 and Figure 28), and therefore ethanol was probably not oxidized via the *C. klyveri*-like pathway. Taxa that comprise acetogens (e.g., *Clostridiaceae* and *Veillonellaceae* in Table A3) did not respond to supplemental ethanol, indicating that ethanol was not consumed by known acetogens. Conversion of ethanol to propionate and acetate was exergonic in ethanol treatments ($\Delta G \approx$ -22 and -23 kJ·mol^{-1} ethanol at 15°C and 5°C, respectively; calculated for 50 µM ethanol, 100 µM of acetate, 100 µM propionate, pH 5.3; Figure 46f and Figure 47f). This process was predicted as the main sink for ethanol in Arctic peat soil, and it was assumed that ethanol oxidation was catalyzed by *Actinobacteria* [445]. However, phylotypes that affiliated to *Actinobacteria* did not respond to ethanol in this study. Instead, OTU35a responded to supplemental ethanol at 5°C and 15°C and was closely related to *Pelobacter propionicus*. *P. propionicus* is capable of ethanol oxidation to propionate and acetate, whereas so far investigated strains do not perform syntrophic ethanol oxidation which is performed by *Pelobacter acetylenicus* and *Pelobacter carbinolicus* [374, 399]. However, low concentrations of propionate and transiently accumulating acetate and H_2 observed in ethanol treatments (Figure 27 and Figure 28) suggested that the detected novel strain of *P. propionicus* degraded ethanol to acetate and H_2 rather than propionate and acetate. Effective scavenging of ethanol-derived propionate by syntrophic propionate oxidizers was unlikely because of the high transient acetate concentrations that made this process thermodynamically unfeasible. Taxa that responded to supplemental propionate were not labled from [^{13}C]ethanol-derived [^{13}C]propionate, further underscoring the assumption that the *P. propionicus*-related taxa in the fen performed syntrophic ethanol oxidation without the production of propionate. These and the previous findings indicate that the pathway of ethanol oxidation varies in different strains of *P. propionicus*. Nevertheless, ethanol oxidation to propionate and acetate represents an H_2-independent alternative to syntrophic ethanol oxidation, which might facilitate ethanol consumption under locally and temporarily occuring elevated H_2 partial pressures in peatlands.

Acetate transiently accumulated to up to 500 µM whereas H_2 partial pressures did not exceed 20 Pa in ethanol treatments at 15°C and 5°C in which syntrophic ethanol oxidation (Reaction 8 of Table 2) was always exergonic (Figure 27, Figure 28, and Figure 32). Thus, effective acetate consumption was not mandatory for syntrophic ethanol oxidizers at the low H_2 partial pressures that were maintained by hydrogenotrophic methanogens (e.g., *Methanocella* and *Methanoregula*) in the ethanol-supplemented microcosms. This was supported by theoretical calculations which indicated that the ΔGs were < -16 kj·mol^{-1} (the thermodynamic limit for syntrophic ethanol oxidation in defined chemostat cocultures of *Pelobacter acetylenicus* and different H_2 oxidizers [399, 400]) even at 1 mM acetate as long as the H_2 partial pressures were below 10 Pa at 15°C and 2 Pa at 5°C (Figure 46e and Figure 47e). Syntrophic ethanol oxidation was a likely sink for ethanol in cellulose-supplemented

microcosms in which H_2 partial pressures were equally low (Figure 9 and Table 17). In contrast, syntrophic ethanol oxidation was unlikely in unsupplemented soil-free root microcosms because of the high H_2 and acetate concentrations that were observed (Figure 15). Root-attached acetogens that were detected based on hydrogenase gene diversity analyses (Figure 20) may have consumed fermentation-derived ethanol in these treatments.

In summary, ethanol is a relatively energy rich primary fermentation product that is probably produced in high quantities in this and other peatlands, but its accumulation is likely limited by the activity of metabolically versatile ethanol-oxidizing microbes.

4.1.2.3.   Known and previously unrecognized butyrate-oxidizing peat-inhabiting syntrophs

Syntrophic butyrate oxidation (Reaction 4 in Table 2) via β-oxidation is thus far the single known pathway for the degradation of butyrate under methanogenic conditions [308, 376, 379, 420]. This pathway depends on H_2 partial pressures of ≤ 10 Pa (or ≤ 10 µM formate) [403], a level that was almost never exceeded in butyrate-supplemented microcosms in which butyrate was rapidly consumed after an initial adaption phase (Figure 29). Acetate transiently accumulated to up to 200 µM in butyrate treatments, indicating that the acetate concentrations were not critical as long as the H_2 partial pressures were low enough to allow syntrophic butyrate oxidation (Figure 46h and Figure 47h). A ΔG of approximately -20 kJ·mol^{-1} (sufficient for the synthesis of approximately ⅓ mol ATP per mol of butyrate) was proposed as the thermodynamic limit for the model syntrophic butyrate oxidizer *Syntrophomonas wolfei* based on the assumption that its ATPase translocates 3 H$^+$ per ATP [383]. Observed ΔGs for syntrophic butyrate oxidation were often > -20 kJ·mol^{-1} (Figure 32), suggesting that less energy is required to sustain syntrophic butyrate oxidation. Alternatively, hydrogenotrophic methanogens juxtaposed to butyrate oxidizers may have maintained H_2 partial pressures that were lower than those measured in the headspace gas phases [63]. Such a scenario could also explain why butyrate did not accumulate to higher concentrations in cellulose-supplemented microcosms in which the high observed acetate concentrations caused ΔGs of -5 to +8 kJ·mol^{-1} (at 15°C).

Two OTUs (OTU79a and OTU26a) were labled in [^{13}C]butyrate-supplemented microcosm (Table A3). OTU79a represented a novel species of *Syntrophomonas*, a genus that comprises several syntrophic butyrate oxidizers including the model organism *S. wolfei* [379, 414]. The detection of *Syntrophomonas* in butyrate-supplemented microcosms of peat soil as well as swamp soil [49], paddy rice soil [251], and a hydrocarbon-contaminated ditch [116] indicates that this genus contributes to syntrophic butyrate oxidation in various soil environments. OTU26a clustered within the *Alphaproteobacteria*, and *Telmatospirillum siberiense* was the

closest cultured relative (Table A3). To date, syntrophic butyrate oxidation is not known for cultured members of the *Alphaproteobacteria*. However, most sequences of OTU 26a were highly similar to a clone sequence retrieved from a butyrate fed anaerobic digestor (JN995370, Figure 35), suggesting a previously unrecognized potential of *Telmatospirillum*-related taxa to degrade butyrate under methanogenic conditions. *Smithella* and *Syntrophus* are other syntrophic taxa that are known to degrade butyrate [252, 283] and were detected in the investigated fen (Table A2 and Table A3). Both genera did not respond on supplemental butyrate and may primarily oxidize propionate (*Smithella*) and aromatic compounds (*Syntrophus*) in the fen as those are their preferred substrates [82, 252, 283].

The results of the butyrate-SIP experiment indicated that the accumulation of butyrate in the Fen Schlöppnerbrunnen is likely prevented by the activity of *Syntrophomonas*- and *Telmatospirillum*-related taxa that represent known and priviously unrecognized syntrophic genera. Despite low H_2 partial pressures, syntrophic butyrate oxidation became thermodynamically unfeasible when acetate accumulated to mM concentrations (e.g., in unsupplemented controls at 5°C during the cellulose experiment; Figure 9). Thus, butyrate might temporarily accumulate in this fen when acetate oxidation (e.g., by aceticlastic methanogens) is rate limiting. This was observed with peat soil of a mire in northern Finnland in which acetate oxidation was likely limited by the low number of aceticlastic methanogens [289].

4.1.2.4. Thermodynamic constraints influencing the dominating pathways of syntrophic propionate oxidation in peatlands

Two contrasting pathways of syntrophic propionate oxidation are known for members of the genera *Syntrophobacter* (Reactions 5 in Table 2) and *Smithella* (Reactions 6 in Table 2), respectively [82, 308, 379, 403, 420, 485]. The ecological consequence of the different pathways is that *Smithella* sp., which produces more acetate and less H_2, thermodynamically are more dependent on effective acetate removal whereas *Syntrophobacter* sp. (and genera with a similar pathway; e.g. *Pelotomaculum*) are more dependent on effective H_2 removal by the methanogenic partner organisms [93]. However, both pathways profit from and at low propionate concentrations depend on low concentrations of H_2 and acetate (Figure 46b, c and Figure 47b, c) [95, 252, 290]. In the conducted microcosm experiments (3.2.3), the thermodynamics for syntrophic propionate oxidation during initial substrate pulses (Figure 32) and later time points (data not shown) were most times more favorable for the *Smithella* pathway compared to the *Syntrophobacter* pathway. However, when acetate transiently accumulated (e.g., the timeframe between day 40 and day 70 in the ethanol treatment at 5°C; Figure 32F) the *Syntrophobacter* pathway became more favorable. These findings and the

general thermodynamic constraints of the different pathways [93] likely explain why *Smithella* and *Syntrophobacter* increased in abundance in the propionate treatment (characterized by low acetate and low H_2 concentrations) whereas solely *Syntrophobacter* was detected in ethanol treatments at 5°C (characterized by transient acetate concentrations of up to 500 μM and H_2 partial pressures as low as 3 Pa). *Syntrophobacter* but not *Smithella* was detected in fresh peat samples, indicating that in situ the ability to tolerate higher transient acetate concentrations is more important than the ability to cope with elevated H_2 partial pressures. This reflects that acetate temporarily accumulates in the peat soil (e.g., in unsupplemented controls at 5°C during the cellulose experiments; Figure 9) whereas elevated H_2 partial pressures in the fen are likely limited to the rhizosphere of sedges, in which acetate concentrations are also high (Figure 15).

Based on the thermodynamic calculations (Figure 32), *Smithella* may have its niche as the dominant propionate oxidizer in the fen under "starving" steady state conditions (i.e., low acetate and low H_2 concentrations which were observed in propionate treatments and unsupplemented controls at 15°C; Figure 25 and Figure 30). However, *Smithella* was observed only in the propionate treatments (Figure 34), suggesting that higher propionate concentrations (resulting in more negative ΔGs of both propionate degrading pathways) were a prerequisite for *Smithella*. Unfourtunately the pathway of energy conservation and the ΔG limit for ATP synthesis of *Smithella* have not been resolved yet. At this timepoint, on may speculate that the *Smithella* pathway delivers more ATP per mol of propionate than the *Syntrophobacter* pathway, and therefore *Smithella* can thrive only under more negative ΔGs than *Syntrophobacter*. A similar relationship between the substrate concentrations and ΔG limits of certain pathways were proposed for different hydrogenotrophic methanogens [434] and different hydrogenotrophic acetogens [393]. Alternatively, *Smithella* may in situ catalyze only the initial conversion of 2 molecules of propionate to butyrate and acetate, and subsequent butyrate oxidation may be catalyzed by a syntrophic butyrate oxidizer. Support for this trophic interaction comes from a study with paddy rice soil in which *Smithella* and *Syntrophomonas* (as the butyrate oxidizer) were labeled presumably from [^{13}C]propionate and [^{13}C]propionate-derived [^{13}C]butyrate, respectively [133]. However, thus far it is not clear whether *Smithella* can conserve energy within the initial part of its pathway. The potential release of butyrate by *Smithella* in the aforementioned study might have been caused by the high propionate concentrations (10 mM) that were supplemented. A deeper knowledge about the energy metabolism of *Smithella* is required to understand its role in syntrophic propionate oxidation in methanogenic ecosystems.

After the gas phase was flushed in unsupplemented controls at 5°C on day 97, the H_2 partial pressure never exceeded 3 Pa and the acetate concentration was always in the range of 10 μM (Figure 24). Under these conditions, endogenous propionate that transiently

accumulated before day 97 to 50 µM was consumed and after 130 days did never exceed the detection limit (1-10 µM). Furthermore, endogenous (or potentially ethanol-derived) propionate was also consumed in ethanol treatments at 5°C in which the transient acetate levels were higher than in the respective control (Figure 28). These results indicated how efficient propionate was scavenged in the microcosms even at low temperatures at which propionate accumulated in unsupplemented controls of the cellulose experiment (Figure 9) and in Arctic peat soil [445]. The ΔGs for *Syntrophobacter*, which was detected in ethanol and control treatments at 5°C, were always less negative than -10 kJ·mol^{-1} underscoring that *Syntrophobacter* can thrive close to thermodynamic equilibrium [390]. However, it is very likely that syntrophic propionate oxidation occurred in microzones in which thermodynamic conditions were more exergonic compared to the bulk soil slurry. Such microzones could occur in microbial aggregates of syntrophic propionate oxidizers juxtaposed to hydrogenotrophic methanogens (Figure 48) [63]. The hydrogenotrophic methanogens within the aggregate could maintain H_2 concentrations that yield thermodynamic conditions that sustain the growth of syntrophs and methanogens [217]. In this regard, H_2 concentrations of 1 Pa would yield a ΔG of approximately -15 kJ mol^{-1} for the syntrophs and -25 kJ mol^{-1} for hydrogenotrophic methanogens (with 10 µM acetate, 10 µM propionate, 3 kPa CO_2, 1.5 kPa CH_4, 15°C, and pH 5.3; Figure 46c).

Almost no 16S rRNA sequences were affiliated to the *Peptococcaceae*, an important propionate-oxidizing taxon detected in microcosms of swamp soil, Arctic peat, and rice field soils [49, 133, 260, 445]. High concentrations of propionate (10 mM) were supplemented to the microcosms with swamp and rice field soils [49, 133, 260]. In the Arctic peat soil, the *Peptococcaceae* were abundant only at low temperatures (3-5°C) under which the concentrations of endogenous propionate ranged between 1 and 7 mM whereas the *Peptococcacea* were replaced by *Bacteroidetes* at moderate (14-16°C) and high (24-26°C) temperatures at which the concentrations of endogenous propionate were below the detection limit at the end of the incubation [445]. Thus, the syntrophic propionate oxidizers within the *Peptococcaceae* (e.g., the genus *Pelotomaculum* [80]) may require higher propionate concentrations (translates to a more negative ΔG) compared to other syntrophic propionate oxidizers, and therefore they may have been not competitive in the propionate treatments, in which 300-750 µM propionate were pulsed repeatedly instead of adding 10 mM once (2.1.2.3).

It was already mentioned that the *Bacteroidetes* were identified as effective propionate scavengers at moderate temperatures in Arctic peat [445], and unclassified *Bacteroidetes* responded to supplemental propionate in the conducted experiments here (Figure 34). To date, none of the cultured *Bacteroidetes* sp. is known to be capable of syntrophic propionate oxidation but the results with the Arctic peat soil and the peat soil from the Fen Schlöppnerbrunnen suggest that syntrophy is a previously unrecognized trait within the

members of this phylum. Many of the presently known *Bacteroidetes* are fermenters that harbor the methylmalonyl-CoA pathway for fermentative propionate production [301]. In propionate syntrophs like *Syntrophobacter* or *Pelotomaculum* the methylmalonyl-CoA pathway is also present and functions in the reverse direction [152, 308, 403, 420]. Thus, the presence of the methylmalonyl-CoA pathway could be another indicator for the potential of the *Bacteroidetes* to function as syntrophic propionate oxidizers in peatlands. Unclassified *Fibrobacteres* were also stimulated by supplemental propionate (Figure 34) and might thus represent novel propionate syntrophs. However, pure cultures of these taxa will be required to proof their syntrophic abilities.

In summary, thermodynamics for syntrophic propionate fermentation were even more critical as those for the butyrate syntrophs under the experimental conditions (Figure 32). This was reflected by the longest adaption time after the initial substrate pulse and the finding that low concentrations of H_2 and acetate were required for syntrophic propionate oxidation (Figure 23-Figure 30). Once the community was adapted, propionate turnover was fast and (endogenous) propionate was degraded even at 5°C (Figure 24 and Figure 26). Nevertheless, propionate production exceeded its consumption when acetate was not effectively scavenged (Figure 9), and in the presence of high concentrations of acetate and H_2, syntrophic propionate oxidizers may even function as source of propionate in the investigated fen and other soil environments [62, 178]. The presence of propionate syntrophs with different strategies for the degradation of propionate as discussed for *Syntrophobacter* and *Smithella* might prevent the accumulation of propionate and resulting acidification during periods of elevated H_2 or acetate in the fen.

4.1.2.5.   Potential roles for *Methanosarcina*, a metabolically versatile methanogen dominating in the peat soil

Based on the high numbers of aceticlastic methanogens (Figure 14 and Figure 37), acetate was the most important methanogenic substrate in microcosms experiments with supplemental cellulose, ethanol, butyrate, and propionate and in the respective unsupplemented controls. Aceticlastic methanogensis was also the dominant methanogenic pathway in other peat soils [290, 445] whereas hydrogenotrophic methanogenesis contributed to most of the methane production in other studies with peat soil [168, 289]. Within the aceticlastic methanogens, *Methanosarcina* was more abundant than *Methanosaeta* in fresh peat and in almost all microcosms. The relative abundance of *Methanosaeta* was higher than that of *Methanosarcina* only in unsupplemented controls at 15°C. Different relative abundancies of *Methanosarcina* and *Methanosaeta* in the different treatments might be due to the different acetate requirements for both genera (1.3.3). Reported threshold concentrations

for acetate were lower for *Methanosaeta* (<10 μM) than for *Methanosarcina* (>100 μM) because these taxa have different mechanisms for the activation of acetate [184]. On the other hand, *Methanosarcina* generates more ATP per mol acetate and tends to outgrow *Methanosaeta* in the presence of higher acetate concentrations [184]. After the preincubation, acetate concentrations only occasionally exceeded 10 μM in unsupplemented controls at 15°C (Figure 25) whereas acetate concentrations of >100 μM were repeatedly measured in most other treatments (Figure 26 to Figure 29). Thus, *Methanosaeta* might have outcompeted *Methanosarcina* under the more 'acetate-starved' conditions in the unsupplemented control at 15°C, whereas *Methanosarcina* may have dominated under 'acetate-rich' conditions in the other treatments.

The scenario above does not explain why *Methanosarcina* also dominated in propionate treatments at 15°C in which acetate concentrations ranged mostly between 10-30 μM (Figure 30), which has not been reported to be sufficient for the growth of *Methanosarcina*. However, thermodynamic calculations indicated that ΔGs for acetate concentrations in the range of 1-10 μM acetate were exergonic enough for *Methanosarcina* to grow under the experimental conditions employed (Figure 46d). In addition, one could speculate that syntrophs with a propionate oxidation pathway similar to *Syntrophobacter* were juxtaposed to hydrogenotrophic methanogens (e.g., *Methanoregula* or *Methanocella*) and *Methanosarcina* (Figure 48). *Methanoregula* and *Methanocella* could sustain very low H_2 concentrations (1 Pa at 15°C or 0.4 Pa at 5°C) that could allow syntrophs to produce acetate concentrations high enough for *Methanosarcina* (50 μM) (Figure 46a, d and Figure 47a,d). Alternatively, syntrophs with a propionate oxidation pathway similar to *Smithella* could be associated with *Methanosarcina* as the hydrogenotrophic methanogen and *Methanosaeta* as aceticlastic methanogen (Figure 48). In this scenario, *Methanosaeta* would decrease local acetate concentrations to approximately 0.1 μM, allowing syntrophs to sustain local H_2 levels high enough for *Methanosarcina* (170 Pa at 15°C and 90 Pa at 5°C) (Figure 46d and Figure 47d).

Species of *Methanosarcina* are metabolically versatile and can grow on methanol (+/- H_2) or methylamines in addition to acetate or H_2-CO_2 [145, 270]. The ability to use different methanogenic substrates would be advantageous for *Methanosarcina* under the substrate limited conditions of peat. Methylamines might be formed from glycine, sarcosine, and betaine fermentation and may get released during lysis of microbial cells as was assumed for Arctic peat soil [445]. Methanol is produced during the degradation of organic matter [380], and methanol stimulated methanogenesis in anoxic microcosms of peat from the investigated fen [487]. It is likely that *Methanosarcina* had to compete for methanol with other more specialized methanol utilizing methanogens with lower thresholds for methanol (and H_2), a competition that occurs in the hindgut of cockroaches [416]. In this regard, 16S rRNA sequences that were

affiliated with *Methanomassiliicoccus luminyensis* (a methanogen that is restricted to growth on methanol plus H_2; [104]) were detected in some treatments.
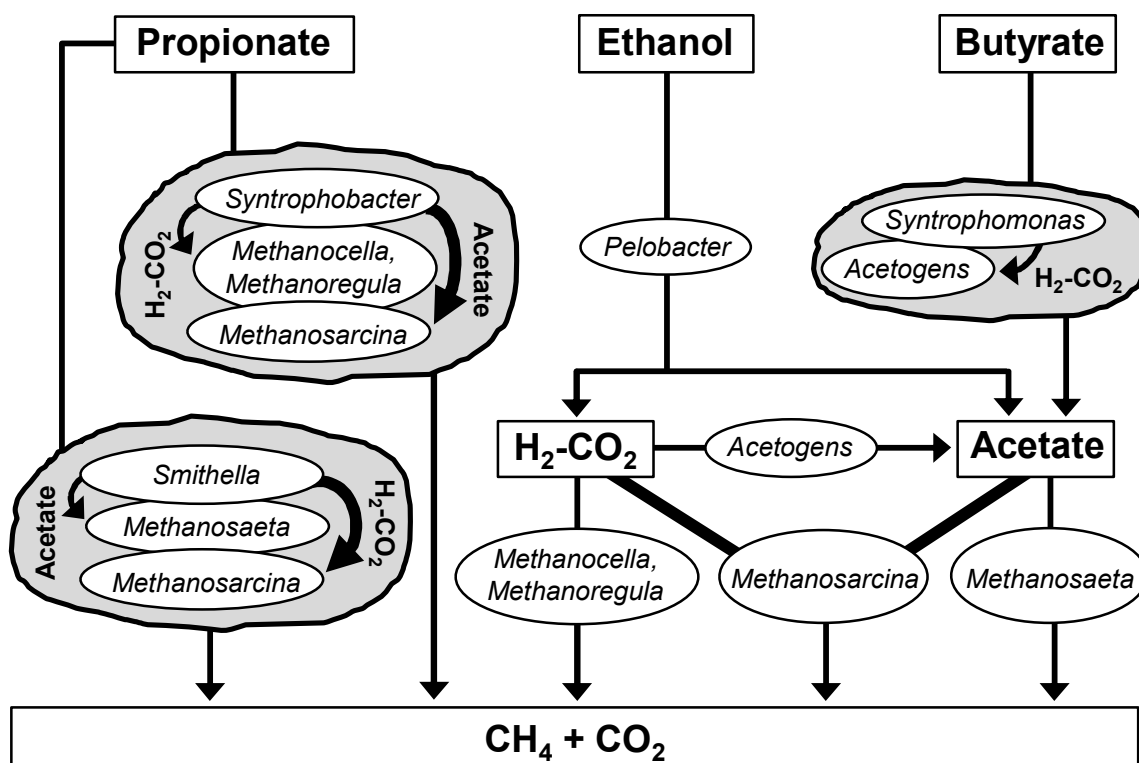
Figure 48   Hypothetical model of syntrophic processes in the Fen Schlöppnerbrunnen.
Thick lines and arrows indicate that *Methanosarcina* has relatively high thresholds for acetate and H_2. Syntrophs in peatlands are most likely juxtaposed to methanogens or acetogens in a matrix that optimizes interspecies transfer of H_2 and acetate.   Propionate oxidation by *Syntrophobacter* is particularly dependent on low H_2 concentrations (maintained by *Methanoregula* or *Methanocella*) and local acetate concentrations could be high enough for *Methanosarcina*.   Propionate oxidation by *Smithella* allows for elevated local H_2 concentrations (high enough for *Methanosarcina*) if acetate concentrations are low (maintained by *Methanosaeta*).   Propionate oxidation by *Syntrophobacter* or *Smithella* could also be coupled to acetogens and aceticlastic methanogens. See Figure 46 and Figure 47 for thermodynamic calculations of pathways potentially involved in syntrophic propionate oxidation. Butyrate oxidation was primarily dependent on low H_2 concentrations as acetate transiently accumulated in butyrate treatments. Ethanol oxidizers might also be located in close proximity to methanogens or acetogens. However calculated ΔGs were exergonic enough to enable a planktonic lifestyle for syntrophic ethanol oxidizers. Formate could be produced by syntrophs in addition to/instead of H_2-CO_2.

4.1.2.6. H_2 vs. formate interspecies transfer in peatlands

H_2 can be replaced by formate as the electron transferring compound between syntrophs and methanogens [376], and it is assumed that syntrophs regulate the extent of formate and H_2 transfer according to the actual thermodynamic constraints and the preference of the

methanogenic partner [152, 308, 383, 403, 485]. Thermodynamics of formate oxidation to H_2 and CO_2 were exergonic and this implies that interspecies H_2 transfer was more favorable than formate transfer for syntrophs in microcosms supplemented with ethanol, butyrate, propionate, and the respective controls at 5°C and 15°C (Figure 46i and Figure 47i). Calculations of diffusion kinetics suggested that formate transfer allows for higher metabolic fluxes when the syntropic and methanogenic prokaryotes are dispensed whereas fluxes are higher for H_2 transfer in densly packed mixed cell aggregates [29, 81, 435, 436]. Under the stable conditions in peatland soils, syntrophic methanogenic consortia likely form mixed cell aggregates (Figure 48) and therefore, H_2 might be the preffered interspecies electron transferring compound even when the thermodynamics for H_2 and formate are in equilibrium. Nevertheless, butyrate and propionate were converted without delay in peat soil microcosms of the investigated fen in the presence of 6 mM supplemental H_2 [338], indicating that peat syntrophs can use formate for interspecies electron transfer when H_2 interspecies transfer becomes thermodynamically unfeasible.

4.1.3.   Variabilities in trophic interactions between acetogens and methanogens in cold and moderately acidic peatlands

The role of acetogens and the extent to which this phylogenetically and physiologically divers group of microbes contributes to the flow of carbon and reductant during the anaerobic degradation of organic matter is not well resolved for peatlands. Acetogens have been shown to be important in cold and moderately acidic lake sediments [61, 331] and a psychrotolerant and acidotolerant acetogen was isolated from a fen [213]. On the other hand, acetogenesis was not an important process in Arctic peat soil [445]. Thus, the presence and activity of acetogens in peatlands likely varies. In the root and soil microcosms experiments conducted during this thesis, potential contributions of acetogens during the mineralization of supplemental cellulose, root biomass, root exudates (e.g., formate), and primary fermentation products (e.g., ethanol, butyrate, and propionate) were observed. In the following, the thermodynamic constraints and the ecological relvance of the acetogens in the Fen Schlöppnerbrunnen are discussed.

4.1.3.1.   Competition between acetogens and methanogens at low H_2 partial pressures and low temperatures in peatlands

Supplemental H_2 and formate stimulated acetate accumulation in the investigated fen, suggesting that acetogens are present and can be activated at higher concentrations of H_2 and formate [148, 176, 178, 384, 487]. When H_2 was consumed completely in these studies,

acetate concentrations decreased and acetate likely was consumed by aceticlastic methanogens [176, 384], indicating that acetogenesis was an intermediary process at higher H_2 concentrations. Inhibition of the methanogenesis in unsupplemented microcosms resulted in the accumulation of acetate but not H_2, indicating that acetogens were able to maintain low H_2 concentrations (< 10 Pa) in peat soil of the fen [384]. However, the studies mentioned above could not show whether acetogenesis contributed to the uptake of H_2 when supplemental H_2 was not present or methanogenesis was not inhibited. Thermodynamically, hydrogenotrophic methanogens can outcompete acetogens at low H_2 concentrations [69]. In this regard, the theoretical limit for hydrogenotrophic methanogenesis was 0.4 and 1 Pa of H_2 at 5°C and 15°C, respectively, under the experimental conditions (Figure 46a and Figure 47a). Such low H_2 partial pressures were measured in microcosms of Arctic peat soil (at 1-30°C), in which hydrogenotrophic methanogens outcompeted acetogens [445]. However, slightly higher H_2 levels (2-5 Pa at 5°C and 5-8 Pa at 15°C) were observed in unsupplemented peat soil microcosms of the investigated fen (Figure 25 and Figure 26), suggesting that endogenous H_2 production exeeded the H_2 uptake capacity of the hydrogenotrophic methanogens [208]. The observed H_2 partial pressures represented the theoretical thermodynamic limit for acetogeneis under the experimental conditions (Figure 46g and Figure 47g), and therefore acetogens could have maintained the observed low H_2 partial pressures. In this regard, the psychrotolerant acetogen *Acetobacterium carbinolicum* HP4 was able to consume H_2 down to 4 Pa and 10 Pa at 4°C and 15°C, respectively [65]. Acetogens with similar capabilities might be present in this and other peatlands, and by keeping the H_2 concentrations low especially at the low temperatures they might facilitate syntrophic oxidation of fermentation products as long as acetate is effectively scavenged by aceticlastic methanogens (Figure 48).

The high number of 16S rRNA sequences that affiliated with aceticlastic methanogens in fresh peat as well as in the anoxic microcosms (Figure 37) suggested that acetate was the major methanogenic substrate in situ at the time point of sampling and in the conducted experiments. This was consistent with a previous study of the Fen Schlöppnerbrunnen [350] and other similar peatlands in which the vegetation was dominated by sedges [132, 195, 355]. In contrast, peatlands dominated by *Sphagnum* mosses showed a high fraction of hydrogenotrophic methanogenesis [47, 132, 168, 232, 337, 355, 481]. A high fraction (> 66% of total CH_4 production) of aceticlastic methanogensis is indicative for acetogenesis whereas hydrogenotrophic methanogensis becomes relatively more important when acetogens do not form acetate [60]. This and the finding that aceticlastic methanogenesis was more prominent in peatlands overgrown by sedges suggests that the importance of acetogens as drivers for aceticlastic methanogenesis depends on the vegetation and thus the quality of the plant organic matter and the availability of root exudates (1.1.2).

In summary, a higher availability of readily degradable organic carbon enhances the chances that H_2 production by fermenters exceeds its consumption by hydrogenotrophic methanogens that are hampered by the low temperatures prevailing in northern peatlands [208]. Under these conditions, acetogens may consume a major fraction of the H_2 and aceticlastic methanogens subsequently consume the acetate produced by fermenters and acetogens.

4.1.3.2. Indications for contrasting activities of acetogens in the rhizosphere of sedges and bulk peat soil

As discussed above, acetogens had to cope with H_2 partial pressures of below 10 Pa in (root-containing) peat soil microcosms of the Fen Schlöppnerbrunnen in which acetogenesis was thermodynamically feasible only because aceticlastic methanogens effectively scavenged acetate. In contrast, H_2 partial pressures were high (>100 Pa) and as a result hydrogenotrophic acetogenesis was exergonic even at acetate concentrations of 3-5 mM in unsupplemented and formate-supplemented soil-free *Carex* root microcosms (Figure 15 and Figure 16). These results indicated the rhizosphere of sedges as a hotspot for acetogens that may feed on H_2 released during fermentative degradation of root biomass. Furthermore, roots of sedges release formate [206] which might be used by acetogens directly or is first converted to H_2 and CO_2 by FHL-containing taxa and subsequently the H_2 is consumed by acetogens. In this regard, [FeFe]-hydrogenase genes of taxa that comprise acetogens (*Veillonellaceae* and *Clostridiaceae*) were detected in soil-free root microcosms (Figure 20), further underscoring that acetogens are present and active in the rhizosphere of sedges in peatlands. Acetogens might be perfectly adapted to the changing redox conditions in the rhizosphere of sedges as they have developed strategies to tolerate O_2 that leaks from roots [38, 175, 222], are able to use different electron acceptors [102], and can convert a variety of electron donors [96, 97, 375] potentially provided from the roots or root attached fermenters. Acetogens have successfully colonized the rhizosphere of various wetland plants [62, 141, 222, 223, 238] and the collective results of the experiments with soil-free *Carex* root microcosms strongly suggest that acetogens are important for the turnover of carbon and reductant in the rhizosphere of peat soil-covering sedges.

High acetate concentrations and low H_2 partial pressures were observed in [^{13}C]cellulose-supplemented microcosms (Figure 9 and Table 17), in which the ΔGs for hydrogenotrophic acetogenesis ranged between -12 to +4 kJ·mol^{-1} at 5°C and +13 to +23 kJ·mol^{-1} at 15°C. Thus, hydrogenotrophic acetogenesis was thermodynamically unfeasible under the experimental conditions. Some acetogens can reverse their metabolism and grow by syntrophic acetate oxidation to H_2 and CO_2 when this becomes thermodynamically feasible [156]. This process

is known to occur in anaerobic digestors, lake sediments and potentially also in peatlands (especially bogs) [168, 191, 288, 318, 389]. On may speculate that syntrophic acetate oxidation occurred at the relatively exergonic ΔGs (up to -23 kJ·mol^{-1}) observed in [^{13}C]cellulose treatments at 15°C whereas this process was more unlikely at 5°C. Interestingly, OTU8b which was distantly related to the acetogen *Holophaga foetida* was abundant in heavy fractions of the [^{13}C]cellulose treatment at 15°C but could not be detected at 5°C (Table 28). 16S rRNA sequences of OTU8b were closely related to an environmental clone sequence (AM409822; Table A2) that was retrieved from sediment samples of the Lake Kinneret, an ecosystem in which syntrophic acetate oxidation occurs [318]. Thus, acetogens related to *Holophaga* might be involved in syntrophic acetate oxidation in peatlands and lake sediments. Syntrophic acetate oxidation might be of ecological relevance in the Fen Schlöppnerbrunnen in the bulk peat soil, in which acetate concentrations can be high and H_2 partial pressures can be low as observed in unsupplemented controls at 5°C during (Figure 9; ΔGs for syntrophic acetate oxidation ranged between -15 to -23 kJ·mol^{-1}). Under such conditions, the combined activity of syntophic acetate oxidizing acetogens and hydrogenotrophic methanogens could prevent further accumulation of acetate and therefore acidification of the peat soil even when the activity of aceticlastic methanogens is low, which can be observed at low pH [209].

The findings in the experiments with soil-free root microcosms and root-containing soil microcosms suggested that within the Fen Schlöppnerbrunnen, acetogens may perform different tasks in the rhizosphere of sedges and in the bulk peat soil: higher H_2 partial pressures potentially stimulate hydrogenotrophic acetogenesis in the rhizosphere whereas temporarily accumulation of acetate in the H_2-limited bulk peat soil might initiate syntrophic acetate oxidation catalyzed by acetogens.

4.1.4. Competiton for methanogenic substrates: methanogens feed on the tip of the iceberg in the Fen Schlöppnerbrunnen

The CO_2:CH_4 ratio is close to 1 in methanogenic ecosystems in which the endogenous organic matter that is mineralized is dominated by plant derived carbohydrates (i.e., the average oxidation state of carbon is 0) and CO_2 is the single dominant electron acceptor that is available [499]. In contrast, CO_2:CH_4 ratios of >1 indicate that alternative respiratory processes are ongoing parallel to methanogenesis [280]. Equimolar production of CO_2 and CH_4 was observed in unsupplemented microcosms of fresh peat soil from a bog site close to the Fen Schlöppnerbrunnen, indicating that methanogensis was the single most important terminal process in this peatland [168]. However, the Fen Schlöppnerbrunnen constantly receives low amounts of alternative electron acceptors from the moving groundwater [5, 219, 326]. In addition to methanogenesis, denitrification, Fe^{3+} reduction and sulfate reduction are

important anaerobic respiratory processes that contribute to the mineralization of organic matter at this fen site [148, 205, 321, 327, 350]. Denitrifiers, Fe^{3+} reducer and sulfate reducer can outcompete methanogens for low concentrations of methanogenic substrates [69, 475]. This was observed in unsupplemented root-free soil microcosms at 15°C, in which only traces of CH_4 were formed and the average $CO_2:CH_4$ ratio after 21 d was 29 (Figure 15). The high $CO_2:CH_4$ ratio confirmed that methanogensis is only one of several respiratory processes that are ongoing in this fen. The average $CO_2:CH_4$ ratio during the initial 20 d preincubation of unsupplemented root-containing soil microcosms at 15°C was 9 (Figure 23) and therefore lower than that in root-free soil microcosms under otherwise similar conditions. The increased importance of methanogenesis in the presence of root biomass suggested that in peatlands methanogens profit from a higher input/availability of degradable carbon sources if they have to compete with other anaerobic respiratory microbes. This is consistent with the finding that $CO_2:CH_4$ ratios were higher in unsupplemented peat soil microcosms of a fen site that was dominated by *Sphagnum* mosses (i.e., low availability of degradable carbon sources) compared to a fen site that was dominated by sedges (i.e., high availability of degradable carbon sources) [493].

Average $CO_2:CH_4$ ratios after the preincubation (days 28-196 at 15°C and days 38-218 at 5°C) were 2.0 and 2.4 in unsupplemented peat soil microcosms at 15°C and 5°C in which CO_2 and CH_4 were the sole detected accumulating endproducts of the mineralization of endogenous carbon sources (Figure 25 and Figure 26). This translates to a fraction of 68% and 60% of the total reductant recovered in CH_4, leaving the remaining fraction of reductant for respiratory processes other than methanogenesis. The $CO_2:CH_4$ ratios as well as the production rates of both gases were relatively stable and only slightly fluctuated over time, indicating that (i) endogenous electron acceptors and donors were available even after 200 days of anoxic incubation, and (ii) methanogenesis was the dominant respiratory process and was ongoing parallel to other respiratory processes. Continuous availability of alternative electron acceptors and co-occurrence of methanogenesis with other respiratory processes has been observed during 240 d of anoxic incubation in a mesocosm experiment with peat soil from the Fen Schlöppnerbrunnen [205]. Sulfate, which is assumed to be recycled rapidly even under anoxic conditions [328], Fe^{3+}, which is present in the form of complex iron oxides in high amounts [219], and humic substances, which make up a huge fraction of the organic matter in peat [441], are the most likely alternative electron acceptors in the fen [205].

Remarkably, reductant derived from supplemental ethanol, butyrate, and propionate was almost completely recovered in CH_4 in microcosms at 15°C and 5°C (Table 27), and therefore a higher availability of carbon and reductant did not stimulate the use of alternative electron acceptors. This and the finding that the $CO_2:CH_4$ ratio did not change much during the prolonged anoxic incubation suggested that anaerobic respiratory microbes can successfully

compete with methanogens for low amounts of electron donors even during prolonged phases of anoxia; but in terms of relative contribution to the total mineralization process, methanogens become more important when the availability of degradable organic carbon sources is higher. The relatively low rate of anaerobic respiration despite an overall high capacitiy to take up electrons is probably caused by a limited rate of sulfate recycling and/or electron transfer to complexed iron oxides and humic substances but not by a low activity of sulfate and Fe^{3+} reducers. This assumption is supported by the finding that CH_4 production was lower in Fe^{3+}- or sulfate-supplemented microcosms compared to unsupplemented controls [257, 350].

The contribution of alternative respiratory processes is likely higher in situ compared to the conducted long-term anoxic microcosms experiments, because O_2 can diffuse from the peat surface and from roots of sedges [38, 475] and can be used by Fe^{2+} and sulfur oxidizers that can speed up the recycling of alternative electron acceptors [117, 328]. In this regard, genera of sulfate reducers (*Desulfomonile*, *Desulfovibrio*, and *Desulfosporosinus*), Fe^{3+} reducers (*Geobacter*, *Geothrix*, *Fervidicella* and *Aciditerrimonas*), and oxidizers of Fe^{2+} and sulfur compounds (*Thiobacillus*, *Sulfuricella*, and *Thiothrix*) were detected in fresh peat, root-containing peat soil microcosms, fresh roots and soil-free root microcosms (Table A2, Table A3, Figure 20, and Figure 22), underscoring the presence of microbes that are involved in iron and sulfur cycling in the Fen [219, 257, 327, 328, 382].

Alternative electron acceptors can be a sink for considerable amounts of reductant in peat of the Fen Schlöppnerbrunnen [205], and methanogens can get outcompeted when the availability of electron donors is low (e.g., in unsupplemented root-free soil microcosms). However, the availability of carbon and reductant derived from root exudates, root and plant biomass likely exceeds the availability of alternative electron acceptors especially at stable anoxic conditions in this fen site that is dominated by sedges. Under such conditions, methanogens will be active parallel to sulfate and Fe^{3+} reducers and collectively prevent an accumulation of fermentation products that has been observed in other peatlands [105].

4.1.5. Trophic links between H_2 metabolizers in the complex anaerobic food web of the Fen Schlöppnerbrunnen

A model of the interwoven anaerobic food web that eventually leads to the complete mineralization of dead plant organic matter in the Fen Schlöppnerbrunnen was constructed (Figure 49). This model is based in part on previous models [100, 384, 487] and includes further functional groups and associated taxa that were heretofore not recognized but were found to be important in the conducted experiments.

Dead plant organic matter is supposed to be the primary carbon source in peatlands. In fens that are overgrown with sedges, the plant biomass is rich in readily degradable

biopolymers like cellulose, hemicellulose, and pectin [313]. These biopolymers have to be hydrolyzed to soluble sugar monomers and oligomers. [^{13}C]cellulose-based 16S rRNA SIP indicated that known cellulolytic taxa (*Ruminococcaceae*, *Telmatobaceter*, and *Prolixibacteraceae*) and potentially also novel unclassified *Bacteria* are involved in cellulose-hydrolysis. Known hemicellulose and pectin degrading taxa belong to the *Clostridiaceae* and *Lachnospiraceae* [344, 478], taxa that were found to be abundant in the conducted experiments. H_2, CO_2, ethanol and organic acids are important fermentation products in this peatland [151, 487], but did not accumulate to a similar extent in the different microcosms studies. Formate, which may also be released by roots of sedges, is probably split by FHL taxa (e.g., *Neisseriaceae* and *Rhodocyclaceae*) to H_2 and CO_2. This reaction may deliver some extra energy during the fermentative metabolism.

Propionate and acetate accumulated regularly whereas butyrate and ethanol were scavenged more efficiently. In the case of acetate, accumulation might simply reflect that acetate production (e.g., by primary and secondary fermenters, and acetogens) exceeded the uptake capacity of aceticlastic methanogens (e.g., *Methanosaeta* and *Methanosarcina*). Accumulation of propionate was thermodynamically coupled to high acetate concentrations and not the result of a low propionate-oxidizing activity. Butyrate and ethanol oxidation were less sensitive to elevated acetate concentrations, explaining why these compounds did not accumulate in most experiments. When in situ concentrations of acetate exceed a certain level syntrophic acetate oxidation becomes thermodynamically feasible and this process might be catalyzed by the uncultured *Holophagaceae* that were abundant in the cellulose treatments at 15°C.

H_2 and formate never accumulated in the conducted experiments indicating that the microbial community was poised to quickly consume these compounds. While methanogens are known to be an important sink for formate and H_2 in peatlands, acetogens might have been also active in the consumption of these intermediates. However, the identity and the in situ relevance of acetogens still needs further evaluation. Fe^{3+}- and sulfate reduction were not in the focus of the conducted experiments but these processes likely contributed to the overall mineralization even at the end of the prolonged anoxic incubations. In situ, Fe^{3+} and sulfate are constantly recycled especially close to sedge roots that can leak O_2. Thus, alternative anaerobic respiratory processes are probably very important in the investigated fen.

The presented model is not intended to be a complete representation of all the taxa that are active in the fen. It merely focuses on the observed processes and detected taxa in the conducted experiments. However, it can be used as a basis to investigate potential activities and identify associated taxa in future studies.
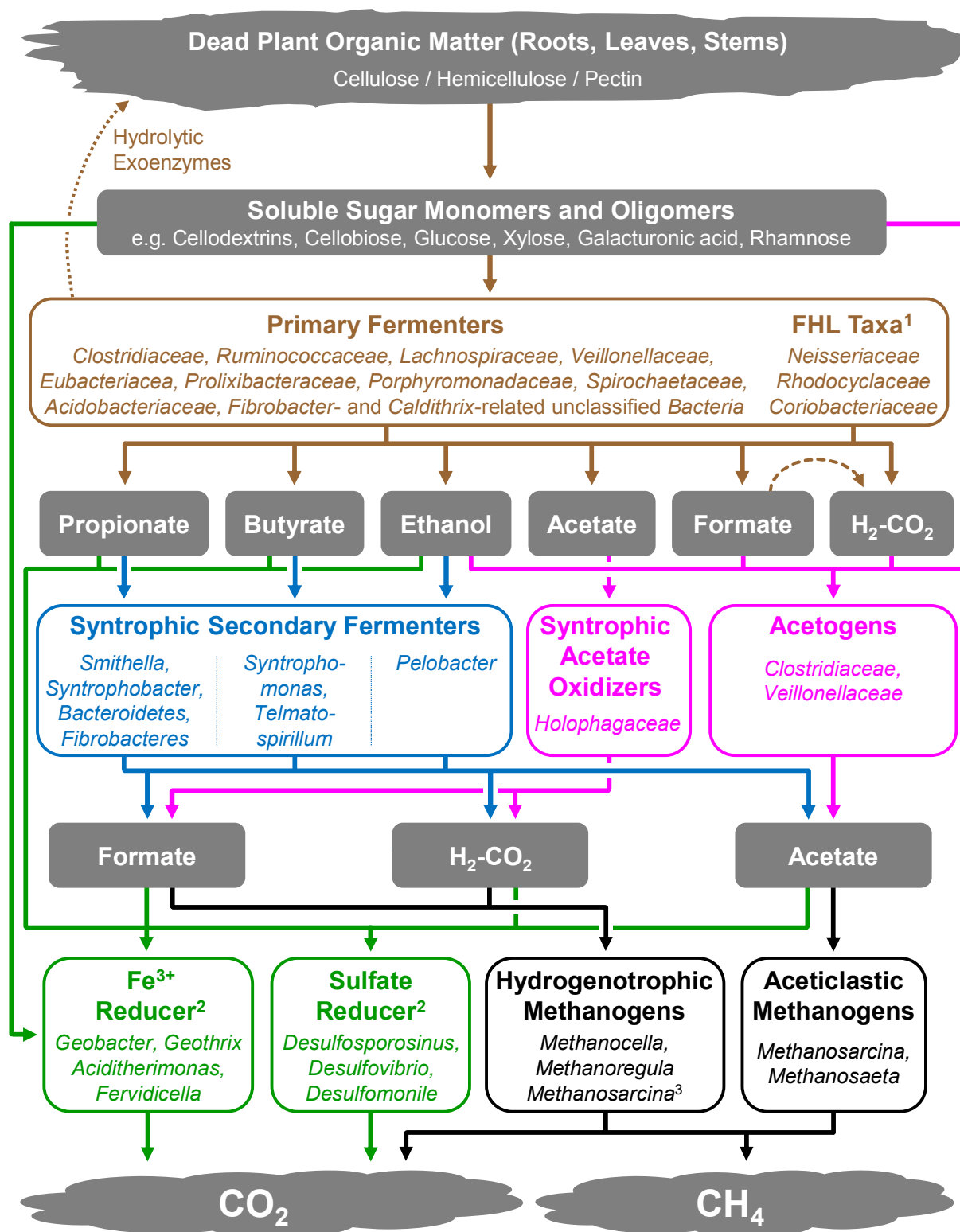
Figure 49   Model of the intermediary ecosystem metabolism in the investigated fen.

Numbers: 1, FHL-containing taxa are likely facultative aerobes that cometabolize formate (dashed arrow) together with a fermentable substrate; 2, Fe^{2+} and sulfide are the reduced endproducts of Fe^{3+} and sulfate reducers, respectively; 3, *Methanosarcina* will be a sink for H_2 only at elevate H_2 partial pressures and *Methanosarcina* is unable to grow on formate. Denitirification and aerobic procceses were not included in the model because these processes were probably of minor importance in the conducted experiments on which the model is based on.

4.2. Hydrogen metabolizers active in the gut of the earthworm *Lumbricus terrestris*

In contrast to peatlands in which H_2 is rapidly turned over and usually does not accumulate on the ecosystem level, high H_2 concentrations can be measured in the gut of the anecic earthworm *L. terrestris* [488]. Furthermore, living individuals of *L. terrestris* can emit H_2 and therefore constitute a mobile source of reductant for H_2-oxidizing microbes in aerated soils [488]. Fermenters that may feed on mucus-derived sugars or organic compounds derived from ingested and disrupted microbial cells are potential H_2 producers but their identities and the hydrogenases they use for H_2 production are not well resolved in the gut of earthworms [490]. Thus, the hydrogenase gene transcript diversity was evaluated in glucose-supplemented gut content microcosms and the microbial community in microcosms supplemented with disrupted microbial cells was analyzed to identify key taxa that are involved in H_2 production in the gut of *L. terrestris*.

4.2.1. H₂-producing glucose fermenters in the gut of *L. terrestris*

16S rRNA based stable isotope probing (16S rRNA SIP) identified members of anaerobic *Clostridiaceae* (known to produce H_2 via [FeFe]-hydrogenases during butyrate fermentation) and facultatively aerobic *Enterobacteriaceae* (known to produce H_2 via group 4 [NiFe]-hydrogenases during mixed acid fermentation [310, 398, 460]), as active, major glucose-fermenting taxa in anoxic gut content microcosms [490]. Abundant sequences that were affiliated with other obligate fermenters (*Peptostreptococcaceae*) and facultative aerobes (*Aeromonadaceae*) were also obtained in the aforementioned study but were not identified as active glucose-utilizing taxa [490]. In this regard, nearly half the CO_2 produced in glucose-supplemented microcosms was attributed to endogenous carbon sources, suggesting that taxa not directly involved in glucose utilization were nonetheless active [490]. One objective of the current study was to identify taxa associated with the production of H_2 in that earlier investigation.

74% of the sequences obtained for group 4 [NiFe]-hydrogenases (amplified with *Gammaproteobacteria*-specific primers NiFegF/R; Table 16) were related to HycE of *E. coli* (Figure 39 and Table 26). The HycE-affiliated amino acid sequences had high identity values (94 to 98%) to those of several species of the genus *Enterobacter* (Table 26). This result and those obtained previously by 16S rRNA SIP [490] reinforces the likelihood that *Enterobacter* and other genera within the *Enterobacteriaceae* can contribute to the production of H_2 in the gut of earthworms. 5% of the sequences that were obtained from transcripts of gammaproteobacterial group 4 [NiFe]-hydrogenases were related to HyfG of *E. coli* (Figure 39

and Table 26). The *hyf* operon, including *hyfG*, has been shown to be silent under several physiological conditions and definitive evidence for HYD4 (the *E. coli* hydrogenase that contains HyfG)-mediated H_2 production has not been obtained [401]. Thus, the presence of a transcript related to *hyfG* in gut content is of special interest, although the function of such a hydrogenase remains unclear.

Aeromonadaceae is another family of facultative aerobes capable of forming H_2 during mixed acid fermentation [421]. Members of the genus *Aeromonas* occur in the earthworm gut [203] and were enriched but not identified as active glucose consumers in the [^{13}C]-glucose 16S rRNA SIP study [490]. In the current study, 21% of the [NiFe]-hydrogenase-affiliated sequences were related to *Aeromonas* sp. (Figure 39 and Table 26). These findings indicate that *Aeromonas* sp. can contribute to the fermentative production of H_2 in the gut of earthworms but they may be less competitive for glucose than other taxa.

Group 4 [NiFe]-hydrogenases are not restricted to the formate hydrogenlyase complex of facultative aerobes within the *Gammaproteobacteria* [158, 460, 461]. In this regard, gene sequence that were amplified with primers NiFe-uniF(b)/R (Table 16) affiliated with group 4 [NiFe]-hydrogenase genes of *Opitutus terrae* (73-78% amino acid identitiy), *Clostridium thermocellum* (70%) and *Caldicellulosiruptor saccharolyticus* (65%). These organisms belong to *Verrucomicrobia* as well as *Ruminococcaceae* and *Thermoanaerobacterales* within the *Firmicutes* and are known to produce H_2 during the fermentation of polymeric substrates [52, 312, 453]. Members of these taxa were not identified as active glucose fermenters in the gut content microcosms [490] but may contribute to fermentative H_2 production via the degradation of mucus-derived substrates in the gut of earthworms. Unfortunately, detection of transcripts indicative of group 4 [NiFe]-hydrogenases failed with primers NiFe-uniF(b)/R.

177 out of 178 [FeFe]-hydrogenase-affiliated sequences amplified from RNA samples of the gut content microcosms clustered with hydrogenase-affiliated sequences of the *Clostridiales* families *Clostridiaceae*, *Lachnospiraceae*, *Peptostreptococcaceae* and *Ruminococcaceae* (Figure 38). Based on 16S rRNA SIP analyses, members of the *Clostridiaceae* were major active glucose fermenters, *Peptostreptococcaceae* were highly abundant but not active in the consumption (i.e., assimilation) of glucose, *Lachnospiraceae* were less abundant, and *Ruminococcaceae* were not detected [490]. BLAST identities of *Clostridiales*-related [FeFe]-hydrogenase-affiliated sequences were considerably lower than were the blast identities of *Gammaproteobacteria*-related group 4 [NiFe]-hydrogenase-affiliated sequences (Table 25 and Table 26). Furthermore, [FeFe]-hydrogenases of *Clostridia* do not cluster according to their family affiliation as do group 4 [NiFe]-hydrogenases of *Gammaproteobacteria* [388]. Thus, the amplified [FeFe]-hydrogenase-affiliated sequences cannot be affiliated unambiguously at the family level. However, based on the 16S rRNA SIP analyses [490], it is likely that most of these hydrogenases belong to organisms of either the

Clostridiaceae or the *Peptostreptococcaceae* and only to a lesser extent the *Lachnospiraceae* and the *Ruminococcaceae*. The diversity of [FeFe]-hydrogenases affiliated to the *Clostridia* was higher than the diversity of group 4 [NiFe]-hydrogenases affiliated to the *Gammaproteobacteria* (Figure 38 and Figure 39). However, a high [FeFe]-hydrogenase diversity is not necessarily correlated to a high diversity of organisms that contain those hydrogenases, since multiple hydrogenases can occur in a single organism (Table A1). Thus, the actual number of different [FeFe]-hydrogenase-containing families in the gut content microcosms might be lower than 13 (the number of OTUs found at 80% threshold similarity).

Both the group 4 [NiFe]-hydrogenase data obtained in this study and the 16S rRNA SIP data obtained before [490] suggested that *Enterobacteriaceae* and *Aeromonadaceae* were the most abundant families of facultative aerobes in the anoxic gut content microcosms. The [FeFe]-hydrogenase-affiliated sequences had lower identity scores to known hydrogenases compared to amplified group 4 [NiFe]-hydrogenase-affiliated sequences, indicating a higher degree of novelty for the [FeFe]-hydrogenases. However, this higher novelty makes determining the affiliation of [FeFe]-hydrogenase-affiliated sequences at the family level less reliable. Nonetheless, [FeFe]-hydrogenase-affiliated sequences clustered in close proximity to hydrogenases of families that were detected with the 16S rRNA SIP analyses (namely *Clostridiaceae*, *Lachnospiraceae* and *Peptostreptococcaceae*) and were affiliated to the order *Clostridiales*.

In summary, group 4 [NiFe]-hydrogenases of facultatively aerobic *Enterobacteriaceae* and *Aeromonadaceae*, members of which are capable of mixed acid fermentation [310], as well as [FeFe]-hydrogenases of anaerobic *Clostridiales*, members of which are capable of butyrate fermentation [39], were detected on the transcript level in anoxic glucose-supplemented gut content microcosms of the earthworm *L. terrestris*. The taxa resolved by the analyses of hydrogenase gene transcripts in the current study were in good accordance with the taxa that were resolved by the analyses of 16S rRNA in the preceding study [490]. Furthermore, the in situ profiles of fermentation products (e.g., fatty acids and H_2) along the alimentary canal of *L. terresris* are indicative of ongoing H_2-producing mixed acid and butyrate fermentations [488]. These collective observations support the assumption that *Enterobacteriaceae* and *Clostridiaceae* are important drivers of H_2 production in the alimentary canal. However, the detection of highly novel hydrogenases that could not be unambiguously phylogenetically assigned suggests that additional taxa may also contribute to fermentative H_2 production in the alimentary canal. These conclusions must be placed in perspective of the experimental conditions employed. The sequence data were derived from anoxic gut content microcosms that simulated many but not all of the in situ conditions in the gut to which ingested soil bacteria are exposed [490] and likewise are from an experiment with only one earthworm species. It is therefore important that future studies determine if the H_2-producing fermentative processes

and taxa resolved in *L. terrestris* are representative of those in different earthworm species and feeding guilds.

4.2.2.   Grinding in the gizzard: how earthworms feed their feeders

It is conceptionalized that a fraction of the ingested microbial cells (especially larger cells like fungal hyphae) are disrupted by the grinding activity in the gizzard [35, 391, 484]. Such a disruption would result in the release of disrupted cell-derived biopolymers (proteins, nucleic acids, lipids, and cellwall carbohydrates like chitin) and their breakdown products (amino acids, nucleotides, glycerol, fatty acids, and sugars) [230]. The earthworm may absorb a fraction of the disrupted cell-derived organics as part of its nutrition [35]. Ingested soil anaerobes that are activiated by the beneficial conditions in the gut (e.g., anoxia, a high water content, mucus-derived sugars and glycoproteins) may also feed on organic compounds derived from disrupted cells. However, such taxa that potentially contribute to the degradation of microbial cells, which were disrupted by the grinding activity of the gizzard, are not resolved. A lysate derived from french pressed yeast cells was supplemented to gut content microcosms to stimulate taxa that in situ may thrive on disrupted cells.

16S rRNA transcript-based analyses of the microbial community indicated that *Clostridium bifermentans* (*Peptostreptococcaceae*) and *Aeromonas* sp. (*Aeromonadaceae*) were the dominant taxa that initially responded on the supplemented cell lysate (Figure 42 and Figure 43). Both taxa are able to ferment proteinaceous substrates and carbohydrates, and *Aeromonas* sp. can hydrolyze DNA and lipids [46, 276], making them excellent utilizer of various organics derived from disrupted cells. Acetate, succinate, formate, H_2 and CO_2 were the major fermentation products that accumulated during the first 6 h of incubation, and these compounds are among the fermentation products that are characteristic for *C. bifermentans* and *Aeromonas* sp. [421, 478]. *C. bifermentans*-related taxa were also abundant but not labled in [^{13}C]glucose-supplemented gut content microcosms of *L. terrestris*, indicating that these taxa did not assimilate supplemental glucose and may have metabolized endogenous carbon compounds in these experiments [490]. This assumption is reinforced by the high abundance of *C. bifermentans* in unsupplemented controls in the present experiments (Figure 42). Thus, disrupted cell-derived organic compounds represent only one of several substrates on which *C. bifermentans* can feed in the gut of earthworm*s.*

With time, the generalistic fermenters *C. bifermentans* and *Aeromonas* sp. that rapidly responded to the supplemented cell lysate were more and more replaced by saccharolytic *Enterobacteriaceae* [33], proteolytic *Clostridiaceae* [34, 285, 363], and physiologically uncharacterized *Lachnospiraceae* (Figure 42). The *Enterobacteriaceae* taxa that were stimulated by cell lysates (Figure 43) were highly similar to those observed in gut content

microcosms supplemented with glucose (a constituent of the mucus of *L. terrestris*) [488, 490]. Thus members of the *Enterobacteriaceae* may profit from the release of sugars derived from disrupted cells (e.g., ribose and deoxyribose from RNA and DNA) or the mucus in the gut of earthworms. In contrast to the *Enterobacteriaceae* sp. that were similar in glucose and cell lysate supplemented microcosms, the proteolytic *Clostridiaceae* observed in the treatments with cell lysate were phylogenetically distinct from those that utilized glucose in the aforementioned study [490]. Therefore, physiologically and phylogenetically distinct fermenters of the *Clostridiaceae* are active in the degradation of carbohydrates and proteins in the gut of earthworms. OTU_Y6 was the only abundant OTU that was stimulated by supplemental cell lysate but was not closely related to any cultured species (Figure 43). This OTU could be affiliated to the *Lachnospiraceae*, a family that comprises cellulolytic, pectinolytic, xylanolytic, and other saccharolytic fermenters as well as acetogens, and syntrophic species [344]. No proteolytic species are known and therefore OTU_Y6 may have been stimulated by carbohydrates and not by cell lysate-derived proteins. However, this needs to be verified.

Based on the earlier findings that formate and H_2 were produced but not consumed in long term incubated gut section homogenates supplemented with glucose [192] and that acetogens were not detected in glucose-supplemented gut content microcosms [490], it was assumed that acetogenesis is not an important process in the gut of earthworms. However, formate consumption started after 6 h in cell lysate treatments and in parallel the production of acetate and CO_2 increased (Figure 40), both observations being indicative for formate-dependent acetogenesis. Furthermore, taxa closely related to *C. glycolicum* (*Peptostreptococcaceae*) and *C. magnum* (*Clostridiaceae*), two species that comprise formate utilizing acetogenic strains [28, 175, 222], increasesd in 16S rRNA transcript abundances (Figure 43). After 20 h, H_2 and CO_2 accumulation slowed down whereas acetate still accumulated at high rates in cell lysate treatments, suggesting that acetogens may have utilized H_2-CO_2 in addition to formate (Figure 40). Ethanol and lactate are also potential substrates for acetogens (Table 4) and accumulated in glucose-supplemented microcosms [490]. Both compounds did not accumulate in cell lysate treatments and therefore may have been scavenged by acetognes. Some strains of *C. glycolicum* can decarboxylate succinate to propionate [45], an activity that was potentially a source for the propionate formed in cell lysate treatments. *C. glycolicum* and *C. magnum* can convert various sugars [28, 175, 222] and might compete with saccharolytic fermenters for the same substrates.

A hypothetical model showing the proposed trophic interactions between the earthworm and the ingested soil microbes is given in Figure 50. The earthworm takes up microbial cells attached to plant litter and soil. Larger cells like that from fungal hyphae, protists, and also vegetative bacterial cells are partially disrupted probably by the grinding activity in the gizzard

[110, 391]. The organic compounds that are released during cell disruption are potent substrates for ingested soil anaerobes. The initial stimulation of fermenters with a broad susbtrate range (*C. bifermentans* and *Aeromonas* sp.) and the subsequent replacement of these taxa by more specialiced fermenters (e.g., proteolytic *Clostridiaceae* and saccharolytic *Enterobacteriaceae*) indicated, that different functional clades of fermenters are active during gut passage from the foregut to the hindgut. These fermenters produce organic acids that can be absorbed by the earthworm as part of its nutrition, although this has not been tested yet. However, the concentrations of organic acids decreased from the midgut to the hindgut in living earthworms [488] and the capacity to absorp these compounds in the digestive tract is a general trait of animals [21, 106, 164, 347, 439]. Thus, it is very likely that earthworms indeed absorbs organic acids derived from fermentation processes in the gut. Acetogens can also contribute to the formation of organic acids and therefore may also play a role in the nutrition of earthworms. In summary, earthworms feed ingested soil anaerobes (i.e., fermenters and acetogens) with disrupted microbial cells, and the anaerobes in turn produce organic acids (acetate, succinate, and propionate) on which the earthworm can feed (*Hypothesis 4*, 1.5).
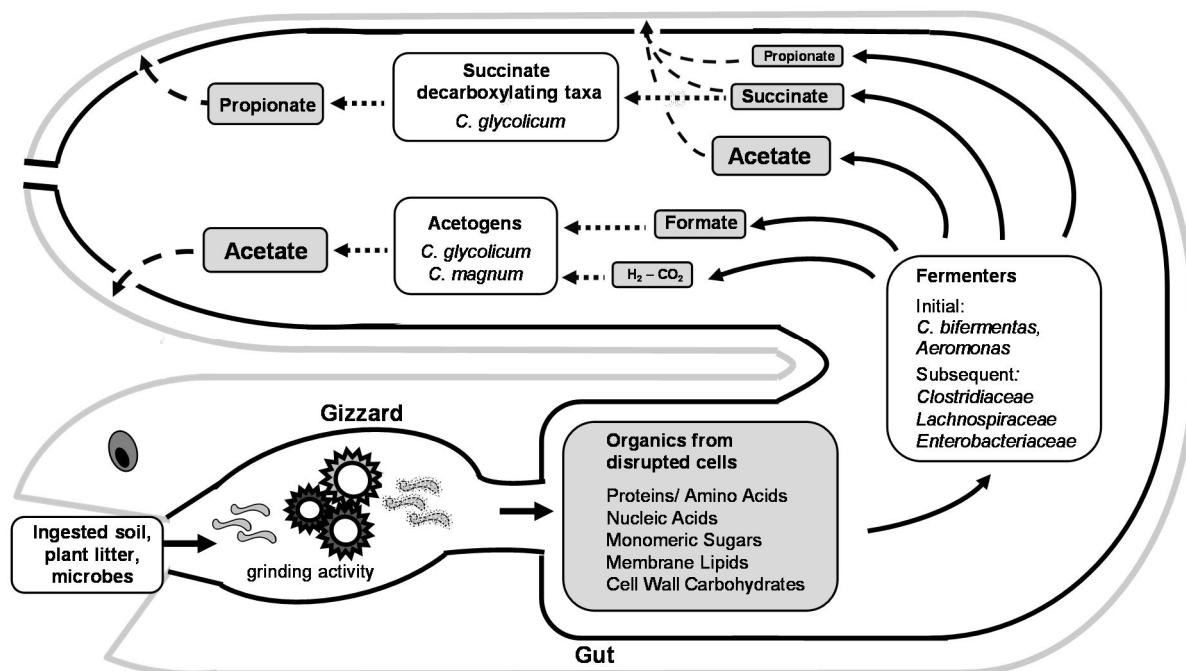
Figure 50 Hypothetical model of anaerobic processes and associated taxa that are stimulated by disrupted microbial cells in the gut of the earthworm *L. terrestris*.

Dashed lines, proposed absorption of organic acids by the earthworm; dotted lines, potential anaerobic processes that might occur in addition to fermentation.

4.3. Peatlands and earthworm guts: anoxic ecosystems with contrasting conditions for H$_2$ metabolizers

Regarding the H$_2$ metabolism, the most striking difference in peatlands and the gut of earthworms is that on the level of the ecosystem H$_2$ is effectively scavenged in the former whereas it accumulates in and is emitted from the latter. In this regard, in situ concentrations of dissolved H$_2$ approximated 0.02-0.1 µM in a peatland soil and 5-6 µM in the gut of the earthworm *Lumbricus terrestris* [18, 488]. The contrasting H$_2$ concentrations observed in both ecosystems result most probably (i) from the thermodynamic constraints that H$_2$ metabolizing microbes have to face and (ii) the stability of anoxic conditions.

The gut of earthworms is characterized by a high availability of sugars and amino acids, which are potentially derived from the mucus, disrupted microbial cells, and plant litter. However, gut passage and therefore the time during which ingested soil microbes experience anoxic conditions is rather short (< 1 d [111, 153, 490]). Thus, fermenters that can quickly adapt to changing redox conditions (e.g., facultative aerobes like *Aeromonadaceae* [421] and *Enterobacteriaceae* [33]) and those that have the potential to fastly turnover a variety of substrates (e.g., *Clostridiaceae* [478] and *Peptostreptococcaceae* [119]) have a strategic adavantage over fermenters that are specialized on stable anoxic and oligotrophic conditions. Primary fermenters, which reduce electron acceptors with low redox potentials during their metabolism (e.g., reduced ferredoxin generated during pyruvate decarboxylation), can produce H$_2$ even in the presence of high H$_2$ concentrations (i.e., those found in the gut of earthworms) [301]. In contrast, syntrophic fermenters are thermodynamically restricted to low H$_2$ concentrations [376] and can therefore not contribute to H$_2$ production in the gut of earthworms. This was supported by the finding that syntrophic taxa were not detected in earthworm gut content microcosms before and after the incubation. Because of the absence of syntrophs, which remove fermentation-derived organic acids (e.g., propionate) in other anaerobic ecosystems (e.g., peatlands), these compounds can accumulate to high concentrations in the gut of earthworms [488]. At the pH neutral conditions that are maintained by the earthworm by excreting calcium carbonate [32, 109], the accumulation of organic acids has no inhibitory effect on the ingested microbes. H$_2$ consuming processes seem to be of minor importance at least in the gut of the used model organism *L. terrestris*. This is another reason why H$_2$ can accumulate to higher concentrations compared to peatlands. The number of methanogens in oxic soils in which these earthworms live is probably too low and the gut transient time is too short to activate an efficiently large number of this functional group. However, methane emissions were observed from other earthworm species indicating that methanogenesis is a potential sink for H$_2$ in some but not all earthworms [89, 395]. Acetogens are a potential sink for H$_2$ and they were active in gut content microcosms supplemented with

disrupted cells and also in unsupplemented controls. However, they generally have a broad substrate spectrum and are certainly not restricted to the use of H_2 in the gut [98]. In this regard, formate dependent acetogenesis was probably an important process in treatments with disrupted cells whereas indications for hydrogenotrophic acetogenesis were weak. In conclusion, H_2 production is thermodynamically limited to primary fermenters and H_2 consuming process are of minor importance in the gut of earthworms. Thus, this ecosystem is poised to accumulate H_2, which eventually diffuses through the worm tissues and is emitted to the surrounding oxic environment, in which aerobic H_2-oxidizing microbes can take it up as a source of energy and reductant.

In Peatlands, the situation for H_2 metabolizers is fundamentally different from that in the gut of earthworms. Basically, the anoxic conditions are rather stable and not restricted to a few hours of gut passage. Thus, complex microbial communities have time to develop and can form an interwoven foodweb. The members of this community have to be well adapted to a limited availability of readily degradable carbon and assimilable nitrogen sources, low pH, and low temperatures [313]. Under such conditions, slow growing oligotrophs that can sustain their energy metabolism even at ΔGs close to the thermodynamic limit are more competitive than fast growing copiophiles that are less efficient in the utilization of their substrates [240]. Primary fermenters are considered a main source of H_2 in peatlands [208], but some of them (especially propionate fermenters) might also be a H_2 sink (Figure 45). Consequently, the net release of H_2 from the primary fermentations might be substantially lower than what is actually formed. An additional and quantitatively highly relevant source of H_2 in peatlands are syntrophs that keep the concentration of primary fermentation products like ethanol, butyrate, and propionate at low non-inhibitory levels. However, the thermodynamic prerequisite for this activity is that H_2 and to a lesser extent acetate are effectively scavenged by methanogens (Figure 47 and Figure 48). Thermodynamic calculations indicated that syntrophs and methanogens might be juxtaposed to each other to optimize the interspecies transfer of H_2. Acetogens are conceptualized mainly as potential sinks for H_2 that compete with methanogens for the same substrate. However, when acetate transiently accumulates, some of them (e.g., *Holophagaceae*) might function as syntrophic acetate oxidizers and therefore as a source of H_2. Such an activity would prevent an accumulation of acetate in the ecosystem. Additional sinks for H_2 in peatlands are alternative respiratory processes like Fe^{3+} and sulfate reduction. Such processes are certainly more important in mesotrophic and eutrophic fens compared to oligotrophic bogs. To sum this up, the rate of H_2 production is determined by the limited availability of degradable carbon sources in peatlands; and because of the presence of various active H_2 consumers, which are not substrate saturated, H_2 will usually not accumulate in peatlands.

4.4. Addressing the hypotheses, limitations and future perspectives

Supplemental cellulose stimulated fermentative processes in peat soil microcosms of the Fen Schlöppnerbrunnen at low temperatures and low pH. This finding indicated that (i) the peat fermenters could readily metabolize cellulose at the harsh in situ-near conditions, and (ii) these fermenters were substrate limited in unsupplemented controls. Thus, the results supported *Hypothesis 1*. The molecular analysis was based on 16S rRNA SIP, and it identified novel bacterial taxa (e.g., *Fibrobacter*-related unclassified *Bacteria*) in addition to physiological characterized fermenters as abundant assimilators of [^{13}C]cellulose-derived carbon. However, whether such novel taxa represent cellulolytic or saccharolytic fermenters remains unclear. Thus, one of the future tasks will be to cultivate cellulolytic fermenters from the investigated fen. In this regard, the recent success in isolating a slow growing facultative aerobic cellulolytic member of the *Acidobacteria* (i.e., *Telmatobacter bradus*) from a similar habitat shows that those previously considered 'unculturable' organisms may not resist a live in the lab if the cultivation methods are appropriate [84, 324].

Peatlands are generally considered as anoxic environments with a low availability of substrates for peat-inhabiting anaerobes. However, fermentation activities were high in unsupplemented soil-free *Carex* root microcosms in which H_2 concentrations were considerably higher than those in root-free and root-containing microcosms. Thus, the rhizosphere of sedges is a hotspot for H_2 producing fermenters in peatlands. Among those H_2 producing fermenters are FHL-containing taxa that can convert formate, which can be released from roots, into H_2 and CO_2. This FHL activity was observed in formate-supplemented root microcosms and might be attributed to facultative aerobic *Betaproteobacteria*. The high H_2 concentrations that were observed in unsupplemented and formate supplemented root microcosms were beneficial for acetogens. In this regard, the high concentrations of acetate in the root microcosms and the detection of hydrogenase genes that were related to those of known acetogens indicated that acetogens are attached to *Carex* roots and likely contribute to the consumption of H_2 in the rhizosphere of sedges. Thus the collective data of the experiments with root microcosms reinforced the *Hypothesis 2*. Methanogens were of minor importance in the conducted experiments with soil-free root microcosms. This might have been caused by the experimental design (i.e., roots were washed with water to remove soil particles). The washing procedure likely removed microbes (methanogens among others) that are in situ present in the rhizosphere but are not tightly attached to the root surfaces. Preparing microcosms with unwashed roots might enhance the methanogenesis rate in similar experiments. In situ, H_2 formed in close proximity to the roots likely diffuses away from the

root surfaces and methanogens that are not proximal but very close to the root probably compete with acetogens and other H_2 oxidizers for H_2 formed in the rhizosphere.

Known syntrophs and novel taxa that heretofore were not recognized as syntrophs were active in peat soil microcosms in which supplemental ethanol, butyrate, and propionate were converted to CH_4 and CO_2. Thermodynamic calculations revealed that especially syntrophic propionate degraders thrived at the thermodynamic limit, and close interactions with methanogens were necessary to maintain exergonic conditions. These results were in support of *Hypothesis 3*. *Alphaproteobacteria*, *Bacteroidetes*, and *Fibrobacteres* were among the potentially novel syntrophic taxa that need to be isolated and physiologically characterized in the future. Other syntrophic processes (e.g., syntrophic degradation of aromatic compounds or acetate) and the associated taxa have rarely been studied in peatlands although these processes are potentially important for the anaerobic mineralization processes. In this regard, uncultured *Holophagaceae* were identified as potential syntrophic acetate oxidizers in cellulose treatments at 15°C, and 16S rRNA transcript sequences related to *Syntrophus* and *Syntrophorhabdus* (i.e., two genera that comprise aromatic compound oxidizing bacteria) were repeatedly detected in the conducted experiments. These processes should be looked at in the future to further resolve the interwoven food web in peatlands.

Acetate, succinate, and propionate rapidly accumulated in earthworm gut content microcosms supplemented with disrupted microbial cells. This underscores the hypothesis that the ingested soil anaerobes that feed on disrupted cells produce organic acids that can potentially be absorbed by the earthworm (*Hypothesis 4*). However, it could not be resolved which of the cell components were utilized by the stimulated taxa like *Peptostreptococcaceae*, *Aeromonadaceae*, and *Enterobacteriaceae*. Instead of cell lysates more defined substrates (e.g., proteins and nucleic acids) could be used in follow-up experiments to determine the substrate range of taxa that are involved in the degradation of microbial cells, which are disrupted by the grinding activity of the gizzard.

Newly designed hydrogenase gene-specific PCR-primers were designed and succesfully applied to identify H_2 metabolizers in both, peat soil and earthworm gut content microcosms, and the established 80% similarity cut-off was appropriate to cluster hydrogenase gene or transcript sequences that most probably belong to organisms of the same family. However, phylogenetic and functional affiliation of environmental hydrogenase sequences is challenging because of the low number of references sequences in the databases and the lack of functional characterized hydrogenases. Furthermore, not all H_2 metabolizers could be covered with the designed primers. In this regard, primers for the amplification of group 3 [NiFe]-hydrogenases are missing to date. This group of hydrogenases is especially important in methanogens and syntrophs and therefore, the design of appropriate PCR-primers specific for genes of such hydrogenases is of high priority.

5. SUMMARY

H_2 is a central intermediate of the complex anaerobic microbioal degradation of plant biomass and in situ concentrations of the gas are generally low because of its ongoing consumption. In contrast, high H_2 concentrations were determined in the gut of the earthworm *Lumbricus terrestris*. These observations raised the question why the anaerobic microbial community in peatlands is poised to effectively scavenge H_2 whereas H_2 production by ingested soil anaerobes exceeds H_2 consumption in the gut of *L. terrestris*. To address this question, H_2-producing and H_2-consuming processes were analyzed in peat soil slurries (soil microcosms) and diluted *L. terrestris* gut contents (gut content microcosms). In order to identify active H_2 metabolizing taxa, gene marker analyses were intended. Hydrogenases are the key enzymes of the H_2 metabolism and therefore represent suitable gene marker for H_2-metabolizing microorgansims. Thus, PCR-primers for the amplification of hydrogenase gene sequences from environmental samples were designed. Furthermore, a sequence similarity cut-off of 80% for the clustering of environmental hydrogenase gene sequences on the family level was established by comparative 16S rRNA-hydrogenase gene analyses.

Cellulose is a major constituent of sedges, which is the dominant vegetation and the major source of organic carbon in the investigated peatland. The polymer was readily degraded mainly to propionate, acetate, and CO_2, whereas an accumulation of H_2 was not observed in peat soil microcosms. Based on process data and thermodynamic calculations, methanogenesis and acetogenesis could be excluded as abundant sinks for cellulose-derived H_2. Propionate fermenters might have cometabolized H_2 and cellulose hydrolysis products. *Fibrobacter*-related unclassified *Bacteria*, *Prolixibacteraceae*, *Porphyromonandaceae*, *Clostridiaceae*, *Ruminococcaceae*, *Acidobacteriaceae*, *Holophagaceae*, and *Spirochaetaceae* were identified as active assimilators of cellulose-derived carbon by 16S rRNA SIP (stable isotope probing). However, the H_2 metabolism and the hydrolytic capabilities especially of the novel taxa remain unresolved. In contrast to the cellulose-supplemented soil microcosms, considerably higher concentrations of H_2 were observed in microcosms with washed roots of *Carex rostrata* (an abundant sedge in the investigated peatland). Hydrogenase gene analyses revealed that several families within the *Firmicutes* (e.g., *Clostridiaceae*, *Ruminococcaceae*, and *Lachnospiraceae*) dominated H_2 production in unsupplemented root microcosms. Formate, which can be excreted by roots, was converted into H_2 and CO_2 by formate hydrogenlyase-containing taxa (e.g., *Betaproteobacteria* and *Acidobacteria*). H_2, derived from the fermentation of endogenous sources or supplemented formate, was primarily consumed by acetogens (e.g., *Clostridiaceae* und *Veillonellaceae*). These finding reinforced the assumption that the rhizosphere of sedges is a hotspot for H_2-evolving fermenters and H_2-consuming acetogens. In addition to primary fermenters, secondary syntrophic fermenters (syntrophs) are considered as major H_2 producers in peatlands. 16S rRNA transcript analyses

identified (i) a novel strain of *Pelobacter propionicus* as syntrophic ethanol oxidizer, (ii) *Syntrophomonas* and *Telmatospirillum*-related taxa as syntrophic butyrate oxidizers, and (iii) *Syntrophobacter*, *Smithella*, unclassified *Bacteroidetes*, and unclassified *Fibrobacteres* as potential syntrophic propionate oxidizers in soil microcosms. CH_4 and CO_2 were the only accumulating endproducts of the propionate, butyrate, and ethanol degradation, suggesting that H_2, formate, and acetate (the fermentation products of the syntrophs) were effectively scavenged by methanogens. Aceticlastic methanogens (*Methanosarcina* and *Methanosaeta*) outnumbered hydrogenotrophic methanogens (*Methanoregula* and *Methanocella*). This might indicate that acetogens were active and competed with hydrogenotrophic methanogens for available H_2.

In a previous study, in which *L. terrestris* gut content microcosms were supplemented with glucose, *Clostridiaceae* and *Enterobacteriaceae* were identified as important primary fermenters and potential producers of H_2 whereas syntrophs, methanogens, and acetogens were not crucial for the H_2 turnover. Hydrogenase transcript analyses corroborated these findings. *Aeromonadaceae* and *Peptostreptococcaceae* were determined as abundant H_2-evolving taxa in addition to *Clostridiaceae* and *Enterobacteriaceae*. However, the former two families were not involved in the degradation of glucose and might have fermented endogenous carbon compounds. Proteins, nucleic acids, and carbohydrates derived from disrupted microbial cells represent potential endogenous substrates that are available in the earthworm gut. *Aeromonas* sp. and *Clostridium bifermentans* (phylogenetically belongs to the *Peptostreptococcaceae*) were indeed stimulated within a few hours after the supplementation of yeast cell lysates to gut content microcosms. Subsequently, proteolytic *Clostridiaceae*, saccharolytic *Enterobacteriaceae*, and unclassified *Lachnospiraceae* partially replaced the initially dominating fermenters. The acetogens *Clostridium glycolicum* and *Clostridium magnum* were also abundant. They probably utilized formate rather than H_2, underscoring the assumption that acetogens are not an important sink for H_2 in the gut of *L. terrestris*.

The collective data indicated that at the oligotrophic conditions prevailing in peatlands (i) H_2, is produced by primary and secondary fermenters and is effectively scavenged by methanogens, acetogens, and propionate fermenters, (ii) the rhizosphere of sedges is a hotspot for H_2 metabolizers, and (iii) novel microbial taxa are involved in the complex anaerobic degradation of plant biomass. In contrast to the oligotrophic peatland soils, huge amounts of readily degradable carbon sources are available for the anaerobic microorganisms in the gut of earthworms. Because of the short gut passage, the anaerobes do not form an interwoven foodweb and consequently, primary and secondary fermentation products are not completely scavenged. Thus, fermentation-derived organic acids can be absorbed by the earthworm whereas H_2 diffuses out of the worm and becomes available for H_2 oxidizers in the soil.

6. ZUSAMMENFASSUNG

In Mooren ist H_2 ein zentrales Intermediat des komplexen anaeroben Abbaus pflanzlicher Biomasse durch Mikroorganismen und aufgrund des stetigen Verbrauchs sind die in situ Konzentrationen dieses Gases für gewöhnlich niedrig. Im Gegensatz dazu wurden hohe H_2-Konzentrationen im Darm des Regenwurms *Lumbricus terrestris* festgestellt. Diese Beobachtungen führten zu der Frage, weshalb die anaeroben Mikroorganismen-gemeinschaften in Mooren H_2 effektiv verbrauchen, wohingegen die aus dem Boden stammenden Anaeroben im Darm von *L. terrestris* mehr H_2 produzieren als sie konsumieren. Um diese Frage beantworten zu können wurden in der vorliegenden Arbeit H_2-bildende und H_2-verbrauchende Prozesse in Moorbodenaufschlämmungen (Bodenmikrokosmen) und verdünntem *L. terrestris*-Darminhalt (Darminhaltmikrokosmen) untersucht. Aktive H_2-metaboilisierende Taxa sollten dabei mittels Genmarkeranalysen identifiziert werden. Hydrogenasen sind die Schlüsselenzyme im H_2-Stoffwechsel und eignen sich daher als Genmarker für H_2-metabolisierende Mikroorganismen. Aus diesem Grund wurden PCR-Primer entwickelt, die eine Amplifikation von Hydrogenasegensequenzen aus Umweltproben ermöglichen. Mittels vergleichender 16S rRNA-Hydrogenase-Genanalyse konnte ein Grenzwert von 80% Sequenzübereinstimmung ermittelt werden, auf dessen Basis sich Hydrogenasegensequenzen aus Umweltproben auf Familienebene zusammenfassen lassen.

Zellulose ist ein Hauptbestandteil von Seggen, der dominierenden Vegetation und somit der Hauptquelle für organischen Kohlenstoff in dem untersuchten Moor. Das Polymer wurde primär zu Propionat, Acetat und CO_2 abgebaut, wohingegen eine Akkumulation von H_2 nicht beobachtet wurde. Basierend auf Prozessdaten und thermodynamischen Kalkulationen konnten Methanogenese und Acetogenese als bedeutende Senken des aus dem Zellulose-abbau-resultierendem H_2 ausgeschlossen werden. Möglicherweise haben Propionat-Gärer H_2 und Zellulose-Hydrolyseprodukte gleichzeitig verstoffwechselt. *Fibrobacter*-verwandte unklassifizierte *Bacteria*, *Prolixibacteraceae*, *Porphyromonandaceae, Clostridiaceae*, *Rumino-coccaceae*, *Acidobacteriaceae*, *Holophagaceae* und *Spirochaetaceae* konnten durch 16S rRNA SIP (stabile Isotopenbeprobung) als aktive Assimilierer von aus der Zellulosehydrolyse stammendem Kohlenstoff identifiziert werden. Der genaue Gärungsstoffwechsel und die hydrolytischen Fähigkeiten insbesondere der neuartigen Taxa bleiben allerdings unbekannt. Im Gegensatz zu den Zellulose-supplementierten Bodenmikrokosmen wurden deutlich höhere H_2-Konzentrationen in Mikrokosmen mit gewaschenen Wurzeln von *Carex rostrata*, eine im untersuchten Moor häufig vorkommende Seggenart, beobachtet. Hydrogenase-Genanalyse offenbarte, dass verschiedene Familien innerhalb der *Firmicutes* (z.B. *Clostridiaceae*, *Ruminococcaceae* und *Lachnospiraceae*) die H_2-Produktion in unsupplementierten Wurzel-Mikrokosmen dominierten. Formiat, das von Wurzeln in den Boden abgegeben werden kann, wurde durch Formiat-Hydrogen-Lyase-besitzende Taxa (z.B. *Betaproteobacteria* und

Acidobacteria) in H_2 und CO_2 umgewandelt. H_2, aus dem Abbau endogener Quellen oder zugegebenem Formiat stammend, wurde hauptsächlich durch Acetogene (z.B. *Clostridiaceae* und *Veillonellaceae*) verbraucht. Diese Ergebnisse bekräftigten die Annahme, dass die Rhizosphäre von Seggen ein Hotspot für H_2-bildende Gärer und H_2-verbrauchende Acetogene ist. Neben primären Gärern werden auch sekundäre syntrophe Gärer (Syntrophe) als wichtige H_2-Produzenten in Mooren erachtet. Mittels 16S rRNA-Transkriptanalyse konnten (i) ein neuer Stamm von *Pelobacter propionicus* als syntropher Ethanoloxidierer, (ii) *Syntrophomonas* und *Telmatospirillum*-verwandte Taxa als syntrophe Butyratoxidierer und (iii) *Syntrophobacter*, *Smithella*, unklassifizierte *Bacteroidetes* und unklassifizierte *Fibrobacteres* als potenzielle syntrophe Propionatoxidierer in Bodenmikrokosmen identifiziert werden. CH_4 und CO_2 waren die einzigen akkumulierenden Endprodukte des Propionat-, Butyrat- und Ethanolabbaus, was darauf hindeutet, dass H_2, Formiat und Acetat (die Gärungsprodukte der Syntrophen) effektiv von Methanogenen beseitigt wurden. Die acetiklastischen Methanogenen (*Methanosarcina* and *Methanosaeta*) waren zahlenmäßig stärker vertreten als die hydrogenotrophen Methanogenen (*Methanoregula* and *Methanocella*). Dies könnte ein Hinweis darauf sein, dass Acetogene aktiv waren und mit hydrogenotorphen Methanogenen um verfügbaren H_2 konkurrierten.

In einer früheren Studie mit Glucose-supplementierten *L. terrestris*-Darminhalt-mikrokosmen konnten *Clostridiaceae* und *Enterobacteriaceae* als wichtige primäre Gärer und potenzielle H_2-Produzenten identifiziert werden, wohingegen Syntrophe, Methanogene und Acetogene nicht entscheidend für den H_2-Umsatz waren. Eine Hydrogenase-Transkriptanalyse bestätigte diese Ergebnisse. Neben den *Clostridiaceae* und *Enterobacteriaceae* wurden auch *Aeromonadaceae* und *Peptostreptococcaceae* als abundante H_2-bildende Taxa ermittelt, obgleich diese nicht am Glucoseabbau beteiligt waren und folglich endogene Kohlenstoffverbindungen vergärten. Als mögliche endogene Substrate, die im Regenwurmdarm verfügbar sind, kommen Proteine, Nukleinsäuren und Kohlenhydrate von lysierten mikrobiellen Zellen in Frage. Tatsächlich konnten *Aeromonas* sp. und *Clostridium bifermentans*, letzterer gehört phylogenetisch zu den *Peptostreptococcaceae*, binnen weniger Stunden durch die Zugabe eines Hefezelllysates in Darminhaltmikrokosmen stimuliert werden. Im weiteren Verlauf des Experiments verdrängten proteolytische *Clostridiaceae*, saccharolytische *Enterobacteriaceae* und unklassifizierte *Lachnospiraceae* zum Teil die eingangs dominierenden Gärer. Die Acetogenen *Clostridium glycolicum* und *Clostridium magnum* waren ebenfalls abundant und konsumierten wahrscheinlich hauptsächlich Formiat und weniger H_2. Dieses Ergebnis bestätigte die Annahme, dass Acetogene keine wichtige Senke für H_2 im Darm von *L. terrestris* darstellen.

Die gesammelten Daten zeigen, dass unter den oligotrophen Bedingungen, die in Moorböden vorherrschen, (i) H_2 von primären und sekundären Gärern gebildet und von

Methanogenen, Acetogenen und Propionatgärern effektiv verbraucht wird, (ii) die Rhizosphäre von Seggen ein Hotspot für H_2-Metabolisierer ist und (iii) neuartige mikrobielle Taxa am komplexen anaeroben Abbau pflanzlicher Biomasse beteiligt sind. Im Gegensatz zu den nährstoffarmen Moorböden finden die anaeroben Mikroorganismen im Regenwurmdarm eine Vielzahl leicht verwertbarer Kohlenstoffquellen vor. Aufgrund der kurzen Verweilzeit im Darm können die Anaeroben allerdings kein verzweigtes Nahrungsnetz bilden, was zur Folge hat, dass primäre und sekundäre Gärungsprodukte nicht vollständig konsumiert werden. Von Gärern gebildete organische Säuren können daher vom Regenwurm absorbiert werden, während H_2 aus dem Wurm diffundiert und H_2-Oxidierern im Boden zur Verfügung steht.

7. REFERENCES

1. **Aaij C, Boerst P.** (1972). The gel electrophoresis of DNA. *Biochim Biophys Acta* **296:** 192-200.
2. **Abbott SL, Cheung WK, Janda JM.** (2003). The genus *Aeromonas*: biochemical characteristics, atypical reactions, and phenotypic identification schemes. *J Clin Microbiol* **41:** 2348-2357.
3. **Ahmed Z, Banu H, Rahman MM, Akhter F, Haque MS.** (2001). Microbial activity on the degradation of lignocellulosic polysaccharides. *J Biol Sci* **1:** 993-997.
4. **Aira M, Monroy F, Dominguez J.** (2009). Changes in bacterial numbers and microbial activity of pig slurry during transit of epigeic and anecic earthworms. *J Hazard Mater* **162:** 1404-1407.
5. **Alewell C, Paul S, Lischeid G, Küsel K, Gehre M.** (2006). Characterizing the redox status in three different forested wetlands with geochemical data. *Environ Sci Technol* **40:** 7609-7615.
6. **Andrews SC, Berks BC, McClay J, Ambler A, Quail MA, Golby P, Guest JR.** (1997) A 12-cistron *Escherichia coli* operon (*hyf*) encoding a pyruvate proton-translocating formate hydrogenlyase system. *Microbiology* **143:** 3633-3647.
7. **Aragano M, Schlegel HG.** (1992). The mesophilic hydrogen-oxidizing (knallgas) bacteria. In: Balows A, Trüper HG, Dworkin M, Harder W, Schleifer K-H (eds). *The Prokaryotes.* Springer: New York, pp 344-384.
8. **Aselmann I, Crutzen PJ.** (1989). Global distribution of natural freshwater wetlands and rice paddies, their net primary productivity, seasonality and possible methane emission. *J Athmos Chem* **8:**307-359.
9. **Ausec L, Kraigher B, Mandic-Mulec I.** (2009). Differences in the activity and bacterial community structure of drained grassland and forest peat soil. *Soil Biol Biochem* **41:** 1874-1881.
10. **Bagramyan K, Mnatsakanyan N, Poladian A, Vassilian A, Trchounian A.** (2002). The roles of hydrogenase 3 and 4, and the F_0F_1-ATPase, in H_2 production by *Escherichia coli* at alkaline and acidic pH. *FEBS Lett* **516:** 172-178.
11. **Bagramyan K, Trchounian A.** (2003). Structural and functional features of formate hydrogen lyase, an enzyme of mixed-acid fermentation from *Escherichia coli*. *Biochem Int* **68:** 1159-1170.
12. **Bais HP, Weir TL, Perry LG, Gilroy S, Vivanco JM.** (2006). The role of root exudates in rhizosphere interactions with plants and other organisms. *Annu Rev Plant Biol* **57:** 233-266.
13. **Balch WE, Fox GE, Magrum LJ, Woese CR, Wolfe RS.** (1979). Methanogens: reevaluation of a unique biological group. *Microbiol Rev* **43:** 260-296.
14. **Barker HA.** (1981). Amino acid degradation by anaerobic bacteria. *Annu Rev Biochem* **50:** 23-40.
15. **Barois I, Brossard M, Lavelle P, Tondoh J, Kanyonyo J, Martínez A, et al.** (1999). Ecology of earthworm species with large environmental tolerance and/or extended distributions. In: Lavelle P, Hendrix P, Brussard L (eds). *Earthworm management in tropical agroecosystems.* CAB International: London, pp 57-86.
16. **Barois I, Lavelle P.** (1986). Changes in respiration rate and some physiochemical properties of a tropical soil during transit through *Pontoscolex corethrurus* (Glossoscolecidae, Oligochaeta). *Soil Biol Biochem* **18:** 539-541.

17. **Bayer EA, Yuval S, Lamed R.** (2006). Cellulose-decomposing bacteria and their enzyme systems. In: Dworkin MM, Falkow S, Rosenberg E, Schleifer KH, Stackebrandt E (eds). *The Prokaryotes*. Springer: New York, pp 578-617.

18. **Beer J, Blodau C.** (2007). Transport and thermodynamics constrain belowground carbon turnover in a northern peatland. *Geochim Cosmochim Acta* **71:** 2989-3002.

19. **Benson DA, Karsch-Mizrachi I, Lipman DJ, Ostell J, Rapp BA, Wheeler DL.** (2000). GenBank. *Nucleic Acids Res* **28:** 15-18.

20. **Bentley DR, Balasubramanian S, Swerdlow HP, Smith GP, Milton M, Brown CG, *et al.*** (2008). Accurate whole human genome sequencing using reversible terminator chemistry. *Nature* **456:** 53-59.

21. **Bergman EN.** (1990). Energy contributions of volatile fatty acids from the gastrointestinal tract in various species. *Physiol Rev* **70:** 567-590.

22. **Bernard L, Chapuis-Lardy L, Razafimbelo T, Razafindrakoto M, Pablo A-L, Legname E, et al.** (2012). Endogeic earthworms shape bacterial functional communities and affect organic matter mineralization in a tropical soil. *ISME J* **6:** 213-222.

23. **Bétian HG, Linehan BA, Bryant MP, Holderman LV.** (1977). Isolation of a cellulolytic *Bacteroides* sp. from human feces. *Appl Environ Microbiol* **33:** 1009-1010.

24. **Bityutskii NP, Kaidun PI, Yakkonen KL.** (2012). The earthworm (*Aporrectodea caliginosa*) primes the release of mobile and available micronutrients in soil. *Pedobiologia* **55:** 93-99.

25. **Blachnik R.** (1998). D'Ans Lax Taschenbuch für Chemiker und Physiker, Vol 3, 4th edn. Springer: Berlin.

26. **Böck A.** (2000). Fermentation. In: Lederberg J (ed). *Encyclopedia of Microbiology*. Vol 20, 2nd ed. Academic press: San Diego pp 343-349.

27. **Bonkowski M, Schäfer M.** (1997). Interactions between earthworms and soil protozoa: a trophic component of the soil food web. *Soil Biol Biochem* **29:** 142-148.

28. **Bomar M, Hippe H, Schink B.** (1991). Lithotrophic growth and hydrogen metabolism by *Clostridium magnum*. *FEMS Microbiol Let* **83:** 347-349.

29. **Boone DR, Johnson RL, Liu Y.** (1989). Diffusion of the interspecies electron carriers H_2 and formate in methanogenic ecosystems and its implications in the measurement of K_m for H_2 or formate uptake. Appl Environ Microbiol **55:** 1735-1741.

30. **Bouché MB.** (1977). Strategies lombriciennes. In: Lohm U, Persson T (eds). *Soil organisms as components of ecosystems.* Vol 25. Ecological Bulletins: Stockholm, pp 122-132.

31. **Bräuer SL, Cadillo-Quiroz H, Ward RJ, Yavitt JB, Zinder SH.** (2011). *Methanoregula boonei* gen. nov., sp. nov., an acidiphilic methanogen isolated from an acidic peat bog. *Int J Syst Evol Micr* **61:** 45-52.

32. **Breidenbach J.** (2002). Normalanatomie und Histologie des Lumbriciden *Lumbricus terrestris* L. (Annelida, Oligochaeta). PhD thesis. University of Münster.

33. **Brenner DJ, Farmer JJ.** (2005). Family I. *Enterobacteriaceae*. In: Brenner DJ, Krieg NR, Staley JT (eds). *Bergey's Manual of Systematic Bacteriology.* 2nd edn. Springer: New York, pp 587-607.

34. **Broda DM, Lawson PA, Bell RG, Musgrave DR.** (1999). *Clostridium frigidicarnis* sp. nov., a psychrotolerant bacterium associated with 'blown pack'spoilage of vacuum-packed meats. *Int J Syst Evol Micr* **49:** 1539-1550.

35. **Brown GG, Barois I, Lavelle P.** (2000). Regulation of soil organic matter dynamics and microbial activity in the drilosphere and the role of interactions with other edaphic functional domains. *Eur J Soil Biol* **36:** 177-198.

36. **Brown GG, Doube BM.** (2004). Functional interactions between earthworms, microorganisms, organic matter, and plants. In: Edwards CA (ed). *Earthworm ecology.* 3rd edn. CRC Press: Boca Raton pp 213-239.

37. **Brown GG, Edwards CA, Brussaard L.** (2004). How earthworms affect plant growth: burrowing into the mechanisms. In: Edwards CA (ed). *Earthworm ecology.* 3rd edn. CRC Press: Boca Raton pp 13-50.

38. **Brune A, Frenzel P, Cypionka H.** (2000). Life at the oxic-anoxic interface: microbial activities and adaptions. *FEMS Microbiol Rev* **24:** 691-710.

39. **Buckel W.** (2005). Special clostridial enzymes and fermentation pathways. In: Dürre P (ed). *Handbook on clostridia*. CRC Press: Boca Raton pp 177-220.

40. **Buckel W, Thauer RK.** (2013). Energy conservation via electron bifurcating ferredoxin reduction and proton/Na$^+$ translocating ferredoxin oxidation. *Biochim Biophys Acta* **1827:** 94-113.

41. **Byzov BA, Nechtitaylo TY, Bumazhkin BK, Kurakov AV, Golyshin PN, Zvyagintsev DG.** (2009). Culturable microorganisms from the earthworm digestive tract. *Mikrobiologiya* **78:** 360-368.

42. **Calusinska M, Happe T, Joris B, Wilmotte A.** (2010). The surprising diversity of clostridial hydrogenases, a comparative genomic perspective. *Microbiology 156:* 1575-1588.

43. **Campbell BJ.** (2013). The family *Acidobacteriaceae*. In: Rosenberg E, DeLong EF, Lory S, Stackebrandt E, Thompson F (eds). *The Prokaryotes – prokaryotic biology and symbiotic associations.* Springer: New York, pp 405–415.

44. **Caporaso JG, Kuczynski J, Stombaugh J, Bittinger K, Bushman FD, Costello EK, et al.** (2010). QIIME allows analysis of high-throughput community sequencing data. *Nat methods* **7:** 335-336.

45. **Chamkha M, Labat M, Patel BK, Garcia JL.** (2001). Isolation of a cinnamic acid-metabolizing *Clostridium glycolicum* strain from oil mill wastewaters and emendation of the species description. *Int J Syst Evol Micr* **51:** 2049-2054.

46. **Chamkha M, Patel BK, Garcia JL, Labat M.** (2001). Isolation of *Clostridium bifermentans* from oil mill wastewaters converting cinnamic acid to 3-phenylpropionic acid and emendation of the species. *Anaerobe* **7:** 189-197.

47. **Chasar LS, Chanton JP, Glaser PH, Siegel DI.** (2000). Methane concentration and stable isotope distribution as evidence of rhizospheric processes: Comparison of a fen and bog in the Glacial Lake Agassiz Peatland complex. *Ann Bot* **86:** 655-663.

48. **Chassard C, Delmas E, Robert C, Bernalier-Donadille A.** (2010). The cellulose-degrading microbial community of the human gut varies according to the presence or absence of methanogens. *FEMS Microbiol Ecol* **74:** 205-213.

49. **Chauhan A, Ogram A.** (2006). Fatty acid-oxidizing consortia along a nutrient gradient in the Florida Everglades. *Appl Environ Microbiol* **72:** 2400-2406.

50. **Cheng KJ, Stewart CS, Dinsdale D, Costerton JW.** (1983). Electron microscopy of bacteria involved in the digestion of plant cell walls. *Anim Feed Sci Technol* **10:** 93-120.

51. **Chin KJ, Hahn D, Hengstmann U, Liesack W, Janssen PH.** (1999). Characterization and identification of numerically abundant culturable bacteria from the anoxic bulk soil of rice paddy microcosms. *Appl Environ Microbiol* **65:** 5042-5049.

52. **Chin KJ, Liesack W, Janssen PH.** (2001). *Opitutus terrae* gen. nov., sp. nov., to accommodate novel strains of the division 'Verrucomicrobia' isolated from rice paddy soil. *Int J Syst Evol Micr* **51:** 1965-1968.

53. **Chin KJ, Lukow T, Conrad R.** (1999). Effect of temperature on structure and function of the methanogenic archaeal community in an anoxic rice field soil. *Appl Environ Microbiol* **65:** 2341-2349.

54. **Clymo RS.** (1963). Ion exchange in *Sphagnum* and its relation to bog ecology. *Ann Bot* **27:** 309-324.

55. **Clymo RS.** (1965). Experiments on breakdown of *Sphagnum* in two bogs. *J Ecol* **53:** 747-758.

56. **Clymo RS.** (1987). The ecology of peatlands. *Sci Prog* **71:** 593-614.

57. **Coates JD, Ellis DJ, Gaw CV, Lovley DR.** (1999). *Geothrix fermentans* gen. nov., sp. nov., a novel Fe[III]-reducing bacterium from a hydrocarbon-contaminated aquifer. *Int J Syst Bacteriol* **49:** 1615-1622.

58. **Collins MD, Lawson PA, Willems A, Cordoba JJ, Fernandez-Garayzabal J, Garcia P, *et al*.** (1994). The phylogeny of the genus *Clostridium*: proposal of five new genera and eleven new species combinations. *Int J Syst Bacteriol* **44:** 812-826.

59. **Condon S.** (1987). Responses of lactic-acid bacteria to oxygen. *FEMS Microbiol Rev* **46:** 269-280.

60. **Conrad R.** (1999). Contribution of hydrogen to methane production and control of hydrogen concentrations in methanogenic soils and sediments. *FEMS Microbiol Ecol* **28:** 193-202.

61. **Conrad R, Bak F, Seitz HJ, Thebrath B, Mayer HP, Schütz H.** (1989). Hydrogen turnover by psychrotrophic homoacetogenic and mesophilic methanogenic bacteria in anoxic paddy soil and lake sediment. *FEMS Microbiol Ecol* **62:** 285-294.

62. **Conrad R, Klose M.** (1999). Anaerobic conversion of carbon dioxide to methane, acetate and propionate on washed rice roots. *FEMS Microbiol Ecol* **30:** 147-155.

63. **Conrad R, Phelps TJ, Zeikus JG.** (1985). Gasmetabolism in support of juxtapositioning of hydrogen-producing and methanogenic bacteria in sewage sludge and lake sediments. *Appl Environ Microbiol* **50:** 595-601.

64. **Conrad R, Schütz H, Babbel M.** (1987). Temperature limitation of hydrogen turnover and methanogenesis in anoxic paddy soil. *FEMS Microbiol Ecol* **45:** 281-289.

65. **Conrad R, Wetter B.** (1990). Influence of temperature on energetics of hydrogen metabolism in homoacetogenic, methanogenic, and other anaerobic bacteria. *Arch Microbiol* **155:** 94-98.

66. **Constant P, Chowdhury SP, Hesse L, Pratscher J, Conrad R.** (2011). Genome data mining and soil survey for the novel group 5 [NiFe]-hydrogenase to explore the diversity and ecological importance of presumptive high-affinity H_2-oxidizing bacteria. *Appl Environ Microbiol* **77:** 6027-6035.

67. **Cooke A.** (1983). The effects of fungi on food selection by *Lumbricus terrestris* L. In: Satchell JE (ed). *Earthworm ecology: from Darwin to vermiculture*. Chapman & Hall: London, pp 365-373.

68. **Cooke A, Luxton M.** (1980). Effect of microbes on food selection by *Lumbricus terrestris*. *Rev Ecol Biol Sol* **17:** 365-370.

69. **Cord-Ruwisch R, Seitz HJ, Conrad R.** (1988). The capacity of hydrogenotrophic anaerobic bacteria to compete for traces of hydrogen depends on the redox potential of the terminal electron acceptor. *Arch Microbiol* **149:** 350-357.

70. **Cornish-Bowden A.** (1985). IUPAC-IUB symbols for nucleotide nomenclature. *Nucleic Acid Red* **13:** 3021-3030.

71. **Crawford DL, Crawford RL, Pometto AL.** (1977). Preparation of specifically radiolabled ^{14}C-(lignin)- and ^{14}C-(cellulose)-lignocelluloses and their decomposition by the microflora of soil. *Appl Environ Microbiol* **33:** 1247-1251.

72. **Crill PM, Martens CS.** (1983). Spatial and temporal fluctuations of methane production in anoxic coastal marine sediments. *Limnol Oceanogr* **28:** 1117-1130.

73. **Curreem SO, Teng JL, Tse H, Yuen KY, Lau SK,Woo PC.** (2011). General metabolism of *Laribacter hongkongensis*: a genome-wide analysis. *Cell Biosci* **1:** 16.

74. **Curry, Schmidt O.** (2007). The feeding ecology of earthworms - a review. *Pedobiologia* **50:** 463-477.

75. **Da Silva SM, Voordouw J, Leitão C, Martins M, Voordouw G, Pereira IAC.** (2013). Function of formate dehydrogenases in *Desulfovibrio vulgaris* Hildenborough energy metabolism. *Microbiology* **159:** 1760-1769.

76. **Daniel O, Anderson JM.** (1992). Microbial biomass and activity in contrasting soil materials after passage through the gut of the earthworm *Lumbricus rubellus* Hoffmeister. *Soil Biol Biochem* **24:** 465-470.

77. **Daniel SL, Drake HL.** (1993). Oxalate-dependent and glyoxylate-dependent growth and acetogenesis by *Clsotridium thermoaceticum*. *Appl Environ Microbiol* **59:** 3062-3069.

78. **Darwin C.** (1881). The formation of vegetable mould through the action of worms, with observations of their habits. Murray: London.

79. **Davidson EA, Janssens IA.** (2006). Temperature sensitivity of soil carbon decomposition and feedbacks to climate change. *Nature* **440:** 165-173.

80. **De Bok FA, Harmsen HJ, Plugge CM, de Vries MC, Akkermans AD, de Vos WM, Stams AJ.** (2005). The first true obligately syntrophic propionate-oxidizing bacterium, *Pelotomaculum schinkii* sp. nov., co-cultured with *Methanospirillum hungatei*, and emended description of the genus *Pelotomaculum*. *Int J Syst Evol Micr* **55:** 1697-1703.

81. **De Bok FAM, Plugge CM, Stams AJM.** (2004). Interspecies electron transfer in methanogenic propionate degrading consortia. *Water Res* **38:** 1368-1375.

82. **De Bok FAM, Stams AJM, Dijkema C, Boone DR.** (2001). Pathway of propionate oxidation by a syntrophic culture of *Smithella propionica* and *Methanospirillum hungatei*. *Appl Environ Microbiol* **67:** 1800-1804.

83. **De Vos P, Ludwig W, Schleifer KH, Whitman WB.** (2009). Family IV. *Paenibacillaceae* fam. nov. In: De Vos P, Garrity GM, Jones D, Krieg NR, Ludwig W, Rainey EA *et al*. (eds). *Bergey's Manual of Systematic Bacteriology*. Vol 3, 2nd edn. Springer: New York, pp 269-327.

84. **Dedysh SN.** (2011). Cultivating uncultured bacteria from northern wetlands: knowledge gained and remaining gaps. *Front Microbiol* **2:** 1-15.

85. **Dedysh SN, Pankratov TA, Belova SE, Kulichevskaya IS, Liesack W.** (2006). Phylogenetic analysis and in situ identification of bacteria community composition in an acidic *Sphagnum* peat bog. *Appl Environ Microbiol* **72:** 2110-2117.

86. **Degelmann DM, Kolb S, Dumont M, Murrell JC, Drake HL.** (2009). *Enterobacteriaceae* facilitate the anaerobic degradation of glucose by forest soil. *FEMS Microbiol Ecol* **68:** 312-319.

87. **Depkat-Jakob PS, Brown GG, Tsai SM, Horn MA, Drake HL.** (2013). Emission of nitrous oxide and dinitrogen by diverse earthworm families from Brazil and resolution of associated denitrifying and nitrate-dissimilating taxa. *FEMS Microbiol Ecol* **83:** 375-391.

88. **Depkat-Jakob PS, Hilgarth M, Horn MA, Drake HL.** (2010). Effect of earthworm feeding guilds on ingested dissimilatory nitrate reducers and denitrifiers in the alimentary canal of the earthworm. *Appl Environ Microbiol* **76:** 6205-6214.

89. **Depkat-Jakob PS, Hunger S, Schulz K, Brown GG, Tsai SM, Drake HL.** (2012). Emission of methane by *Eudrilus eugeniae* and other earthworms from Brazil. *Appl Environ Microbiol* **78:** 3014–3019.

90. **Desvaux M.** (2005). *Clostridium cellulolyticum*: model organism of mesophylic cellulolytic Clostridia. *FEMS Microbiol Rev* **29:** 741-764.

91. **Dharmadi Y, Murarka A, Gonzalez R.** (2006). Anaerobic Fermentation of Glycerol by Escherichia coli: A New Platform for Metabolic Engineering. *Biotechnol Bioeng* **94:** 821-829.

92. **Doi RH.** (2008). Cellulases of mesophilic microorganisms. *Ann NY Acad Sci* **1125:** 267-279.

93. **Dolfing J.** (2013). Syntrophic propionate oxidation via butyrate: a novel window of opportunity under methanogenic conditions. *Appl environ microbiol* **79:** 4515-4516.

94. **Dolfing J, Jiang B, Henstra AM, Stams AJM, Plugge CM.** (2008). Syntrophic growth on formate: a new microbial niche in anoxic environments. *Appl Environ Microbiol* **74:** 6126-6131.

95. **Dong X, Plugge CM, Stams AJM.** (1994). Anaerobic degradation of propionate by a mesophilic acetogenic bacterium in coculture and triculture with different methanogens. *Appl Environ Microbiol* **60:** 2834-2838.

96. **Drake HL.** (1994). Acetogenesis, acetogenic bacteria, and the Acetyl-CoA "Wood/Ljungdahl" pathway: past and current perspectives. In: Drake HL (ed). *Acetogenesis*. Chapman & Hall: New York, pp 3-60.

97. **Drake HL, Daniel SL, Küsel K, Matthies C, Kuhner C, Braus-Stromeyer S.** (1997). Acetogenic bacteria: what are the *in situ* consequences of their diverse metabolic versatilities? *Biofactors* **6:** 13-24.

98. **Drake HL, Gößner AS, Daniel SL.** (2008). Old acetogens, new light. In: Wiegel J, Maier RJ, Adams MWW (eds). *Incredible anaerobes: From physiology to genomics to fuels.* New York Academy of Science: Boston, pp 100-128.

99. **Drake HL, Horn MA.** (2007). As the worm turns: the earthworm gut as a transient habitat for soil microbial biomes. *Annu Rev Microbiol* **61:** 169-189.

100. **Drake HL, Horn MA, Wüst PK.** (2009). Intermediary ecosystem metabolism as a main driver of methanogenesis in acidic wetland soil. *Environ Microbiol Rep* **1:** 307-318.

101. **Drake HL, Küsel K.** (2005). Acetogenic clostridia. In: Dürre P (ed). *Handbook on Clostridia*. CRC-Press: Boca Raton, pp 719-746.

102. **Drake HL, Küsel K, Matthies C.** (2002). Ecological consequences of the phylogenetic and physiological diversities of acetogens. *A Van Leeuw J Microb* **81:** 203-213.

103. **Drake HL, Küsel K, Matthies C.** (2006). Acetogenic prokaryotes. In: Balows A, Trüper HG, Dworkin M, Harder W, Schleifer K-H (eds). *The Prokaryotes*. 3rd ed. Springer: New York pp 354-420.

104. **Dridi B, Fardeau M-L, Ollivier B, Raoult D, Drancourt M.** (2012). *Methanomassiliicoccus luminyensis* gen. nov., sp. nov., a methanogenic archaeon isolated from human faeces. *Int J Syst Evol Micr* **62:** 1902-1907.

105. **Duddleston KN, Kinney MA, Kiene RP, Hines ME.** (2002). Anaerobic microbial biogeochemistry in a northern bog: Acetate as a dominant metabolic end product. *Global Biogeochem Cy* **16:** 11-1–11-9.

106. **Duke GE.** (1997). Gastrointestinal physiology and nutrition in wild birds. *Proc Nutr Soc* **56:** 1049-1056.

107. **Duncan SH, Barcenilla A, Stewart CS, Pryde SE, Flint HJ.** (2002). Acetate utilization and butyryl CoA:acetate CoA transferase in human colonic bacteria. *Appl Environ Microbiol* **68:** 5186-5190.

108. **Dwyer DF, Weeg-Aerssens E, Shelton DR, Tiedje J.** (1988). Bioenergetic Conditions of bytyrate metabolism by a syntrophic, anaerobic bacterium coculture with hydrogen-

oxidizing methanogenic and sulfidogenic bacteria. *Appl Environ Microbiol* **54:** 1354-1359.

109. **Edwards CA, Bohlen BJ.** (1996). Biology and ecology of earthworms. 3rd ed. Chapman & Hall: London.

110. **Edwards CE, Fletcher KE.** (1988). Interactions between earthworms and microorganisms in organic-matter breakdown. *Agricul Ecosys Environ* **24:** 235-247.

111. **Edwards CA, Lofty JR.** (1977). Biology of earthworms. 2nd ed. Chapman & Hall: London, pp 141-173.

112. **Eichorst SA, Kuske CR, Schmidt TM.** (2011). Influence of plant polymers on the distribution and cultivation of bacteria in the phylum *Acidobacteria*. *Appl Environ Microbiol* **77:** 586-596.

113. **Egert M, Marhan S, Wagner B, Scheu S, Friedrich MW.** (2004). Molecular profiling of 16S rRNA genes reveals diet-related differences of microbial communities in soil, gut, and casts of *Lumbricus terrestris* L. (Oligochaeta: Lumbricidae). *FEMS Microbiol Ecol* **48:** 187-197.

114. **Eisenhauer N, Scheu S.** (2008). Earthworms as drivers of the competition between grasses and legumes. *Soil Biol Biochem* **40:** 2650-2659.

115. **Eisenhauer N, Schuy M, Butenschoen O, Schau S.** (2009). Direct and indirect effects of endogeic earthworms on plant seeds. *Pedobiologia* **52:** 151-162.

116. **Embree M, Liu JK, Al-Bassam MM, Zengler K.** (2015). Networks of energetic and metabolic interactions define dynamics in microbial communities. *Proc Natl Acad Sci USA* **112:** 15450-15455.

117. **Emerson D, Weiss JV, Megonigal JP.** (1999). Iron-oxidizing bacteria are associated with ferric hydroxide precipitates (Fe-plaque) on the roots of wetland plants. *Appl Environ Microbiol* **65:** 2758-2761.

118. **Eurola S, Hicks S, Kaakinen E.** (1984). Key to Finnish mire types. In: Moore PD (ed). *European mires*. Academic Press: London, pp 11-17.

119. **Ezaki T.** (2009). Family VII. *Peptostreptococcaceae* fam. nov. In: De Vos P, Garrity GM, Jones D, Krieg NR, Ludwig W, Rainey EA et al. (eds). *Bergey's Manual of Systematic Bacteriology*. Vol 3, 2nd edn. Springer: New York, pp 1008-1015.

120. **Faust L, Szendy M, Plugge CM, van den Brink PFH, Temmink H, Rijnaarts HHM.** (2015). Characterization of the bacterial community involved in the bioflocculation process of wastewater organic matter in high-loaded MBRs. *Appl Microbiol Biotechnol* **99:** 5327-5337.

121. **Fedosov DV, Podkopaeva DA, Miroshnichenko ML, Bonch-Osmolovskaya EA, Lebedinsky AV, Grabovich MY.** (2006). Investigation of the catabolism of acetate and peptides in the new anaerobic thermophilic bacterium *Caldithrix abyssi*. *Microbiology* 75: 119-124.

122. **Felske A, Wolterink A, van Lis R, Akkermans ADL.** (1998). Phylogeny of the main bacterial 16S rRNA sequences in Drentse A grassland soils (the Netherlands). *Appl Environ Microbiol* **64:** 871-879.

123. **Flint HJ, Bayer EA, Rincon MT, Lamed R, White BA.** (2008). Polysaccharide utilization by gut bacteria: potential for new insights from genomic analysis. *Nat Rev Micro* **6:** 121-131.

124. **Fontaine S, Bardoux G, Benest D, Verdier B, Mariotti A, Abbadie L.** (2004). Mechanisms of the priming effect in a Savannah soil amended with cellulose. *Soil Sci Soc Am J* **68:** 125-131.

125. **Fox GE, Pechman KJ, Woese CR.** (1977). Comparative cataloging of 16S ribosomal ribonucleic acid: molecular approach to procaryotic systematics. *Int J Syst Bacteriol* **27:** 44-57.

126. **Freeman C, Ostle N, Kang H.** (2001). An enzymic 'latch' on a global carbon store: a shortage of oxygen locks up carbon in peatlands by restraining a single enzyme. *Nature* **409:** 149.

127. **Frimmer U, Widdel F.** (1989). Oxidation of ethanol by methanogenic bacteria. *Arch Microbiol* **152:** 479-483.

128. **Frolking S, Roulet NT, Moore TR, Richard PJH, Lavoie M, Muller SD.** (2001). Modeling northern peatland decomposition and peat accumulation. *Ecosystems* **4:** 479-498.

129. **Fukuzaki S, Nishio N, Shobayashi M, Nagai S.** (1990). Inhibition of the fermentation of propionate to methane by hydrogen, acetate, and propionate. *Appl Environ Microbiol* **56:** 719–723.

130. **Furlong MA, Singleton DR, Coleman DC, Whitman WB.** (2002). Molecular and culture-based analyses of prokaryotic communities from an agricultural soil and the burrows and casts of the earthworm *Lumbricus rubellus*. *Appl Environ Microbiol* **68:** 1265-1279.

131. **Gajalakshmi S, Abbasi SA.** (2004). Earthworms and vermicomposting. *Ind J Biotech* **3:** 486-494.

132. **Galand PE, Fritze H, Conrad R, Yrjälä K.** (2005). Pathways for methanogenesis and diversity of methanogenic archaea in three boreal peatland ecosystems. *Appl Environ Microbiol* **71:** 2195-2198.

133. **Gan Y, Qiu Q, Liu P, Rui J, Lu Y.** (2012). Syntrophic oxidation of propionate in rice field soil at 15 and 30°C under methanogenic conditions. *Appl Environ Microbiol* **78:** 4923-4932.

134. **Gerstberger P.** (2001a). Naturräumliche und geomorphologische Übersicht über das Fichtelgebirge. In: Gerstberger P (ed). *Waldökosystemforschung in Nordbayern: Die BITÖK-Untersuchungsflächen im Fichtelgebirge und Steigerwald. Bayreuther Forum Ökologie.* Vol 90. BayCEER: Bayreuth, pp 1-4.

135. **Gerstberger P.** (2001b). Zur Vegetation des Fichtelgebirges. In: Gerstberger P (ed). *Waldökosystemforschung in Nordbayern: Die BITÖK-Untersuchungsflächen im Fichtelgebirge und Steigerwald. Bayreuther Forum Ökologie.* Vol 90. BayCEER: Bayreuth, pp 5-10.

136. **Given PH, Dickinson CH.** (1975). Biochemistery and microbiology of peats. In: Paul EA, McLaren AD (eds). *Soil biochemistery*. Marcel Dekker: New York, pp 123-212.

137. **Good IJ.** (1953). The population frequencies of species and the estimation of population parameters. *Biometrika* **40:** 237-264.

138. **Gore AJP.** (1983). Ecosystems of the world (4A), Mires, Swamp, Bog, Fen and Moor. Vol. 2. Elsevier: Amsterdam, pp 1-34.

139. **Gorham E.** (1991). Northern peatlands: role in the carbon cycle and probable responses to climate warming. *Ecol Appl* **1:** 182-195.

140. **Gößner A, Devereux R, Ohnemüller N, Acker G, Stackebrandt E, Drake HL.** (1999). *Thermicanus aegyptius* gen. nov., sp. nov., isolated from oxic soil, a facultative microaerophile that grows commensally with the thermophilic acetogen *Moorella thermoacetica*. *Appl Environ Microbiol* **65:** 5124-5133.

141. **Gößner AS, Küsel K, Schulz D, Trenz S, Acker G, Lovell CR, Drake HL**. (2006). Trophic interaction of the aerotolerant anaerobe *Clostridium intestinale* and the acetogen

Sporomusa rhizae sp. nov. isolated from roots of the black needlerush *Juncus roemerianus*. *Microbiology* **152:** 1209-1219.

142. **Graentzdoerffer A, Rauh D, Pich A, Andreesen JR.** (2003). Molecular and biochemical characterization of two tungsten- and selenium-containing formate dehydrogenases from *Eubacterium acidaminophilum* that are associated with components of an iron-only hydrogenase. *Arch Microbiol* **179:** 116-130.

143. **Green Mr, Sambrook J.** (2012). Molecular cloning. A laboratory manual. 4th edn. Cold Spring Harbor Laboratory Press: New York.

144. **Griffiths RI, Whiteley AS, O'Donnel AG, Bailey MJ.** (2000). Rapid method for coextraction of DNA and RNA from natural environments for analysis of ribosomal DNA- and rRNA-based microbial community composition. *Appl Environ Microbiol* **66:** 5488-5491.

145. **Gunnigle E, McCay P, Fuszard M, Botting CH, Abram F, O'Flaherty V.** (2013). A functional approach to uncover the low-temperature adaption strategies of the archaeon *Methanosarcina barkeri*. *Appl Environ Microbiol* **79:** 4210-4219.

146. **Haas BJ, Gevers D, Earl AM, Feldgarden M, Ward DV, Giannoukos G, *et al*.** (2011). Chimeric 16S rRNA sequence formation and detection in Sanger and 454-pyrosequenced PCR amplicons. *Genome Res* **21:** 494-504.

147. **Hackmann TJ, Firkins J.** (2015). Electron transport phosphorylation in rumen butyrivibrios: unprecedented ATP yield for glucose fermentation to butyrate. *Front Microbiol* **6:** 622.

148. **Hädrich A, Heuer VB, Herrmann M, Hinrichs KU, Küsel K.** (2012). Origin and fate of acetate in an acidic fen. *FEMS Microbiol Ecol* **81:** 339-354.

149. **Hakobyan M, Sargsyan H, Bagramyan K.** (2005). Proton translocation coupled to formate oxidation in anaerobically grown fermenting *Escherichia coli*. *Biophys Chem* **115:** 55-61.

150. **Halsall DM, Goodchild DJ.** (1986). Nitrogen fixation associated with development and localization of mixed populations of *Cellulomonas* sp. and *Azospirillum brasilense* grown on cellulose or wheat straw. *Appl Environ Microbiol* **51:** 849-854.

151. **Hamberger A, Horn MA, Dumont MG, Murrell JC, Drake HL.** (2008). Anaerobic consumers of monosaccharides in a moderately acidic fen. *Appl Environ Microbiol* **74:** 3112-3120.

152. **Hamilton JJ, Contreras MC, Reed JL.** (2015). Thermodynamics and H_2 transfer in a methanogenic, syntrophic community. *PLoS Comput Biol* **11:** e1004364.

153. **Hartenstein R, Amico L.** (1983). Production and carrying-capacity for the earthworm *Lumbricus terrestris* in culture. *Soil Biol Biochem* **15:** 51-54.

154. **Hartman WH, Richardson CJ, Vigalys R, Bruland GL.** (2008). Environmental and anthropogenic controls over bacterial communities in wetland soils. *Proc Natl Acad Sci USA* **105:** 17842-17847.

155. **Hartwich K, Poehlein A, Daniel R.** (2012). The purine-utilizing bacterium *Clostridium acidurici* 9a: a genome-guided metabolic reconsideration. *PLoS One* **7:** e51662.

156. **Hattori S.** (2008). Syntrophic acetate-oxidizing microbes in methanogenic environments. *Microbes Environ* **23:** 118-127.

157. **Heck KL, Vanbelle G, Simberloff D.** (1975). Explicit calculation of rarefaction diversity measurement and determination of sufficient sample size. *Ecology* **56:** 1459-1461.

158. **Hedderich R, Forzi L.** (2005). Energy-converting [NiFe] hydrogenases: more than just H_2 activation. *J Mol Microbiol Biotechnol* **10:** 92-104.

159. **Heidelberg JF, Seshadri R, Haveman SA, Hemme CL, Paulsen IT, Kolonay JF, *et al.*** (2004). The genome sequence of the anaerobic, sulfate-reducing bacterium *Desulfovibrio vulgaris* Hildenborough. *Nat Biotechnol* **22:** 554–559.

160. **Henderson C.** (1980). The influence of extracellular hydrogen on the metabolism of *Bacteroides ruminicola*, *Anaerovibrio lipolytica* and *Selenomonas ruminantium*. *J Gen Microbiol* **119:** 485-491.

161. **Hendrickson OQ.** (1990). Asymbiotic nitrogen fixation and soil metabolism in three Ontario forests. *Soil Biol Biochem* **22:** 967-971.

162. **Hengstmann U, Chin KJ, Janssen PH, Liesack W.** (1999). Comparative phylogenetic assignment of environmental sequences of genes encoding 16S rRNA and numerically abundant culturable bacteria from an anoxic rice paddy soil. *Appl Environ Microbiol* **65:** 5050–5058.

163. **Herlemann DPR, Labrenz M, Jürgens K, Bertilsson S, Waniek JJ, Andersson AF.** (2011). Transitions in bacterial communities along the 2000 km salinity gradient of the Baltic Sea. *ISME J* **5:** 1571-1579.

164. **Hogan ME, Slaytor M, O'Brien RW.** (1985). Transport of volatile fatty acids across the hindgut of the cockroach *Panesthia cribrata* Saussure and the termite *Mastotermes darwiniensis* Froggatt. *J Insect Physiol* **31:** 587-591.

165. **Holt RA, Cairns AJ, Morris JG.** (1988). Production of butanol by *Clostridium puniceum* in batch and continuous culture. Appl Microbiol Biotechnol **27:** 319-324.

166. **Hornor SG, Mitchell MJ.** (1981). Effect of the earthworm *Eisenia foetida* (*Oligochaeta*) on fluxes of volatile carbon and sulfur compounds from sewage sludge. *Soil Biol Biochem* **13:** 367–372.

167. **Horn MA, Drake HL, Schramm A.** (2006a). Nitrous oxide reductase genes (*nosZ*) of denitrifying microbial populations in soil and the earthworm gut are phylogenetically similar. *Appl Environ Microbiol* **72:** 1019-1026.

168. **Horn MA, Matthies C, Küsel K, Schramm A, Drake HL.** (2003). Hydrogenotrophic methanogenesis by moderately acid-tolerant methanogens of a methane-emitting acidic peat. *Appl Environ Microbiol* **69:** 74-83.

169. **Horn MA, Mertel R, Kästner M, Gehre M, Drake HL.** (2006b). In vivo emission of dinitrogen by earthworms via denitrifying bacteria in the gut. *Appl Environ Microbiol* **72:** 1013-1018.

170. **Horn MA, Schramm A, Drake HL.** (2003). The earthworm gut: an ideal habitat for ingested N_2O-producing microorganisms. Appl Environ Microbiol **69:** 1662-1669.

171. **Horner DS, Foster PG, Embley TM.** (2000). Iron hydrogenases and the evolution of anaerobic eukaryotes. *Mol Biol Evol* **17:** 1695-1709.

172. **Horner DS, Heil B, Happe T, Embley TM.** (2002). Iron hydrogenases - ancient enzymes in modern eukaryotes. *Trends Biochem Sci* **27:** 148-153.

173. **Huang X-F, Liu YJ, Dong JD, Qu LY, Zhang Y-Y, Wang F-Z, Tian X-P, Zhang S.** (2014). *Mangrovibacterium diazotrophicum* gen. nov., sp. nov., a nitrogen-fixing bacterium isolated from a mangrove sediment, and proposal of *Prolixibacteraceae* fam. nov. *Int J Syst Evol Micr* **64:** 875-881.

174. **Hungate RE.** (1969). A roll tube method for the cultivation of strict anaerobes. In: Norris JR, Ribbons DW (eds). *Methods in microbiology*. Academic press: New York, pp 117-132.

175. **Hunger S, Gößner AS, Drake HL.** (2011). Trophic links between the acetogen *Clostridium glycolicum* KHa and the fermentative anaerobe *Bacteroides xylanolyticus* KHb, isolated from Hawaiian forest soil. *Appl Environ Microbiol* **77:** 6281-6285.

176. **Hunger S, Gößner AS, Drake HL.** (2015). Anaerobic trophic interactions of contrasting methane-emitting mire soils: processes versus taxa. *FEMS Microbiol Ecol* **91:** fiv045.

177. **Hunger S, Schmidt O, Gößner AS, Drake HL.** (2016). Formate-derived H_2, a driver of hydrogenotrophic processes in the root-zone of a methane-emitting fen. *Environ Microbiol* (published online ahead of print; doi: 10.1111/1462-2920.13301).

178. **Hunger S, Schmidt O, Hilgarth M, Horn MA, Kolb S, Conrad R, Drake HL.** (2011). Competing formate- and carbon dioxide-utilizing prokaryotes in an anoxic methane-emitting fen soil. *Appl Environ Microbiol* **77:** 3773-3785.

179. **Hurlbert SH.** (1971). The nonconcept of species diversity: a critique and alternative parameters. *Ecology* **52:** 577-586.

180. **Ianotti EL, Kafkewitz D, Wolin MJ, Bryant MP.** (1973). Glucose fermentation products of *Ruminococcus albus* grown in continuous culture with *Vibrio succinogenes*: changes caused by interspecies transfer of H_2. *J Bacteriol* **114:** 1231-1240.

181. **Ihssen J, Horn MA, Matthies C, Gößner A, Schramm A, Drake HL.** (2003). N_2O-producing microorganisms in the gut of the earthworm *Aporrectodea caliginosa* are indicative of ingested soil bacteria. *Appl Environ Microbiol* **69:** 1655-1661.

182. **Imachi H, Sakai S, Nagai H, Yamaguchi T, Takai K.** (2009). *Methanofollis ethanolicus* sp. nov., an ethanol-utilizing methanogen isolated from a lotus field. *Int J Syst Evol Micr* **59:** 800-805.

183. **Jackson MB, Armstrong W.** (1999). Formation of aerenchyma and the process of plant ventilation in relation to soil flooding and submergence. *Plant Biol* **1:** 274-287.

184. **Jetten MSM, Stams AJM, Zehnder AJB.** (1992). Methanogenesis from acetate: a comparison of the acetate metabolism in *Methanothrix soehngenii* and *Methanosarcina* spp. *FEMS Microbiol Rev* **88:** 181-198.

185. **Johnson DB, Stallwood B, Kimura S, Hallberg KB.** (2006). Isolation and characterization of *Acidicaldus organivorus*, gen. nov., sp. nov.: a novel sulfur oxidizing, ferric iron-reducing thermo-acidophilic heterotrophic *Proteobacterium*. *Arch Microbiol* **185:** 212-221.

186. **Johnson DB, Yajie L, Okibe N.** (2008). "Bioshrouding": a novel approach for securing reactive mineral tailings. *Biotechnol Lett* **30:** 445-449.

187. **Jones CG, Lawton JH, Shachak M.** (1994). Organisms as ecosystem engineers. *Oikos* **69:** 373-386.

188. **Jones DL.** (1998). Organic acids in the rhizosphere–a critical review. *Plant Soil* **205:** 25–44.

189. **Jones JG, Simon BM, Gardener S.** (1982). Facctors affecting methanogenesis and associated anaerobic processes in the sediments of a stratified eutrophic lake, *J Gen Microbiol* **128:** 1-11.

190. **Jouquet P, Dauber J, Lagerlöf J, Lavelle P, Lepage M.** (2006). Soil invertebrates as ecosystem engineers: intended and accidental effects on soil and feedback loops. *Appl Soil Ecol* **32:** 153-164.

191. **Karakashev D, Batstone DJ, Trably E, Angelidaki I.** (2006). Acetate oxidation is the dominant methanogenic pathway from acetate in the absence of *Methanosaetaceae*. *Appl Environ Microbiol* **72:** 5138-5141.

192. **Karsten GR, Drake HL.** (1995). Comparative assessment of the aerobic and anaerobic microfloras of earthworm guts and forest soils. *Appl Environ Microbiol* **61:** 1039-1044.

193. **Karsten GR, Drake HL.** (1997). Denitrifying bacteria in the earthworm gastrointestinal tract and *in vivo* emission of nitrous oxide (N_2O) by earthworms. *Appl Environ Microbiol* **63:** 1878-1882.

194. **Kaster AK, Moll J, Parey K, Thauer RK.** (2011). Coupling of ferredoxin and heterodisulfide reduction via electron bifurcation in hydrogenotrophic methanogenic archaea. *P Natl Acad Sci USA* **108:** 2981-2986.

195. **Kelly CA, Dise NB, Martens CS.** (1992). Temporal variations in the stable carbon isotopic composition of methane emitted from Minnesota peatlands. *Global Biogeochem Cy* **6:** 263-269.

196. **Kempher ML, Madigan MT.** (2012). Phylogeny and photoheterotrophy in the acidophilic phototrophic purple bacterium *Rhodoblastus acidophilus*. *Arch Microbiol* **194:** 567-574.

197. **King GM.** (1990). Dynamics and controls of methane oxidation in a Danish wetland sediment. *FEMS Microbiol Ecol* **74:** 309-324.

198. **King GM, Roslev P, Skovgaard H.** (1990). Distribution and rate of methane oxidation in sediments of the Florida Everglades. *Appl Environ Microbiol* **56:** 2902-2911.

199. **Kishimoto N, Kosako Y, Tano T.** (1991). *Acidobacterium capsulatum* gen. nov., sp. nov.: an acidophilic chemoorganotrophic bacterium containing menaquinone from acidic mineral environment. *Curr Microbiol* **22:** 1-7.

200. **Kjeldsen KU, Loy A, Jakobsen TF, Thomsen TR, Wagner M, Ingvorsen K.** (2007). Diversity of sulfate-reducing bacteria from an extreme hypersaline sediment, Great Salt Lake (Utah). *FEMS Microbiol Ecol* **60:** 287-298.

201. **Kjøller A, Struwe S.** (1980). Microfungi of decomposing red alder leaves and their substrate utilization. *Soil Biol Biochem* **12:** 425-431.

202. **Klindworth A, Pruesse E, Schweer T, Peplies J, Quast C, Horn M, Glöckner FO.** (2013). Evaluation of general 16S ribosomal RNA gene PCR primers for classical and next- generation sequencing- based diversity studies. *Nucleic Acids Res* **41:** e1.

203. **Knapp BA, Podmirseg SM, Seeber J, Meyer E, Insam H.** (2009). Diet-related composition of the gut microbiota of *Lumbricus rubellus* as revealed by a molecular fingerprinting technique and cloning. *Soil Biol Biochem* **41:** 2299-2307.

204. **Knee EM, Gong FC, Gao MS, Teplitski M, Jones AR, Foxworth A, Mort AJ, Bauer WD.** (2001). Root mucilage from pea and its utilization by rhizosphere bacteria as a sole carbon source. *Mol Plant Microbe In* **14:** 775–784.

205. **Knorr K-H, Blodau C.** (2009). Impact of experimental drought and rewetting on redox transformations and methanogenesis in mesocosms of a northern fen soil. *Soil Biol Biochem* **41:** 1187-1198.

206. **Koelbener A, Ström L, Edwards PJ, Olde Venterink H.** (2010). Plant species from mesotrophic wetlands cause relatively high methane emissions from peat soil. *Plant Soil* **326:** 147-158.

207. **Kojima H, Fukui M.** (2010). *Sulfuricella denitrificans* gen. nov., sp. nov., a sulfur-oxidizing autotroph isolated from a freshwater lake. *Int J Syst Evol Micr* **60:** 2862-2866.

208. **Kotsyurbenko OR.** (2005). Trophic interactions in the methanogenic microbial community of low-temperature terrestrial ecosystems. *FEMS Microbiol Ecol* **53:** 3-13.

209. **Kotsyurbenko OR, Friedrich MW, Simankova MV, Nozhevnikova AN, Golyshin PN, Timmis KN, Conrad R.** (2007). Shift from aceticlastic to H_2-dependent methanogenesis in a West Siberian peat bog at low pH values and isolation of an acidophilic *Methanobacterium* strain. *Appl Environ Microbiol* **73:** 2344-2348.

210. **Kotsyurbenko OR, Glagolev MV, Nozhevnikova AN, Conrad R.** (2001). Competition between homoacetogenic bacteria and methanogenic archaea for hydrogen at low temperature. *FEMS Microbiol Ecol* 38:153-159.

211. **Kotsyurbenko OR, Nozhevnikova AN, Soloviova TI, Zavarzin GA.** (1996). Methanogenesis at low temperatures by microflora of tundra wetland soil. *A Van Leeuw J Microb* **69:** 75-86.

212. **Kotsyurbenko OR, Nozhevnikova AN, Zavarzin GA.** (1993). Methanogenic degradation of organic matter by anaerobic bacteria at low temperature. *Chemosphere* **27:** 1745-1761.

213. **Kotsyurbenko OR, Simankova MV, Nozhevnikova AN, Zhilina TN, Bolotina NP, Lysenko AM, Osipov GA.** (1995). New species of psychrophilic acetogens: *Acetobacterium bakii* sp. nov., *A. paludosum* sp. nov., *A. fimetarium* sp. nov. *Arch Microbiol* **163:** 29-34.

214. **Kremer C, Pettolino F, Bacic A, Drinnan A.** (2004). Distribution of cell wall components in *Sphagnum* hyaline cells and in liverwort and hornwort elaters. *Planta* **219:** 1023–1035.

215. **Kröger A.** (1974). Electron-transport phosphorylation coupled to fumarate reduction in anaerobically grown *Proteus rettgeri*. Biochim Biophys Acta **347:** 273-289.

216. **Kröger A, Biel S, Simon J, Gross R, Unden G, Lancaster CRD.** (2002). Fumarate respiration of *Wolinella succinogenes*: enzymology, energetics and coupling mechanism. *Biochim Biophys Acta* **1553:** 23-38.

217. **Krylova NI, Conrad R.** (1998). Thermodynamics of propionate degradation in methanogenic paddy soil. *FEMS Microbiol Ecol* **26:** 281-288.

218. **Kuhner CH, Matthies C, Acker G, Schmittroth M, Gößner AS, Drake HL.** (2000). *Clostridium akagii* sp. nov. and *Clostridium acidisoli* sp. nov.: acid-tolerant, N_2-fixing clostridia isolated from acidic forest soil and litter. *Int J Syt Evol Micr* **50:** 873-881.

219. **Küsel K, Blöthe M, Schulz D, Reiche M, Drake HL.** (2008). Microbial reduction of iron and porewater biogeochemistery in acidic peatlands. *Biogesciences* **5:** 1537-1549.

220. **Küsel K, Drake HL.** (1995). Effect of environmental parameters on the formation and turnover of acetate in forest soils. *Appl Environ Microbiol* **61:** 3667–3675.

221. **Küsel K, Drake HL.** (1996). Anaerobic capacities of leaf litter. *Appl Environ Microbiol* **62:** 4216-4219.

222. **Küsel K, Karnholz A, Trinkwalter T, Devereux R, Acker G, Drake HL.** (2001). Physiological ecology of *Clostridium glycolicum* RD-1, an aerotolerant acetogen isolated from sea grass roots. *Appl Environ Microbiol* **67:** 4734-4741.

223. **Küsel K, Pinkart HC, Drake HL, Devereux R.** (1999). Acetogenic and sulfate-reducing bacteria inhabiting the rhizoplane and deep cortex cells of the seagrass *Halodule wrightii*. *Appl Environ Microbiol* **65:** 5117-5123.

224. **Küsel K, Wagner C, Drake HL.** (1999). Enumeration and metabolic product profiles of the anaerobic microflora in the mineral soil and litter of a beech forest. *FEMS Microb Ecol* **29:** 91–103.

225. **Laiho R.** (2006). Decomposition in peatlands: Reconciling seemingly contrasting results on the impacts of lowered water levels. *Soil Biol Biochem* **38:** 2011-2024.

226. **Lambers H, Mougel C, Jaillard B, Hinsinger P.** (2009). Plant-microbe-soil interactions in the rhizosphere: an evolutionary perspective. *Plant Soil* **321:** 83-115.

227. **Lancaster CRD, Sauer US, Groß R, Haas AH, Graf J, Schwalbe H, *et al*.** (2005). Experimental support for the "E pathway hypothesis" of coupled transmembrane e$^-$ and H$^+$ transfer in dihemic quinol:fumarate reductase. *Proc Natl Acad Sci USA* **102:** 18860-18865.

228. **Landsdown JM, Quay PD, King SL.** (1992). CH_4 production via CO_2 reduction in a temperate bog: a source of ^{13}C-depleted CH_4. *Geochim Cosmochim Acta* 56: 3493-3503.

229. **Lane DJ.** (1991). 16S/23S rRNA sequencing. In: Stackebrandt E, Goodfellow M (eds). *Nucleic acid techniques in bacterial systematic*. John Wiley & Sons: New York, pp 115-175.

230. **Lange HC, Heijnen JJ.** (2001). Statistical reconciliation of the elemental and molecular biomass composition of *Saccharomyces cerevisiae*. *Biotechnol Bioeng* **75:** 334-344.

231. **Lange NA.** (1967). Handbook of Chemistry. McGraw-Hill: New York.

232. **Lansdown JM, Quay PD, King SL.** (1992). CH_4 production via CO_2 reduction in a temperate bog: A source of ^{13}C-depleted CH_4. *Geochim Cosmochim Acta* **56:** 3493-3503.

233. **Laossi K-R, Noguera CD, Bartolomé-Lasa A, Mathieu J, Blouin M, Barot S.** (2009). Effects of an endogeic and an anecic earthworm on the competition between four annual plants and their relative fecundity. *Soil Biol Biochem* **41:** 1668-1673.

234. **Lattaud C, Zhang BG, Locati S, Rouland C, Lavelle P.** (1997). Activities of the digestive enzymes in the gut and in tissue culture of a tropical geophagous earthworm, *Polypheretima elongate* (Megascolecidae). *Soil Biol Biochem* **29:** 335-339.

235. **Lau H-T, Faryna J, Triplett EW.** (2006). *Aquitalea magnusonii* gen. nov., sp. nov., a novel Gram-negative bacterium isolated from a humic lake. *Int J Syst Evol Micr* **56:** 867-871.

236. **Lavelle P, Lattaud C, Trigo D, Barois I.** (1995). Mutualism and biodiversity in soils. *Plant Soils* **170:** 23-33.

237. **Lavelle P, Bignell D, Legape M, Wolters V, Roger P, Ineson P, Heal OW, Ghillion S.** (1997). Soil function in a changing world: the role of invertebrate ecosystem engineers. *Eur J Soil Biol* **33:** 159-193.

238. **Leaphart AB, Friez MJ, Lovell CR.** (2003). Formyltetrahydrofolate synthetase sequences from salt marsh plant roots reveal a diversity of acetogenic bacteria and other bacterial functional groups. *Appl Environ Microbiol* **69:** 693-696.

239. **Lee KE.** (1985). Earthworms. Their ecology and relationships with soil and land use. Academic Press: Sydney.

240. **Lele U, Watve MG.** (2014). Bacterial growth rate and growth yield: is there a relationship? *Proc Indian Natn Sci Acad* **80:** 537-546.

241. **Leschine SB.** (1995). Cellulose degradtion in anaerobic environments. *Annu Rev Microbiol* **49:** 399-426.

242. **Lehtovirta-Morley LE, Stoecker K, Vilcinskas A, Prosser JI, Nicol GW.** (2011). Cultiviation of an olbligate acidophilic ammonia oxidizer from a nitrifying acid soil. *P Natl Acad Sci USA* **108:** 15892-15897.

243. **Lever MA.** (2011). Acetogenesis in the energy-starved deep biosphere – a paradox? *Front Microbiol* **2:** 284.

244. **Li T, Mazéas L, Sghir A, Leblon G, Bouchez T.** (2009). Insights into networks of functional microbes catalyzing methanization of cellulose under mesophilic conditions. *Environ Microbiol* **11:** 889-904.

245. **Liesack W, Bak F, Kreft JU, Stackebrandt E.** (1994). *Holophaga foetida* gen. nov., sp. nov., a new, homoactogenic bacterium degrading methoxylated aromatic compounds. *Arch Microbiol* **162:** 85-90.

246. **Lim JK, Bae SS, Kim TW, Lee J-H, Lee HS, Kang SG.** (2012). Thermodynamics of formate-oxidizing metabolism and implications for H_2 production. *Appl Environ Microbiol* **78:** 7393-7397.

247. **Limmer C, Drake HL.** (1996). Nonsymbiotic N_2-fixation by acidic and pH-neutral forest soils: aerobic and anaerobic differentials. *Soil Biol Biochem* **28:** 177-183.

248. **Lin X, Handley KM, Gilbert JA, Kostka JE.** (2015). Metabolic potential of fatty acid oxidation and anaerobic respiration by abundant members of *Thaumarchaeota* and *Thermoplasmata* in deep anoxic peat. *ISME J* **9:** 2740-2744.

249. **Lipson DA, Haggerty JM, Srinivas A, Raab TK, Sathe S, Dinsdale EA.** (2013). Metagenomic insights into anaerobic metabolism along an Arctic peat soil profile. *PLoS One* **8:** e64659.

250. **Lischeid G, Moritz K, Bittersohl J.** (2001). Hydrologie im Einzugsgebiet Lehstenbach. In: Gerstberger P (ed). *Waldökosystemforschung in Nordbayern: Die BITÖK-Untersuchungsflächen im Fichtelgebirge und Steigerwald. Bayreuther Forum Ökologie.* Vol 90. BayCEER: Bayreuth, pp 91-101.

251. **Liu P, Qiu Q, Lu Y.** (2011). *Syntrophomonadaceae*-affiliated species as active butyrate-utilizing syntrophs in paddy field soil. *Appl Environ Microbiol* **77:** 3884-3887.

252. **Liu Y, Balkwill DL, Aldrich HC, Drake GR, Boone DR.** (1999). Characterization of the anaerobic propionate-degrading syntrophs *Smithella propionica* gen. nov., sp. nov. and *Syntrophobacter wolinii*. *Int J Syst Bacteriol* **49:** 545-556.

253. **Ljungdahl LG.** (1994). The acetyl-CoA pathway and the chemiosmotic generation of ATP during acetogenesis. In: Drake HL (ed). *Acetogenesis*. Chapman & Hall: New York, pp 63-87.

254. **Ljungdahl L, Eriksson KE.** (1985). Ecology of microbial cellulose degradation. *Adv Microb Ecol* **8:** 237-299.

255. **Logsdon SD, Linden DR.** (1992). Interactions of earthworms with soil physical conditions influencing plant growth. *Soil Sci* **154:** 330-337.

256. **Loveley DR.** (1991). Dissimilarory Fe(III) and Mn(IV) reduction. *Microbiol Rev* **55:** 259-287.

257. **Loy A, Küsel K, Lehner A, Drake HL, Wagner M.** (2004). Microarray and functional gene analyses of sulfate-reducing prokaryotes in low-sulfate, acidic fens reveal cooccurrence of recognized genera and novel linages. *Appl Environ Microbiol* **70:** 6998-7009.

258. **Lubbers IM, van Groenigen KJ, Fonte SJ, Six J, Brussaard L, von Groenigen JW** (2013) Greenhouse gas emissions from soils increased by earthworms. *Nature Climate Change* **3:** 187-194.

259. **Lueders T, Manefield M, Friedrich MW.** (2004). Enhanced sensitivity of DNA- and rRNA-nased stable isotope probing by fractionation and quantitative analysis of isopycnic centrifugation gradients. *Environ Microbiol* **6:** 73-78.

260. **Lueders T, Pommerenke B, Friedrich MW.** (2004). Stable-isotope probing of microorganisms thriving at thermodynamic limits: syntrophic propionate oxidation in flooded soil. *Appl Environ Microbiol* **70:** 5778-5786.

261. **Ludwig W, Schleifer KH.** (1994). Bacterial phylogeny based on 16S and 23S rRNA sequence analysis. *FEMS Microbiol Rev* **15:** 155-173.

262. **Ludwig W, Schleifer KH, Whitman WB.** (2009). Revised road map to the phylum *Firmicutes*. In: De Vos P, Garrity GM, Jones D, et al. (eds). *Bergey's Manual of Systematic Bacteriology*. 2nd edn, Vol 3: The *Firmicutes*. New York: Springer, pp 1-13.

263. **Ludwig W, Strunk O, Klugbauer S, Klugbauer N, Weizenegger M, Neumaier J, *et al*.** 1998. Bacterial phylogeny based on comparative sequence analysis. *Electrophoresis* **19:** 554-568.

264. **Ludwig W, Strunk O, Westram R, Richter L, Meier H, Yadhukumar, *et al*.** (2004). ARB: a software environment for sequence data. *Nucleic Acids Res* **32:** 1363-1371.

265. **Luli GW, Strohl WR.** (1990). Comparison of growth, acetate production, and acetate inhibition of *Escherichia coli* strains in batch and fed-batch fermentations. *Appl Environ Microbiol* **56:** 1004-1011.

266. **Lund BM, Brocklehurst TF, Wyatt GM.** (1981). Characterization of strains of *Clostridium puniceum* sp. nov., a pink-pigmented, pectolytic bacterium. *J Gen Microbiol* **122:** 17-26.

267. **Lynd RL, Weimer PJ, van Zyl WH, Pretorius IS.** (2002). Microbial Cellulose Utilization: Fundamentals and Biotechnology. *Microbiol Mol Biol R* **66:** 506-577.

268. **Macfarlane S, Macfarlane GT.** (2003). Regulation of short-chain fatty acid production. *P Nutr Soc* **62:** 67-72.

269. **Macy JM, Ljungdahl LG, Gottschalk G.** (1978). Pathway of succinate and propionate formation in *Bacteroides fragilis*. *J Bacteriol* **134:** 84-91.

270. **Maestrojuán GM, Boone DR.** (1991). Characterization of *Methanosarcina barkeri* MS^T and 227, *Methanosarcina mazei* S-6^T, and *Methanosarcina vacuolata* Z-761^T. *Int J Syst Bacteriol* **41:** 267-274.

271. **Maglione G, Russell JB, Wilson DB.** (1997). Kinetics of cellulose digestion by *Fibrobacter succinogenes* S85. *Appl Environ Microbiol* **63:** 665-669.

272. **Maltby E Immirzi P.** (1993). Carbon dynamics in peatlands and other wetland soils, regional and global perspectives. *Chemosphere* **27:** 999-1023.

273. **Manefield M, Whiteley AS, Griffiths RI, Bailey MJ.** (2002). RNA stable isotope probing, a novel means of novel means of linking microbial community function to phylogeny. *Appl Environ Microbiol* **68:** 5367-5373.

274. **Mansell GP, Syers JK, Gregg PEH.** (1981). Plant availability of phosphorus in dead herbage ingested by surface-casting earthworms. *Soil Biol Biochem* **13:** 163-167.

275. **Martin A, Cortez J, Barois I, Lavelle P.** (1987). Les mucus intestinaux de Ver de Terre, moteur de leurs interactions avec la microflore. *Rev Ecol Biol Sol* **24:** 549-558.

276. **Martin-Carnahan A, Joseph SW.** (2005). Genus I. *Aeromonas*. In: Brenner DJ, Krieg NR, Staley JT (eds). *Bergey's manual of systematic bacteriology*. 2nd edn. Springer: New York, pp 557-578.

277. **Matthies C, Griesshammer A, Schmittroth M, Drake HL.** (1999). Evidence for involvement of gut-associated denitrifying bacteria in emission of nitrous oxide (N_2O) by earthworms obtained from garden and forest soils. *Appl Environ Microbiol* **65:** 3599-3604.

278. **Matzner E, Huwe B.** (2004). Antrag auf Einrichtung einer Forschungsgruppe der DFG zum Thema "Dynamik von Bidenprozessen bei extremen meteorologischen Randbedingungen", Teilprojekt "Zentrale Experimente". Universität Bayreuth, Bayreuth.

279. **Mba CC.** (1988). Biomass and vermicompost production by the earthworm *Eudrilus eugeniae* (Kinberg). *Rev Biol Trop* **37:** 11–13.

280. **McCarty PL.** (1972). Energetics of organic matter degradation. In: Mitchell R (ed). *Water Pollution Microbiology.* John Wiley and Sons: New York, pp 91-118.

281. **McDonald JE, Houghton JNI, Rooks DJ, Allison HE, McCarthy AJ.** (2012). The microbial ecology of anaerobic cellulose degradation in municipal waste landfill sites: evidence of a role for fibrobacteres. *Environ Microbiol* **14:** 1077-1087.

282. **McInerney MJ, Bryant MP.** (1981). Basic principles of bioconversions in anaerobic digestion and methanogenesis. In: Sofer SS and Zaborsky OR (eds). *Biomass Conversion Processes for Energy and Fuels.* Plenum: New York, pp 277-296.

283. **McInerney MJ, Rohlin L, Mouttaki H, Kim UM, Krupp RS, Rios-Hernandez L *et al*.** (2007). The genome of *Syntrophus aciditrophicus*: life at the thermodynamic limit of microbial growth. *Proc Natl Acad Sci USA* **104:** 7600-7605.

284. **McInerney MJ, Sieber JR, Gunsalus RP.** (2009). Syntrophy in anaerobic global carbon cycles. *Curr Opin Biotech* **20:** 623-632.

285. **Mechichi T, Fardeau ML, Labat M, Garcia JL, Verhe F, Patel BK.** (2000). *Clostridium peptidivorans* sp. nov., a peptide-fermenting bacterium from an olive mill wastewater treatment digester. *Int J Syst Evol Micr* **50:** 1259-1264.

286. **Meselson M, Stahl FW.** (1958). The replication of DNA in *Escherichia coli. Proc Natl Acad Sci USA* **44:** 671-682.

287. **Messing J.** (1983). New M13 vectors for cloning. *Method Enzymol* **101:** 20-78.

288. **Metje M.** (2006). Terminale Prozesse des anaeroben Abbaus in sauren Torfmooren der Subarktis und des südlichen Boreals. *Dissertation an der Philipps-Universität Marburg/Lahn.*

289. **Metje M, Frenzel P.** (2005). Effect of Temperature on anaerobic ethanol oxidation and methanogenesis in acidic peat from a northern wetland. *Appl Environ Microbiol* **71:** 8191-8200.

290. **Metje M, Frenzel P.** (2007). Methanogenesis and methanogenic pathways in a peat from subarctic permafrost. *Environ Microbiol* **9:** 954-964.

291. **Meuer J, Bartoschek S, Koch J, Künkel A, Hedderich R.** (1999). Purification and catalytic properties of Ech hydrogenase from *Methanosarcina barkeri*. *Eur J Biochem* **265:** 325-335.

292. **Meyer J.** (2007). [Fe-Fe] hydrogenases and their evolution: a genomic perspective. *Cell Mol Life Sci* **64:** 1063-1084.

293. **Meyerdierks A, Kube M, Kostadinov I, Teeling H, Glöckner FO, Reinhardt R, Amann R.** (2010). Metagenome and mRNA expression analyses of anaerobic methanotrophic archaea of the ANME-1 group. *Environ Microbiol* **12:** 422-39.

294. **Miki T, Yokokawa T, Matsui K.** (2014). Biodiversity and multifunctionality in a microbial community: a novel theoretical approach to quantify functional redundancy. *Proc R Soc B* **281:** 20132498.

295. **Miles HB.** (1963). Soil protozoa and earthworm nutrition. *Soil Sci* **95:** 407-409.

296. **Miroshnichenko ML, Kolganova, TV, Spring S, Chernyh N, Bonch-Osmolovskaya.** (2010). *Caldithrix palaeochoryensis* sp. nov., a thermophilic, anaerobic, chemo-organotrophic bacterium from a geothermally heated sediment, and emended description of the genus *Caldithrix*. *Int J Syst Evol Micr* **60:** 2120-2123.

297. **Miroshnichenko ML, Kostrikina NA, Chernyh NA, Pimenov NV, Tourova TP, Antipov AN, *et al.*** (2003). *Caldithrix abyssi* gen. nov., sp. nov., a nitrate-reducing thermophilic, anaerobic bacterium isolated from a Mid-Atlantic Ridge hydrothermal vent, represents a novel bacterial lineage. *Int J Syst Evol Micr* **53:** 323-329.

298. **Misoph M, Drake HL.** (1996). Effect of CO_2 on the fermentation capacities of the acetogen *Peptostreptococcus productus* U-1. *J Bacteriol* **178:** 3140-3145.

299. **Mitchell WJ.** (1998). Physiology of carbohydrate to solvent conversion by clostridia. *Adv Microb Physiol* **39:** 31-130.

300. **Mizrahi I.** (2013). Rumen Symbioses. In: Rosenberg E, DeLong EF, Lory S, Stackebrandt E, Thompson F (eds). *The Prokaryotes – prokaryotic biology and symbiotic associations.* Springer: New York, pp 533–544.

301. **Moat AG, Foster JW, Spector MP.** (2002). Fermentation pathways. In: Moat AG, Foster JW, Spector MP (eds). *Microbial Physiology*. 4th edn. Wiley-Liss: New York pp 412-433.

302. **Montgomery L, Flesher B, Stahl D.** (1988). Transfer of *Bacteroides succinogenes* (Hungate) to *Fibrobacter* gen. nov. as *Fibrobacter succinogenes* comb. nov. and description of *Fibrobacter intestinalis* sp. nov. *Int J Syst Bacteriol* **38:** 430-435.

303. **Moody SA, Briones MJI, Piearce TG, Dighton J.** (1995). Selective consumption of decomposing wheat-straw by earthworms. *Soil Biol Biochem* **27:** 1209-1213.

304. **Moore PD.** (1990). Soil and ecology: Temperate wetlands. In: Williams M (ed). *Wetlands: a threatened landscape*. Blackwell Publishers: Oxford, pp. 95-114.

305. **Moran MA, Benner R, Hudson RE.** (1989). Kinetics of microbial degradation of vascular plant material in two wetland ecosystems. *Oecologia* **79:** 158-167.

306. **Mori Y.** (1995). Nutritional interdependence between *Thermoanaerobacter thermo-hydrosulfuricus* and *Clostridium thermocellum*. *Arch Microbiol* **164:** 152-154.

307. **Mormile MR, Gurijala KR, Robinson JA, McInerney MJ, Suflita JM.** (1996). The importance of hydrogen in landfill fermentations. *Appl Environ Microbiol* **62:** 1583-1588.

308. **Müller N, Worm P, Schink B, Stams AJM, Plugge CM.** (2010). Syntrophic butyrate and propionate oxidation processes: from genomes to reaction mechanisms. *Environ Microbiol Rep* **2:** 489-499.

309. **Mußmann M, Brito I, Pitcher A, Damste JSS, Hatzenpichler R.** (2011). Thaumarchaeotes abundant in refinery nitrifying sludges express *amoA* but are not obligate autotrophic ammonia oxidizers. *Proc Natl Acad Sci USA* **108:** 16771-16776.

310. **Nandi R, Sengupta S.** (1998). Microbial production of hydrogen: an overview. *Crit Rev Microbiol* **24:** 61-84.

311. **Nechitaylo TY, Timmis KN, Golyshin PN.** (2009). 'Candidatus Lumbricincola', a novel lineage of uncultured *Mollicutes* from earthworms of family *Lumbricidae*. *Environ Microbiol* **11:** 1016-1026.

312. **Ng TK, Weimer PJ, Zeikus JG.** (1977). Cellulolytic and physiological properties of *Clostridium thermocellum*. *Arch Microbiol* **114:** 1-7.

313. **Nilsson M.** (2002) Mire Ecosystems. In: eLS. John Wiley & Sons Ltd: Chichester. http://www.els.net [doi: 10.1038/npg.els.0003194].

314. **Nilsson M, Mikkela C, Sundh I, Granberg G, Svensson BH, Ranneby B.** (2001). Methane emission from Swedish mires: national and regional budgets and dependence on mire vegetation. *J Geophys Res Atmos* **106:** 20847-20860.

315. **Nohrstedt HÖ.** (1988). Effect of liming and N-fertilization on denitrification and N_2-fixation in an acid coniferous forest floor. *Forest Ecol Manag* **24:** 1-13.

316. **Nozaki M, Miura C, Tozawa Y, Miura T.** (2009). The contribution of endogenous cellulose digestion in the gut of earthworm (*Pheretima hilgendorfi*: Megascolecidae). *Soil Biol Biochem* **41:** 762-769.

317. **Nozhevnikova AN, Kotsyurbenko OR, Simankova MV.** (1994). Acetogenesis at low temperature. In: Drake HL (ed). *Acetogenesis*. Chapman & Hall: New York, pp 416-431.

318. **Nüsslein B, Chin KJ, Eckert W, Conrad R.** (2001). Evidence for anaerobic syntrophic acetate oxidation during methane production in the profundal sediment of subtropical Lake Kinneret (Israel). *Environ Microbiol* **3:** 460-470.

319. **Painter TJ.** (1991). Lindow man, Tollund man and other peat-bog bodies: the preservative and antimicrobial action of sphagnan, a reactive glycuronoglycan with tanning and sequestering properties. *Carbohyd Polym* **15:** 123-142.

320. **Palmer K, Drake HL, Horn MA.** (2009). Genome-derived criteria for assigning environmental *narG* and *nosZ* sequences to operational taxonomic units of nitrate reducers. *Appl Environ Microbiol* **75:** 5170-5174.

321. **Palmer K, Drake HL, Horn MA.** (2010). Association of novel and highly diverse acid-tolerant denitrifiers with N_2O fluxes of an acidic fen. *Appl Environ Microbiol* **76:** 1125-1134.

322. **Pankratov TA, Dedysh SN.** (2010) *Granulicella paludicola* gen. nov., sp. nov., *Granulicella pectinivorans* sp. nov., *Granulicella aggregans* sp. nov., *Granulicella rosea* sp. nov., acidophilic, polymer-degrading acidobacteria from *Sphagnum* peat bogs. *Int J Syst Evol Micr* **60:** 2951-2959.

323. **Pankratov TA, Ivanova AO, Dedysh SN, Liesack W.** (2011). Bacterial populations and environmental factors controlling cellulose degradation in an acidic *Sphagnum* peat. *Environ Microbiol* **13:** 1800-1814.

324. **Pankratov TA, Kirsanova, LA, Kaparullina EN, Kevbrin VV, Dedysh SN.** (2012). *Telmatobacter bradus* gen. nov., sp. nov., a cellulolytic facultative anaerobe from

subdivision 1 of the *Acidobacteria*, and emended description of *Acidobacterium capsulatum* Kishimoto *et al*. 1991. *Int J Syst Evol Micr* **62:** 430-437.

325. **Parlé JN.** (1963). Microorganisms in the intestine of earthworms. *J Gen Microbiol* **31:** 1-13.

326. **Paul S, Küsel K, Alewell C.** (2006). Reduction processes in forest wetlands: Tracking down heterogeneity of source/sink functions with a combination of methods. *Soil Biol Biochem* **38:** 1028-1039.

327. **Pester M, Bittner N, Deevong P, Wagner M, Loy A.** (2010). A 'rare biosphere' microorganism contributes to sulfate reduction in a peatland. *ISME J* **4:** 1591-1602.

328. **Pester M, Knorr K-H, Friedrich MW, Wagner M, Loy A.** (2012). Sulfate-reducing microorganisms in wetlands – fameless actors in carbon cycling and climate change. *Front Microbiol* **3:** 1-19.

329. **Peters V, Conrad R.** (1995). Methanogenic and other strictly anaerobic bacteria in desert soil and other oxic soils. *Appl Environ Microbiol* **61:** 1673–1676.

330. **Peyret N, Senevirante PA, Allawi HT, SantaLucia J.** (1999). Nearest-neighbour thermodynamics and NMR of DNA sequences with internal A·A, C·C, G·G, and T·T mismatches. *Biochemistery* **38:**1028-1039.

331. **Phelps TJ, Zeikus JG.** (1984). Influence of pH on terminal carbon metabolism in anoxic sediments from a mildly acidic lake. *Appl Environ Microbiol* **48:** 1088-1095.

332. **Philippot L, Raaijmakers JM, Lemanceau P, van der Putten WH.** (2013). Going back to the roots: the microbial ecology of the rhizosphere. *Nat Rev Microbiol* **11:** 789-799.

333. **Piearce TG, Philips MJ.** (1980). The fate of ciliates in the earthworm gut: an in vitro study. *Microb Ecol* **5:** 313-319.

334. **Piearce TG, Roggero N, Tipping R.** (1994). Earthworms and seeds. *J Biol Edu* **28:** 195-202.

335. **Poehlein A, Schmidt S, Kaster A-K, Goenrich M, Vollmers J, Thürmer A, *et al*.** (2012). An ancient pathway combining carbon dioxide fixation with the generation and utilization of a sodium ion gradient for ATP synthesis. PLoS ONE **7:** e33439.

336. **Pohlschroeder M, Leschine SB, Canale-Parola E.** (1994). *Spirochaeta caldaria* sp. nov., a thermophilic bacterium that enhances cellulose degradation by *Clostridium thermocellum*. *Arch Microbiol* **161:** 17-24.

337. **Popp TJ, Chanton JP, Whiting GJ, Grant N.** (1999). Methane stable isotope distribution at a Carex dominated fen in north central Alberta. *Global Biogeochem Cy* **13:** 1063-1077.

338. **Potapow N.** (2011). Syntrophe Propionat- und Butyratoxidation im Niedermoorboden. *Bachelor thesis at the University of Bayreuth.*

339. **Prabha ML, Jayaraaj IA, Jeyaraaj R, Rao S.** (2007). Comparative studies on the digestive enzymes in the gut of earthworms, *Eudrilus eugeniae* and *Eisenia fetida*. *Ind J Biotech* **6:** 567-569.

340. **Pruesse E, Peplies J, Glöckner FO.** (2012). SINA: accurate high-throughput multiple sequence alignment of ribosomal RNA genes. *Bioinformatics* **28:** 1823-1829.

341. **Pruesse E, Quast C, Knittel K, Fuchs B, Ludwig W, Peplies J, Glöckner FO.** (2007). SILVA: a comprehensive online resource for quality checked and aligned ribosomal RNA sequence data compatible with ARB. *Nucleic Acids Res* **35:** 7188-7196.

342. **Purkhold U, Pommerening-Röser A, Juretschko S, Schmid MC, Koops HP, Wagner M.** (2000). Phylogeny of all recognized species of ammonia oxidizers based on comparative 16S rRNA and *amoA* sequence analysis: implications for molecular diversity surveys. *Appl Environ Microbiol* **66:** 5368-5382.

343. **Rahemtulla F, Lovtrup S.** (1975). Comparative biochemistry of invertebrate mucopolysaccharides. 3. *Oligochaeta* and *Hirudinea*. *Comp Biochem Physiol B, Biochem Mol Biol* **50:** 627-629.

344. **Rainey FA.** (2009a). Family V. *Lachnospiraceae* fam. nov. In: De Vos P, Garrity GM, Jones D, Krieg NR, Ludwig W, Rainey EA et al. (eds). *Bergey's Manual of Systematic Bacteriology*. Vol 3, 2nd edn. Springer: New York, pp 921-968.

345. **Rainey FA.** (2009b). Family VIII. *Ruminococcaceae* fam. nov. In: De Vos P, Garrity GM, Jones D, Krieg NR, Ludwig W, Rainey EA et al. (eds). *Bergey's Manual of Systematic Bacteriology*. Vol 3, 2nd edn. Springer: New York, pp 1016-1043.

346. **Rainey FA.** (2009c). Family X. *Veillonellaceae*. In: De Vos P, Garrity GM, Jones D, Krieg NR, Ludwig W, Rainey EA *et al*. (eds). *Bergey's Manual of Systematic Bacteriology*. Vol 3, 2nd edn. Springer: New York, pp 1059-1129.

347. **Rechkemmer G, Rönnau K, Engelhardt WV.** (1988). Fermentation of polysaccharides and absorption of short chain fatty acids in the mammalian hindgut. *Comp Biochem Physiol* **90:** 563-568.

348. **Reddell P, Spain AV.** (1991). Transmission of effective Frankia (Actinomycetales) propagules in casts of the endogeic earthworm *Pontoscolex corethrurus* (Oligochaeta, Glossoscolecidae). *Soil Biol Biochem* **23:** 775-778.

349. **Reddy GS, Nagy M, Garcia-Pichel F.** (2006). *Belnapia moabensis* gen. nov., sp. nov., an alphaproteobacterium from biological soil crusts in the Colorado Plateau, USA. *Int J Syst Evol Micr* **56:** 51-58.

350. **Reiche M, Torburg G, Küsel K.** (2008). Competition of Fe(III)reduction and methanogenesis in an acidic fen. *FEMS Microbiol Ecol* **65:** 88-101.

351. **Reiche M, Hädrich A, Lischeid G, Küsel K.** (2009). Impact of manipulated drought and heavy rainfall events on peat mineralization processes and source-sink functions of an acidic fen. *J Geophys Res* **114:** G02021.

352. **Rinne J, Riutta T, Pihlatie M, Aurela M, Haapanala S, Tuovinen J-P, Tuittila E-S, Vesala T.** (2007). Annual cycle of methane emission from aboreal fen measured by the eddy covariance technique. *Tellus* **59B:** 449-457.

353. **Robert C, Chassard C, Lawson PA, Bernalier-Donadille A.** (2007). *Bacteroides cellulosilyticus* sp. nov., a cellulolytic bacterium from the human gut microbial community. *Int J Syst Evol Micr* **57:** 1516-1520.

354. **Rodhe H.** (1990). A comparison of the contribution of various gases to the greenhouse-effect. *Science* **248:** 1217-1219.

355. **Rooney-Varga JN, Giewat MW, Duddleston KN, Chanton JP, Hines ME.** (2007). Links between archaeal community structure, vegetation type and methanogenic pathway in Alaskan peatlands. *FEMS Microbiol Ecol* **60:** 240-251.

356. **Rose TM, Schultz ER, Henikoff JG, Pietrokovski S, McCallum CM, Henikoff S.** 1998. Consensus-degenerate hybrid oligonucleotide primers for amplification of distantly related sequences. *Nucleic Acids Res* **26:** 1628-1635.

357. **Roulet NT, Kelly CA, Klinger LF, Moore TR, Protz R, Ritter JA, Rouse WR.** (1994). Role of the Hudson Bay Lowland as a source of atmospheric methane. *J Geophys Res* **99:** 1439-1454.

358. **Russell JB.** (1985). Fermentation of cellodextrins by cellulolytic and noncellulolytic rumen bacteria. *Appl Environ Microbiol* **49:** 572–576.

359. **Russell JB.** (1991). Intracellular pH of acid tolerant ruminal bacteria. *Appl Environ Microbiol* **57:** 3383-3384.

360. **Russell JB, Muck RE, Weimer PJ.** (2009). Quantitative analysis of cellulose degradation and growth of cellulolytic bacteria in the rumen. *FEMS Microbiol Ecol* **67:** 183–197.

361. **Saiki RK, Gelfand DH, Stoffel S, Scharf SJ, Higuchi R, Horn GT, Mullis KB, Erlich HA.** (1988). Primer-directed enzymatic amplification of DNA with a thermostable DNA polymerase. *Science* **239:** 487-489.

362. **Sakai S, Imachi H, Hanada S, Ohashi A, Harada H, Kamagata Y.** (2008) *Methanocella paludicola* gen. nov., sp. nov., a methane-producing archaeon, the first isolate of the lineage 'Rice Cluster I', and proposal of the new order *Methanocellales* ord. nov. *Int J Syst Evol Micr* **58:** 929-936.

363. **Sallam A, Steinbüchel A.** (2009). *Clostridium sulfidigenes* sp. nov., a mesophilic, proteolytic, thiosulfate-and sulfur-reducing bacterium isolated from pond sediment. *Int J Syst Evol Micr* **59:** 1661-1665.

364. **Sambrook J, Russell D.** (2001). Molecular cloning: A laboratory manual. 3rd ed. CSH press: Cold Spring Harbor.

365. **Samperdo L, Jeannotte R, Whalen JK.** (2006). Trophic transfer of fatty acids from gut microbiota to the earthworm *Lumbricus terrestris* L. *Soil Biol Biochem* **38:** 2188-2198.

366. **Samperdo L, Whalen JK.** (2007). Changes in the fatty acid profiles through the digestive tract of the earthworm *Lumbricus terrestris* L. *Appl Soil Ecol* **35:** 226-236.

367. **Sanger F, Nicklen S, Coulson AR.** (1977). DNA sequencing with chain-terminating inhibitors. *Proc Natl Acad Sci USA* **74:** 5463-5467.

368. **Sapra R, Bagramyan K, Adams MWW.** (2003). A simple energy-conserving system: proton reduction coupled to proton translocation. *Proc Natl Acad Sci USA* **100:** 7545-7550.

369. **Sauter M, Böhm R, Böck A.** (1992). Mutational analysis of the operon (*hyc*) determining hydrogenase 3 formation in *Escherichia coli*. *Mol Microbiol* **6:** 1523-1532.

370. **Sawers RG.** (2005). Formate and its role in hydrogen production in *Escherichia coli*. *Biochem Soc Trans* **33:** 42-46.

371. **Scheifinger CC, Wolin MJ.** (1973). Propionate formation from cellulose and soluble sugars by combined cultures of *Bacteroides succinogenes* and *Selenomonas ruminantium*. *Appl Microbiol* **26:** 789-795.

372. **Schellenberger S, Kolb S, Drake HL.** (2010). Metabolic responses of novel cellulolytic and saccharolytic agricultural soil *Bacteria* to oxygen. *Environ Microbiol* **12:** 845-861.

373. **Scheu S.** (1987). Microbial activity and nutrient dynamics in earthworm casts. *Biol Fertil Soils* **5:** 230-234.

374. **Schink B.** (1984). Fermentation of 2,3-butanediol by *Pelobacter carbinolicus* sp. nov. and *Pelobacter propionicus* sp. nov., and evidence for propionate formation from C2 compounds. *Arch Microbiol* 137: 33-41.

375. **Schink B.** (1994). Diversity, ecology, and isolation of acetogenic bacteria. In: Drake HL (ed). *Acetogenesis*. Chapman & Hall: New York, pp 273-302.

376. **Schink B.** (1997). Energetics of syntrophic cooperation in methanogenic degradation. *Microbiol Mol Biol Rev* **61:** 262-280.

377. **Schink B, Kremer DR, Hansen TA.** (1987). Pathway of propionate formation from ethanol in *Pelobacter propionicus*. *Arch Microbiol* **147:** 321-327.

378. **Schink B, Pfennig N.** (1982). *Propionigenium modestum* gen. nov. sp. nov. a new strictly anaerobic, nonsporing bacterium growing on succinate. *Arch Microbiol* **133:** 209-216.

379. **Schink B, Stams AJM.** (2013). Syntrophism among Prokaryotes. In: Rosenberg E, DeLong EF, Lory S, Stackebrandt E, Thompson F (eds). *The Prokaryotes*. Springer: Berlin, pp 471-493.

380. **Schink B, Zeikus JG.** (1980). Microbial methanol formation: a major end product of pectin metabolism. *Curr Microbiol* **4:** 387-389.

381. **Schloss PD, Handelsman J.** (2005). Introducing DOTUR, a computer program for defining operational taxonomic units and estimating species richness. *Appl Environ Microbiol* **71:** 1501-1506.

382. **Schmalenberger A, Drake HL, Küsel K.** (2007). High unique diversity of sulfate-reducing prokaryotes characterized in a depth gradient in an acidic fen. *Environ Microbiol* **9:** 1317-1328.

383. **Schmidt A, Müller N, Schink B, Schleheck D.** (2013). A proteomic view at the biochemistry of syntrophic butyrate oxidation in *Syntrophomonas wolfei*. *PloS one* **8:** e56905.

384. **Schmidt O.** (2008). Diversität bakterieller [Fe-Fe]-Hydrogenasen in einem sauren Niedermoor: Bedeutung für den intermediären H_2-Metabolismus. *Diploma thesis at the University of Bayreuth.*

385. **Schmidt O, Drake HL, Horn MA.** (2010). Hitherto unknown [FeFe]-hydrogenase gene diversity in anaerobes and anoxic enrichments from a moderately acidic fen. *Appl Environ Microbiol* **76:** 2027-2031.

386. **Schmidt O, Hink L, Horn MA, Drake HL.** (2016). Peat: Home to novel syntrophic species that feed acetate- and hydrogen-scavenging methanogens. *ISME J* (published online ahead of print; doi: 101038/ismej.2015.256).

387. **Schmidt O, Horn MA, Kolb S, Drake HL.** (2015). Temperature impacts differentially on the methanogenic food web of cellulose-supplemented peatland soil. *Environ Microbiol* **17:** 720-734.

388. **Schmidt O, Wüst PK, Hellmuth S, Borst K, Horn MA, Drake HL.** (2011). Novel [NiFe]- and [FeFe]-hydrogenase gene transcripts indicative of active facultative aerobes and obligate anaerobes in earthworm gut contents. *Appl Environ Microbiol* **77:** 5842-5850.

389. **Schnürer A, Zellner G, Svensson BH.** (1999). Mesophilic syntrophic acetate oxidation during methane formation in biogas reactors. *FEMS Microbiol Ecol* **29:** 249-261.

390. **Scholten JCM, Conrad R.** (2000). Energetics of syntrophic propionate oxidation in defined batch and chemostat cocultures. *Appl Environ Microbiol* **66:** 2934-2942.

391. **Schönholzer F, Hahn D, Zeyer J.** (1999). Origins and fate of fungi and bacteria in the gut of *Lumbricus terrestris* L. studied by image analysis. *FEMS Microbiol Ecol* **28:** 235-248.

392. **Schuchmann K, Müller V.** (2012). A bacterial electron-bifurcating hydrogenase. *J Biol Chem* **287:** 31165-31171.

393. **Schuchmann K, Müller V.** (2014). Autotrophy at the thermodynamic limit of life: a model for energy conservation in acetogenic bacteria. *Nat Rev Microbiol* **12:** 809-821.

394. **Schultz JE, Weaver PF.** (1982). Fermentation and anaerobic respiration by *Rhodospirillum rubrum* and *Rhodopseudomonas capsulate*. *J Bacteriol* **149:** 181-190.

395. **Schulz K, Hunger S, Brown GC, Tsai SM, Cerri CC, Conrad R, Drake HL.** (2015). Methanogenic food web in the gut contents of methane-emitting earthworm Eudrilus eugeniae from Brazil. *ISME J* **9:** 1778-1792.

396. **Schut GI, Adams MWW.** (2009). The iron-hydrogenase of *Thermotoga maritima* utilizes ferredoxin and NADH synergistically: a new perspective on anaerobic hydrogen production. *J Bacteriol* **191:** 4451-4457.

397. **Schwartz C.** (1973). Anaerobiosis and oxygen consumption of some strains of Propionibacterium and a modified method for comparing the oxygen sensitivity of various anaerobes. *Z Allg Mikrobiol* **13:** 681-691.

398. **Schwartz E, Fritsch J, Friedrich B.** (2013). H_2-metabolizing prokaryotes. In: Rosenberg E, DeLong E, Lory S, Stackebrandt E, Thompson F (eds). *The prokaryotes: prokaryotic physiology and biochemistry*. Vol 3, 4th ed. Springer: New York pp 120-199.

399. **Seitz H-J, Schink B, Pfennig N, Conrad R.** (1990). Energetics of syntrophic ethanol oxidation in defined chemostat cocultures. 1. Energy requirement for H_2 production and H_2 oxidation. *Arch Microbiol* **155:** 82-88.

400. **Seitz H-J, Schink B, Pfennig N, Conrad R.** (1990). Energetics of syntrophic ethanol oxidation in defined chemostat cocultures. 2. Energy sharing in biomass production. *Arch Microbiol* **155:** 89-93.

401. **Self WT, Hasona A, Shanmugam KT.** (2004). Expression and regulation of a silent operon, *hyf*, coding for hydrogenase 4 isoenzyme in *Escherichia coli*. *J Bacteriol* **186:** 580-587.

402. **Shi Y, Weimer PJ.** (1996). Utilization of individual cellodextrins by three predominant ruminal cellulolytic bacteria. *Appl Environ Microbiol* **62:** 1084-1088.

403. **Sieber JR, McInerney MJ, Gunsalus RP.** (2012). Genomic insights into syntrophy: the paradigm for anaerobic metabolic cooperation. *Annu Rev Microbiol* **66:** 429-452.

404. **Singleton DR, Hendrix PF, Coleman DC, Whitman WB.** (2003). Identification of uncultured bacteria tightly associated with the intestine of the earthworm *Lumbricus rubellus* (Lumbricidae; Oligochaeta). *Soil Biol Biochem* **35:** 1547-1555.

405. **Singh BK, Bardgett RD, Smith P, Ready DS.** (2010). Microorganisms and climate change: terrestrial feedbacks and mitigation options. *Nat Rev Microbiol* **8:** 779-790.

406. **Sizova MV, Panikov NS, Spiridonova EM, Slobodova NV, Tourova TP.** (2007). Novel facultative anaerobic acidotolerant *Telmatospirillum sibiriense* gen. nov., sp. nov. isolated from mesotrophic fen. *Syst Appl Microbiol* **30:** 213-220.

407. **Sizova MV, Panikov NS, Tourova TP, Flanagan PW.** (2003). Isolation and characterization of oligotrophic acido-tolerant methanogenic consortia from a Sphagnum peat bog. *FEMS microbiol ecol* **45:** 301-315.

408. **Sjörs H.** (1981). The zonation of northern peatlands and their importance for the carbon balance of the atmosphere. *Int J Ecol Environ Sci* **7:** 11-14.

409. **Smith EA, Macfarlane GT.** (1997). Dissimilatory amino acid metabolism in human colonic bacteria. *Anaerobe* **3:** 327-337.

410. **Smith RL, Ceazan ML, Brooks MH.** (1994). Autotrophic, hydrogen-oxidizing, denitrifying bacteria in groundwater, potential agents for bioremediation of nitrate contamination. *Appl Environ Microbiol* **60:** 1949-1955.

411. **Smith MR, Mah RA.** (1978). Growth and methanogenesis by *Methanosarcina* strain 227 on acetate and methanol. *Appl Environ Microbiol* **36:** 870-879.

412. **Soboh B, Linder D, Hedderich R.** (2004). A multisubunit membrane-bound [NiFe] hydrogenase and an NADH-dependent Fe-only hydrogenase in the fermenting bacterium *Thermoanaerobacter tengcongensis*. *Microbiology* **150:** 2451-2463.

413. **Soudzilovskaia NA, Cornelissen JH, During HJ, van Logtestijn RS, Lang SI, Aerts R.** (2010). Similar cation exchange capacities among bryophyte species refute a presumed mechanism of peatland acidification. *Ecology* **91:** 2716-26.

414. **Sousa DZ, Smidt H, Alves MM, Stams AJM.** (2007). *Syntrophomonas zehnderi* sp. nov., an anaerobe that degrades long-chain fatty acids in co-culture with *Methanobacterium formicicum*. *Int J Syst Evol Micr* **57:** 609-615.

415. **Spain AV, Saffigna PG, Wood AW.** (1990). Tissue carbon sources of *Pontoscolex corethrurus* (Oligochaeta: Glossoscolecidae) in a sugarcane ecosystem. *Soil Biol Biochem* **29:** 703-706.

416. **Sprenger WW, Hackstein JHP, Keltjens JT.** (2007). The competitive success of *Methanomicrococcus blatticola*, a dominant methylotrophic methanogen in the cockroach hindgut, is supported by high substrate affinities and favorable thermodynamics. *FEMS Micobiol Ecol* **60:** 266-275.

417. **Stackebrandt E, Ebers J.** (2006). Taxonomic parameters revisited: tarnished gold standards. *Microbiol Today* **33:** 152-155.

418. **Stackebrandt E, Goebel BM.** (1994). Taxonomic note: a place for DNA-DNA reassociation and 16S rRNA sequence analysis in the present species definition in bacteriology. *Int J Syst Bacteriol* **44:** 846-849.

419. **Stahl DA, Amann R.** (1991). Development and application of nucleic acid probes in bacterial systematic. In: Stackebrandt E, Goodfellow M (eds). *Nucleic acid techniques in bacterial systematic*. John Wiley & Sons: New York, pp 205-248.

420. **Stams AJ, Plugge CM.** (2009). Electron transfer in syntrophic communities of anaerobic bacteria and archaea. *Nat Rev Microbiol* **7:** 568-577.

421. **Stanier RY, Adams GA.** (1944). The nature of the *Aeromonas* fermentation. *J Bacteriol* **38:** 168-171.

422. **Stephen KD, Ara JRM, Daulat W, Clymo RS.** (1998). Root-mediated gas transport in the peat determined by argon diffusion. *Soil Biol Biogeochem* **30:** 501-508.

423. **Storch V, Welch U.** (1999). Kükenthals Leitfaden für das zoologische Praktikum. 24th edn. Spektrum Akademischer Verlag: Heidelberg.

424. **Ström L, Mastepanov M, Christensen TR.** (2005). Species-specific effects of vascular plants on carbon turnover and methane emissions from wetlands. *Biogeochemistry* **75:** 65-82.

425. **Stumm W, Morgan JJ.** (1981). Aquatic chemistry. An introduction emphasizing chemical equilibria in natural waters. Wiley: Chichester.

426. **Suen G, Weimer PJ, Stevenson DM, Aylward FO, Boyum J, Deneke J, *et al.*** (2011) The complete genome sequence of *Fibrobacter succinogenes* S85 reveals a cellulolytic and metabolic specialist. *PLoS ONE* **6:** e18814.

427. **Sumner ME.** (1999). Handbook of soil science. CRC press: Boca Raton.

428. **Šustr V, Šimek M.** (2009). Methane release from millipedes and other soil invertebrates in Central Europe. *Soil Biol Biochem* **41:** 1684–1688.

429. **Tamura K, Peterson D, Peterson N, Stecher G, Nei M, Kumar S.** (2011). MEGA5: molecular evolutionary genetics analysis using maximum likelihood, evolutionary distance, and maximum parsimony methods. *Mol Biol Evol* **28:** 2731-2739.

430. **Tard C, Pickett CJ.** (2009). Structural and functional analogues of the active sites of the [Fe]-, [NiFe]-, and [FeFe]-hydrogenases. *Chem Rev* **109:** 2245-2274.

431. **Thauer RK.** (1998). Biochemistery of methanogenesis: a tribute to Marjory Stephenson. *Microbiology* **144:** 2377-2406.

432. **Thauer RK, Jungermann K, Decker K.** (1977). Energy conservation in chemotrophic bacteria. *Bacteriol Rev* **41:** 100-180.

433. **Thauer RK, Kaster AK, Goenrich M, Schick M, Hiromoto T, Shima S.** (2010). Hydrogenases from methanogenic archaea, nickel, a novel cofactor, and H_2 storage. *Annu Rev Biochem* **79:** 507-536.

434. **Thauer RK, Kaster AK, Seedorf H, Buckel W, Heddrich R.** (2008). Methanogenic archaea: ecologically relevant differences in energy conservation. *Nat Rev Microbiol* **6:** 579-591.

435. **Thiele JH, Chartrain M, Zeikus JG.** (1988). Control of interspecies electron flow during anaerobic digestion: role of floc formation in syntrophic methanogenesis. *Appl Environ Microbiol* **54:** 10-19.

436. **Thiele JH, Zeikus JG.** (1988). Control of interspecies electron flow during anaerobic digestion: significance of formate transfer versus hydrogen transfer during syntrophic methanogenesis in flocs. *Appl Environ Microbiol* **54:** 20-29.

437. **Thompson JD, Higgins DG, Gibson TJ.** (1994). CLUSTAL W: improving the sensitivity of progressive multiple sequence alignment through sequence weighting, position-specific gap penalties and weight matrix choice. *Nucleic Acid Res* **22:** 4673-4680.

438. **Tillinghast EK, O'Donnell R, Eves D, Calvert E, Taylor J.** (2001). Water-soluble luminal contents of the gut of the earthworm *Lumbricus terrestris* L. and their physiological significance. *Compar Biol Physiol* **129:** 345-353.

439. **Titus E, Ahearn GA.** (1991). Transintestinal acetate transport in a herbivorous teleost: anion exchange at the basolateral membrane. *J Exp Biol* **156:** 41-61.

440. **Tiwari SC, Tiwar BK, Mishra RR.** (1989). Microbial populations, enzyme activities and nitrogen-phosphorus-potassium enrichment in earthworm casts and in the surrounding soil of a pineapple plantantion. *Biol Fertil Soils* **8:** 178-182.

441. **Trckova M, Matlova L, Hudcova H, Faldyna M, Zraly Z, Dvorska L, Beran V, Pavlik I.** (2005). Peat as a feed supplement for animals: a review. *Vet Med* **50:** 361-377.

442. **Trigo D, Barois I, Garvin MH, Huerta E, Irisson S, Lavelle P.** (1999). Mutualism between earthworms and soil microflora. *Pedobiologia* **43:** 866-873.

443. **Trchounian A, Sawers RG.** (2014). Novel insights into the bioenergetics of mixed-acid fermentation: Can hydrogen and proton cycles combine to help maintain a proton motive force? *IUBMB Life* **66:** 1-7.

444. **Tsutsuki K, Kuwatsuka S.** (1979). Chemical studies on soil humic acids. *Soil Sci Plant Nutr* **25:** 373-384.

445. **Tveit AT, Ulrich T, Frenzel P, Svenning MM.** (2015). Metabolic and trophic interactions modulate methane production by Arctic peat microbiota in response to warming. *Proc Natl Acad Sci USA* **112:** E2507-E2516.

446. **Ueki A, Akasaka H, Suzuki D, Ueki K.** (2006). *Paludibacter propionicigenes* gen. nov., sp. nov., a novel strictly anaerobic, Gram-negative, propionate-producing bacterium isolated from plant residue in irrigated rice-field soil in Japan. *Int J Syst Evol Micr* **56:** 39-44.

447. **Urakami T, Sasaki J, Suzuki KI, Komagata K.** (1995). Characterization and description of *Hyphomicrobium denitrifcans* sp. nov. *Int J Syst Microbiol* **45:** 528-532.

448. **Uren NC.** (2001). Types, amounts, and possible functions of compounds released into the rhizosphere by soil-grown plants. In: Pinton R, Varanini Z, Nannipieri P (eds). *The rhizosphere: biochemistry and organic substances at the soil-plant interface.* Marcel Dekker Inc: New York pp 19-40.

449. **Uz I, Ogram AV.** (2006). Cellulolytic and fermentative guilds in eutrophic soils of the Florida Everglades. *FEMS Microbiol Ecol* **57:** 396–408.

450. **Van de Werken HJG, Verhaart MRA, VanFossen AL, Willquist K, Lewis DL, Nichols JD et al.** (2008). Hydrogenomics of the extremly thermophilic bacterium *Caldicellulo-siruptor saccharolyticus. Appl Environ Microbiol* **74:** 6720-6729.

451. **Van Gylswyk NO, Hippe H, Rainey FA.** (1996). *Pseudobutyrivibrio ruminis* gen. nov., sp. nov., a butyrate-producing bacterium from the rumen that closely resembles *Butyrivibrio fibrisolvens* in phenotype. *Int J Syst Bacteriol* **46:** 559-563.

452. **Van Gylswyk NO, Van der Toorn JJTK.** (1985). *Eubacterium uniforme* sp. nov. and *Eubacterium xylanophilum* sp. nov., fibre-digesting bacteria from the rumina of sheep fed corn stover. *Int J Syst Bacteriol* **35:** 323-326.

453. **Van Niel EWJ, Budde MAW, de Haas GG, van der Wal FJ, Claassen PAM, Stams AJM.** (2002). Distinctive properties of high hydrogen producing extreme thermophiles, *Caldicellulosiruptor saccharolyticus* and *Thermotoga elfii*. *Int J Hydrogen Energ* **27:** 1391-1398.

454. **Vanwonterghem I, Jensen PD, Dennis PG, Hugenholtz P, Rabaey K, Tyson GW.** (2014). Deterministic processes guide long-term synchronized population dynamics in replicate anaerobic digesters. *ISME J* **8:** 2015-2028.

455. **Vanwonterghem I, Jensen PD, Rabaey K, Tyson GW.** (2015). Temperature and solids retention time control microbial population dynamics and volatile fatty acid production in replicated anaerobic digesters. *Sci Rep* **5:** 8496.

456. **Vardar-Schara G, Maeda T, Wood TK.** (2007). Metabolically engineered bacteria for producing hydrogen via fermentation. *Microbiol Biotechnol* **1:** 107-125.

457. **Veal DA, Lynch JM.** (1987). Associative cellulolysis and nitrogen fixation by co-cultures of *Trichoderma harzianum* and *Clostridium butyricum*: the effects of ammonium nitrogen on these processes. *J Appl Bacteriol* **63:** 245-253.

458. **Veldcamp H.** (1960). Isolation and characteristics of *Treponema zuelzerae* nov. spec., an anaerobic, free-living spirochete. *Anton Van Lee J M S* **26:** 103-125.

459. **Verhoeven JTA, Liefveld WM.** (1997). The ecological significance of organochemical compounds in Sphagnum. *Acta Bot Neer* **46:** 117–130.

460. **Vignais PM, Billoud B, Meyer J.** (2001). Classification and phylogeny of hydrogenases. *FEMS Microbiol Rev* **25:** 455-501.

461. **Vignais PM, Billoud B.** (2007). Occurrence, classification, and biological function of hydrogenases: an overview. *Chem Rev* **107:** 4206-4272.

462. **Von Stockar U, Liu JS.** (1999). Does microbial life feed on negative entropy? Thermodynamic analysis of microbial growth. *Biochim Biophys Acta* **1412:** 191-211.

463. **Wagner C, Grießhammer A, Drake HL.** (1996). Acetogenic capacities and the anaerobic turnover of carbon in a Kansas prairie soil. *Appl Environ Microbiol* **62:** 494-500.

464. **Walker TS, Bais HP, Grotewold E, Vivanco JM.** (2003). Root exudation and rhizosphere biology. *Plant Physiol* **132:** 44-51.

465. **Wang J, Hersketh JD, Wooley JT.** (1986). Preexisting channels and soybean rooting patterns. *Soil Sci* **141:** 432-437.

466. **Wang S, Huang H, Kahnt J, Mueller AP, Köpke M, Thauer RK.** (2013). NADP-specific electron-bifurcating [FeFe]-hydrogenase in a functional complex with formate dehydrogenase in *Clostridium autoethanogenum* grown on CO. *J Bacteriol* **195:** 4373-4386.

467. **Wang S, Huang H, Kahnt J, Thauer RK.** (2013). *Clostridium acidurici* electron-bifurcating formate dehydrogenase. *Appl Environ Microbiol* **79:** 6176-6179.

468. **Ward NL, Challacombe JF, Janssen PH, Henrissat B, Coutinho PM, Wu M, *et al*.** (2009). Three genomes from the phylum *Acidobacteria* provide insight into the lifestyles of these microorganisms in soil. *Appl Environ Microbiol* **75:** 2046-2056.

469. **Warikoo V, McInerney JM, Robinson JA, Suflita JM.** (1996). Interspecies acetate transfer influences the extent of anaerobic benzoate degradation by syntrophic consortia. *Appl Environ Microbiol* **62:** 26-32.

470. **Watkins NE, SantaLucia J.** (2005). Nearest-neighbor thermodynamics of deoxyinosine pairs in DNA duplexes. *Nucleic Acids Res* **33:**6258-6267.

471. **Weedon JT, Aertsa R, Kowalchuka GA, van Logtestijna R, Andringaa D, van Bodegom PM.** (2013). Temperature sensitivity of peatland C and N cycling: does substrate supply play a role? *Soil Biol Biochem* **61:** 109-120.

472. **Weimer PJ, Zeikus G.** (1977). Fermentation of cellulose and cellobiose by *Clostridium thermocellum* in the absence and presence of *Methanobacterium thermoautotrophicum*. *Appl Environ Microbiol* **33:** 289-297.

473. **Weller R, Weller JW, Ward DM.** (1991). 16S rRNA sequences of uncultivated hot spring cyanobacterial mat inhabitants retrieved as randomly primed complementary DNA. *Appl Environ Microbiol* **57:** 1146-1151.

474. **Wells JE, Russell JB, Shi Y, Weimer PJ.** (1995). Cellodextrin efflux by the cellulolytic ruminal bacterium *Fibrobacter succinogenes* and its potential role in the growth of nonadherent bacteria. *Appl Environ Microbiol* **61:** 1757-1762.

475. **Westermann P.** (1993). Wetland and swamp microbiology. In: Ford TE (ed). *Aquatic microbiology: an ecological approach.* Blackwell Publishers: Oxford, pp. 215-238.

476. **Westheide W, Rieger R.** (2007). Spezielle Zoologie Teil 1: Einzeller und Wirbellose Tiere. Spektrum Akademischer Verlag: Munich.

477. **Whiteley AS, Thomson B, Lueders T, Manefield M.** (2007). RNA stable isotope probing. *Nat Protoc* 2: 838-844.

478. **Wiegel J.** (2009). Family I. *Clostridiaceae*. In: De Vos P, Garrity GM, Jones D, Krieg NR, Ludwig W, Rainey EA *et al*. (eds). *Bergey's Manual of Systematic Bacteriology*. Vol 3, 2nd edn. Springer: New York, pp 736-864.

479. **Williams RT, Crawford RL.** (1983a). Effects of various physiochemical factors on microbial activity in peatlands: aerobic biodegradative processes. *Can J Microbiol* **29:** 1430-1437.

480. **Williams RT, Crawford RL.** (1983b). Microbial diversity of Minnesota peatlands. *Microb Ecol* **9:** 201-214.

481. **Williams RT, Crawford RL.** (1984). Methane production in Minnesota peatlands. *Appl Environ Microbiol* **50:** 1542-1544.

482. **Wolin MJ.** (1990). Rumen fermentation: biochemical interactions between the populations of a microbial community. In: Akin DE et al. (eds). *Microbial and plant opportunities to improve lignocellulose utilization by ruminants.* Elsevier Science Publications: New York, pp 237–251.

483. **Wood HG, Ljungdahl LG.** (1991). Autotrophic character of acetogenic bacteria. In: Shively JM, Barton LL (eds). *Variations in autotrophic life*. Academic Press: San Diego, pp 201-250.

484. **Wolter C, Scheu S.** (1999). Changes in bacterial numbers and hyphal length during the gut passage through *Lumbricus terrestris* (Lumbricidae, Oligochaeta). *Pedobiologia* **43:** 891-900.

485. **Worm P, Stams AJ, Cheng X, Plugge CM.** (2011). Growth- and substrate-dependent transcription of formate dehydrogenase and hydrogenase coding genes in *Syntrophobacter fumaroxidans* and *Methanospirillum hungatei*. *Microbiology* **157:** 280-289.

486. **Wu W-M, Jain MK, Zeikus JG.** (1994). Anaerobic degradation of normal- and branched-chain fatty acids with four or more carbons to methane by a methanogenic triculture. *Appl Environ Microbiol* **60:** 2220-2226.

487. **Wüst PK, Horn MA, Drake HL.** (2009a). Trophic links between fermenters and methanogens in a moderatley acidic fen soil. *Environ Microbiol* **11:** 1395-1409.

488. **Wüst PK, Horn MA, Drake HL.** (2009b). In situ hydrogen and nitrous oxide as indicators of concomitant fermentation and denitrification in the alimentary canal of the earthworm *Lumbricus terrestris*. *Appl Environ Microbiol* **75:** 1852-1859.

489. **Wüst PK, Horn MA, Henderson G, Janssen PH, Rehm BH, Drake HL.** (2009). Gut-associated denitrification and in vivo emission of nitrous oxide by the earthworm families *Megascolecidae* and *Lumbricidae* in New Zealand. *Appl Environ Microbiol* **75:** 3430-3436.

490. **Wüst PK, Horn MA, Drake HL.** (2011). *Clostridiaceae* and *Enterobacteriaceae* as active fermenters in earthworm gut content. *ISME J* **5:** 92-106.

491. **Wüst PK, Nacke H, Kaiser K, Marhan S, Sikorski J, Kandeler E *et al*.** (2016). Estimates of the bacterial ribosome content and diversity in soils are significantly affected by different nucleic acid extraction methods. *Appl Environ Microbiol* (published online ahead of print; doi: 10.1128/AEM.00019-16).

492. **Yarza P, Richter M, Peplies J, Euzéby J, Amann R, Schleifer KH, Ludwig W, Glöckner FO, Rosselló-Móra R.** (2008). The All-species living tree project: a 16S rRNA-based phylogenetic tree of all sequenced type strains. *Syst Appl Microbiol* **31:** 241-250.

493. **Yavitt JB, Seidman-Zager M.** (2006). Methanogenic conditions in northern peat soils. *Geomicrobiol J* **23:** 119-127.

494. **Zehnder AJB.** (1978). Ecology of methane formation. In: Mitchell R (ed). *Water Pollution Microbiology*, Vol. 2. John Wiley & Sons: London, pp 349-376.

495. **Zehnder AJB, Stumm W.** (1988). Geochemistry and biochemistry of anaerobic habitats. In: Zehnder AJB (ed). *Biology of anaerobic microorganisms*. John Wiley & Sons: New York, pp 1-38.

496. **Zhang C, Yang H, Yang F, Ma Y.** (2009). Current progress on butyric acid production by fermentation. *Curr Microbiol* **59:** 656-663.

497. **Zhang Z, Schwartz S, Wagner L, Miller W.** (2000). A greedy algorithm for aligning DNA sequences. *J Comput Biol* **7:** 203-214.

498. **Zeikus JG, Winfrey MR.** (1976). Temperature limitation of methanogenesis in aquatic sediments. *Appl Environ Microbiol* **31:** 99-107.

499. **Zinder SH.** (1993). Physiological ecology of methanogens. In: Ferry JG (ed). *Methanogens: Ecology, Physiology, Biochemistry and genetics*. Chapman & Hall: London, pp 128-206.

500. **Zinder SH.** (1994). Syntrophic acetate oxidation and "reversible acetogenesis". In: Drake HL (ed). *Acetogenesis*. Chapman & Hall: New York, pp 386-415.

501. **Zoltai SC, Pollett FC.** (1983). Wetlands in Canada: Their classification, distribution and use. In: Gore AJP (ed). *Ecosystems of the World (4B), Mires, Swamp, Bog, Fen and Moor*. Vol 2, Elsevier: Amsterdam, pp 245-268.

8. ACKNOWLEDGMENTS

First of all, I want to thank my supervisor Prof. Harold L. Drake for giving me the opportunity to work on versatile and interesting projects, for countless constructive and motivating discussions, for all the financial support, and of course for getting up on his soap box from where he kindly shared decades of life- and science-expieriences.

Special thank goes to PD Dr. Marcus Horn who was helpful on numerous occacions (e.g., paitiently introducing me into the world of ARB during my first breaths at the department).

Thanks also goes to PD Dr. Steffen Kolb for excellent discussions especially during the lab seminars.

I want to thank Linda Hink, Ralf Mertel, Maik Hilgarth, Katharina Borst, Susanne Hellmuth, and Natalie Potapow for all the work in the lab that was necessary to conduct all of the experiements.

To all the other (past and present) transient and permanent Ömiks, thank you for an unmatched positive working atmosphere. You were always supportive in the good and in the bad times.

And I want to thank the University of Bayreuth for financial support.

I thank Bernd Rehm for giving me the opportunity to come to his lab in New Zealand and I thank all the people in his lab and the Massey Mooloos for the great time in Aoteaora.

I have to further thank all the members of the C1-GRCs. For a guy who felt in love with thermodynamics, proton motive forces, and electron bifurcation, there is no better place to be.

And than there is the world outside the lab and outside science…

Thanks to all my team mates from Teutonia Netzschkau and the Team Doktorspiele at the Uni Bayreuth.

I thank all my friends for all the fun times over the years.

Special thanks goes to my family who always supported me in any critical and less critical situations.

And finally, I want to thank Nadine for the steady encouragements and the daily support.

9. PUBLICATIONS

Some of the information in this dissertation is based on information published in the following papers:

Schmidt O, Hink L, Horn MA, Drake HL. (2016). Peat: Home to novel syntrophic species that feed acetate- and hydrogen-scavenging methanogens. *ISME J* (published online ahead of print; doi: 101038/ismej.2015.256).

Hunger S, Schmidt O, Gößner AS, Drake HL. (2016). Formate-derived H_2, a driver of hydrogenotrophic processes in the root-zone of a methane-emitting fen. *Environ Microbiol* (published online ahead of print; doi: 10.1111/1462-2920.13301).

Schmidt O, Horn MA, Kolb S, Drake HL. (2015). Temperature impacts differentially on the methanogenic food web of cellulose-supplemented peatland soil. *Environ Microbiol* **17:** 720-734.

Schmidt O, Wüst PK, Hellmuth S, Borst K, Horn MA, Drake HL. (2011). Novel [NiFe]- and [FeFe]-hydrogenase gene transcripts indicative of active facultative aerobes and obligate anaerobes in earthworm gut contents. *Appl Environ Microbiol* **77:** 5842-5850.

Hunger S, Schmidt O, Hilgarth M, Horn MA, Kolb S, Conrad R, Drake HL. (2011). Competing formate- and carbon dioxide-utilizing prokaryotes in an anoxic methane-emitting fen soil. *Appl Environ Microbiol* **77:** 3773-3785.

Schmidt O, Drake HL, Horn MA. (2010). Hitherto unknown [FeFe]-hydrogenase gene diversity in anaerobes and anoxic enrichments from a moderately acidic fen. *Appl Environ Microbiol* **76:** 2027-2031.

In addition to the already published papers, one further manuscript is in preparation:

Zeibich L, Schmidt O, Drake HL. (2016). Ingested soil anaerobes feeding on disrupted microbial cells in the gut of *Lumbricus terrestris*. *In preparation.*

One paper was published that is not related to the experiments of this dissertation:

Hay ID, Schmidt O, Filitcheva J, Rehm BHA. (2012). Identification of a periplasmic AlgK-AlgX-MucD multiprotein complex in *Pseudomonas aeruginosa* involved in biosynthesis and regulation of alginate. *Appl Microbiol Biotechnol* **93:** 215-227.

10. (EIDESSTATTLICHE) VERSICHERUNGEN UND ERKLÄRUNGEN

(§ 5 Nr. 4 PromO)

Hiermit erkläre ich, dass keine Tatsachen vorliegen, die mich nach den gesetzlichen Bestimmungen über die Führung akademischer Grade zur Führung eines Doktorgrades unwürdig erscheinen lassen.

(§ 8 S. 2 Nr. 5 PromO)

Hiermit erkläre ich mich damit einverstanden, dass die elektronische Fassung meiner Dissertation unter Wahrung meiner Urheberrechte und des Datenschutzes einer gesonderten Überprüfung hinsichtlich der eigenständigen Anfertigung der Dissertation unterzogen werden kann.

(§ 8 S. 2 Nr. 7 PromO)

Hiermit erkläre ich eidesstattlich, dass ich die Dissertation selbständig verfasst und keine anderen als die von mir angegebenen Quellen und Hilfsmittel benutzt habe.

(§ 8 S. 2 Nr. 8 PromO)

Ich habe die Dissertation nicht bereits zur Erlangung eines akademischen Grades anderweitig eingereicht und habe auch nicht bereits diese oder eine gleichartige Doktorprüfung endgültig nicht bestanden.

(§ 8 S. 2 Nr. 9 PromO)

Hiermit erkläre ich, dass ich keine Hilfe von gewerblichen Promotionsberatern bzw. - vermittlern in Anspruch genommen habe und auch künftig nicht nehmen werde.

………………………………………………………………………………….

Ort, Datum, Unterschrift

11. APPENDICES

Table A1   16S rRNA and hydrogenase gene sequences from the GeneBank database used for primer design and threshold similarity calculations

Organism	GeneBank accession numbers			
	16S rRNA	Group 1 [NiFe]	Group 4 [NiFe]	[FeFe]
Abiotrophia defectiva ATCC 49176	ACIN02000013			EEP25573
Acetivibrio cellulolyticus CD2	L35516			EFL59652
Acetonema longum DSM 6540	AFGF01000106	EGO64044		
Acidaminococcus fermentans DSM 20731	X78017			ADB48307
Acidaminococcus sp. D21	ACGB01000071			EEH90332
Acidiphilum cryptum JF5	CP000697	ABQ29564		
Acidithiobacillus ferrooxidans ATCC 53993	CP001132	ACH85068		
Acidithiobacillus sp. GGI221	AEFB01001296	EGQ63604		
Acidobacterium capsulatum ATCC 51196	CP001472	ACO31874		
Actinobacillus pleuropneumoniae AP76	CP001091	ACE62037		
Actinobacillus succinogenes 130Z	CP000746	ABR74640		
Aeromonas caviae Ae398	AM184292	ZP_08520477		
Aeromonas hydrophila ATCC 7966	CP000462	ABK36783	ABK37281	
Aeromonas salmonicida A449	CP000644	ABO89869	ABO89889	
Aeromonas veronii B565	CP002607	AEB50179		
Aggregatibacter actinomycetemcomitans D11S1	M75038		ACX83106	
Aggregatibacter actinomycetemcomitans SC1083	AB512008	EGY34510		
Aggregatibacter aphrophilus NJ8700	CP001607	ACS97204	ACS97518	
Aggregatibacter segnis ATCC 33393	AEPS01000017	EFU67641		
Akkermansia muciniphila ATCC BAA835	CP001071	ACD05938		
Alistipes putredinis DSM 17216	ABFK02000016			EDS04615*
Alkalilimnicola ehrlichii MLHE1	CP000453	ABI57370		
Alkaliphilus metalliredigens QMF	CP000724			ABR50188*
				ABR46866*
Alkaliphilus oremlandii OhILAs	CP000853			ABW18477*
				ABW18537*
Allochromatium vinosum DSM 180	CP001896	ADC62958	EER67355	
		ADC63225		
Altermomonas macleodii Deep ecotype	CP001103	AEA96484		
Ammonifex degensii KC4	CP001785		ACX51701	ACX52870
				ACX52871
Anaerococcus hydrogenalis DSM 7454	ABXA01000039			EEB35646*
Anaerofustis stercorihominis DSM 17244	ABIL02000006			EDS71847*
Anaeromyxobacter dehalogans 2CPC	CP000251	ABC80254		
Anaeromyxobacter sp. Fw1095	CP000769	ABS24737		
		ABS27701		
Anaeromyxobacter sp. K	CP001131	ACG71750		
Anaerostipes caccae DSM 14662	ABAX03000023			EDR99311*
				EDR98979*
				EDR97978*
Anaerotruncus colihominis DSM 17241	ABGD02000032			EDS09197*
Aquifex aeolicus VF5	AE000657	AAC06861		
		AAC07046		
Arcobacter butzleri JV22	AEPT01000071	EFU68957		
		EFU68964		
Arcobacter nitrofigilis DSM 7299	CP001999	ADG91706		
		ADG93019		
		ADG93024		
Arsenophonus nasoniae SK14	M90801		CBA72198	
Azoarcus sp. BH72	AM406670	CAL96403		
Azorhizobium caulinodans ORS 571	AP009384	BAF86597		
Azospirillum amazonense Y2	AB568111	EGX99467		
Azospirillum sp. B510	AP010946	BAI75493		

Organism	GeneBank accession numbers			
	16S rRNA	Group 1 [NiFe]	Group 4 [NiFe]	[FeFe]
Azotobacter chroococcum MCD1	AB696770	CAA37134		
Azotobacter vinelandii DJ	CP001157	ACO81146		
Bacterioides caccae ATCC 43185	X83951			EDM20695*
Bacteroides capillosus ATCC 29799	AY136666			EDN01243*
				EDM99349*
Bacteroides intestinalis DSM 17393	ABJL02000008			EDV04390*
Bacteroides ovatus ATCC 8483	AB050108			EDO09736*
Bacteroides pectinophilus ATCC 43243	ABVQ01000036			EEC57378*
Bacteroides sp. 2_2_4	ABZZ01000168			EEO54032
Bacteroides sp. 3_1_19	ADCJ01000062	EFI09015		
Bacteroides sp. D1	ACAB01000173			EEO49244
Bacteroides sp. D2	ACGA01000077			ZP_05757528
Bacteroides thetaiotaomicron VPI5482	AE015928			AAO75231*
Beijerinckia indica ATCC 9039	CP001016	ACB94793		
Bilophila sp. 4_1_30	ADCO01000112	EGW42944		
		EGW43974		
Bilophila wadsworthia 3_1_6	ADCP01000166	EFV44255		
		EFV44642		
Blastocystis sp. NandIIb				ACD10930*
Blautia hansenii DSM 20583	ABYU01000028			EED58806*
Blautia hydrogenotrophica DSM 10507	ACBZ01000217			EEG50720
Bradyrhizobium japonicum USDA 110	BA000040	BAC46986		
		BAC52206		
Bradyrhizobium sp. BTAi1	CP000494	ABQ34188		
		ABQ39839		
Bradyrhizobium sp. ORS278	CU234118	CAL75562		
Burkholderia phymatum STM815	CP001043	ACC76258		
Burkholderia vietnamiensis G4	CP000614	ABO58857		
Caldanaerobacter subterraneus subsp. *pacificus* DSM 12653	ABXP01000200		EEB75698	EEB76457
Caldanaerobacter subterraneus subsp. *tengcongensis* MB4	AE008691		AAM23431	AAM24150*
			NP_623297	
Caldicellulosiruptor bescii DSM 6725	CP001393		ACM60187	EEB43498*
Caldicellulosiruptor saccharolyticus DSM 8903	CP000679		ABP67131	ABP67449*
Calditerrivibrio nitroreducens	CP002347	ADR18012		
Caminibacter mediatlanticus TB2	ABCJ01000002	EDM23779	EDM24561	
		EDM24031	EDM24040	
Campylobacter coli RM2228	AAFL01000001	EAL57408		
Campylobacter concisus 13826	CP000792	EAT97620	EAT98913	
Campylobacter curvus 525.92	CP000767	EAU00111	EAT99623	
Campylobacter fetus 8240	CP000487	ABK83093	ABK82203	
Campylobacter gracilis RM3268	ACYG01000026	EEV18132	EEV16988	
Campylobacter hominis ATCC BAA381	CP000776	ABS52559		
Campylobacter jejuni 81176	CP000538	EAQ72716		
Campylobacter lari RM2100	CP000932	ACM64042		
Campylobacter showae RM3277	ACVQ01000030	EET79938	EET79392	
Campylobacter upsaliensis JV21	AEPU01000040	EFU71732		
Campylobacterales bacterium GD 1	ABXD01000012		EDZ61142	
Candidatus Accumulibacter phosphatis clade IIA UW1	CP001715	ACV35577		
Candidatus Aciduliprofundum boonei T469	ABSD01000024		EDY37019	
Candidatus Cloacamonas acidaminovorans	CU466930			CAO81042*
Candidatus Desulforudis audaxviator MP104C	CP000860		ACA59613	ACA58722*
				ACA58720*
				ACA59846*
				ACA60050*
Candidatus Koribacter versatilis Ellin345	CP000360	ABF43240		
Candidatus Kuenenia stuttgartiensis	CT573071		CAJ72523	
Candidatus Solibacter usitatus Ellin6076	CP000473	ABJ87839		

Organism	GeneBank accession numbers			
	16S rRNA	Group 1 [NiFe]	Group 4 [NiFe]	[FeFe]
Carboxydibrachium pacificum DSM 12653b				EEB76457*
Carboxydothermus hydrogenoformans Z2901	CP000141		ABB14885	
Centipeda periodontii DSM 2778	AF458222	EGK61248		
Chlorobaculum parvum NCIB 8327	CP001099	ACF11699		
Chlorobium ferrooxidans DSM 13031	AASE01000013	EAT58409		
Chlorobium limicola DSM 245	CP001097	ACD89935		
Chlorobium luteolum DSM 273	AM050131	ABB24306		
Chlorobium phaeobacteroides BS1	CP001101	ACE04513		
Chloroherpeton thalassium ATCC 35110	CP001100	ACF15111		
Citreicella sp. SE45	ACNW01000104	EEX12879		
Citrobacter koseri ATCC BAA895	NR_102823	ABV15444	ABV15142	
Citrobacter rodentium ICC168	FN543502	CBG90254	CBG89819	
Citrobacter youngae ATCC 29220	AB273741	EFE05954		
	AB273741	EFE08022		
Clostridium acetobutylicum ATCC 824	AE001437			AAB03723*
Clostridium bartlettii DSM 16795	ABEZ02000021			EDQ97529*
				EDQ97512*
				EDQ95962*
				EDQ97666*
Clostridium beijerinckii NCIMB 8052	X68180			ABR36110*
				ABR35913*
				ABR36220*
				ABR33945*
Clostridium bolteae ATCC BAA613	AJ505482			EDP18661*
				EDP18642*
				EDP12448*
				EDP12468*
Clostridium botulinum E3 str. Alaska E43	L37592			ACD51739*
				ACD51579*
				ACD51947*
				ACD53356*
Clostridium butyricum	X68178			ABO42543*
				ABE76296*
Clostridium carboxidivorans P7	ADEK01000015			EET88267
Clostridium cellulolyticum H10	CP001348		ACL77656	ACL76574*
				EAV71737*
				ACC76640*
Clostridium cellulovorans 743B	X73438			EES30144
Clostridium difficile 630	X73450			CAJ70211*
				CAJ70310*
Clostridium hathewayi DSM13479	AJ311620			EFD01748
Clostridium hiranonis DSM 13275	AB023970			EEA85586*
Clostridium hylemonae DSM 15053	AB023973			EEC87176*
				EEC86762*
Clostridium klyveri DSM 555	CP000673			EDK34269*
				EDK32892*
Clostridium lentocelloum DSM5427	X71851			EFG99835
				EFH00280
Clostridium nexile DSM 1787	X73443			EEA80933*
				EEA83613*
Clostridium novyi NT	X68188			ABK61978*
				ABK60500*
Clostridium papyrosolvens DSM 2782	X71852		EEU59882	EEU58396
				EEU59818
				EEU57394
				EEU60511
Clostridium paraputrificum	X73445			BAD29951*
Clostridium pasteurianum	AB536773			AAA23248*
Clostridium perfringens C str. JGS1495	CP000246			EDS78838*

Organism	GeneBank accession numbers			
	16S rRNA	Group 1 [NiFe]	Group 4 [NiFe]	[FeFe]
Clostridium phytofermentans ISDg	CP000885		ABX42106	EDS80043* ABX44152* ABX40477* ABX42424*
Clostridium ramosum DSM 1402	ABFX02000008			EDS19309*
Clostridium saccharobutylicum	AM998793			AAA85785*
Clostridium saccharoperbutylacetonicum	U16122			AAV86076*
Clostridium scindens ATCC 35704	ABFY02000057			EDS05023* EDS06718* EDS06575*
Clostridium sp. L250				EDO58161*
Clostridium sp. M62/1	ACFX02000046			ZP_06346611
Clostridium sp. SS2/1	ABGC03000041			EDS20618*
Clostridium spiroforme DSM 1552	X73441			EDS74444*
Clostridium sporogenes ATCC 15579	X68189			EDU36979*
Clostridium thermocellum ATCC 27405	CP000568		ABN54216	ABN51580* ABN51668* ABN54199*
Clostridium tyrobutyricum JM1	M59113			ACI42788*
Collinsella aerofaciens ATCC 25986	AB011814		EBA40524	EBA39488*
Collinsella tanakaei YIT 12063	ADLS01000035	EGX70943		
Coprococcus comes ATCC 27758	ABVR01000038			EEG91467 EEG90163
Coprothermobacter proteolyticus DSM 5265	CP001145		ACI16934	ACI17295*
Corynebacterium amycolatum SK46	ABZU01000033	EEB63853		
Corynebacterium diphtheriae NCTC13129	CP003215	CAE49190		
Corynebacterium glucuronolyticum ATCC 51867	ABYP01000081	EEI25974		
Cronobacter sakazakii ATCC BAA894	EF088378		ABU77315	
Cronobacter turicensis z3032	EF059891		CBA30403	
Cryptobacterium curtum DSM 15641	CP001682	ACU94556	ACU94432 ACU93832	
Cupriavidus metallidurans CH34	CP000352	ABF08182		
Dechloromonas aromatica RCB	CP000089	AAZ48698 AAZ48715		
Dechlorosoma suillum PS	CP003153	EGW61456		
Deferribacter desulfuricans SSM1	AP011529	BAI79588		
Dehalococcoides ethenogenes 195	AX814128		AAW39859	AAW40508*
Dehalococcoides sp. BAV1	CP000688		ABQ17368	ABQ16813*
Dehalococcoides sp. CBDB1	AJ965256		CAI82992	CAI82422*
Dehalococcoides sp. GT	CP001924			ADC73542
Dehalococcoides sp. VS	ABFQ01000011		ACZ61901	EDO70419*
Denitrovibrio acetiphilus DSM 12809	CP001968	ADD67992 ADD69246		
Desulfarculus baarsii DSM 2075	CP002085	ADK84769		
Desulfatibacillum alkenivorans AK01	CP001322	ACL03969		
Desulfitobacterium hafniense DCB2	AF403181		ACL22289	BAE86501* BAE82725*
Desulfitobacterium hafniense Y51	AP008230	BAE84028		
Desulfobacterium autotrophicum HRM2	CP001087	ACN15334		
Desulfobulbus propionicus DSM 2032	CP002364	ADW19453		
Desulfohalobium retbaense DSM 5692	CP001734	ACV67568		
Desulfomicrobium baculatum DSM 4028	CP001629	ACU88885		
Desulfotalea psychrophila LSv54	CR522870	CAG35304		CAG35208*
Desulfotomaculum acetoxidans DSM 771	ABTQ01000001		ACV61704	EEN16608 ACV64533
Desulfotomaculum reducens MI1	CP000612			ABO49009* ABO51790* ABO50179* ABO50182*

Organism	GeneBank accession numbers			
	16S rRNA	Group 1 [NiFe]	Group 4 [NiFe]	[FeFe]
Desulfovibrio aespoeensis Aspo2	CP002431	ADU63581		
Desulfovibrio aespoeensis DSM 10631	X95230		EFA67421	
Desulfovibrio alaskensis G20	CP000112	ABB40549		
		ABB38935		
Desulfovibrio desulfuricans ATCC 27774	CP001358	ACL48744	ACL49568	ABB99078*
		ACL48945	ACL49781	ABB37276*
				AAK11625*
Desulfovibrio fructosovorans JJ	AECZ01000068	EFL49300		CAA72423*
				AAA87057*
Desulfovibrio gigas	DQ447183		AAP51029	
Desulfovibrio magneticus RS1	AP010904	BAH75051	BAH73768	BAH73739
				BAH74274
Desulfovibrio piger ATCC 29098	AF192152	EEB32528	EEB32729	
Desulfovibrio salexigens DSM 2638	CP001649	ACS79977	YP_002992827	EEC62363*
				EEC59248*
Desulfovibrio sp. 3_1_syn3	ADDR01000239	EFL85988		
		EFL86218		
Desulfovibrio sp. 6_1_46AFAA	ACWM01000085	EGW52406		
Desulfovibrio sp. A2	AGFG01000025	EGY25754		
		EGY27556		
Desulfovibrio sp. FW1012B	ADFE01000082		EFC18761	EFC19500
Desulfovibrio vulgaris Miyazaki F	CP001197	ACL07227		
		ACL08678		
Desulfovibrio vulgaris Hildenborough	AF418179		AAS94913	AAS96246*
			AAS96764	AAS96248*
Desulfurispirillum indicum S5	CP002432	ADU65820		
Desulfurivibrio alkaliphilus AHT2	CP001940	ADH85599		
Desulfurobacterium thermolithotrophum DSM 11699	CP002543	ADY73108		
Desulfurococcus kamchatkensis 1221n	EU167539		ACL11347	
			ACL10743	
Dethiobacter alkaliphilus AHT 1	EF422412			EEG77316
Dethiosulfovibrio peptidovorans DSM 11002	ABTR01000010		EEK27429	
Dialister invisus DSM 15470	ACIM01000043		EEW97982	
Dickeya dadantii 3937	CP002038	ADM99253	ACZ77465	
Dickeya zeae Ech1591	CP001655	ACT06275	ACT07540	
Dictyoglomus thermophilum H612	CP001146			ACI81165*
Dictyoglomus turgidum DSM 6724	CP001251			ACK41850*
Dorea formicigenerans ATCC 27755	AAXA02000015			EDR47355*
				EDR46534*
Dorea longicatena DSM 13814	AJ132842			EDM62429*
Edwardsiella ictaluri 93146	CP001600	ACR69825	ACR70412	
		ACR70545		
Edwardsiella tarda EIB202	CP001135	ACY85199	ACY85728	
		ACY85833		
Eggerthella lenta DSM 2243	CP001726	ACV55246	ACV55542	
Eggerthella sp. YY7918	AP012211	BAK44398		
Elusimicrobium minutum Pei191	CP001055		ACC98682	ACC98088*
Endosymbiont of *Riftia pachyptila*	AFOC01000137	EGV51840		
Endosymbiont of *Tevnia jerichonana*	AFZB01000059	EGW53439		
Enterobacter aerogenes IAM1183	AJ251468		ABQ42614	
Enterobacter cancerogenus ATCC 35316	Z96079		ZP_05970021	
Enterobacter cloacae SCF1	CP002272	ADO48716		
Enterobacter radicincitans DIV140	AY563134		CBB97123	
Enterobacter sp. 638	CP000653		ABP61858	
Escherichia albertii TW07627	ABKX01000012	EDS90078	EDS93944	
Escherichia coli K12 substr. MG1655	ANWG01000004	AAC74058	AAC75763	
		AAC76030	AAC75540	
Escherichia fergusonii ATCC 35469	CU928158	CAQ88640	CAQ88231	
Escherichia sp. 4_1_40B	ACDM02000056	ZP_05437191		

Organism	GeneBank accession numbers			
	16S rRNA	Group 1 [NiFe]	Group 4 [NiFe]	[FeFe]
Ethanoligenens harbinense YUAN3	AY295777			EFD40314
Eubacterium acidaminophilum	AF071416			CAC39231*
Eubacterium eligens ATCC 27750	L34420			ACR71237
Eubacterium hallii DSM 3352	ACEP01000116			EEG37282
Eubacterium siraeum DSM 15702	ABCA03000043			EDS00330*
Ferrimonas balearica DSM 9799	CP002209	ADN75300		
Fervidobacterium nodosum Rt17B1	CP000771			ABS60092*
				ABS60103*
Flavobacterium johnsoniae UW101	CP000685	ABQ06918		
Flexistipes sinusarabici DSM 4947	CP002858	AEI14334		
		AEI14618		
Frankia sp. EAN1pec	CP000820	ABW12806		
Frankia sp. EUN1f	ADGX01000271	EFC80541		
Fusobacterium gonidiaformans ATCC 25563	ACET01000043			ZP_05630409
Fusobacterium mortiferum ATCC 9817	ACDB01000061			EEO35500
Fusobacterium sp. 3_1_5R	ACDD01000078			ZP_05617405
Fusobacterium sp. D12	ACDG01000169			ZP_05627425
Fusobacterium ulcerans ATCC 49185	ACDH01000090			ZP_05633280
Fusobacterium varium ATCC 27725	ACIE01000009			EES65225
Geobacillus sp. Y4.1MC1	CP002293	ADP74797		
Geobacillus thermoglucosidasius C56YS93	CP002835	AEH48076		
Geobacter bemidjiensis Bem	CP001124	ACH38387	ACH37100	
		ACH40138		
Geobacter lovleyi SZ	CP001089	ACD93883		
		ACD95771		
Geobacter metallireducens GS15	CP000148	ABB33544		
Geobacter sp. M18	CP002479	ADW11942	EET35469	EET35462
		ADW12702		
		ADW14550		
Geobacter sp. M21	CP001661	ACT17187		
		ACT18944		
Geobacter sulfurreducens KN400	CP002031	ADI82960		
Geobacter uraniireducens Rf4	CP000698	ABQ24758	ABQ25011	
		ABQ25079		
		ABQ26136		
Glaciecola sp. 4H37+YE5	CP002526	AEE25410		
Gordonibacter pamelaeae 7101b	FP929047	CBL04553		
Haemophilus haemolyticus M21127	AFQP01000035	EGT74314		
Haemophilus parainfluenzae ATCC 33392	AEWU01000024	EGC73072		
Haemophilus pittmaniae HK 85	AFUV01000004	EGV04852		
Haliscomenobacter hydrossis DSM 1100	CP002691	AEE49707		
Halorhabdus utahensis DSM 12940	ABTZ01000001		ACV12394	
Halothermothrix orenii H 168	CP001098			EAR78776*
				EAR79475*
				ACL69059*
Helicobacter acinonychis Sheeba	AM260522	CAJ99542		
Helicobacter bilis ATCC 43879	ACDN01000023	EEO24116		
Helicobacter bizzozeronii CIII1	FR871757	CCB80005		
Helicobacter canadensis MIT 985491	ABQS01000108	EFR48731		
Helicobacter cinaedi CCUG 18818	ABQT01000054	EFR46581		
Helicobacter felis ATCC 49179	FQ670179	CBY83366		
Helicobacter hepaticus ATCC 51449	AE017125	AAP76654		
Helicobacter mustelae 12198	M35048	CBG40247		
Helicobacter pullorum MIT 985489	ABQU01000097	EEQ62631		
Helicobacter pylori F57	AP011945	BAJ59730		
Helicobacter suis HS1	ADGY01000105	EFX42983		
Helicobacter winghamensis ATCC BAA430	ACDO01000013	EEO25716		
Heliobacillus mobilis	AB100835			CAJ44289*
Heliobacterium modesticaldum Ice1	CP000930	ABZ82825		ABZ83545*

Organism	GeneBank accession numbers			
	16S rRNA	Group 1 [NiFe]	Group 4 [NiFe]	[FeFe]
Hippea maritima DSM 10411	CP002606	ABZ84052 AEA34063		
Holdemania filiformis DSM 12042	Y11466			EEF67834*
Hydrogenimonas thermophila EP1551%	AB105048	BAH02018		
Hydrogenivirga sp. 1285R11	ABHJ01000001	EDP75031 EDP75720		
Hydrogenobacter thermophilus TK6	AP011112	BAI68562 BAI69471		
Hydrogenobaculum sp. Y04AAS1	CP001130	ACG56745		
Hydrogenovibrio marinus	D86374	BAK19334		
Hyphomicrobium sp. MC1	FQ859181	CCB63689		
Jonquetella anthropi E3_33 E1	ACOO02000004			EEX48260
Klebsiella oxytoca HP1	U78183		ABR12482	
Klebsiella pneumoniae MGH 78578	CP000647		ABR78459	
Kosmotoga olearia TBF 19.5.1	EU980631		ACR79287	
Labrenzia aggregata IAM 12614	AAUW01000023	EAV40966		
Laribacter hongkongensis HLHK9	AF389085			ACO75311
Lawsonia intracellularis PHE/MN100	AM180252	CAJ54494		
Magnetococcus marinus MC1	CP000471	ABK45003		
Magnetospirillum gryphiswaldense MSR1	CU459003	CAM75723		
Magnetospirillum magneticum AMB1	AP007255	BAE50451		
Magnetospirillum magnetotacticum MS1	Y10110	ZP_00052632		
Mannheimia succiniciproducens MBEL55E	AE016827	AAU38968		
Marichromatium purpuratum 984	AFWU01000015	EGV22308 EGV23964		
Marinitoga piezophila KA3	AF326121			EEB81756*
Megamonas hypermegale ART12/1	AJ420107	CBL05748		
Megasphaera elsdenii	U95027			AAF22114*
Methanobrevibacter smithii ATCC 35061	CP000678		ABQ86517 ABQ87268	
Methanocaldococcus fervens AG86	AF056938		ACV24169 ACV23967	
Methanocaldococcus jannaschii DSM 2661	L77117		AAB98504 AAB99031	
Methanocaldococcus vulcanius M7	AF051404		ACX72347 ACX72499	
Methanocella paludicola SANAE	AB196288		BAI60595 BAI62712	
Methanococcus aeolicus Nankai3	CP000743		ABR55958 ABR55894	
Methanococcus maripaludis S2	BX950229		CAF31018 CAF30709	
Methanococcus vannielii SB	CP000742		ABR54679 ABR54380	
Methanocorpusculum labreanum Z	AF095267		ABN06746 ABN07129	
Methanoculleus marisnigri JR1	M59134		ABN57115 ABN56293	
Methanopyrus kandleri AV19	M59932		AAM01678	
Methanoregula boonei 6A8	CP000780		ABS54552	
Methanosarcina barkeri Fusaro	AF028692		AAZ69133	
Methanosarcina mazei Go1	X69874		AAM32020	
Methanosphaera stadtmanae DSM 3091	CP000102		ABC57814	
Methanosphaerula palustris E19c	CP001338		ACL17991	
Methanospirillum hungatei JF1	M60880		ABD41812 ABD41467 ABD42287	
Methanothermobacter thermautotrophicus Delta H	Z37156		AAB84904 AAB85727	

Organism	GeneBank accession numbers			
	16S rRNA	Group 1 [NiFe]	Group 4 [NiFe]	[FeFe]
Methylacidiphilum infernorum V4	AM900833	ACD83374		
Methylibium petroleiphilum PM1	CP000555	ABM95780		
Methylococcus capsulatus Bath	AE017282	AAU90583		
Methylocystis sp. ATCC 49242	AEVM01000005	EFX98064		
Methylomonas methanica MC09	CP002738	AEG00196		
Methylosinus trichosporium OB3b	ADVE01000118	EFH02837		
Methyloversatilis universalis FAM5	AFHG01000027	EGK70321		
Mitsuokella multacida DSM 20544	ABWK02000005	EEX69175		EEC93934*
Mobiluncus curtisii ATCC 43063	CP001992	ADI67100		
Mobiluncus mulieris ATCC 35243	ACKW01000035	EEJ53163		
Moorella thermoacetica ATCC 39073	CP000232		ABC20475	ABC20019* ABC20183*
Mucilaginibacter paludis DSM 18603	AEIH02000003	EFQ73191		
Nautilia profundicola AmH	CP001279	ACM92168	ACM92209 ACM93715	
Neocallimatrix frontalis				AAK60409*
Neptuniibacter caesariensis MED92	AY136116	EAR61269		
Nitratifractor salsuginis DSM 16511	CP002452	ADV45348		
Nitratiruptor sp. SB1552	AP009178	BAF70074		
Novosphingobium nitrogenifigens DSM 19370	AEWJ01000057	EGD60642		
Nyctotherus ovalis				AAU14235* CAA76373*
Oligotropha carboxidovorans OM5	CP002826	AEI08137		
Opitutus terrae PB901	AJ229235		ACB77392	ACB74828*
Oscillochloris trichoides DG6	ADVR01000146	EFO80542		
Parabacteroides distasonis ATCC 8503	CP000140	ABR43551		ABR42810*
Parabacteroides johnsonii DSM 18315	ABYH01000014			EEC97198*
Parabacteroides merdae ATCC 43148	EU136586			EDN84324*
Paracoccus denitrificans PD1222	CP000490	ABL71179		
Parasutterella excrementihominis YIT 11859	AFBP01000029	EGG57582		
Pasteurella dagmatis ATCC 43325	M75051		EEX50402	
Pectobacterium atrosepticum SCRI1043	BX950851	CAG74138	CAG74151	
Pelagibaca bermudensis HTCC2601	AATQ01000003	EAU46677		
Pelobacter carbinolicus DSM 2380	CP000142			ABA88877* ABA88849* ABA89741*
Pelobacter propionicus DSM 2379	CP000482		YP_903174 YP_902443 YP_900284	ABK99106*
Pelodictyon phaeoclathratiforme BU1	CP001110	ACF44087		
Pelotomaculum thermopropionicum SI	AB035723			BAF58849* BAF60191* BAF59558*
Peptostreptococcus anaerobius 653L	AY326462			EFD04254
Persephonella marina EXH1	AF188332	ACO03535		
Petrotoga mobilis SJ95	Y15479			ABX31447* ABX31867*
Photobacterium angustum S14	AY900628	EAS64810		
Photobacterium damselae CIP 102761	ADBS01000001	EEZ41179	EEZ39259	
Photobacterium profundum 3TCK	DQ027054		EAS44663	
Piromyces sp. E2				AAL90459*
Polaromonas naphthalenivorans CJ2	CP000529	ABM37283		
Prosthecochloris aestuarii DSM 271	CP001108	ACF45900		
Proteus mirabilis ATCC 29906	ACLE01000013	EEI46552	CAR44989	
Proteus penneri ATCC 35198	ABVP01000020	EEG84707	EEG86883	
Providencia alcalifaciens DSM 30120	ABXW01000071	EEB45846	EEB46381	
Providencia rettgeri DSM 1131	ACCI02000101	EFE54495		
Providencia rustigianii DSM 4541	AM040489	EFB72814	EFB72310	
Pseudotrichonympha grassii				BAF82036*

Organism	GeneBank accession numbers			
	16S rRNA	Group 1 [NiFe]	Group 4 [NiFe]	[FeFe]
Psychromonas sp. CNPT3	DQ027056		EAS39386	
Pyramidobacter piscolens W5455	EU309492		EFB91372	EFB89727
Pyrococcus abyssi GE5	AY099167		NP_126404	
			CAB50378	
Pyrococcus furiosus DSM 3638	AE009950		AAL81558	
Pyrococcus horikoshii OT3	D45214		BAA30544	
Ralstonia eutropha H16	AM260479	AAP85758		
Rhizobium leguminosarum UPM791	AY509900	CAA37149		
Rhodobacter capsulatus SB 1003	CP001312	ADE84533		
Rhodobacter sp. SW2	ACYY01000039	EEW24942		
		EEW25312		
Rhodobacter sphaeroides 2.4.1	CP000143	ABA79667		
Rhodoferax ferrireducens T118	CP000267	ABD71789		
Rhodomicrobium vannielii ATCC 17100	CP002292	ADP70241		
Rhodopseudomonas palustris BisA53	CP000463	ABJ05184		
Rhodopseudomonas palustris BisB18	AB498818		ABD90092	ABJ07787*
			ABD90024	
Rhodospirillum rubrum ATCC 11170	CP000230	ABC21963	ABC21121	
			ABC22226	
Roseiflexus castenholzii DSM 13941	CP000804	ABU59201		
Roseiflexus sp. RS1	CP000686	ABQ90699		
Roseovarius sp. TM1035	ABCL01000005	EDM30628		
Ruminococcus gnavus ATCC 29149	X94967			EDN76601*
Ruminococcus lactaris ATCC 29176	ABOU02000049			EDY34146
Ruminococcus obeum ATCC 29174	X85101			EDM86254*
Ruminococcus torques ATCC 27756	AAVP02000002			EDK25445*
Sagittula stellata E37	AAYA01000001	EBA05805		
Salmonella bongori NCTC 12419	FR877557	CCC30452		
		CCC30723		
		CCC31798		
Salmonella enterica serovar Typhimurium 14028S	X80681		ACY89857	
Salmonella enterica serovar Paratyphi A ATCC 9150	CP000026	AAV77264		
		AAV78851		
Sebaldella termitidis ATCC 33386	ABUO01000016			EEP36362
Selenomonas artemidis F0399	GQ422716	EFW28714		
Selenomonas flueggei ATCC 43531	AF287803	EEQ49256		
Selenomonas infelix ATCC 43532	ACZM01000023	EHG21561		
Selenomonas noxi F0398	ADGH01000012	EHG24722		
Selenomonas sp. oral taxon 137 str. F0430	AENV01000002	EFR39968		
Selenomonas sputigena ATCC 35185	ACKP02000033	EEX77124		EEX77934
Serratia odorifera 4Rx13	AJ233432		EFA15879	
Serratia proteamaculans 568	CP000826		ABV41531	
Shewanella amazonensis SB2B	CP000507	ABL99884		
Shewanella baltica OS117	CP002811	AEH13746		
Shewanella decolorationis S12	FJ589032	ABL07495		ABD48098*
Shewanella frigidimarina NCIMB 400	CP000447	ABI71950		
Shewanella halifaxensis HAWEB4	CP000931	ABZ76821		ABZ75974*
Shewanella loihica PV4	CP000606	ABO23630		
Shewanella oneidensis MR1	AE014299	AAN55145		AAN56895*
Shewanella pealeana ATCC 700345	CP000851	ABV87352		
Shewanella piezotolerans WP3	AJ551090	ACJ29375		
Shewanella sediminis HAWEB3	AJ551090	ABV36518		
Shewanella sp. ANA3	CP000469			ABK46949*
Shewanella sp. MR4	CP000446	ABI38895		ABI40318*
Shewanella sp. MR7	CP000444	ABI43144		
Shewanella sp. W3181	CP000503	ABM24758		
Shigella boydii 521682	AFGE01000015	EGI91794		
Shigella boydii CDC 308394	CP001063		ACD09395	
			ACD10019	

Organism	GeneBank accession numbers			
	16S rRNA	Group 1 [NiFe]	Group 4 [NiFe]	[FeFe]
Shigella dysenteriae Sd197	CP000034	ABB63095	ABB62946	
Shigella dysenteriae Sd197	CP000034		ABB62726	
Shigella flexneri 2a str. 2457T	AE014073		AAP18056	
Shigella flexneri 5 8401	CP000266	ABF05112		
Shigella sonnei 53G	ADUU01000047	EFZ53847		
Shigella sonnei Ss046	CP000038		AAZ89472	
			AAZ89197	
Sideroxydans lithotrophicus ES1	CP001965	ADE11850		
Slackia exigua ATCC 700122	ACUX02000005	EEZ61275	EEZ61671	
Slackia heliotrinireducens DSM 20476	CP001684	ACV22318	ACV22361	ACV22672
Staphylothermus marinus F1	X99560		ABN69134	
			ABN70159	
Subdoligranulum variabile DSM 15176	ACBY01000115		EFB75401	EFB75894
Sulfobacillus acidophilus TPY	CP002901	AEJ40416		
Sulfuricurvum kujiense DSM 16994	CP002355	ADR34711		
		ADR34716		
Sulfurihydrogenibium azorense AzFu1	AF528192	ACN99030		
Sulfurimonas autotrophica DSM 16294	CP002205	ADN09357		
Sulfurimonas denitrificans DSM 1251	CP000153	ABB44712		
Sulfurimonas gotlandica GD1	AFRZ01000001	EDZ61592		
		EDZ61659		
		EDZ61663		
Sulfurospirillum deleyianum DSM 6946	CP001816	ACZ12129	ACZ12881	
Sulfurovum sp. NBC371	AP009179	BAF72603		
		BAF72612		
Sutterella wadsworthensis 3_1_45B	ADMF01000048	EFW02846		
Symbiobacterium thermophillum IAM 14863	AP006840			BAD42191*
				BAD42274*
Syntrophobacter fumaroxidans MPOB	CP000478	ABK18626		ABK16545*
				ABK16541
Syntrophomonas wolfei Goettingen	DQ666175			ABI69222*
				ABI69725*
				ABI68331*
Syntrophus acidotrophicus SB	CP000252			ABC76974*
Thermanaerovibrio acidaminovorans DSM 6589	ABUW01000006			EEP4294
Thermoanaerobacter ethanolicus CCSD1	L09162			EEU63102
Thermoanaerobacter italicus Ab9	AJ250846		EET56929	EET56892
Thermoanaerobacter mathranii A3	Y11279		EET64481	EET63443
Thermoanaerobacter pseudethanolicus ATCC 33223	CP000924			ABY95106*
Thermoanaerobacter sp. X514	CP000923			ABY93410*
Thermoanaerobacterium saccharolyticum JW/SLYS485	L09169		ACA51666	ACA51661*
Thermoanaerobacterium thermosaccharolyticum DSM 571	FJ465165		EET54167	EET54977
Thermococcus barophilus MP	AY099172		EDY41627	
			EDY41343	
			EDY41719	
Thermococcus gammatolerans EJ3	CP001398		ACS32538	
			ACS32746	
			ACS32561	
Thermococcus kodakarensis KOD1	D38650		BAD86280	
Thermococcus litoralis DSM 5473	AY099180		ABW05546	
Thermococcus onnurineus NA1	CP000855		ACJ17083	
			ACJ15761	
Thermococcus sibiricus MM 739	CP001463		ACS90352	
			ACS90338	
Thermococcus sp. AM4	ABXN01000014		EEB73628	
			EEB73425	
Thermocrinis albus DSM 14484	CP001931	ADC89740		
		ADC90045		

Organism	GeneBank accession numbers			
	16S rRNA	Group 1 [NiFe]	Group 4 [NiFe]	[FeFe]
Thermodesulfatator indicus DSM 15286	CP002683	AEH44173		
Thermodesulfobacterium sp. OPB45	CP002829	AEH22983		
Thermodesulfovibrio yellowstonii DSM 11347	CP001147	ACI21456	ACI21046	ACI22150* ACI20377*
Thermofilum pendens Hrk 5	X14835		ABL77593 ABL78470	
Thermosinus carboxydivorans Nor1	AAWL01000016	EAX46314 EAX46613	EAX48205	EAX48145*
Thermosipho africanus TCF52B	DQ657057			ACJ75249* ACJ76239*
Thermosipho melanesiensis BI429	Z70248			ABR30357* ABR31445*
Thermotoga lettingae TMO	AF355615			ABV33518* ABV33907*
Thermotoga maritima MSB8	M21774			AAD36496* AAD35293*
Thermotoga neapolitana DSM4359	CP000916			ACM23243*
Thermotoga petrophila RKU1	AJ872269			ABQ47381* ABQ46743*
Thermotoga sp. RQ2	AJ872273			ABC09663* ACB09099*
Thermotogales bacterium TBF 19.5.1b				EEB54378*
Thermovibrio ammonificans HB1	CP002444	ADU97088		
Thioalkalivibrio sulfidophilus HLEbGr7	CP001339	ACL72352		
Thioalkalivibrio thiocyanoxidans ARh 4	AGFB01000001	EGZ34490		
Thiobacillus denitrificans ATCC 25259	CP000116	AAZ97328		
Thiocapsa marina 5811	AFWV01000002	EGV20327 EGV20369		
Thiocapsa roseopersicina BBS	AF112998	AAC38282		
Thiocystis violascens DSM 198	CP003154	EGZ46833 EGZ50170 EGZ38182 EGZ46931		
Thiomicrospira crunogena XCL2	CP000109	ABB42627		
Thiomonas intermedia K12	CP002021	ADG32405		
Thiorhodococcus drewsii AZ1	AFWT01000001	EGV32883 EGV33622 EGV33659		
Thiorhodospira sibirica ATCC 700588	AGFD01000020	EGZ50867		
Thiorhodovibrio sp. 970	AFWS02000055	EGZ52773 EGZ53354 EGZ54324		
Treponema denticola ATCC 30405	AE017226			AAS12110*
Trichomonas vaginalis G3				EAY17406* EAY19300* EAY23026*
uncultured methanogenic archaeon RCI	AM114193		CAJ37062 CAJ35909	
uncultured Parabasalid eukaryote				BAF82038*
uncultured Termite group1 bacterium phylotype RsD17				BAG14005*
Veillonella atypica ACS134VCol7a	AEDS01000059	EFL57821		
Veillonella dispar ATCC 17748	ACIK02000004	EEP65753		
Veillonella parvula ATCC 17745	ADFU01000009	EFB85382		
Veillonella sp. 6_1_27	ADCW01000016	EFG25700		
Veillonella sp. oral taxon 158 str. F0412	AENU01000007	EFR60886		
Veillonella sp. oral taxon 780 str. F0422	AFUJ01000023	EGS38836		
Vibrio furnissii CIP 102972	X76336		EEX41800	
Victivallis vadensis ATCC BAA548	ABDE01000031			EDM95131* EDM95636*

Organism	GeneBank accession numbers			
	16S rRNA	Group 1 [NiFe]	Group 4 [NiFe]	[FeFe]
Wolinella succinogenes DSM 1740	BX571657	CAA46303	CAE10852	
Xanthobacter autotrophicus Py2	CP000781	ABS67418		
Yersinia aldovae ATCC 35236	AF366376	EEP95197	EEP97130	
Yersinia bercovieri ATCC 43970	AB682283	EEQ06478	EEQ07006	
Yersinia enterocolitica subsp. enterocolitica 8081	M59292		CAL12837	
Yersinia enterocolitica subsp. palearctica Y11	FR729477	CBY25779		
Yersinia frederiksenii ATCC 33641	AF366379	EEQ13283	EEQ14814	
Yersinia intermedia ATCC 29909	AF366380	EEQ18538	EEQ18748	
Yersinia kristensenii ATCC 33638	ACCA01000078	EEP92066	EEP93037	
Yersinia mollaretii ATCC 43969	AF366382	EEQ08984	EEQ08775	
Yersinia rohdei ATCC 43380	ACCD01000071	EEQ00964	EEQ04074	
Yersinia ruckeri ATCC 29473	EU401667		EEP98895	

*Sequences were used for the design of [FeFe]-hydrogenase primers.

Table A2   Phylogenetic affiliation and relative abundances of bacterial family-level and subfamily-level OTUs observed in [^{13}C]cellulose treatments.

Phylogenic Affiliation of OTUs [a]	OTU	Reference Sequence (Acc. no.)	Closest related sequence (Acc. no.)	Max. ident. [%]	Closest cultured relative (Acc. no.)	Max. ident. [%]	Relative Abundance of OTUs in clone library [b]						
							total	15°C				5°C	
								$t_{40}H$	$t_{40}L$	t_0H	t_0L	$t_{80}H$	$t_{80}L$
Acidobacteria							19.7	19.4	24.0	16.4	30.0	10.7	19.0
Acidobacteria							17.0	8.8	23.4	13.9	30.0	10.1	17.2
Acidobacteriales (Subdivision 1)													
Acidobacteriaceae	3						8.9	8.8	9.4	6.1	13.3	9.5	6.9
	3a	150LH12 (HG324378)	Uncultered bacterium (FR732377)	99	Bacterium K-5b2 (AF524860)	95	1.5	0.0	3.5	0.6	5.3	0.0	2.9
	3b	15EHF18 (HG324491)	Uncultered bacterium (JF309192)	95	*Candidatus* Koribacter versatilis Ellin345 (CP000360)	93	0.6	3.5	0.0	0.0	0.0	4.8	0.0
	3c	15ELH23 (HG324551)	Uncultered bacterium (GU127747)	99	*Candidatus* Koribacter versatilis Ellin345 (CP000360)	94	1.4	0.0	4.1	1.8	2.7	0.0	2.9
	3d	150LB20 (HG324591)	Uncultered bacterium (HQ598096)	95	*Acidobacterium capsulatum* (CP001472)	93	0.1	0.0	0.0	0.0	0.7	0.0	0.0
	3e	15EHA5 (HG324381)	Uncultered bacterium (FR720621)	99	*Telmatobacter bradus* (AM887760)	98	1.9	4.1	1.2	2.4	4.0	4.8	1.1
	3f	150HC11 (HG324450)	Uncultered bacterium (HQ599053)	97	*Edaphobacter modestus* (DQ528760)	91	0.6	1.2	0.6	1.2	0.7	0.0	0.0
Subdivision 2	7	150LD12 (HG324356)	Uncultered bacterium (GU127790)	99	*Acidobacterium capsulatum* (CP001472)	84	2.5	0.0	7.6	1.2	6.0	0.0	0.6
Subdivision 3	5	150HE2 (HG324432)	Uncultered bacterium (EF125937)	98	*Solibacter usitatus* (CP000473)	98	4.7	0.0	6.4	4.8	9.3	0.6	7.5
Subdivision 6	65	150HA20 (HG324554)	Uncultered bacterium (AY963342)	99	*Holophaga foetida* (NR_036891)	82	0.3	0.0	0.0	1.2	0.0	0.0	0.6
Subdivision 13	81	150LG21 (HG324780)	Uncultered bacterium (AB364765)	99	*Symbiobacterium thermophilum* (AP006840)	84	0.4	0.0	0.0	0.0	0.7	0.0	1.7
Subdivision 15	52	150HC16 (HG324649)	Uncultered bacterium (HQ597963)	98	*Acidobacterium capsulatum* (CP001472)	86	0.2	0.0	0.0	0.6	0.7	0.0	0.0
Holophagae													

Phylogenic Affiliation of OTUs [a]	OTU	Reference Sequence (Acc. no.)	Closest related sequence (Acc. no.)	Max. ident. [%]	Closest cultured relative (Acc. no.)	Max. ident. [%]	Relative Abundance of OTUs in clone library [b]						
							total	15°C				5°C	
								$t_{40}H$	$t_{40}L$	t_0H	t_0L	$t_{80}H$	$t_{80}L$
Holophagales (Subdivision 8)													
Holophagaceae	8						2.7	10.6	0.6	2.4	0.0	0.6	1.7
	8a	150HB18 (HG324553)	Uncultered bacterium (GQ339218)	99	*Geothrix fermentans* (NR_036779)	96	0.8	0.0	0.0	2.4	0.0	0.6	1.7
	8b	15EHG2 (HG324848)	Uncultered bacterium (AM409822)	97	*Holophaga foetida* (NR_036891)	93	1.9	10.6	0.6	0.0	0.0	0.0	0.0
Actinobacteria													
Actinobacteria							5.2	1.2	12.9	3.6	8.0	0.6	5.2
Acidimicrobiales													
Acidimicrobiaceae	18	15ELA1 (HG324864)	Uncultered bacterium (GU127806)	99	*Aciditerrimonas ferrireducens* (AB517669)	93	1.1	0.6	2.3	0.6	2.0	0.0	1.1
Actinomycetales													
Thermomonosporaceae	10	150LE1 (HG324357)	Uncultered bacterium (FR732204)	100	*Actinoallomurus purpureus* (NR_041651)	95	3.1	0.6	7.0	1.8	4.7	0.6	4.0
Coriobacteriales													
Coriobacteriaceae	73	150HD20 (HG324567)	Uncultered bacterium (JX505359)	99	*Atopobium vaginae* (AJ585206)	88	0.1	0.0	0.0	0.6	0.0	0.0	0.0
Gaiellales													
Gaiellaceae	37	150LE23 (HG324607)	Uncultered bacterium (AB659065)	96	*Gaiella occulta* (JF423906)	87	0.4	0.0	0.6	0.6	1.3	0.0	0.0
Solirubrobacterales													
Conexibacteraceae	26	15ELE7 (HG324313)	Uncultered bacterium (JF145738)	98	*Conexibacter arvalis* (AB597950)	95	0.5	0.0	2.9	0.0	0.0	0.0	0.0
Bacteroidetes							10.9	22.4	2.3	12.7	0.0	20.8	5.7
Bacteroida													
Bacteroidales													
Porphyromonadaceae	9	150HF16 (HG324577)	Uncultered bacterium (JN626532)	99	*Paludibacter propionigenes* (NR_074577)	99	4.4	9.4	0.0	2.4	0.0	12.5	1.7

Phylogenic Affiliation of OTUs [a]	OTU	Reference Sequence (Acc. no.)	Closest related sequence (Acc. no.)	Max. ident. [%]	Closest cultured relative (Acc. no.)	Max. ident. [%]	Relative Abundance of OTUs in clone library [b]						
							total	15°C				5°C	
								$t_{40}H$	$t_{40}L$	t_0H	t_0L	$t_{80}H$	$t_{80}L$
Prolixibacter-related *Bacteroidetes*	4						5.1	11.8	2.3	4.8	0.0	7.7	3.4
	4a	15ELF7 (HG324338)	Uncultered bacterium (HM141899)	99	Bacterium PB90-2 (AJ229236)	95	2.9	7.6	2.3	2.4	0.0	1.8	2.9
	4c	5BEL1F07 (HG325250)	Uncultered bacterium (HQ178850)	99	*Prolixibacter bellariivorans* (AB541983)	89	0.2	0.0	0.0	0.0	0.0	0.6	0.6
	4b	15EHB11 (HG324797)	Uncultered bacterium (EF562547)	94	*Prolixibacter bellariivorans* (AB541983)	88	2.0	4.1	0.0	2.4	0.0	5.4	0.0
Sphingobacteria							1.3	1.2	0.0	5.5	0.0	0.6	0.6
Sphingobacteriales							0.7	0.0	0.0	3.0	0.0	0.6	0.6
Chitinophagaceae	79	150HH7 (HG324718)	Uncultered bacterium (FJ475457)	98	*Niastella populi* (EU877262)	94	0.2	0.0	0.0	0.6	0.0	0.0	0.6
Sphingobacteriaceae	23	150HB17 (HG324642)	Uncultered bacterium (FR732370)	98	*Solitalea koreensis* (NR_044568)	87	0.5	0.0	0.0	2.4	0.0	0.6	0.0
Unclassified *Sphingobacteria* I	51	15EHD4 (HG324389)	Uncultered bacterium (AB237705)	86	*Alkaliflexus imshenetskii* (NR_042317)	84	0.1	0.6	0.0	0.0	0.0	0.0	0.0
Unclassified *Sphingobacteria* II	55	15EHH16 (HG324501)	Uncultered bacterium (JX505131)	98	*Cytophaga fermentans* (AB517712)	86	0.3	0.6	0.0	1.2	0.0	0.0	0.0
Unclassified *Sphingobacteria* III	70	150HG14 (HG324696)	Uncultered bacterium (JN626598)	90	*Paludibacter propionigenes* (NR_074577)	89	0.1	0.0	0.0	0.6	0.0	0.0	0.0
Unclassified *Sphingobacteria* IV	78	150HF10 (HG324681)	Uncultered bacterium (AM945454)	99	*Solitalea koreensis* (NR_044568)	88	0.1	0.0	0.0	0.6	0.0	0.0	0.0
Chlorobi													
Ignavibacteria													
Ignavibacteriales													
Ignavibacteriaceae	74	150LA22 (HG324589)	Uncultered bacterium (AB364876)	99	*Ignavibacterium album* (NR_074698)	85	0.3	0.0	0.0	0.0	0.7	0.0	1.1
Chloroflexi							2.1	1.8	1.8	1.2	4.7	0.6	2.9
Anaerolineae													
Anaerolineales													

Phylogenic Affiliation of OTUs [a]	OTU	Reference Sequence (Acc. no.)	Closest related sequence (Acc. no.)	Max. ident. [%]	Closest cultured relative (Acc. no.)	Max. ident. [%]	Relative Abundance of OTUs in clone library [b]						
								15°C				5°C	
							total	$t_{40}H$	$t_{40}L$	t_0H	t_0L	$t_{80}H$	$t_{80}L$
Anaerolineaceae	64	150LC10 (HG324735)	Uncultered bacterium (GQ860297)	99	Leptolinea tardivitalis (NR_040971)	92	0.2	0.0	0.6	0.0	0.7	0.0	0.0
Ktedonobacteria							0.6	0.6	0.6	0.6	0.0	0.6	1.1
Ktedonobacterales													
Ktedonobacteraceae	61	150HA15 (HG324630)	Uncultered bacterium (FJ037000)	99	Ktedonobacter racemifer (NR_042472)	92	0.3	0.6	0.0	0.6	0.0	0.0	0.6
Unclassified Ktendobacteria	84	15ELE13 (HG324918)	Uncultered bacterium (AM773926)	99	Ktedonobacter racemifer (NR_042472)	89	0.3	0.0	0.6	0.0	0.0	0.6	0.6
Unclassified Chloroflexi I	29	15EHA17 (HG324461)	Uncultered bacterium (FR732102)	99	Bellilinea caldifistulae (NR_041354)	82	0.8	1.2	0.0	0.0	2.0	0.0	1.7
Unclassified Chloroflexi II	41	150LC2 (HG32460)	Uncultered bacterium (AB658204)	97	Thermanaerothrix daxensis (HM596746)	84	0.3	0.0	0.0	0.0	2.0	0.0	0.0
Unclassified Chloroflexi III	50	15ELH6 (HG324327)	Uncultered bacterium (DQ450737)	99	Acidimicrobium ferrooxidans (NR_074390)	83	0.2	0.0	0.6	0.6	0.0	0.0	0.0
Firmicutes							12.5	12.9	3.5	8.5	3.3	38.7	7.5
Bacilli													
Bacillales							0.4	0.0	0.6	0.6	1.3	0.0	0.0
Bacillaceae	90	150LH10 (HG324377)	Uncultered bacterium (EU773370)	99	Bacillus psychrosaccharolyticus (AB681415)	99	0.1	0.0	0.0	0.0	0.7	0.0	0.0
Paenibacillaceae	30	15ELB3 (HG324308)	Uncultered bacterium (HQ764278)	99	Paenibacillus xylanilyticus (NR_029169)	99	0.3	0.0	0.6	0.6	0.7	0.0	0.0
Clostridia							12.0	12.9	2.9	7.9	2.0	38.1	7.5
Clostridiales							11.9	12.9	2.9	7.9	1.3	38.1	7.5
Clostridiaceae	6						9.3	7.1	1.8	4.8	0.7	34.5	6.3
	6a	15EHD20 (HG324468)	Uncultered bacterium (AM159328)	99	Clostridium puniceum (NR_026105)	99	1.6	2.4	0.0	3.0	0.7	3.6	0.0
	6b	15ELF14 (HG324538)	Uncultered bacterium (FJ542892)	98	Clostridium acidisoli (NR_028898)	98	7.3	2.9	1.2	1.8	0.0	31.0	6.3

| Phylogenic Affiliation of OTUs [a] | OTU | Reference Sequence (Acc. no.) | Closest related sequence (Acc. no.) | Max. ident. [%] | Closest cultured relative (Acc. no.) | Max. ident. [%] | Relative Abundance of OTUs in clone library [b] | | | | | | |
| | | | | | | | total | 15°C | | | | 5°C | |
								$t_{40}H$	$t_{40}L$	t_0H	t_0L	$t_{80}H$	$t_{80}L$
	6c	15ELE5 (HG324925)	Uncultered bacterium (AM159328)	99	Clostridium frigoris (NR_036822)	99	0.1	0.0	0.6	0.0	0.0	0.0	0.0
	6d	15EHG10 (HG324844)	Uncultered bacterium (AB487631)	98	Clostridium cylindrosporum (Y18179)	93	0.3	1.8	0.0	0.0	0.0	0.0	0.0
Lachnospiraceae	63	150HE21 (HG324676)	Uncultered bacterium (EU181081)	99	Roseburia faecis (AB661433)	96	0.1	0.0	0.0	0.6	0.0	0.0	0.0
Peptococcaceae	31	15ELA6 (HG324332)	Uncultered bacterium (HM481392)	98	Desulfosporosinus lacus (NR_042202)	97	0.5	0.6	1.2	0.6	0.0	0.0	0.6
Ruminococcaceae	15						2.0	5.3	0.0	1.8	0.7	3.6	0.6
	15a	15EHH5 (HG324403)	Uncultered bacterium (AM159453)	97	Clostridium cellulosi (FJ465164)	94	1.8	5.3	0.0	1.2	0.0	3.6	0.6
	15b	150LD5 (HG324752)	Uncultered bacterium (FM956748)	98	Sporobacter termitidis (NR_044972)	95	0.2	0.0	0.0	0.6	0.7	0.0	0.0
Thermoanaerobacterales													
Thermoanaerobacteraceae	80	150LF22 (HG324774)	Uncultered bacterium (AB486478)	99	Clostridium tertium (AB689162)	90	0.1	0.0	0.0	0.0	0.7	0.0	0.0
Negativicutes													
Selenomonadales													
Veillonellaceae	97	5BEH1F11 (HG325190)	Uncultered bacterium (AB486409)	99	Psychrosinus fermentans (DQ767881)	98	0.1	0.0	0.0	0.0	0.0	0.6	0.0
Lentisphaerae													
Lentisphaeria													
Victivallales													
Victivallaceae	68	15ELD22 (HG324908)	Uncultered bacterium (HM481332)	97	Victivallis vadensis (JQ346729)	85	0.2	0.6	0.6	0	0	0	0
Planctomycetes							5.3	1.8	6.4	4.8	4.0	0.0	14.4
Planctomycea	13												
Planctomycetales													
Planctomycetatceae							5.0	1.8	6.4	3.6	4.0	0.0	13.8

Phylogenic Affiliation of OTUs [a]	OTU	Reference Sequence (Acc. no.)	Closest related sequence (Acc. no.)	Max. ident. [%]	Closest cultured relative (Acc. no.)	Max. ident. [%]	Relative Abundance of OTUs in clone library [b]						
								15°C				5°C	
							total	t40H	t40L	t0H	t0L	t80H	t80L
	13a	15ELA5 (HG324306)	Uncultered bacterium (HQ265093)	97	*Gemmata* sp. SD2-6 (GQ889476)	91	2.0	0.0	4.7	1.8	1.3	0.0	4.0
	13b	150LA7 (HG324345)	Uncultered bacterium (EF667618)	97	*Pirellula staleyi* (NR_074521)	86	0.8	0.6	0.0	1.2	2.7	0.0	0.6
	13c	150HB7 (HG324426)	Uncultered bacterium (JX504972)	99	*Singulisphaera rosea* (FN391026)	92	1.9	0.0	1.8	0.6	0.0	0.0	8.6
	13d	15EHD14 (HG324816)	Uncultered bacterium (EU344930)	99	*Schlesneria paludicola* (NR_042466)	87	0.3	1.2	0.0	0.0	0.0	0.0	0.6
Unclassified *Planctomycetes* I	57	150HH22 (HG324712)	Uncultered bacterium (HQ496487)	98	*Phycisphaera mikurensis* (NR_074491)	77	0.1	0.0	0.0	0.6	0.0	0.0	0.0
Unclassified *Planctomycetes* II	89	150HG3 (HG324702)	Uncultered bacterium (AM774208)	100	*Phycisphaera mikurensis* (NR_074491)	81	0.1	0.0	0.0	0.6	0.0	0.0	0.0
Unclassified *Planctomycetes* III	98	5BEL2E07 (HG325286)	Uncultered bacterium (EF018297)	97	*Candidatus* Brocadia fulgida (EU478693)	82	0.1	0.0	0.0	0.0	0.0	0.0	0.6
Proteobacteria							26.8	4.7	36.8	46.7	40.0	1.8	32.2
Alphaproteobacteria							14.1	3.5	22.8	28.5	16.7	0.6	13.2
Caulobacterales													
Caulobacteraceae	54	150HB5 (HG324444)	Uncultered bacterium (JF223137)	98	*Phenylobacterium immobile* (NR_026498)	97	0.2	0.0	0.6	0.6	0.0	0.0	0.0
Rhizobiales							10.3	1.8	12.9	22.4	15.3	0.0	10.3
	2						10.0	1.8	12.9	20.6	15.3	0.0	10.3
unclassified *Rhizobiales* I	2a	150HH5 (HG324458)	uncultured Bacterium (HM488704)	99	*Methylocystis* sp. H2s (FN422003)	95	1.6	1.8	0.6	1.8	2.7	0.0	2.9
Beijerinkiaceae	2b	150HG7 (HG324437)	Uncultered bacterium (HE614759)	99	*Methylocapsa aurea* (FN433469)	99	2.6	0.0	4.1	5.5	4.7	0.0	1.7
Bradyrhizobiaceae-Rhodoblastus	2c	15ELF10 (HG324320)	Uncultered bacterium (FR732224)	99	*Rhodoblastus acidophilus* (JN399240)	98	0.7	0.0	1.2	1.8	0.7	0.0	0.6

Phylogenic Affiliation of OTUs [a]	OTU	Reference Sequence (Acc. no.)	Closest related sequence (Acc. no.)	Max. ident. [%]	Closest cultured relative (Acc. no.)	Max. ident. [%]	Relative Abundance of OTUs in clone library [b]						
							total	15°C				5°C	
								$t_{40}H$	$t_{40}L$	t_0H	t_0L	$t_{80}H$	$t_{80}L$
Methylocystaceae	2d	15ELF3 (HG324317)	Uncultured bacterium (DQ202242)	99	*Methylocystis heyeri* (AM283543)	99	1.1	0.0	1.8	3.6	1.3	0.0	0.0
Unclassified *Rhizobiales* II	2e	15ELA4 (HG324331)	Uncultured bacterium (EU359939)	99	*Blastochloris sulfoviridis* (NR_037121)	94	0.2	0.0	0.6	0.0	0.7	0.0	0.0
Bradyrhizobiaceae	2f	150HD5 (HG324430)	Uncultured bacterium (GQ402719)	100	*Bradyrhizobium elkanii* (EU481825)	99	1.1	0.0	1.2	1.8	2.0	0.0	1.7
Unclassified *Rhizobiales* III	2g	150LB5 (HG324349)	Uncultured bacterium (AY913267)	99	*Rhodoplanes elegans* (NR_029125)	95	1.4	0.0	2.3	1.2	1.3	0.0	3.4
Hyphomicrobiaceae-Rhodomicrobium	2h	150LF1 (HG324363)	Uncultered bacterium (AB364708)	99	*Rhodomicrobium vanielii* (AM691111)	98	1.0	0.0	1.2	3.0	2.0	0.0	0.0
Unclassified *Rhizobiales* IV	47	150LH17 (HG324787)	Uncultered bacterium (JQ384371)	98	*Bradyrhizobium japonicum* (NR_074322)	90	0.3	0.0	0.0	1.8	0.0	0.0	0.0
Rhodospirillales							3.6	1.8	9.4	5.5	1.3	0.6	2.9
Acetobacteraceae	11	15ELA2 (HG324866)	Uncultered bacterium (GU127727)	99	*Acidisphaera rubrifaciens* (NR_037119)	94	1.7	1.2	3.5	2.4	0.7	0.6	1.7
Rhodospirillaceae	27	150HG10 (HG324439)	Uncultered bacterium (GU270803)	99	*Telmatospirillum siberiense* (NR_041925)	99	0.5	0.0	1.8	1.2	0.0	0.0	0.0
Unclassified *Rhodospirillales* I	14	15ELG4 (HG324322)	Uncultered bacterium (FR732495)	99	*Azospirillum amazonense* (HM485596)	90	1.1	0.6	3.5	1.2	0.0	0.0	1.1
Unclassified *Rhodospirillales* II	59	150LH8 (HG324376)	Uncultered bacterium (AB364710)	99	*Dongia mobilis* (FJ455532)	92	0.2	0.0	0.0	0.6	0.7	0.0	0.0
Unclassified *Rhodospirillales* III	71	15ELF23 (HG324933)	Uncultered bacterium (EU360041)	96	*Azospirillum amazonense* (HM485596)	91	0.1	0.0	0.6	0.0	0.0	0.0	0.0
Betaproteobacteria							3.7	1.2	2.3	7.9	4.7	0.0	6.3
Burkholderiales							0.7	0.0	0.0	1.2	2.0	0.0	1.1
Comamonadaceae	28	150LG23 (150LG23)	Uncultured bacterium (JN626527)	99	*Albidiferax ferrireducens* (NR_074760)	98	0.5	0.0	0.0	1.2	2.0	0.0	0.0
Unclassified *Burkholderiales*	93	5BEL1F01 (HG325102)	Un bacterium (GQ402786)	99	*Ralstonia eutropha* (CP000091)	93	0.2	0.0	0.0	0.0	0.0	0.0	1.1

Phylogenic Affiliation of OTUs [a]	OTU	Reference Sequence (Acc. no.)	Closest related sequence (Acc. no.)	Max. ident. [%]	Closest cultured relative (Acc. no.)	Max. ident. [%]	Relative Abundance of OTUs in clone library [b]						
							total	15°C				5°C	
								$t_{40}H$	$t_{40}L$	t_0H	t_0L	$t_{80}H$	$t_{80}L$
Gallionellales													
Gallionellaceae	16	150HE17 (HG324570)	Uncultered bacterium (GQ339210)	98	*Sideroxydans lithotrophicus* (DQ386859)	96	1.3	0.0	1.2	1.2	1.3	0.0	4.0
Hydrogenophilales													
Hydrogenophilaceae	46	150HF23 (HG324691)	Uncultered bacterium (JQ723670)	99	*Ferritrophicum radicicola* (DQ386263)	96	0.5	0.0	0.0	1.8	0.7	0.0	0.6
Neisseriales													
Neisseriaceae	36	15EHF15 (HG324837)	Uncultered bacterium (GU270675)	99	*Paludibacterium yongneupense* (AB682439)	99	0.4	0.6	0.0	1.8	0.0	0.0	0.0
Rhodocyclales													
Rhodocyclaceae	24	150HB8 (HG324446)	Uncultered bacterium (JN697733)	99	*Uliginosibacterium gangwonense* (AB682440)	99	0.6	0.6	0.0	1.8	0.7	0.0	0.6
Unclassified *Betaproteobacteria*	66	15ELB8 (HG324886)	Uncultered bacterium (AF431270)	98	*Burkholderia ferrariae* (NR_04389)	93	0.2	0.0	1.2	0.0	0.0	0.0	0.0
Deltaproteobacteria							7.8	0.0	10.5	8.5	17.3	0.6	10.9
Desulfobacterales													
Desulfobulbaceae	32	150LA3 (HG324344)	Uncultered bacterium (EU981255)	99	*Desulfocapsa thiozymogenes* (NR_029306)	92	0.6	0.0	1.8	0.0	1.3	0.0	0.6
Desulfovibrionales													
Desulfovibrionaceae	42	150LB10 (HG324352)	Uncultered bacterium (JQ086920)	99	*Desulfovibrio idahonensis* (AJ582758)	98	0.3	0.0	0.6	0.0	1.3	0.0	0.0
Desulfuromonadales													
Geobacteraceae	17	150LA15 (HG324588)	Uncultered bacterium (FM956386)	99	*Geobacter psychrophilus* (NR_043075)	98	2.1	0.0	1.2	2.4	5.3	0.6	3.4
Myxococcales							1.1	0.0	2.3	0.6	1.3	0.0	2.3
Cystobacteriaceae	86	150HA24 (HG324634)	Uncultered bacterium (HQ622736)	98	*Anaeromyxobacter dehalogans* (NR_074927)	94	0.1	0.0	0.0	0.6	0.0	0.0	0.0
Polyangiaceae	43	150LF3 (HG324364)	Uncultered bacterium (EU360029)	99	*Byssovorax cruenta* (NR_042341)	97	0.7	0.0	1.2	0.0	0.7	0.0	2.3

Phylogenic Affiliation of OTUs [a]	OTU	Reference Sequence (Acc. no.)	Closest related sequence (Acc. no.)	Max. ident. [%]	Closest cultured relative (Acc. no.)	Max. ident. [%]	Relative Abundance of OTUs in clone library [b]						
								15°C				5°C	
							total	$t_{40}H$	$t_{40}L$	t_0H	t_0L	$t_{80}H$	$t_{80}L$
Unclassified *Myxococcales* I	48	15ELD21 (HG324907)	Uncultered bacterium (JQ367119)	99	*Haliangium ochraceum* (NR_074917)	87	0.2	0.0	1.2	0.0	0.0	0.0	0.0
Unclassified *Myxococcales* II	91	150LA21 (HG324724)	Uncultered bacterium (GU172194)	98	*Cystobacter fustus* (AJ233898)	90	0.1	0.0	0.0	0.0	0.7	0.0	0.0
Syntrophobacterales							2.5	0.0	2.3	5.5	4.7	0.0	2.9
Syntrophaceae	44						1.3	0.0	0.6	3.6	2.0	0.0	1.7
	44a	15ELH14 (HG324542)	Uncultered bacterium (DQ404734)	99	*Desulfobacca acetoxidans* (NR_074955)	90	0.6	0.0	0.6	1.2	0.0	0.0	1.7
	44b	150LE4 (HG324359)	Uncultered bacterium (AB630476)	97	*Smithella propionica* (NR_024989)	93	0.7	0.0	0.0	2.4	2.0	0.0	0.0
Syntrophobacteraceae	19	150LA8 (HG324346)	Uncultered bacterium (FR732208)	99	*Syntrophobacter wolinii* (X70906)	95	0.8	0.0	1.8	1.2	2.0	0.0	0.0
Syntrophorhabdaceae	67	150HA13 (HG324628)	Uncultered bacterium (AB364745)	99	*Syntrophorhabdus aromaticivorans* (AB212873)	93	0.4	0.0	0.0	0.6	0.7	0.0	1.1
Unclassified *Deltaproteobacteria* (GR-WP 33-30)	20	150LA11 (HG324347)	Uncultered bacterium (DQ451494)	99	*Angiococcus disciformis* (AJ233911)	84	1.2	0.0	2.3	0.0	3.3	0.0	1.7
Gammaproteobacteria							1.1	0.0	1.2	1.8	1.3	0.6	1.7
Aeromonadales													
Aeromonadaceae	94	5BEHM02 (HG325048)	Uncultered bacterium (FJ535215)	99	*Tolumonas auensis* (CP001616)	99	0.1	0.0	0.0	0.0	0.0	0.6	0.0
Chromatiales													
Ectothiorhodospiraceae	99	5BEL2G08 (HG325295)	Uncultered bacterium (JN133837)	99	*Acidiferrobacter thiooxydans* (AF387301)	89	0.1	0.0	0.0	0.0	0.0	0.0	0.6
Xanthomonadales													
Solimonadaceae	40	150LH13 (HG324618)	Uncultered bacterium (GU366822)	99	*Steroidobacter denitrificans* (NR_044309)	91	0.6	0.0	1.2	0.0	1.3	0.0	1.1
Unclassified *Gammaproteobacteria* I	53	150HF4 (HG324434)	Uncultered bacterium (JX223446)	97	*Thiohalospira halophila* (EU368849)	87	0.2	0.0	0.0	1.2	0.0	0.0	0.0

Phylogenic Affiliation of OTUs [a]	OTU	Reference Sequence (Acc. no.)	Closest related sequence (Acc. no.)	Max. ident. [%]	Closest cultured relative (Acc. no.)	Max. ident. [%]	Relative Abundance of OTUs in clone library [b]						
								15°C				5°C	
							total	$t_{40}H$	$t_{40}L$	t_0H	t_0L	$t_{80}H$	$t_{80}L$
Unclassified *Gammaproteobacteria* II	69	150HH10 (HG324706)	Uncultered bacterium (AM991261)	98	*Methylmicrobium album* (NR_029244)	92	0.1	0.0	0.0	0.6	0.0	0.0	0.0
Spirochaetes							1.8	5.9	1.8	0.0	0.7	1.8	0.6
Spirochaetes													
Spirochaetales													
Spirochaetaceae	12	15EHC22 (HG324466)	Uncultered bacterium (AB658126)	99	*Spirochaeta zuelzare* (FR749929)	96	1.3	5.9	0.0	0.0	0.0	1.8	0.0
Unclassified *Spirochaetes*	33	15ELA16 (HG324514)	Uncultered bacterium (AB659121)	98	*Spirochaeta caldaria* (NR_074757)	84	0.5	0.0	1.8	0.0	0.7	0.0	0.6
Verrucomicrobia							0.7	0.0	0.6	0.6	0.7	1.8	0.6
Opitutae							0.2	0.0	0.0	0.6	0.7	0.0	0.0
Opitutales													
Opitutaceae	92	150LB3 (HG324731)	Uncultered bacterium (GU127816)	99	*Opitutus terrae* (NR_074978)	96	0.1	0.0	0.0	0.0	0.7	0.0	0.0
Puniceicoccales													
Puniceicoccaceae	62	150HC12 (HG324648)	Uncultered bacterium (AB718832)	98	*Coraliomargarita akajimensis*	87	0.1	0.0	0.0	0.6	0.0	0.0	0.0
Unclassified *Verrucomicrobia* I	82	15ELA18 (HG324865)	Uncultered bacterium (AM162456)	99	*Prosthecobacter debontii* (AJ966882)	85	0.3	0.0	0.6	0.0	0.0	0.6	0.6
Unclassified *Verrucomicrobia* II	95	5BEH1C07 (HG325178)	Uncultered bacterium (HQ330617)	96	*Alterococcus agarolyticus* (NR_036763)	85	0.2	0.0	0.0	0.0	0.0	1.2	0.0
Unclassified *Bacteria*							14.4	29.4	9.4	6.7	7.3	23.2	9.8
Fibrobacter-related unclassified *Bacteria*	1						11.4	27.1	4.7	5.5	2.0	20.8	7.5
	1a	15EHH9 (HG324421)	Uncultured bacterium (FR732203)	99	*Fibrobacter succinogenes* (CP001792)	79	3.6	11.8	3.5	4.2	2.0	0.0	0.0
	1b	15EHE2 (HG324392)	Uncultured bacterium (JN697815)	90	*Fibrobacter succinogenes* (CP001792)	79	7.7	15.3	1.2	0.6	0.0	20.8	7.5

Phylogenic Affiliation of OTUs [a]	OTU	Reference Sequence (Acc. no.)	Closest related sequence (Acc. no.)	Max. ident. [%]	Closest cultured relative (Acc. no.)	Max. ident. [%]	Relative Abundance of OTUs in clone library [b]						
								15°C				5°C	
							total	$t_{40}H$	$t_{40}L$	t_0H	t_0L	$t_{80}H$	$t_{80}L$
	1c	150HD1 (HG324451)	Uncultured bacterium (JN697815)	90	*Desulfovibrio cuneatus* (NR_036969)	80	0.1	0.0	0.0	0.6	0.0	0.0	0.0
Vampirovibrio-related unclassified *Bacteria*	22	15EHA10 (HG324406)	Uncultured bacterium (JQ624955)	98	*Vampirovibrio chlorellavorus* (HM038000)	82	0.9	2.4	0.0	0.6	0.0	2.4	0.0
Candidate division BRC1 a	58	150LE21 (HG324762)	Uncultered bacterium (AB656628)	98	*Desulfobacca acetoxidans* (NR_074955)	85	0.2	0.0	0.0	0.0	1.3	0.0	0.0
Candidate division BRC1 b	72	15ELD4 (HG324912)	Uncultered bacterium (AJ390444)	98	*Geoalkalibacter ferrihydriticus* (NR_043709)	85	0.1	0.0	0.6	0.0	0.0	0.0	0.0
Unclassified *Bacteria* I	25	15ELA10 (HG324307)	Uncultered bacterium (AB657077)	90	*Desulfomicrobium baculatum* (NR_074900)	82	0.6	0.0	1.8	0.6	0.7	0.0	0.6
Unclassified *Bacteria* II	35	150LF23 (HG324613)	Uncultered bacterium (AB656120)	97	*Geothermobacter ehrlichii* (NR_042754)	86	0.3	0.0	1.2	0.0	0.7	0.0	0.0
Unclassified *Bacteria* III	39	150LE18 (HG324761)	Uncultered bacterium (HM228769)	98	*Atopobium vaginae* (JQ5119723)	86	0.3	0.0	0.0	0.0	2.0	0.0	0.0
Unclassified *Bacteria* IV	75	150LH19 (HG324620)	Uncultered bacterium (AB656778)	99	*Geothermobacter ehrlichii* (NR_042754)	84	0.1	0.0	0.0	0.0	0.7	0.0	0.0
Unclassified *Bacteria* V	83	15ELD5 (HG324913)	Uncultered bacterium (JF181265)	98	*Geothermobacter ehrlichii* (NR_042754)	85	0.2	0.0	0.6	0.0	0.0	0.0	0.6
Unclassified *Bacteria* VI	85	15ELH8 (HG324958)	Uncultered bacterium (JN023430)	99	*Aminomonas paucivorans* (AF072581)	88	0.1	0.0	0.6	0.0	0.0	0.0	0.0
Unclassified *Bacteria* VII	96	5BEL1H12 (HG325265)	Uncultered bacterium (GU127775)	98	*Clostridium papyrosolvens* (NR_026102)	81	0.2	0.0	0.0	0.0	0.0	0.0	1.1

[a]OTUs were assigned to taxa based on their phylogenic position in the SILVA 16S rRNA tree (2.6.1.2).

[b]t_0 and t_{40} are 0 and 40 d of incubation, respectively, after 17 d of preincubation at 15°C, and t_{80} is 80 d of incubation after 22 d of pre-incubation (2.1.2.1). L and H are 'light' and 'heavy' fractions, respectively (Figure 6).

Table A3 Relative abundancies and phylogenetic affiliations of bacterial family-level OTUs.

Phylogenic affiliation [a]	OTU	Reference sequence (acc. no.)	Acc. no. of closest relative	I [b] [%]	Closesest cultured relative (acc. no.)	I [b] [%]	total	FP	EH	EL	BH	BL	P	C	E	C
											15°C				5°C	
											Relative abundance [%] [c]					
Proteobacteria							45.0	46.9	62.7	42.9	31.9	41.5	47.1	40.7	50.0	39.3
Betaproteobacteria							3.2	5.0	1.7	0.8	0.8	2.2	3.7	0.9	7.1	7.1
Burkholderiales							1.8	2.8	1.7	0.0	0.8	0.7	2.2	0.9	2.7	4.8
Comamonadaceae	1						0.1	0.0	0.0	0.0	0.8	0.0	0.0	0.0	0.0	0.0
Pelomonas	1a	BButH3P4D05 (LK024657)	HM111641	99	*Pelomonas saccharophila* (AB681917)	99	0.1	0.0	0.0	0.0	0.8	0.0	0.0	0.0	0.0	0.0
Alcaligenaceae	2						1.1	1.1	0.0	0.0	0.0	0.7	2.2	0.9	2.7	2.4
uncultured	2a	BButL8P5B07 (LK024718)	DQ451484	99	*Cupriavidus campinensis* (NR_025137)	92	1.1	1.1	0.0	0.0	0.0	0.7	2.2	0.9	2.7	2.4
Oxalobacteraceae	3						0.6	1.7	1.7	0.0	0.0	0.0	0.0	0.0	0.0	2.4
Massilia	3a	BEtH3P3B02 (LK024555)	JX989230	99	*Massilia timonae* (FR799435)	99	0.6	1.7	1.7	0.0	0.0	0.0	0.0	0.0	0.0	2.4
Hydrogenophilales							0.6	0.6	0.0	0.0	0.0	0.0	0.0	0.0	3.6	2.4
Hydrogenophilaceae	4						0.6	0.6	0.0	0.0	0.0	0.0	0.0	0.0	3.6	2.4
uncultured	4a	BEt5P8E06 (LK025008)	HG325081	99	*Thiobacillus aquaesulis* (HE971728)	95	0.4	0.0	0.0	0.0	0.0	0.0	0.0	0.0	3.6	0.0
uncultured	4b	Bt0P13G11 (LK025286)	AB240525	98	*Sulfuricella denitrificans* (AP013066)	93	0.3	0.6	0.0	0.0	0.0	0.0	0.0	0.0	0.0	2.4
Nitrosomonadales							0.4	0.0	0.0	0.8	0.0	0.7	1.5	0.0	0.0	0.0
Nitrosomonadaceae	5						0.4	0.0	0.0	0.8	0.0	0.7	1.5	0.0	0.0	0.0
uncultured	5a	BProP7C11 (LK024911)	DQ404836	99	*Nitrosospira* sp. III7 (AY123809)	91	0.4	0.0	0.0	0.8	0.0	0.7	1.5	0.0	0.0	0.0
Neisseriales							0.3	1.7	0.0	0.0	0.0	0.0	0.0	0.0	0.0	0.0
Neisseriaceae	6	Bt0P13A06 (LK025219)	GU270775	100	*Paludibacterium yongneupense* (AB682439)	96	0.3	1.7	0.0	0.0	0.0	0.0	0.0	0.0	0.0	0.0
Rhodocyclales							0.1	0.0	0.0	0.0	0.0	0.7	0.0	0.0	0.0	0.0
Rhodocyclaceae	7	BButL9P10C07 (LK025161)	FJ592534	99	*Propionivibrio limicola* (NR_025455)	96	0.1	0.0	0.0	0.0	0.0	0.7	0.0	0.0	0.0	0.0

Phylogenic affiliation [a]	OTU	Reference sequence (acc. no.)	Acc. no. of closest relative	I [b] [%]	Closesest cultured relative (acc. no.)	I [b] [%]	Relative abundance [%] [c]									
							total	FP	15°C						5°C	
									EH	EL	BH	BL	P	C	E	C
UCT N117	8	BEt5P17D03 (LK025551)	KC605613	99	*Sideroxydans paludicola* (DQ386858)	93	0.1	0.0	0.0	0.0	0.0	0.0	0.0	0.0	0.9	0.0
Gammaproteobacteria							1.2	3.9	0.0	0.8	0.0	0.0	0.0	2.7	0.9	1.2
Xanthomonadales							0.8	2.2	0.0	0.0	0.0	0.0	0.0	2.7	0.9	1.2
uncultured	9	BCon15P7F03 (LK024938)	GU127724	99	*Steroidobacter denitrificans* (NR_044309)	90	0.8	2.2	0.0	0.0	0.0	0.0	0.0	2.7	0.9	1.2
Legionellales							0.1	0.0	0.0	0.8	0.0	0.0	0.0	0.0	0.0	0.0
Legionellaceae	10						0.1	0.0	0.0	0.8	0.0	0.0	0.0	0.0	0.0	0.0
Legionella	10a	BEtL9P6G01 (LK024856)	KC620607	98	*Legionella worsleiensis* (NR_044971)	98	0.1	0.0	0.0	0.8	0.0	0.0	0.0	0.0	0.0	0.0
Enterobacterales							0.2	1.1	0.0	0.0	0.0	0.0	0.0	0.0	0.0	0.0
Enterobacteriaceae	11						0.2	1.1	0.0	0.0	0.0	0.0	0.0	0.0	0.0	0.0
Serratia	11a	Bt0P14D10 (LK025336)	AM403659	99	*Rahnella aquatilis* (AY253919)	98	0.2	1.1	0.0	0.0	0.0	0.0	0.0	0.0	0.0	0.0
NKB5	12	Bt0P13C05 (LK025242)	JF270457	99	*Nitrosococcus halophilus* (NR_074790)	87	0.1	0.6	0.0	0.0	0.0	0.0	0.0	0.0	0.0	0.0
Alphaproteobacteria							29.2	33.5	16.9	35.3	22.7	34.1	30.9	31.0	28.6	25.0
Rhizobiales							18.7	24.0	10.2	26.3	5.9	22.2	22.8	20.4	17.0	13.1
Bradyrhizobiaceae	13						6.4	6.1	0.8	10.5	0.8	5.2	11.8	8.8	7.1	4.8
*Bradyrhizobium*_1	13a	BProP7C04 (LK024904)	JX099945	99	*Bradyrhizobium japonicum* (AB513467)	99	2.7	1.7	0.0	3.8	0.8	2.2	8.1	0.0	5.4	1.2
Rhodoblastus	13b	Bt0P8B09 (LK024980)	AF408958	99	*Rhodoblastus acidophilus* (JN399240)	99	3.7	4.5	0.8	6.8	0.0	3.0	3.7	8.8	1.8	3.6
Xanthobacteraceae	14						2.2	1.1	0.8	3.8	0.0	3.7	2.9	3.5	0.9	3.6
uncultured	14a	BButL8P5A07 (LK024708)	EU680439	98	*Rhodoplanes elegans* (NR_029125)	95	1.6	1.1	0.8	3.0	0.0	3.0	2.9	0.9	0.9	1.2
Pseudolabrys	14b	BEtL9P3F12 (LK024602)	JX505027	99	*Pseudolabrys taiwanensis* (EU938323)	97	0.6	0.0	0.0	0.8	0.0	0.7	0.0	2.7	0.0	2.4
Beijerinckiaceae	15						2.0	3.4	1.7	3.8	0.8	5.2	1.5	0.0	0.0	0.0

Phylogenic affiliation [a]	OTU	Reference sequence (acc. no.)	Acc. no. of closest relative	I [b] [%]	Closest cultured relative (acc. no.)	I [b] [%]	Relative abundance [%] [c]									
							total	FP	15°C						5°C	
									EH	EL	BH	BL	P	C	E	C
uncultured	15a	BButL8P5A03 (LK024704)	HG324448	99	*Methylocapsa acidiphila* (NR_028923)	98	2.0	3.4	1.7	3.8	0.8	5.2	1.5	0.0	0.0	0.0
alpha1 cluster	16	BEtH3P3A07 (LK024549)	FR732133	99	*Methylosinus trichosporium* (AJ431385)	96	4.0	7.3	5.9	4.5	3.4	3.7	2.2	1.8	2.7	2.4
Methylocystaceae	17						2.6	2.8	0.8	2.3	0.8	1.5	2.9	5.3	4.5	2.4
Methylocystis	17a	BButL9P5H02 (LK024780)	HQ844544	99	*Methylocystis heyeri* (NR_042531)	98	2.6	2.8	0.8	2.3	0.8	1.5	2.9	5.3	4.5	2.4
Hyphomicrobiaceae	18						1.1	2.2	0.0	1.5	0.0	1.5	1.5	0.0	1.8	0.0
Rhodomicrobium	18a	BEtL9P3F11 (LK024601)	HG324619	99	*Rhodomicrobium vannielii* (AB250621)	97	0.9	2.2	0.0	1.5	0.0	0.0	1.5	0.0	1.8	0.0
Hyphomicrobium	18b	BButL8P5B10 (LK024721)	JX504970	100	*Hyphomicrobium sulfonivorans* (AY305006)	96	0.2	0.0	0.0	0.0	0.0	1.5	0.0	0.0	0.0	0.0
Family Incertae Sedis *Rhizomicrobium*	19	BButL8P5C06 (LK024727)	GU134924	99	*Rhizomicrobium electricum* (NR_108115)	96	0.2	0.0	0.0	0.0	0.0	1.5	0.0	0.0	0.0	0.0
Rhodobiaceae	20	BCon15P16B08 (LK025457)	GU270794	99	*Thermovum composti* (AB563785)	93	0.1	0.0	0.0	0.0	0.0	0.0	0.0	0.9	0.0	0.0
Methylobacteriaceae	21						0.1	0.6	0.0	0.0	0.0	0.0	0.0	0.0	0.0	0.0
Methylobacterium	21a	Bt0P14F02 (LK025349)	JF176677	99	*Methylobacterium cerastii* (FR733885)	99	0.1	0.6	0.0	0.0	0.0	0.0	0.0	0.0	0.0	0.0
KF-JG30-B3	22	Bt0P13F07 (LK025274)	JN851645	99	*Methylosinus trichosporium* (AB648997)	92	0.1	0.6	0.0	0.0	0.0	0.0	0.0	0.0	0.0	0.0
Caulobacterales							0.9	0.6	0.0	0.8	0.0	0.7	2.9	1.8	0.9	0.0
Caulobacteraceae	23						0.9	0.6	0.0	0.8	0.0	0.7	2.9	1.8	0.9	0.0
uncultured	23a	BProP7A10 (LK024888)	EF221337	99	*Caulobacter segnis* (NR_074208)	96	0.9	0.6	0.0	0.8	0.0	0.7	2.9	1.8	0.9	0.0
Sphingomonadales							0.1	0.6	0.0	0.0	0.0	0.0	0.0	0.0	0.0	0.0
Sphingomonadaceae	24						0.1	0.6	0.0	0.0	0.0	0.0	0.0	0.0	0.0	0.0
Sandarakinorhabdus	24a	Bt0P8D04 (LK024995)	JX172565	100	*Sandarakinorhabdus* sp. JJ2202 (JX304656)	98	0.1	0.6	0.0	0.0	0.0	0.0	0.0	0.0	0.0	0.0
Rhodospirillales							9.5	8.4	6.8	7.5	16.8	11.1	5.1	8.8	10.7	11.9

Phylogenic affiliation [a]	OTU	Reference sequence (acc. no.)	Acc. no. of closest relative	I [b] [%]	Closest cultured relative (acc. no.)	I [b] [%]	Relative abundance [%] [c]									
									15°C						5°C	
							total	FP	EH	EL	BH	BL	P	C	E	C
Acetobacteraceae	25						5.7	5.6	3.4	3.0	5.0	5.2	2.9	8.8	8.9	10.7
uncultured	25a	BProP7C12 (LK024912)	HM060104	99	*Acidisphaera rubrifaciens* (NR_037119)	95	4.3	3.4	3.4	0.8	4.2	5.2	2.9	6.2	7.1	8.3
Acidisoma	25b	Bt0P8D03 (LK024994)	HG324557	99	*Rhodovastum atsumiense* (AB381935)	94	0.2	0.6	0.0	0.0	0.0	0.0	0.0	0.0	0.0	1.2
Rhodovastum	25c	BCon15P7G06 (LK024953)	KF581239	97	*Rhodovastum atsumiense* (AB381935)	97	1.1	1.7	0.0	2.3	0.8	0.0	0.0	2.7	0.9	1.2
Acidocella	25d	BEt5P17E08 (LK025568)	HQ595222	98	*Asaia bogorensis* (AB682008)	95	0.1	0.0	0.0	0.0	0.0	0.0	0.0	0.0	0.9	0.0
Rhodospirillaceae	26						1.6	1.7	0.8	0.0	10.9	0.7	0.0	0.0	0.0	0.0
uncultured	26a	BButL8P5C07 (LK024728)	AJ292593	99	*Telmatospirillum siberiense* (DQ094180)	95	1.4	0.6	0.8	0.0	10.9	0.7	0.0	0.0	0.0	0.0
Inquilinus	26b	Bt0P14A07 (LK025303)	HM488730	99	*Rhodospirillum centenum* (NR_074105)	90	0.2	1.1	0.0	0.0	0.0	0.0	0.0	0.0	0.0	0.0
DA111	27	BEtH3P6B05 (LK024803)	HG324329	99	*Azospirillum amazonense* (NR_104981)	90	2.2	1.1	2.5	4.5	0.8	5.2	2.2	0.0	1.8	1.2
Rickettsiales							0.1	0.0	0.0	0.8	0.0	0.0	0.0	0.0	0.0	0.0
Family Incertae Sedis *Candidatus* Odyssella	28	BEtL9P3G05 (LK024607)	FJ849470	99	*Trojanella thessalonices* (AF069496)	93	0.1	0.0	0.0	0.8	0.0	0.0	0.0	0.0	0.0	0.0
Deltaproteobacteria							11.4	4.5	44.1	6.0	8.4	5.2	12.5	6.2	13.4	6.0
Myxococcales							0.9	1.1	0.8	0.0	2.5	1.5	0.0	0.0	0.9	1.2
uncultured 1	29	BButH4P4G02 (LK024688)	EU300006	99	*Kofleria flava* (HF543825)	88	0.2	0.0	0.0	0.0	1.7	0.0	0.0	0.0	0.0	0.0
Polyangiaceae	30	BEtH4P6C12 (LK024820)	JN540279	98	*Phaselicystis flava* (NR_044523)	92	0.4	0.6	0.8	0.0	0.0	0.0	0.0	0.0	0.9	1.2
uncultured 2	31	BButL8P5A04 (LK024705)	AB661018	99	*Polyangium thaxteri* (AJ233943)	89	0.2	0.0	0.0	0.0	0.0	1.5	0.0	0.0	0.0	0.0
Myxococcaceae	32	Bt0P14H01 (LK025364)	EF667661	98	*Anaeromyxobacter dehalogenans* (CP001359)	90	0.2	0.6	0.0	0.0	0.8	0.0	0.0	0.0	0.0	0.0

Phylogenic affiliation [a]	OTU	Reference sequence (acc. no.)	Acc. no. of closest relative	I [b] [%]	Closesest cultured relative (acc. no.)	I [b] [%]	Relative abundance [%] [c]									
							total	FP	15°C						5°C	
									EH	EL	BH	BL	P	C	E	C
GR-WP33-30	33	BButH4P4F05 (LK024679)	GQ918797	99	Geothermobacter ehrlichii (NR_042754)	84	0.7	0.0	0.8	1.5	2.5	0.7	0.0	0.0	0.0	1.2
Desulfuromonadales							5.3	0.0	39.8	3.0	0.8	0.0	0.7	0.0	6.3	0.0
BVA18	34	BButH3P4A12 (LK024631)	HG324643	99	Geobacter psychrophilus (NR_043075)	96	0.2	0.0	0.8	0.0	0.8	0.0	0.0	0.0	0.0	0.0
Desulfuromonadaceae	35						4.4	0.0	35.6	1.5	0.0	0.0	0.7	0.0	4.5	0.0
Pelobacter	35a	BEtH4P3C04 (LK024567)	AM159357	98	Pelobacter propionicus (NR_074975)	98	4.4	0.0	35.6	1.5	0.0	0.0	0.7	0.0	4.5	0.0
Geobacteraceae	36						0.7	0.0	3.4	1.5	0.0	0.0	0.0	0.0	1.8	0.0
Geobacter 1	36a	BEtL8P3E04 (LK024582)	AB273881	98	Geobacter bremensis (NR_026076)	96	0.4	0.0	0.8	1.5	0.0	0.0	0.0	0.0	1.8	0.0
Geobacter 8	36b	BEtH4P6C07 (LK024815)	AB656651	99	Geobacter hephaestius (AY737507)	98	0.3	0.0	2.5	0.0	0.0	0.0	0.0	0.0	0.0	0.0
Syntrophobacterales							3.9	3.4	0.0	1.5	1.7	3.0	11.8	4.4	5.4	3.6
Syntrophobacteraceae	37						1.6	1.7	0.0	0.0	0.8	0.0	5.1	1.8	3.6	1.2
Syntrophobacter	37a	BProP15F01 (LK025420)	AM162452	98	Syntrophobacter wolinii (X70906)	95	1.6	1.7	0.0	0.0	0.8	0.0	5.1	1.8	3.6	1.2
Syntrophaceae	38						2.3	1.7	0.0	1.5	0.8	3.0	6.6	2.7	1.8	2.4
Syntrophus	38a	BButH3P4C09 (LK024649)	AB364719	99	Syntrophus aciditrophicus (NR_102776)	92	0.2	0.0	0.0	0.0	0.8	0.0	0.0	0.0	0.0	1.2
Smithella	38b	BProP7B10 (LK024899)	FQ658588	98	Smithella propionica (NR_024989)	97	0.6	0.0	0.0	0.0	0.0	0.0	5.1	0.0	0.0	0.0
Desulfobacca-related	38c	BButL9P5F09 (LK024763)	GU127781	99	Desulfobacca acetoxidans (NR_074955)	89	0.4	0.6	0.0	0.0	0.0	1.5	0.0	0.0	0.9	0.0
Desulfomonile	38d	BCon15P7E06 (LK024929)	EF667559	98	Desulfomonile tiedjei (NR_074118)	96	1.2	1.1	0.0	1.5	0.0	1.5	1.5	2.7	0.9	1.2
Order Incertae Sedis							0.4	0.0	0.0	0.0	0.8	0.0	0.0	1.8	0.9	0.0
Syntrophorhabdaceae	39	BCon15P16C03 (LK025463)	EU399665	98	Syntrophorhabdus aromaticivorans (NR_041306)	95	0.4	0.0	0.0	0.0	0.8	0.0	0.0	1.8	0.9	0.0

Phylogenic affiliation [a]	OTU	Reference sequence (acc. no.)	Acc. no. of closest relative	I [b] [%]	Closest cultured relative (acc. no.)	I [b] [%]	Relative abundance [%] [c]									
									15°C						5°C	
							total	FP	EH	EL	BH	BL	P	C	E	C
Desulfovibrionales							0.3	0.0	2.5	0.0	0.0	0.0	0.0	0.0	0.0	0.0
Desulfovibrionaceae	40						0.3	0.0	2.5	0.0	0.0	0.0	0.0	0.0	0.0	0.0
Desulfovibrio	40a	BEtH3P3A05 (LK024547)	AB364720	97	*Desulfovibrio marrakechensis* (KF536746)	96	0.3	0.0	2.5	0.0	0.0	0.0	0.0	0.0	0.0	0.0
Spirochaetae							1.3	0.0	0.0	0.0	2.5	0.7	2.2	2.7	1.8	3.6
Spirochaetes							1.3	0.0	0.0	0.0	2.5	0.7	2.2	2.7	1.8	3.6
Spirochaetales							1.3	0.0	0.0	0.0	2.5	0.7	2.2	2.7	1.8	3.6
Spirochaetaceae	41						1.3	0.0	0.0	0.0	2.5	0.7	2.2	2.7	1.8	3.6
Spirochaeta	41a	BButH3P4D09 (LK024661)	AB234282	98	*Spirochaeta stenostrepta* (AB541984)	84	0.8	0.0	0.0	0.0	2.5	0.7	0.7	1.8	1.8	0.0
Treponema	41b	BProP7C01 (LK024901)	KF581660	99	*Treponema zuelzerae* (NR_104797)	98	0.3	0.0	0.0	0.0	0.0	0.0	1.5	0.0	0.0	1.2
uncultured	41c	BCon5P18F11 (LK025652)	AB658226	99	*Treponema caldaria* (NR_074757)	89	0.3	0.0	0.0	0.0	0.0	0.0	0.0	0.9	0.0	2.4
Bacteroidetes							3.1	3.4	0.0	0.0	1.7	1.5	8.1	4.4	4.5	4.8
Bacteroidia							0.5	0.0	0.0	0.0	0.0	0.0	0.7	0.0	1.8	3.6
Bacteroidales							0.5	0.0	0.0	0.0	0.0	0.0	0.7	0.0	1.8	3.6
Porphyromonadaceae	42						0.5	0.0	0.0	0.0	0.0	0.0	0.7	0.0	1.8	3.6
Paludibacter	42a	BProP7B07 (LK024896)	FR732486	99	*Paludibacter propionicigenes* (NR_074577)	97	0.5	0.0	0.0	0.0	0.0	0.0	0.7	0.0	1.8	3.6
Sphingobacteriia							1.2	2.8	0.0	0.0	0.8	1.5	2.2	0.9	0.9	0.0
Sphingobacteriales							1.2	2.8	0.0	0.0	0.8	1.5	2.2	0.9	0.9	0.0
S15A-MN91	43	BButL9P5H11 (LK024789)	AM409843	97	*Owenweeksia hongkongensis* (NR_074100)	87	0.6	1.1	0.0	0.0	0.8	0.7	1.5	0.9	0.0	0.0
WCHB1-69	44	BButL8P5A08 (LK024709)	JF829179	99	*Owenweeksia hongkongensis* (NR_074100)	91	0.5	1.7	0.0	0.0	0.0	0.7	0.7	0.0	0.9	0.0
Prolixibacter-related	45	BProP7B06 (LK024895)	HG324396	99	*Sunxiuqinia faeciviva* (NR_108114)	89	0.7	0.0	0.0	0.0	0.0	0.0	1.5	2.7	1.8	1.2

Phylogenic affiliation [a]	OTU	Reference sequence (acc. no.)	Acc. no. of closest relative	I [b] [%]	Closest cultured relative (acc. no.)	I [b] [%]	Relative abundance [%] [c]									
									15°C						5°C	
							total	FP	EH	EL	BH	BL	P	C	E	C
vadinHA17	46	BButH3P4B09 (LK024639)	HG324501	100	Cytophaga fermentans (AB517712)	91	0.3	0.6	0.0	0.0	0.8	0.0	0.0	0.9	0.0	0.0
SB5	47	BProP15C03 (LK025392)	FJ902094	96	Owenweeksia hongkongensis (NR_074100)	87	0.4	0.0	0.0	0.0	0.0	0.0	3.7	0.0	0.0	0.0
Chlorobi							1.2	1.1	0.8	2.3	0.0	0.7	2.2	1.8	1.8	0.0
Ignavibacteria							0.8	0.6	0.8	2.3	0.0	0.7	0.7	1.8	0.0	0.0
Ignavibacteriales							0.8	0.6	0.8	2.3	0.0	0.7	0.7	1.8	0.0	0.0
BSV26	48	BEtH4P3C02 (LK024565)	AB661083	99	Ignavibacterium album (NR_074698)	84	0.3	0.0	0.8	0.8	0.0	0.0	0.7	0.0	0.0	0.0
BSV26b	49	BCon15P7E12 (LK024935)	EU644261	98	Ignavibacterium album (NR_074698)	85	0.4	0.6	0.0	0.0	0.0	0.7	0.0	1.8	0.0	0.0
uncultured	50	BEtL9P3G02 (LK024604)	JX981698	99	Ignavibacterium album (NR_074698)	93	0.2	0.0	0.0	1.5	0.0	0.0	0.0	0.0	0.0	0.0
Chlorobia							0.4	0.6	0.0	0.0	0.0	0.0	1.5	0.0	1.8	0.0
Chlorobiales							0.4	0.6	0.0	0.0	0.0	0.0	1.5	0.0	1.8	0.0
OPB56	51	BEt5P8E01 (LK025003)	HG324870	97	Rhodothermus marinus (CP003029)	83	0.4	0.6	0.0	0.0	0.0	0.0	1.5	0.0	1.8	0.0
Fibrobacteres							1.6	0.0	0.0	0.8	0.0	0.7	5.1	2.7	5.4	0.0
Fibrobacteria							1.6	0.0	0.0	0.8	0.0	0.7	5.1	2.7	5.4	0.0
Fibrobacterales							1.6	0.0	0.0	0.8	0.0	0.7	5.1	2.7	5.4	0.0
Fibrobacteraceae	52	BEt5P8F11 (LK025023)	GQ340200	98	Bartonella washoensis (AB519064)	84	0.3	0.0	0.0	0.0	0.0	0.7	0.0	0.0	1.8	0.0
B122	53	BProP7C03 (LK024903)	JQ367579	99	Desulfatibacillum aliphaticivorans (NR_025694)	80	1.3	0.0	0.0	0.8	0.0	0.0	5.1	2.7	3.6	0.0
Planctomycetes							5.5	4.5	2.5	12.8	4.2	10.4	3.7	2.7	3.6	3.6
Planctomycetacia							5.0	3.9	2.5	11.3	4.2	10.4	3.7	0.9	3.6	2.4
Planctomycetales							5.0	3.9	2.5	11.3	4.2	10.4	3.7	0.9	3.6	2.4
Planctomycetaceae	54						5.0	3.9	2.5	11.3	4.2	10.4	3.7	0.9	3.6	2.4
Isosphaera	54a	BButL9P5F10 (LK024764)	EF663268	99	Isosphaera sp. PX4 (KF467528)	93	1.1	1.1	0.8	0.8	0.0	5.9	0.0	0.0	0.0	0.0
Singulisphaera	54b	BEtL9P6G02 (LK024857)	FJ466090	99	Singulisphaera rosea (FN391026)	95	0.2	0.0	0.0	1.5	0.0	0.0	0.0	0.0	0.0	0.0

Phylogenic affiliation [a]	OTU	Reference sequence (acc. no.)	Acc. no. of closest relative	I [b] [%]	Closest cultured relative (acc. no.)	I [b] [%]	Relative abundance [%] [c]									
									15°C						5°C	
							total	FP	EH	EL	BH	BL	P	C	E	C
Gemmata	54c	BEtL9P6F06 (LK024850)	GQ402654	98	*Gemmata obscuriglobus* (NR_037010)	94	0.1	0.0	0.0	0.8	0.0	0.0	0.0	0.0	0.0	0.0
Zavarzinella	54d	BButH4P4G12 (LK024695)	JN867696	99	*Zavarzinella formosa* (NR_042465)	86	0.2	0.0	0.0	0.0	1.7	0.0	0.0	0.0	0.0	0.0
uncultured 1	54e	BEtL8P6E09 (LK024841)	HG324527	99	*Telmatocola sphagniphila* (JN880417)	85	1.6	0.6	0.8	6.0	1.7	0.7	1.5	0.0	2.7	0.0
uncultured 2	54f	BButL9P5H07 (LK024785)	GU127742	98	*Candidatus* Anammoximicrobium moscowii (KC467065)	89	1.0	1.1	0.0	1.5	0.0	3.0	0.7	0.9	0.0	1.2
uncultured 3	54g	BEtH3P6A10 (LK024797)	JQ376396	98	*Telmatocola sphagniphila* (JN880417)	82	0.1	0.0	0.8	0.0	0.0	0.0	0.0	0.0	0.0	0.0
uncultured 4	54h	BProP7D04 (LK024915)	EF018763	99	*Telmatocola sphagniphila* (JN880417)	83	0.3	0.0	0.0	0.0	0.0	0.0	1.5	0.0	0.9	0.0
Planctomyces	54i	Bt0P13B07 (LK025232)	FJ624888	99	*Planctomyces maris* (NR_025327)	89	0.5	1.1	0.0	0.8	0.8	0.7	0.0	0.0	0.0	1.2
Phycisphaerae							0.5	0.6	0.0	1.5	0.0	0.0	0.0	1.8	0.0	1.2
WD2101 soil group	55	BEtL8P3E02 (LK024580)	HF952502	99	*Phycisphaera mikurensis* (NR_074491)	80	0.2	0.0	0.0	0.8	0.0	0.0	0.0	0.0	0.0	1.2
CPla-3 termite group *Bacteria*	56	BEtL9P6G04 (LK024859)	DQ088001	98	*Phycisphaera mikurensis* (NR_074491)	80	0.4	0.6	0.0	0.8	0.0	0.0	0.0	1.8	0.0	0.0
Verrucomicrobia							3.3	3.9	0.0	0.0	0.0	0.7	2.2	10.6	6.3	8.3
Spartobacteria							0.3	0.0	0.0	0.0	0.0	0.0	0.0	2.7	0.0	0.0
Chthoniobacterales							0.3	0.0	0.0	0.0	0.0	0.0	0.0	2.7	0.0	0.0
LD29	57	BCon15P7E05 (LK024928)	JX100065	99	*Verrucomicrobium spinosum* (NR_026266)	92	0.3	0.0	0.0	0.0	0.0	0.0	0.0	2.7	0.0	0.0
OPB35 soil group	58	BProP7D08 (LK024919)	GQ402552	98	*Prosthecobacter dejongeii* (NR_026021)	85	1.9	2.2	0.0	0.0	0.0	0.0	2.2	4.4	6.3	2.4
Opitutae							0.8	0.6	0.0	0.0	0.0	0.7	0.0	1.8	0.0	6.0

Phylogenic affiliation [a]	OTU	Reference sequence (acc. no.)	Acc. no. of closest relative	I [b] [%]	Closesest cultured relative (acc. no.)	I [b] [%]	Relative abundance [%] [c]									
							total	FP	15°C						5°C	
									EH	EL	BH	BL	P	C	E	C
Opitutales							0.8	0.6	0.0	0.0	0.0	0.7	0.0	1.8	0.0	6.0
Opitutaceae	59						0.8	0.6	0.0	0.0	0.0	0.7	0.0	1.8	0.0	6.0
Opitutus	59a	BCon15P7G05 (LK024952)	JN626549	99	*Opitutus terrae* (NR_074978)	96	0.8	0.6	0.0	0.0	0.0	0.7	0.0	1.8	0.0	6.0
S-BQ2-57 soil group	60	BCon15P7G11 (LK024956)	KC358349	99	*Prosthecobacter debontii* (AJ966882)	88	0.3	0.6	0.0	0.0	0.0	0.0	0.0	1.8	0.0	0.0
unknown	61	Bt0P14C12 (LK025328)	EU680463	97	*Methylacidiphilum infernorum* (NR_074583)	84	0.1	0.6	0.0	0.0	0.0	0.0	0.0	0.0	0.0	0.0
Lentisphaerae							0.3	0.0	0.0	0.0	0.0	0.0	0.0	0.9	1.8	0.0
Lentisphaeria							0.3	0.0	0.0	0.0	0.0	0.0	0.0	0.9	1.8	0.0
WCHB1-41	62	BCon15P7E03 (LK024926)	DQ642404	99	*Prosthecobacter vanneervenii* (AJ966883)	83	0.1	0.0	0.0	0.0	0.0	0.0	0.0	0.9	0.0	0.0
Victivallales							0.2	0.0	0.0	0.0	0.0	0.0	0.0	0.0	1.8	0.0
Victivallaceae	63						0.2	0.0	0.0	0.0	0.0	0.0	0.0	0.0	1.8	0.0
Victivallis	63a	BEt5P8F01 (LK025014)	JN398085	99	*Victivallis vadensis* (JQ346729)	89	0.2	0.0	0.0	0.0	0.0	0.0	0.0	0.0	1.8	0.0
Candidate division OP3	64	BButH4P4H05 (LK024698)	FQ660114	97	*Desulfarculus baarsii* (NR_074919)	81	1.2	3.4	0.0	0.0	0.8	0.0	2.2	0.9	0.9	1.2
Acidobacteria							13.8	8.9	23.7	21.1	11.8	27.4	8.1	7.1	6.3	8.3
Acidobacteria							13.4	8.9	22.9	21.1	10.9	25.9	8.1	7.1	5.4	8.3
Acidobacteriales							8.8	5.0	21.2	15.8	5.0	13.3	5.1	4.4	3.6	4.8
Acidobacteriaceae (Subgroup_1)	65						8.8	5.0	21.2	15.8	5.0	13.3	5.1	4.4	3.6	4.8
Telmatobacter	65a	BEtH3P6A06 (LK024794)	HG324995	99	*Telmatobacter bradus* (AM887760)	97	1.7	1.1	5.1	1.5	0.8	3.0	0.7	1.8	0.0	1.2
Granulicella	65b	BCon5P8H07 (LK025039)	FR720609	99	*Granulicella pectinivorans* (AM887757)	95	0.4	1.7	0.0	0.0	0.0	0.0	0.0	0.0	0.9	1.2
Koribacter	65c	BEtH3P6A12 (LK024799)	GU270763	99	*Candidatus* Koribacter versatilis (NR_074350)	94	6.6	2.2	16.1	14.3	4.2	10.4	4.4	2.7	2.7	2.4
Subgroup 3 Solibacter	66	BEtL8P3E06 (LK024584)	JN851510	99	*Candidatus* Solibacter usitatus (NR_074351)	95	2.9	2.8	1.7	3.0	4.2	3.7	2.9	2.7	1.8	3.6

Phylogenic affiliation [a]	OTU	Reference sequence (acc. no.)	Acc. no. of closest relative	I [b] [%]	Closesest cultured relative (acc. no.)	I [b] [%]	Relative abundance [%] [c]									
									15°C						5°C	
							total	FP	EH	EL	BH	BL	P	C	E	C
Subgroup 2	67	BButL8P5C05 (LK024726)	HG324440	99	*Acidobacterium capsulatum* (AB561885)	83	1.2	0.6	0.0	1.5	0.8	7.4	0.0	0.0	0.0	0.0
Subgroup 13	68	BEtL9P3G06 (LK024608)	JN168351	99	*Symbiobacterium thermophilum* (AP006840)	81	0.4	0.6	0.0	0.8	0.8	0.7	0.0	0.0	0.0	0.0
JH-WHS99	69	BButL8P5B11 (LK024722)	AB364816	99	*Acidobacterium capsulatum* (AB561885)	86	0.1	0.0	0.0	0.0	0.0	0.7	0.0	0.0	0.0	0.0
Holophagae							0.4	0.0	0.8	0.0	0.8	1.5	0.0	0.0	0.9	0.0
Holophagales							0.4	0.0	0.8	0.0	0.8	1.5	0.0	0.0	0.9	0.0
Holophagaceae	70	BButH4P4E07 (LK024670)	AB659009	99	*Geothrix fermentans* (HF559181)	95	0.4	0.0	0.8	0.0	0.8	1.5	0.0	0.0	0.9	0.0
Nitrospirae							0.6	0.0	0.0	0.8	0.0	0.0	2.2	0.0	0.0	3.6
Nitrospira							0.6	0.0	0.0	0.8	0.0	0.0	2.2	0.0	0.0	3.6
Nitrospirales							0.6	0.0	0.0	0.8	0.0	0.0	2.2	0.0	0.0	3.6
Nitrospiraceae	71						0.5	0.0	0.0	0.8	0.0	0.0	2.2	0.0	0.0	2.4
Nitrospira	71a	BProP7B09 (LK024898)	JQ793080	100	*Nitrospira japonica* (AB818959)	96	0.3	0.0	0.0	0.0	0.0	0.0	1.5	0.0	0.0	1.2
uncultured	71b	BProP7D03 (LK024914)	AB659372	99	*Candidatus* Magnetoovum mohavensis (GU979422)	90	0.3	0.0	0.0	0.8	0.0	0.0	0.7	0.0	0.0	1.2
Sh765B-TzT-35	72	BCon5P18D01 (LK025624)	AB661498	99	*Candidatus* Methylomirabilis oxyfera (NR_102979)	91	0.1	0.0	0.0	0.0	0.0	0.0	0.0	0.0	0.0	1.2
TM6	73	BCon5P18H12 (LK025673)	JF261647	99	*Desulfobacterium indolicum* (NR_028897)	80	0.4	1.1	0.0	0.0	0.0	0.0	0.0	0.0	0.0	2.4
Candidate division BRC1	74	BButH4P4G07 (LK024691)	AM159309	96	*Geoalkalibacter ferrihydriticus* (NR_043709)	84	0.4	0.6	0.0	0.0	0.8	0.0	1.5	0.9	0.0	0.0
Firmicutes							6.3	13.4	1.7	2.3	26.1	0.0	2.9	3.5	1.8	1.2
Bacilli							1.1	3.4	0.0	1.5	0.0	0.0	0.7	1.8	0.9	0.0
Bacillales							1.1	3.4	0.0	1.5	0.0	0.0	0.7	1.8	0.9	0.0
Paenibacillaceae	75						1.1	3.4	0.0	1.5	0.0	0.0	0.7	1.8	0.9	0.0

Phylogenic affiliation [a]	OTU	Reference sequence (acc. no.)	Acc. no. of closest relative	I [b] [%]	Closesest cultured relative (acc. no.)	I [b] [%]	Relative abundance [%] [c]									
									15°C						5°C	
							total	FP	EH	EL	BH	BL	P	C	E	C
Paenibacillus	75a	BEtL9P6F09 (LK024853)	KC620702	99	*Paenibacillus caespitis* (AM745263)	99	1.1	3.4	0.0	1.5	0.0	0.0	0.7	1.8	0.9	0.0
Clostridia							4.7	8.4	1.7	0.8	24.4	0.0	2.2	1.8	0.0	1.2
Clostridiales							4.7	8.4	1.7	0.8	24.4	0.0	2.2	1.8	0.0	1.2
Ruminococcaceae	76						1.7	4.5	0.0	0.8	5.0	0.0	0.7	1.8	0.0	1.2
uncultured 1	76a	BButH4P4E04 (LK024667)	JX224003	95	*Clostridium aldrichii* (X71846)	88	0.4	0.0	0.0	0.0	4.2	0.0	0.0	0.0	0.0	0.0
uncultured 2	76b	BButH3P4C07 (LK024647)	AB630537	95	*Acetivibrio cellulolyticus* (NR_025917)	94	1.2	4.5	0.0	0.8	0.8	0.0	0.7	0.9	0.0	1.2
uncultured 3	76c	BCon15P7H11 (LK024962)	HG324403	99	*Clostridium cellulosi* (FJ465164)	95	0.1	0.0	0.0	0.0	0.0	0.0	0.0	0.9	0.0	0.0
Clostridiaceae	77						0.7	3.9	0.0	0.0	0.0	0.0	0.7	0.0	0.0	0.0
Clostridium	77a	BProP7A12 (LK024890)	JQ625252	99	*Clostridium puniceum* (X71857)	99	0.7	3.9	0.0	0.0	0.0	0.0	0.7	0.0	0.0	0.0
vadinBB60	78	BEtH4P3C08 (LK024571)	JQ625004	97	*Clostridium thermocellum* (L09173)	88	0.1	0.0	0.8	0.0	0.0	0.0	0.0	0.0	0.0	0.0
Syntropho-monadaceae	79						2.1	0.0	0.8	0.0	19.3	0.0	0.0	0.0	0.0	0.0
Syntrophomonas	79a	BButH3P4B12 (LK024641)	JQ599687	98	*Syntrophomonas zehnderi* (NR_044008)	95	2.1	0.0	0.8	0.0	19.3	0.0	0.0	0.0	0.0	0.0
Peptococcaceae 2	80						0.1	0.0	0.0	0.0	0.0	0.0	0.7	0.0	0.0	0.0
Desulfosporosinus	80a	BProP15G04 (LK025433)	JX222948	98	*Desulfosporosinus lacus* (NR_042202)	97	0.1	0.0	0.0	0.0	0.0	0.0	0.7	0.0	0.0	0.0
Negativicutes							0.4	1.7	0.0	0.0	1.7	0.0	0.0	0.0	0.0	0.0
Selenomonadales							0.4	1.7	0.0	0.0	1.7	0.0	0.0	0.0	0.0	0.0
Veillonellaceae	81						0.4	1.7	0.0	0.0	1.7	0.0	0.0	0.0	0.0	0.0
Zymophilus	81a	Bt0P8B12 (LK024982)	AM910671	99	*Zymophilus paucivorans* (HE582763)	99	0.3	1.7	0.0	0.0	0.0	0.0	0.0	0.0	0.0	0.0
uncultured	81b	BButH3P4B08 (LK024638)	JX564342	95	*Sporomusa malonica* (HE962129)	90	0.2	0.0	0.0	0.0	1.7	0.0	0.0	0.0	0.0	0.0

Phylogenic affiliation [a]	OTU	Reference sequence (acc. no.)	Acc. no. of closest relative	I [b] [%]	Closesest cultured relative (acc. no.)	I [b] [%]	Relative abundance [%] [c]									
									15°C						5°C	
							total	FP	EH	EL	BH	BL	P	C	E	C
OPB54	82	BEt5P17C10 (LK025546)	DQ125652	99	*Pelotomaculum thermopropionicum* (AP009389)	86	0.1	0.0	0.0	0.0	0.0	0.0	0.0	0.0	0.9	0.0
Actinobacteria							8.0	6.1	5.1	14.3	4.2	9.6	6.6	10.6	6.3	9.5
Actinobacteria							3.8	2.2	2.5	6.8	3.4	6.7	1.5	2.7	4.5	4.8
Frankiales							3.5	1.7	1.7	6.8	3.4	6.7	1.5	2.7	3.6	4.8
Acidothermaceae	83						3.5	1.7	1.7	6.8	3.4	6.7	1.5	2.7	3.6	4.8
Acidothermus	83a	BButH3P4D02 (LK024654)	GQ203391	99	*Actinoallomurus purpureus* (NR_041651)	95	3.5	1.7	1.7	6.8	3.4	6.7	1.5	2.7	3.6	4.8
Actinomycetales							0.2	0.6	0.0	0.0	0.0	0.0	0.0	0.0	0.9	0.0
Streptomycetaceae	84						0.2	0.6	0.0	0.0	0.0	0.0	0.0	0.0	0.9	0.0
Streptomyces	84a	Bt0P14C05 (LK025323)	HM270025	99	*Streptomyces aomiensis* (AB522686)	97	0.2	0.6	0.0	0.0	0.0	0.0	0.0	0.0	0.9	0.0
Propionibacteriales							0.1	0.0	0.8	0.0	0.0	0.0	0.0	0.0	0.0	0.0
Propionibacteriaceae	85						0.1	0.0	0.8	0.0	0.0	0.0	0.0	0.0	0.0	0.0
Propionibacterium	85a	BEtH4P3D07 (LK024576)	JQ512928	99	*Propionibacterium acnes* (CP003293)	99	0.1	0.0	0.8	0.0	0.0	0.0	0.0	0.0	0.0	0.0
Acidimicrobiia							2.2	2.2	0.0	5.3	0.0	2.2	1.5	5.3	0.9	2.4
Acidimicrobiales							2.2	2.2	0.0	5.3	0.0	2.2	1.5	5.3	0.9	2.4
uncultured 1	86	BButL9P5G01 (LK024767)	GU127771	99	*Aciditerrimonas ferrireducens* (AB517669)	90	1.9	2.2	0.0	4.5	0.0	2.2	1.5	5.3	0.9	0.0
uncultured 2	87	BEtL9P3G01 (LK024603)	FR732407	98	*Aciditerrimonas ferrireducens* (AB517669)	89	0.3	0.0	0.0	0.8	0.0	0.0	0.0	0.0	0.0	2.4
Thermoleophilia							1.9	1.7	2.5	2.3	0.8	0.7	3.7	2.7	0.9	2.4
Solirubrobacterales							1.4	1.7	0.8	2.3	0.0	0.7	2.2	1.8	0.9	2.4
TM146	88	BEtH3P3B10 (LK024563)	GU270680	99	*Solirubrobacter ginsenosidimutans* (NR_108192)	94	1.2	1.7	0.8	2.3	0.0	0.0	1.5	0.9	0.9	2.4
Conexibacteraceae	89	BProP15G01 (LK025431)	JX100297	98	*Conexibacter woesei* (NR_074830)	95	0.3	0.0	0.0	0.0	0.0	0.7	0.7	0.9	0.0	0.0
Gaiellales							0.5	0.0	1.7	0.0	0.8	0.0	1.5	0.9	0.0	0.0

Phylogenic affiliation [a]	OTU	Reference sequence (acc. no.)	Acc. no. of closest relative	I [b] [%]	Closesest cultured relative (acc. no.)	I [b] [%]	Relative abundance [%] [c]									
									15°C						5°C	
							total	FP	EH	EL	BH	BL	P	C	E	C
uncultured 1	90	BButH4P4H02 (LK024696)	HG324607	99	*Gaiella occulta* (JF423906)	84	0.4	0.0	1.7	0.0	0.8	0.0	0.7	0.9	0.0	0.0
uncultured 2	91	BProP15E09 (LK025417)	AB821115	98	*Gaiella occulta* (JF423906)	93	0.1	0.0	0.0	0.0	0.0	0.0	0.7	0.0	0.0	0.0
Chloroflexi							3.8	2.2	0.0	2.3	5.9	2.2	2.2	7.1	7.1	8.3
Anaerolineae							1.0	0.6	0.0	0.0	3.4	0.0	0.0	1.8	2.7	1.2
Anaerolineales							1.0	0.6	0.0	0.0	3.4	0.0	0.0	1.8	2.7	1.2
Anaerolineaceae	92						1.0	0.6	0.0	0.0	3.4	0.0	0.0	1.8	2.7	1.2
uncultured	92a	BCon15P7F10 (LK024945)	GU127800	98	*Bellilinea caldifistulae* (NR_041354)	87	1.0	0.6	0.0	0.0	3.4	0.0	0.0	1.8	2.7	1.2
Dehalococcoidia							0.4	0.0	0.0	0.0	0.8	0.0	0.7	2.7	0.0	0.0
vadinBA26	93	BButH3P4D01 (LK024653)	GU127773	99	*Dehalogenimonas alkenigignens* (NR_109657)	89	0.4	0.0	0.0	0.0	0.8	0.0	0.7	1.8	0.0	0.0
FW22	94	BCon15P16C11 (LK025471)	JX981787	99	*Dehalogenimonas alkenigignens* (NR_109657)	88	0.1	0.0	0.0	0.0	0.0	0.0	0.0	0.9	0.0	0.0
Ktedonobacteria							0.3	0.6	0.0	0.8	0.0	0.7	0.0	0.0	0.0	0.0
Ktedonobacterales							0.3	0.6	0.0	0.8	0.0	0.7	0.0	0.0	0.0	0.0
Ktedonobacteraceae	95	BEtL8P3E05 (LK024583)	DQ830092	99	*Ktedonobacter racemifer* (AB510917)	90	0.1	0.0	0.0	0.8	0.0	0.0	0.0	0.0	0.0	0.0
HSB_OF53-F07	96	BButL9P5G02 (LK024768)	HQ265071	99	*Ktedonobacter racemifer* (AB510917)	88	0.2	0.6	0.0	0.0	0.0	0.7	0.0	0.0	0.0	0.0
SHA-26	97	BButH3P4A03 (LK024622)	FR687081	97	*Dehalococcoides mccartyi* (NR_102515)	84	0.2	0.0	0.0	0.0	1.7	0.0	0.0	0.0	0.0	0.0
JG37-AG-4	98	BCon15P7E07 (LK024930)	DQ450737	99	*Acidimicrobium ferrooxidans* (KC852080)	86	0.4	0.6	0.0	0.0	0.0	0.0	0.0	0.9	1.8	0.0
uncultured	99	BEtL10P6H02 (LK024868)	FR732107	99	*Bellilinea caldifistulae* (NR_041354)	82	1.6	0.6	0.0	1.5	0.0	1.5	1.5	1.8	2.7	7.1
Candidate division OP11							0.2	0.0	0.0	0.0	0.0	0.0	0.7	0.9	0.0	0.0

Phylogenic affiliation [a]	OTU	Reference sequence (acc. no.)	Acc. no. of closest relative	I [b] [%]	Closesest cultured relative (acc. no.)	I [b] [%]	Relative abundance [%] [c]									
									15°C						5°C	
							total	FP	EH	EL	BH	BL	P	C	E	C
uncultured 1	100	BProP7B03 (LK024892)	EU266852	99	*Thermothrix thiopara* (L77877)	79	0.1	0.0	0.0	0.0	0.0	0.0	0.7	0.0	0.0	0.0
uncultured 2	101	BCon15P7G03 (LK024950)	FJ482198	99	*Hippea jasoniae* (NR_108510)	79	0.1	0.0	0.0	0.0	0.0	0.0	0.0	0.9	0.0	0.0
SM2F11	102	BButL9P5H03 (LK024781)	KC607326	98	*Candidatus* Magnetobacterium bavaricum (FP929063)	83	0.3	0.6	0.0	0.0	0.0	0.7	0.0	0.0	0.0	1.2
Candidate division OD1							1.0	0.0	2.5	0.0	5.0	0.0	1.5	0.0	0.0	0.0
uncultured 1	103	BEtH4P3C11 (LK024573)	HM992553	98	*Arthrobacter bergerei* (KF254744)	78	0.3	0.0	0.8	0.0	1.7	0.0	0.0	0.0	0.0	0.0
uncultured 2	104	BButH4P4F10 (LK024684)	HM481385	96	*Plumaria plumosa* (DQ026678)	77	0.6	0.0	0.8	0.0	3.4	0.0	1.5	0.0	0.0	0.0
uncultured 3	105	BEtH3P6B10 (LK024808)	FQ659551	96	*Pelobacter massiliensis* (NR_104786)	77	0.1	0.0	0.8	0.0	0.0	0.0	0.0	0.0	0.0	0.0
Cyanobacteria							1.7	2.8	0.8	0.8	3.4	1.5	0.7	1.8	0.9	2.4
Oscillatoriales							0.1	0.6	0.0	0.0	0.0	0.0	0.0	0.0	0.0	0.0
Phormidium	106	Bt0P13B10 (LK025235)	DQ444144	99	*Phormidium autumnale* (DQ493873)	99	0.1	0.6	0.0	0.0	0.0	0.0	0.0	0.0	0.0	0.0
Nostocales							0.1	0.6	0.0	0.0	0.0	0.0	0.0	0.0	0.0	0.0
Nostocaceae	107						0.1	0.6	0.0	0.0	0.0	0.0	0.0	0.0	0.0	0.0
Nostoc	107a	Bt0P13E05 (LK025265)	KF494248	99	*Nostoc punctiforme* (HQ700838)	98	0.1	0.6	0.0	0.0	0.0	0.0	0.0	0.0	0.0	0.0
4C0d-2	108	BButH4P4F02 (LK024676)	HE775583	99	*Gloeobacter kilaueensis* (CP003587)	85	0.4	0.0	0.8	0.0	3.4	0.0	0.0	0.0	0.0	0.0
MLE1-12	109	BEtL8P3F04 (LK024594)	JQ379900	100	*Calothrix* sp. LCRSM-1413 (JN705664)	90	0.4	0.6	0.0	0.8	0.0	0.0	0.0	0.0	0.0	2.4
WD272	110	BButL9P5F08 (LK024762)	HM312833	99	*Heliophilum fasciatum* (HE582752)	81	0.7	1.1	0.0	0.0	0.0	1.5	0.7	1.8	0.9	0.0
Armatimonadetes							0.6	1.1	0.0	0.0	1.7	0.7	0.7	0.0	0.9	0.0
Chthonomonadetes							0.5	1.1	0.0	0.0	1.7	0.0	0.7	0.0	0.9	0.0
Chthonomonadales							0.5	1.1	0.0	0.0	1.7	0.0	0.7	0.0	0.9	0.0

Phylogenic affiliation [a]	OTU	Reference sequence (acc. no.)	Acc. no. of closest relative	I [b] [%]	Closest cultured relative (acc. no.)	I [b] [%]	Relative abundance [%] [c]									
									15°C						5°C	
							total	FP	EH	EL	BH	BL	P	C	E	C
Chthonomonadaceae	111	BButH4P4E09 (LK024672)	HQ264928	99	Chthonomonas calidirosea (NR_103954)	91	0.5	1.1	0.0	0.0	1.7	0.0	0.7	0.0	0.9	0.0
Fimbriimonas-related	112	BButL8P5C12 (LK024733)	AB672137	98	Fimbriimonas ginsengisoli (GQ339893)	91	0.1	0.0	0.0	0.0	0.0	0.7	0.0	0.0	0.0	0.0
Elusimicrobia							0.5	0.0	0.0	0.0	0.0	1.5	0.0	0.9	0.9	2.4
Elusimicrobia							0.5	0.0	0.0	0.0	0.0	1.5	0.0	0.9	0.9	2.4
Lineage I (Endomicrobia)	113	BCon15P7F07 (LK024942)	JN039001	98	Candidatus Endomicrobium trichonymphae (AY512588)	92	0.1	0.0	0.0	0.0	0.0	0.0	0.0	0.9	0.0	0.0
Lineage II	114	BEt5P17A11 (LK025524)	FJ405885	97	Kofleria flava (HF543825)	79	0.2	0.0	0.0	0.0	0.0	0.7	0.0	0.0	0.9	0.0
Lineage IV							0.3	0.0	0.0	0.0	0.0	0.7	0.0	0.0	0.0	2.4
unkown 1	115	BCon5P18D02 (LK025625)	FR667831	98	Elusimicrobium minutum (NR_074114)	84	0.2	0.0	0.0	0.0	0.0	0.0	0.0	0.0	0.0	2.4
unkown 2	116	BButL9P10D06 (LK025172)	HG529135	98	Candidatus Endomicrobium trichonymphae (AY512588)	81	0.1	0.0	0.0	0.0	0.0	0.7	0.0	0.0	0.0	0.0

[a]OTUs were assigned to taxa based on their phylogenic position in the SILVA 16S rRNA tree (2.6.1.2).

[b]I, blastn identity

[c]FP, fresh peat; E, B or P: ethanol, butyrate, or propionate treatments; C, unsupplemented controls; L and H are 'light' and 'heavy' fractions (Figure 7).